BINAURAL INTERACTION IN HEARING IMPAIRED LISTENERS

by

Kaigham Jacob Gabriel

B.S. University of Pittsburgh (1977)

S.M. Massachusetts Institute of Technology (1979)

SUBMITTED TO THE DEPARTMENT OF ELECTRICAL ENGINEERING AND COMPUTER SCIENCE IN PARTIAL FULFILLMENT OF THE REQUIREMENTS FOR THE DEGREE OF

DOCTOR OF SCIENCE

at the

MASSACHUSETTS INSTITUTE OF TECHNOLOGY

August 30, 1983

Signature of Author _____
Department of Electrical Engineering and Computer Science August 30, 1983

Certified by _____
H. Steven Colburn, Thesis Supervisor

Accepted by _____

MASSACHUSETTS INSTITUTE OF TECHNOLOGY
OCT 4 1983
Archives

BINAURAL INTERACTION IN HEARING IMPAIRED LISTENERS

by

Kaigham Jacob Gabriel

The binaural hearing of four hearing impaired listeners was tested in interaural time discrimination, interaural intensity discrimination, interaural correlation discrimination and binaural detection experiments. All tests were conducted on each subject using third-octave bands of noise centered at 250, 500, 1000, 2000 and 4000 Hz. In general, the pattern of loss in binaural hearing was independent of the pattern of loss as measured by current audiometric techniques. By augmenting a simple, representative, narrowband model of binaural interaction with an interaural-differences averager, the results from the interaural time and intensity discrimination tests were used to predict and relate the correlation discrimination and binaural detection results. For both hearing impaired and normal listeners, this study suggests that narrowband correlation discrimination and NOSπ detection can be characterized by a listener's sensitivity to interaural time and intensity differences.

THESIS SUPERVISOR: H. Steven Colburn

TITLE: Principal Research Scientist

Research Laboratory of Electronics

Acknowledgment

I always have trouble with this part. It's been four years since I last had to write an acknowledgment to a thesis. Let's hope I never have to write another one. I'm feeling sort of emotional right now, so before this gets real soppy, I thank you all for your friendship, your guidance, your enthusiasm and your patience. Success in all your endeavors.

Table of Contents

Chapter 1 Introduction

Motivation 1-3

Chapter 2 Previous Work

A. Normal Listeners 2-5

i) Interaural Time Disc. 2-5
ii) Interaural Intensity Disc. ... 2-7
iii) Interaural Correlation Disc. . 2-8
iv) Binaural Detection 2-9

B. Hearing Impaired Listeners 2-10

C. Models of Binaural Interaction .. 2-15

Chapter 3 Experiments

A. Subjects 3-1

B. Stimuli 3-3

i) Interaural Time Disc. 3-3
ii) Interaural Intensity Disc. ... 3-4
iii) Interaural Correlation Disc. . 3-5
iv) Binaural Detection 3-6

C. Procedure 3-7

Sequential Testing Rule 3-8

Chapter 4 Experimental Results

A. Normal Listeners 4-1

i) Interaural Time Disc. 4-1
ii) Interaural Intensity Disc. ... 4-2
iii) Interaural Correlation Disc. . 4-2
iv) Binaural Detection 4-2

B. Impaired Listeners 4-3

i) Interaural Time Disc. 4-3
ii) Interaural Intensity Disc. ... 4-5
iii) Interaural Correlation Disc. . 4-6
iv) Binaural Detection 4-8

C. Binaural Audiograms 4-9

D. Relationships Among the Tasks ... 4-12

Chapter 5 A Model of Binaural Interaction

A. Outline of the Model 5-1

B. Elements of the Model 5-3

C. Comments 5-5

D. Estimation of Model Parameters .. 5-7

i) Separate Time and Intensity Differences 5-9
ii) Sum of Differences (SID) 5-9

Chapter 6 Characterization of Stimulus Interaural Differences

A. Analytical Evaluation 6-2

i) Correlation Stimuli 6-2
ii) Detection Stimuli 6-7

B. Numerical Computation 6-9

Chapter 7 Binaural Performance Based on Stimulus Variability

A. Distribution of Averaged Interaural Differences 7-2

B. Model Predictor Equations 7-4

i) Separate Time and Intensity Differences 7-5

a) Intensity Alone 7-6
b) Time Alone 7-8
c) Linear Sum of Diff. 7-9
d) Optimal Combination 7-10

ii) Sum of Interaural Diff. (SID). 7-11

Chapter 8 Predictions of the Model

A. Separate Time and Intensity Differences 8-1

B. Normal Listeners 8-2

i) Correlation Discrimination Predictions 8-3
ii) NOSπ Threshold Predictions .. 8-3

C. Impaired Listeners 8-6

i) Correlation Discrimination Predictions 8-6
ii) NOSπ Threshold Predictions .. 8-8

D. Relative Use Of Interaural Cues . 8-9

Chapter 9 Conclusions and Remarks

A. Psychophysical Results 9-1

B. Modelling Results 9-5

Appendix I Waveform Generation

Appendix II Sequential Testing Methods

Appendix III Estimation of Model Parameters

Appendix IV Predictor Equations for Correlation Discrimination and NOSπ Detection

Footnotes

Table 3.1
Table 7.1

Figure Captions

References

Figures

CHAPTER 1

INTRODUCTION AND MOTIVITATION

Binaural hearing is the sensory processing of the sounds at the two ears which extracts auditory information not present at either ear alone. The utilization of this binaural information enables us to locate sounds in the environment, focus on specific sounds within a multitude of different masking sounds, and perceive the spaciousness of sounds.

The physical differences between the acoustic signals which provide binaural information include differences in the spectral characteristics of the sounds, differences in the arrival times of sounds at the two ears and differences in the intensities of the sounds at the two ears. In natural environments, these differences arise from different path geometries (different path lengths, differences in the diffraction of sounds caused by the head and body, etc.) involved in the transmission of the sound from the source to the two ears.

From an evolutionary point of view, it is clear that binaural hearing is an advantage. The degree to which our distant ancestors were able to distinguish and locate the sounds of predators (and prey) was directly related to their chances for survival. Certain

aspects of our present-day interactions with the environment, although less exotic and primitive, are still dependent on binaural hearing. Warnings about the direction of approaching people or objects, and perceptions in complex or noisy environments are greatly enhanced by our binaural hearing.

A substantial number of experiments have been performed on normal listeners in an effort to quantify our ability to perceive binaural information. Many of these experiments have measured the ability of human listeners to discriminate interaural differences of simple sounds presented in controlled listening situations. Although these sounds would not normally be encountered in natural environments, their interaural differences can be finely controlled and extraneous, contaminating factors can be eliminated. For example, by presenting electronically generated and controlled sounds over headphones, arbitrary interaural time differences can be created with no interaural intensity differences. Such a stimulus configuration would be difficult, if not impossible, to achieve with naturally occuring sounds.

In conjunction with the experimental efforts, theoretical models of binaural hearing in normal listeners have also been developed. Like all succesful models, these provide an economical framework within which the different experimental results in binaural hearing are organized. This organization naturally leads to an exposition of relationships between the different results which might not otherwise be apparent. In addition, the more succesful a model is at organizing data, the more binaural performance in many different binaural tasks can be characterized by

a set of experiments which specify the parameter values of such a model. Most of these models have been functional descriptions of the processes presumed to be performed by the physiological system and imply no specific correspondence between physiological processes and a model's elements.

Motivation

Hearing impairments at the peripheral level (the portion of the auditory system which transduces acoustic signals at the ear into neural firing patterns) or at a higher, more central neurophysiological level (or both) can result in a significant degradation of binaural hearing (Durlach et al., 1980). In the everyday life of an impaired listener, the degradation can manifest itself as an inability to localize sound sources or an inability to function in complex auditory environments. This can have dangerous consequences in situations such as work environments and traffic, where auditory warnings are important. Moreover, binaural hearing deficits can have social and psychological consequences when impaired listeners avoid or are uncomfortable in situations with many speakers because their binaural impairments make it difficult to focus on a single speaker.

With few exceptions, current clinical procedures do not include measurements of binaural capabilities in hearing impaired listeners. Because the standard audiometric evaluation of hearing impairments involves separately testing each ear, little or no information is provided about the effect of an impairment on binaural hearing. In

fact, some multiple sclerosis patients show audiometrically normal hearing and yet exhibit severe degradation in binaural hearing (Hausler and Levine, 1980).

The lack of any binaural tests in clinical evaluations is primarily due to not knowing what to measure. It is not clear what aspect of binaural hearing (e.g., interaural time discrimination, interaural intensity discrimination, or binaural target-in-masker detection) should be tested. Moreover, due to constraints on testing time, it is necessary to test only a minimum set of capabilities. The ability to characterize binaural performance in a variety of different binaural tasks with a few, representative set of tests, requires a description of binaural interaction successful at relating the different types of binaural phenomena. To date, none of the current models of binaural interaction have been shown to be capable of relating even the above four phenomena in normal listeners under the same set of assumptions (Colburn and Durlach, 1978).

A way to determine the subset of measurements necessary to characterize impaired binaural hearing in an individual subject is to obtain: (a) results from a number of different binaural experiments, each performed on every impaired subject in the study; and (b) a model of binaural interaction which can simulate simply a given impairment's effect on binaural hearing. Such a model should focus on the use of binaural information to effect performance (and hence, on the relations between the different tests), rather than on any detailed assumptions about how such information is obtained.

The first requirement is a consequence of the differences in binaural hearing abilities encountered across different impaired listeners, even for listeners with the same audiological description (Durlach et al., 1980 ; Hausler and Colburn, 1981). An implicit assumption in the modelling of normal listeners is that they all have similar binaural hearing. Results from different studies (with different subjects and on different binaural phenomena) are integrated and considered equivalent to results from a single extensive study on one normal listener. For impaired listeners, this assumption is not valid. Thus, the different types of binaural experiments must all be performed on each impaired listener used in a study if any valid model of impaired binaural hearing is to be developed.

The requirements on the model are made because different types of impairment have varying, complicated, or unknown physiological origins. Thus, in a model intended to explore interrelationships between binaural phenomena, it is more general (and easier) to describe the overall effect an impairment has on the way in which binaural information is processed, rather than on any specific description of the impairment. Although models with more detailed descriptions of the impairments are possible, it is not evident that such modelling will necessarily improve our ability to relate the different binaural hearing phenomena.

This study presents an attempt to define the minimum set of measurements required to characterize binaural performance in a restricted, but representative, set of binaural experiments for a variety of impaired listeners.

The experiments in this study focused on the frequency dependence of four binaural phenomena: interaural time (fine structure) discrimination, interaural intensity discrimination, binaural masked detection, and interaural correlation discrimination. These four binaural tests were chosen as being descriptive of the functional aspects of the binaural hearing as described earlier in this chapter. As will be seen in the next chapter, interaural time and intensity discrimination is related to localization ability, binaural masked detection to focusing ability, and interaural correlation discrimination to the perception of spaciousness or extent of the acoustic image.

Our interest in the frequency dependence of impaired binaural hearing is generated by several factors. One, for narrowband signals it is generally accepted that, in normal listeners, the binaural system is most sensitive to interaural time differences at low frequencies (less than 1500 Hz) and roughly equaly sensitive to interaural intensity differences at all frequencies. As such, for narrowband stimuli, performance in different binaural tasks (with both interaural time and intensity cues available) is believed to be mediated by interaural time processing at low frequencies and interaural intensity processing at high frequencies. The extent to which this frequency delineation between interaural time and intensity processing exists in impaired listeners can be an important factor in determining the nature of the impairment and can have consequences for both the type of interaural information and the way in which interaural information is processed in binaural hearing aids.

Two, comparison of binaural hearing impairments to current, audiometrically defined monaural losses would be more meaningful and facilitated by a frequency dependent measure of binaural hearing.

Finally, the auditory system is known to be tonotopically organized up to the level of the VIIIth nerve bundle (Kiang *et al.*, 1965) and at least as far as the superior olivary complex (Guinan *et al.*, 1972). Thus, a frequency dependent measure of binaural hearing loss may also delineate regions of physiological loss in the peripheral and central portions of the auditory system.

Because of our interest in the frequency dependence of binaural hearing, we have chosen to use narrowband (one-third octave wide) noise at five different center frequencies. We used noise waveforms instead of pure tones for the following reasons. One, the basic theoretical thrust of this study is an attempt to relate four different binaural phenomena. As such, we wanted to use the same stimuli in both the detection and discrimination tasks. Thus, the narrowband noise used in the discrimination experiments were the same noise waveforms used in the detection experiments. Two, as is discussed in chapter 2, certain binaural impairments are not apparent when testing with wideband stimuli and are apparent only when a narrowband stimulus is used (Hausler et al., 1983).

Chapter 2 reviews a selection of binaural phenomena and models relevant to this study. This includes a description of binaural hearing in normal listeners, a general description of current binaural interaction models, and a brief review of past research on binaural hearing in impaired listeners.

Chapter 3 describes the experiments, stimuli and subjects used in the study. A new, general method of psychophysical testing was developed, which has been particularly useful in the testing of hearing impaired listeners.

In Chapter 4 the results of the experiments are presented and discussed in relation to the impaired subjects' audiograms and to normal listeners' performance. In addition, we present a new description of binaural performance (" binaural audiograms ") which reveal some interesting patterns of loss not apparent in the traditional representations of binaural performance.

Chapter 5 presents a model of binaural interaction for a single frequency band which uses only interaural time and interaural intensity differences of narrowband stimuli as the variables of binaural information. Moreover, this model limits the performance of normal listeners and simulates the effects of an impairment by the magnitudes of noise terms added to the ideally processed interaural time and intensity differences of the stimuli.

In Chapter 6, a characterization of the stimuli used in the binaural experiments is given in terms of their interaural phase (time) and intensity differences. Probability distributions for the two difference variables are presented along with an approximate simplified second-order statistical description of the distributions.

In Chapter 7, the model discussed in Chapter 5 and the results given in Chapter 6 are combined to estimate the parameters of the noisy binaural information processing. This leads to prediction equations for narrowband binaural experiments in which stimulus interaural time and intensity characteristics are known.

Chapter 8 presents the predictions of the class of models (represented by the model of chapter 5) under different assumptions concerning the combination of interaural time and intensity differences. An argument is made for a weighted linear combination of the two differences as a near-optimal combination scheme and the one which best agrees with normal and impaired binaural hearing results.

Finally, Chapter 9 discusses the results of the tests and the model in relation to: (1) clinical and academic research on hearing impaired listeners, (2) testing and modelling of binaural interaction in normal listeners and (3) the development of binaural hearing aids. In addition, generalizations and possible extensions of the model to other binaural phenomena are discussed.

CHAPTER 2

PREVIOUS WORK

We begin with a review of binaural phenomena in normal and hearing impaired listeners which are of particular relevance to this study. Specifically, we consider the frequency dependence of narrowband binaural phenomena. In general, we cite results from studies which used narrowband noise stimuli similar to the ones which were used in this study.

In addition, we review past models of binaural interaction and suggest a refinement to such models which unify predictions for lateralization and detection phenomena.

The majority of the studies discussed in this chapter characterized the sensitivity of the binaural system to the different interaural cues by performing discrimination tests. Discrimination ability is often described in terms of a just-noticeable-difference (jnd). A jnd is defined as the difference (along some dimension, e.g., interaural time or intensity) between a reference stimulus and a test stimulus which corresponds to some specified level of performance. Similarly, detection capability is characterized in terms of a signal-to-noise ratio in a signal- plus-noise stimulus which is just noticeably

different from a stimulus with only noise present.

Localization (the apparent source position for an externalized signal) and lateralization (the phenomena related to the laterality of an auditory image perceived to be within the head) ability has been tested by measuring sensitivity to interaural time (fine structure) differences and intensity differences. Lord Rayleigh was the first to suggest that different types of binaural cues are used at different frequencies to effect localization. In his duplex theory of binaural hearing, he proposed that the binaural system localizes on the basis of interaural time differences at low frequencies and interaural intensity differences at high frequencies.

To a first order, this description is still valid today. Mills (1960) compared jnds in interaural phase and intensity of pure tones, relative to a diotic (interauraly identical signals) reference, to minimum audible angles (MAAs) measured from directly in front of a listener in free-field. For frequencies below 6000 Hz, he was able to predict the MAAs obtained from the interaural phase (or equivalently, interaural time) and intensity jnds. For frequencies below approximately 1500 Hz, interaural phase jnds were consistent with observed MAAs, while above 1500 Hz, interaural intensity differences predicted the observed MAAs.

More recently, Domnitz and Colburn (1977) measured interaural time and intensity jnds for a 500 Hz tone at various reference time and intensity differences. In addition, they also measured the subjective lateral position of a 500 Hz tone (with position matching

experiments) for the same set of subjects and reference interaural differences. The interaural time jnds were predicted by a simple model of lateralization which used a Gaussian position variable the mean of which was determined from the lateralization data and the variance of which was determined from the intensity discrimination results. In later work, Stern and Colburn (1978) were able to succesfully predict the same set of lateralization data using a model that explicitly included a description of auditory-nerve activity. This model, referred to as the position-variable model, will be discussed in more detail later in this chapter

The increased detectability of sounds in the background of maskers due to binaural interaction have been tested in the past by measuring the binaural masking level difference (MLD) in several, different interaural signal-to-noise configuration. The MLD is defined as the difference between the threshold of a target signal in the presence of a masker for some "reference" interaural configuration and the threshold of the same signal in a different interaural configuration. The largest such difference in thresholds occurs between a diotic (interaurally identical) signal in the presence of a diotic masker (usually termed NOSO) and the same signal 180 degrees out of phase between the two ears in the presence of the same diotic masker (NOSπ). We chose to test this particular difference in our experiments because (1) it produces the largest difference in signal thresholds and hence, one which we presumed to be the easiest difference to detect by impaired listeners and (2), it has recently been tested on a large number of hearing impaired listeners by several investigators (Lynn et al., 1981 ; Jerger et

al., 1982 ; Noffsinger, 1982). In further discussions, when the term MLD is used, it is with reference to this difference measured in decibels.

Interaural correlation discrimination, while not a classic or frequently measured binaural phenomenon, tests discrimination of a "pure" binaural difference. There are no monaural cues in the stimuli which contaminate the measurement of binaural capability. In the detection experiments, the presence of the target increases the energy of the total stimulus at the target frequency. While these increases are small for normal signal thresholds, it is possible that for impaired listeners (with increased thresholds) these monaural cues would play a larger role in binaural detection experiments.

In addition, Pollack and Trittipoe (1959 a,b) suggested that the interaural cross-correlation provides a direct measure of the perceptual fusion of binaural stimuli. More recently, Lindemann (1982) has proposed that interaural cross-correlation functions (computed in different frequency bands) of sounds received at the two ears provide a measure of the acoustic "spaciousness" of the sounds. Finally, a large number of binaural interaction models compute as their binaural processor output a function which is essentially the interaural cross-correlation of the signals (Colburn and Durlach, 1978).

Note that for all four experiments performed, the reference conditions were diotic stimuli. Sensitivity to interaural time, intensity and correlation differences are best (smallest jnds) when

reference conditions are diotic (Domnitz and Colburn, 1977 ; Kearney, 1979 ; Pollack and Trittipoe, 1959a).Because discrimination performance is best at this reference condition, we thought that impaired listeners (with interaurally symmetric losses) would find this task easiest to perform. Moreover, in terms of natural interactions with the environment, the diotic reference condition (corresponding to straight-ahead sound sources) is the one usually encountered.

A. Binaural Phenomena in Normal Listeners

To date, there exists in the literature a substantial amount of data from experiments related to the frequency dependence of binaural interaction in normal-hearing listeners. A comprehensive review of these studies up to the early 1970s is available in Durlach and Colburn (1978). In this section, we focus on the four experiments introduced above.

i) Interaural Time Discrimination

Klumpp and Eady (1956) measured interaural time using several bands of narrowband noise at various center frequencies. Using a 2-second duration signal presented at levels of 60 - 80 dB SPL (total noise power), they measured an average jnd of 14 usecs for a band of noise ranging from 425 - 600 Hz and a jnd of 62 usecs for a band of noise ranging from 3056 - 3344 Hz.

Interaural time jnds for normal listeners using narrowband noise at center frequencies of 500 Hz (100 Hz wide) and 4000 Hz (500 Hz) were reported by Hawkins (1977) in a study of impaired listeners. At a stimulus level of 85 dB SPL (total noise power), average time jnds were 17 usec for the 500 Hz noise and 61 usecs for the 4000 Hz noise.

McFadden and Pasanen (1976), using narrowband waveforms centered at 500 Hz (100 Hz wide) and 4000 Hz (500 Hz wide), measured average time jnds of 17 usec at 500 Hz and 42 usecs at 4000 Hz.

A relatively small time jnd at high frequencies was measured by Henning (1974) using a 600 Hz wide band of noise centered at 3900 Hz. He reported average time jnds of approximately 20 usecs. The discrepency between the high-frequency results of the latter two and former two studies are most likely due to differences in the low-frequency energy of the different stimuli.

In a more recent experiment concerned with the effect of low-frequency energy in high-frequency time discrimination, Bernstein and Trahiotis (1982) measured interaural time jnds for narrowband noise centered at 4000 Hz as a function of the low-frequency-skirt slopes of the noise. At the steepest slope tested (24 dB/octave, and thus the condition which had the least amount of low frequency energy) the average jnd obtained (at a stimulus level of 70 dB SPL) was approximately 80 usecs.

As is seen in Figure 2.1 (an aggregation of the results reviewed here), sensitivity to interaural time differences for normal listeners is best in the frequency region between 250 - 1000 Hz, gradually increasing to approximately 80 usecs at 4000 Hz. The jnds observed for narrowband noise are consistent with low-frequency time jnds observed for tonal stimuli at frequencies corresponding to the center frequencies of the noise waveforms (Klump and Eady, 1956 ; Durlach and Colburn, 1978).

ii) Interaural Intensity Discrimination

Hawkins (1977), in an ancilllary experiment, measured intensity jnds (using the same narrowband noise as in the time discrimination experiment) for one normal-hearing listener. At 85 dB SPL, a 0.9 dB intensity jnd was measured for the 500-Hz noise and a 0.6 dB intensity jnd was measured for the 4000-Hz noise.

Zurek and Leshowitz (1975), in a study comparing interaural intensity jnds and frequency selectivity, measured interaural intensity jnds for a 250 ms, 100-Hz wide noise centered at 500 Hz. At 60 dB SPL (total noise power), they measured average intensity jnds of 1.5 dB, about a factor of two larger than the jnds reported by Hawkins.

We have not been able to find any other studies which measured interaural intensity jnds of narrowband noise waveforms.

The results presented by Hawkins are consistent with intensity discrimination of tonal stimuli. Intensity discrimination of tone bursts in normals is approximately constant at 0.8 dB for frequencies between 200 and 1000 Hz, grasually decreasing to approximately 0.6 dB at 4000 Hz (Durlach and Colburn, 1978). Results from the two narrowband studies are presented in Figure 2.2.

iii) Interaural Correlation Discrimination

Compared to interaural time discrimination, sensitivity to differences in interaural correlation has received relatively little attention. Due to the paucity of correlation discrimination data, we review wideband correlation data in addition to the single study which has measured narrowband correlation jnds.

Despite the importance of interaural correlation processing in models of binaural hearing, only three papers (Pollack and Trittipoe, 1959 a,b; Gabriel and Colburn, 1981) have directly reported on the ability of listeners to discriminate interaural correlation. In this type of task, the correlation, a measure of the degree to which the signals at the two ears are similar, is varied and a subject is asked to distinguish changes in correlation between a reference correlation value and some test correlation value.

Pollack and Trittipoe (1959 a,b) measured the correlation jnd of wideband (6800 Hz) Gaussian noise for a variety of reference correlations. At a reference correlation of unity (interaurally

identical stimuli), they measured a jnd of approximately 0.04, i.e. discrimination performance was 75% correct when subjects compared perfectly correlated noise (ρ = 1) to a slightly decorrelated noise (ρ = 0.96).

No definitive studies have measured correlation jnds as a function of frequency. Gabriel and Colburn (1981), measured interaural correlation jnds for a 500 Hz narrowband noise waveform as a function of the noise bandwidth. At a bandwidth of 115 Hz, they reported an average correlation jnd of 0.008 and a value of 0.03 for wideband (0 - 4kHz) noise.

iv) Binaural Detection

Although many researchers have performed binaural MLD experiments (see Durlach and Colburn, 1978), few have reported the individual thresholds obtained in the NOSO and NOSπ signal-noise configuration. Since the focus of this study is the binaural "unmasking" ability as evidenced by NOSπ thresholds, the threshold data are discussed (not MLDs). As noted above, NOSO results are measured for comparison and as an upper bound on performance. In the following sections, detection results are reported in units of 10log(E/No).

Hirsch and Webster (1949), measured NOSO and NOSπ detection thresholds using a 250 Hz target masked by three different masker waveforms. For a 50-Hz wide masker centered at 250 Hz, the average NOSO threshold was found to be 6.0 dB and the average NOSπ

threshold was -5.0 dB.

Bourbon (1966), in a study on the effects of masker bandwidth on MLDs, measured NOSO and NOSπ detection thresholds for a 500 Hz target. Using a stimulus duration of 150 msec (with 25 msec rise/fall times) he measured an average NOSO threshold equal to 8 dB and an average NOSπ threshold equal to - 9 dB, for a noise masker bandwidth equal to 130 Hz (approximately equal to a one-third octave noise).

Wightman (1971), in a similar study on the effects of masker bandwidth on the MLD, reported NOSO and NOSπ detection thresholds for an 800 Hz target. With the "heavily filtered" stimuli, he reported an average NOSO threshold of 10 dB and average NOSπ thresholds of -4 dB for an 800-Hz target masked by a 200 Hz wide, 800-Hz centered noise masker.

Most recently, Zurek *et al.* (1983) measured NOSO and NOSπ thresholds for a 4000 Hz tone with various masker bandwidths. For a masker bandwidth of 1000 Hz, he obtained average NOSO thresholds of 14 dB and average NOSπ thresholds of 9.0 dB.

These results are plotted together in Figure 2.3. In generall, the results are in agreement with wideband MLD results reported in other studies (Durlach and Colburn, 1978). As a function of the tonal, target signal frequency in the background of a broadband masking noise, the MLD shows a maximum of approximately 15 dB in the region between 250 to 500 Hz, remaining constant up to approximately 1000 Hz. For frequencies above 1000 Hz the MLD decreases monotonically to approximately 4 dB at 4000 Hz.

B. Binaural Phenomena in Impaired Listeners

In contrast to the experimental results on normal-hearing listeners, relatively little is known about binaural interaction in hearing-impaired listeners, and even less about the frequency dependence of binaural interaction. Results from experiments (up to 1978) on binaural interaction in hearing impaired listeners are reviewed in Durlach et al. (1981).

Although many different clinical tests are employed in the diagnosis of hearing impairments (Davis and Silverman, 1970), the most common description of impaired hearing is the audiogram. For each ear separately, pure tone thresholds relative to normal thresholds are obtained at frequencies spaced one octave apart and plotted versus tone frequency. Impairments are sometimes categorized on the basis of the frequency dependence of the loss. For example, flat-loss listeners are impaired listeners whose threshold levels are elevated by a relatively constant amount at all frequencies, and hence have a relatively flat audiogram.

Current clinical tests can also classify losses in terms of the general underlying physiological impairments. There typically are two such descriptions: conductive losses and sensori-neural losses.

Conductive losses are impairments of the external and middle ear function. These two portions of the auditory system transmit the acoustic signal from the environment to the cochlea (the site of

transduction from mechanical energy into neural firing patterns). Conductive losses are clinically defined by differences between bone-conducted hearing thresholds and air-conducted thresholds (commonly refered to as the air-bone gap). Typically, conductive-loss listeners show normal bone-conducted thresholds but air-bone gaps of approximately 40 - 60 dB (Davis and Silverman, 1970).

Sensori-neural losses are impairments in the inner ear (or cochlear-losses) and neural pathways of the auditory system. Sensori-neural losses are difficult to describe in general and can result in complicated and different impairments.

Hawkins (1977), measured interaural time discrimination from a reference delay of zero usec for narrowband noises centered at 500 and 4000 Hz. Their impaired subjects were 6 listeners with bilaterally symmetric, sensori-neural losses: 2 high-frequency-loss listeners, 2 low-frequency-loss listeners, and 2 flat-loss listeners. Hawkins found that for all impairments there was a substantial degradation of interaural time discrimination that was not simply relatable to the magnitude of the audiometric loss. In particular, both the high-frequency-loss listeners and the flat-loss-listeners had larger than normal time jnds for the low frequency narrowband noise. In addition, Hawkins and Wightman (1980) measured interaural intensity jnds for two of their subjects and found no correlation between interaural time and interaural intensity discrimination. For example, at 4000 Hz, the flat-loss subject with a very abnormal time jnd (approximately 622 usec) had a normal intensity jnd (approximately 0.8 dB).

Subjects for the survey conducted by Hausler et al., (1983) included 39 normals, 17 unilateral or bilateral conductive losses, 7 bilateral sensori-neural losses with good speech discrimination, and 7 bilateral sensori-neural losses with poor speech discrimination. Furthermore, in conjunction with another study on brain stem auditory evoked potentials, the survey also included 26 multiple sclerosis patients, all of whom had normal audiograms and better than 88% speech discrimination.

All of the hearing-impaired subjects (aside from the multiple sclerosis patients) had moderate to severe hearing losses (> 35 dB). The stimuli for all the tests were 1-sec bursts of wideband noise (0.25 - 10 kHz) presented at a level of 65 dB SPL for the normal listeners and 85 dB SPL for the hearing-impaired listeners.

Although most of the tests performed on the subjects in this study used wideband stimuli, Hausler and Colburn also performed additional tests on bilaterally symmetric, sensori-neural loss listeners using one-third-octave bands of noise at center frequencies of 500 and 3300 Hz.

They found that the listener with good speech discrimination (> 92 %) had normal time jnds at both 500 Hz (20 usecs) and 3300 Hz (30 usecs). In contrast, the person with poor speech discrimination gave very abnormal time jnds at 3300 Hz (> 500 usecs) but a near normal time jnd at 500 Hz (30 usecs).

Since the wideband time jnds were near normal (< 40 usecs) for the majority of bilaterally symmetric, sensori-neural loss listeners; regardless of their speech discrimination scores, the above result suggests that there are frequency regions of impaired binaural activity which are apparent only the non-impaired frequency regions are not stimulated.

Each MS subject showed abnormal localization in at least one localization test -- a significant result since all the MS subjects had normal audiograms and normal speech discrimination scores. Another finding (consistent with the findings of Hawkins, 1977) obtained from testing the MS patients was the apparent independence of the binaural system's processing of interaural time and interaural intensity. There were MS subjects with normal intensity jnds but abnormal time jnds, abnormal intensity jnds but normal time jnds, and subjects with both time and intensity jnds abnormal. This suggests (but does not require) different physiological mechanisms for the processing of interaural time and intensity differences.

In addition to these studies, many clinical investigators have tested the efficacy of the MLD as a diagnostic tool for neurological disorders (Noffsinger et al., 1975 ; Olsen et al., 1976 ; Lynn et al., 1981). In a recent study, Noffsinger (1982) measured MLDs of a 500 Hz tone masked by a wideband noise for 180 unilateral and bilateral, sensori-neural loss subjects. Results showed that 46% of the cochlear-loss subjects had abnormal MLDs (defined by Noffsinger as MLDs less than 8 dB) while 76% of the subjects with impairments of the VIIIth nerve had abnormal MLDs. This suggests that sensori-neural impairments have a significant effect on the MLD and

supports the notion of using binaural detection experiments as diagnostic tests.

Jerger et al. (1982) in an exhaustive test of 649 impaired listeners, measured the MLD for a 500 Hz tone masked by a broadband noise. MLDs for 71 bilaterally symmetric (symmetric within 9 dB interaural threshold differences), sensori-neural loss subjects were obtained. The reduction in the MLD was found to be directly proportional to the threshold loss at 500 Hz. For hearing losses of 0 - 20 dB, no significant reduction was observed in the MLDs (approximately equal to 11 dB). For losses in the range from 20 - 40 dB, MLDs were reduced to approximately 7 dB. For losses in the range of 40 - 60 dB, MLDs were essentially non-existent (about 1 dB).

Unfortunately, in both the Jerger and Noffsinger studies, the individual thresholds for the NOSO and NOSπ configurations were not reported and it is hard to determine whether normal MLDs correspond to normal NOSO and NOSπ thresholds. Moreover, it is not clear whether abnormal MLD were a result of increased NOSπ thresholds and normal NOSO thresholds or differential increases in both the NOSO and NOSπ thresholds.

C. Models of Binaural Interaction

Most models of binaural interaction can be described by a block diagram of the form shown in Figure 2.4. Individual models differ from one another in the detailed assumptions about (1) the

peripheral processing of the signals, and (2) the form of the binaural interaction mechanism.

The peripheral transduction of the stimuli usually includes a critical-band filter, the narrow (1/3 octave wide) frequency region over which the peripheral auditory system combines stimuli. Moreover, the peripheral transduction is assumed to be done imperfectly, and is generally degraded by some form of noisy processing. This noisy processing reflects psychophysical evidence of internal "noise" limiting performance in monaural and binaural tasks and physiological recordings of the intrinsically random neural activity. The embodiment of this noisy processing has varied from an additive noise term (Osman, 1971) to a detailed, physiologically consistent description of the stimulus transduction into neural firing patterns (Colburn, 1973).

The binaural interaction portion of the model typically computes the cross-correlation of the signals at the two ears. The embodiment of the cross-correlation operation in different models varies from a functional description (either explicitly (Sayers and Cherry, 1957 ; Osman, 1971) or implicitly (in the calculation of the energy in the difference between the interaural signals in the EC model, Durlach, 1963) to a presumed neural coincidence mechanism which effects an interaural correlation measurement (Jeffress, 1949; Colburn, 1973).

The decision mechanism is assumed to have available to it the two monaural channel outputs and the output of the binaural interaction mechanism. For stimulus configurations in which the

output of the binaural mechanism provides information which improves performance, the decision mechanism is presumed to use the binaural information. Similarly, for stimulus configurations in which the binaural output provides less information than the monaural, the decision process is assumed to use the better monaural channel.

These models have mainly been applied to performance predictions in binaural detection and lateralization experiments. Colburn and Durlach (1978) have extensively analyzed the predictions of the different models and the dependence of these predictions on the different modelling assumptions. With regard to the purpose of this study, instead of concentrating on the success of the predictions in any one of the tasks, we focus on past attempts at relating discrimination and detection tasks within the framework of a single model. Our ability to relate these two tasks will determine to what extent different binaural phenomena can be characterized by results from a small number of "elementary" experiments.

Starting with Webster (1951) and followed by Jeffress et al.,(1956), many researchers have suggested that the increased detectability of signals in configurations with interaural differences is directly related to processes which effect lateralization. Specifically, Webster (1951) hypothesizes that improvements in binaural detection are due to interaural time differences resulting from the addition of interaurally different signals and maskers.

Thus, given a measure of sensitivity to interaural time differences (for example, a measure of the just-noticeable interaural time difference) and a description of the interaural time differences resulting from the addition of a signal to a masker, one can predict that the signal level at threshold is that level required to produce the just-noticeable amount of interaural time difference.

Hafter (1971), in relating a lateralization model to binaural signal-in-noise detection, assumed a binaural decision variable, $\bar{\Delta}$, which was weighted sum of the instantaneous interaural time and intensity differences. No internal noise was explicitly assumed since Hafter was primarily concerned with the relation between the different binaural detection configurations. Using such a model, Hafter was succesful at predicting the dependence of the MLD as a function of signal-to-noise interaural phase configuration, Θ, for values of Θ ranging from 0 to π. Domnitz and Colburn (1976) point out that such a fit is not dependent on the specific model assumed but is a function of the stimulus parameters. In addition, because his binaural decision variable also included the contribution of interaural intensity differences, Hafter's lateralization model, like the model presented by Durlach (1964), is capable of predicting high-frequency MLDs. Previously, models which used only interaural phase differences as the binaural cues (Jeffress et al., 1956) were unsuccesful at predicting high-frequency MLDs.

Note however, that the value of Hafter's binaural decision variable (a sort of compound interaural time difference) calculated at signal-to-noise threshold in the NOSπ configuration is approximately 90 usecs. Clearly, if such a model were to be applied to localization and detection, it would not be able to predict both the observed 10-20 usec time jnds and the observed signal-to-noise thresholds in an NOSπ paradigm.

Another, more recent, model which also combines interaural time and intensity differences is the position-variable model mentioned in the beginning of this chapter (Stern and Colburn, 1978). In its original conception, this model generated a binaural timing display of neural coincidence counts after a fixed interaural delay, τ, between pairs of fibers of the same characteristic frequency. This distribution of coincidence counts is then weighted by the relative number of fibers with the assumed interaural delays and a timing function (designated $L_T(\tau)$) is obtained.

Stern included an analogous interaural intensity function, $L_I(\tau)$, transformed to units of interaural delay so that the two functions could be combined. $L_I(\tau)$ was assumed to be Gaussian in form with a fixed width, W_I and a "mean" equal to $M_I(\Delta\alpha)$, a function dependent on the interaural intensity difference. A position function, $L_P(\tau)$, was then formed from the product of $L_T(\tau)$ and $L_I(\tau)$. The binaural decision variable used in effecting lateralization, $\hat{P}$, was obtained by calculating the centroid of this resultant position function.

To date, this model has not been applied to detection data, but has been quite succesful at predicting subjective lateral-position data and interaural discrimination of time in the presence of noise (Stern and Bachorski, 1983)

In general , if the parameter values of any model of the type discussed in this section are chosen to fit interaural time jnds, the predicted binaural detection thresholds are 15 to 20 dB lower than the observed thresholds (Colburn and Durlach, 1978). Although these two tasks are related and performance may be effected by identical processes, it is not necessarily true that the two are identical tasks for the decision mechanism. In lateralization experiments, the decision is looking based on shifts in the mean value of the binaural variable, while in binaural detection experiments (and in correlation discrimination experiments), the decision is based on changes in the width (or variance) of the binaural variables distribution. In the analysis to follow, important consequences can be seen to follow from these differences.

CHAPTER 3

EXPERIMENTS

We tested four hearing-impaired listeners in four fundamental binaural experiments ; (1) interaural time discrimination, (2) interaural intensity discrimination, (3) interaural correlation discrimination and (4) binaural detection. The same stimuli and the same paradigm were used for all the subjects in all the experiments.

A. Subjects

The two criteria for subject selection were bilaterally symmetric (within 5 dB), sensori-neural hearing loss with no known differences in physiological damage between the two ears. This simplified the issue of signal level presentations (see Durlach, et al., 1981) and allowed us to present signals of equal SPLs at the two ears.

The subjects used in this study were three subjects with moderate-to-severe bilaterally symmetric hearing losses diagnosed as sensori-neural in origin and a Multiple Sclerosis (MS) patient with no hearing loss. Two of these subjects had noise-induced high-frequency losses (both subjects had been regular pistol

shooters) and had audiograms which matched within plus or minus 5 dB at all frequencies tested (cf., Figures 3.1 and 3.2). These subjects were 48 and 65 years old, had good speech discrimination scores and did not wear hearing aids. The third subject was diagnosed as having presbycusis of the strial-atrophy type (Schucknecht, 1974) and showed a relatively flat loss (Figure 3.3) with slightly larger losses at the higher frequencies. This subject was 62 years old, had poor speech discrimination scores, regularly wore a hearing aid in her everyday life, but did not wear it during the experiments performed in this study. The fourth subject had normal hearing as measured in (cf., Figure 3.4) standard audiological tests, but had been diagnosed as having MS. This subject was 30 years old, did not wear a hearing aid, and had normal speech discrimination scores.

In addition to the impaired subjects, we tested two normal listeners, one of whom was the author, the other an undergraduate student , aged 28 and 19 respectively. These subjects were tested in a subset of the conditions tested with the hearing-impaired listeners in order (1) to provide a comparison of the methods used in this study by comparing our normal results to previous data and (2) to fill in "gaps" in the normal data, particularly in interaural intensity and interaural correlation experiments.

B. Stimuli

Stimuli for the discrimination tests were one-third-octave bands of noise centered around five of the frequencies usually tested in pure-tone audiometry (250, 500, 1000, 2000 and 4000 Hz). Stimuli for the detection experiments were the same narrowband noises (as maskers) and pure tones at the corresponding center frequencies (as target signals). All the noise stimuli used in the experiments were synthesized on a computer from sums of random amplitude, random phase cosines (see Appendix I). The digital waveforms were stored on disk and were reconstructed over dual D/A channels (at a 10 kHz sampling rate) followed by lowpass filters with 4.5 kHz cutoff frequencies. In all the experiments, stimulus interval durations of 300 msec (rise-fall times of 15 msec; on-time of 270 msec) and interstimulus interval durations of 100 msec were used.

Stimulus levels at each frequency were held constant across the different binaural tests. These levels were different for each subject, but were above threshold and within the range of comfortable listening (generally 30 dB above a subject's threshold). Table 3.1 lists the stimulus levels for each subject at the five testing frequencies.

The stimulus waveforms presented to the left and right ears in each of the the experiments were constructed according to the methods described below.

i) Interaural Time Discrimination

Interaural time differences less than 100 usecs were created by synthesizing sets of 16 independent waveforms, each with time differences (relative to the zero-standard set) ranging from 2.5 to 47.5 usec in steps of 5 usecs. Thus, a total of 11, 16-waveform sets were generated at each of the five different center frequencies.

Interaural time differences greater than 100 usecs were created by delaying presentation in one D/A channel. This was done for ease of presentation since it was easier to delay the waveform outputs by multiple sample values (at large interaural delays) rather than generate sets of delayed waveforms. Note that this causes a total waveform (envelope (onset) and fine structure) delay. For delays less than 100 usec, only a delay of the fine structure was created.

For any one presentation, the delayed waveform was presented to either the left or right ear in the first interval and then to the opposite ear in the second interval

$$x_L(t) = n_i(t) \qquad x_L(t) = n_j(t - \tau/2)$$

or

$$x_R(t) = n_i(t - \tau/2) \qquad x_R(t) = n_j(t)$$

where τ is the interaural time difference and $n_i(t)$ or $n_j(t)$ is one of the 16 waveforms chosen at random. The ear to which the delay was first presented was chosen randomly with equal probability.

ii) Interaural Intensity Discrimination

Interaural intensity differences were created by attenuating and amplifying one of 64 uncorrelated waveforms chosen at random. For any one presentation, the attenuated waveform was presented to either the left or right ear in the first interval and then to the opposite ear in the second interval

$$x_L(t) = A\,n_i(t) \qquad x_L(t) = B\,n_j(t)$$

or

$$x_R(t) = B\,n_i(t) \qquad x_R(t) = A\,n_j(t)$$

where A and B are the waveform amplitudes such that $20\log(B/A) = \Delta\alpha/2$ and $\Delta\alpha$ is equal to the interaural intensity difference in dB. Since it is possible to perform this task by listening to one ear only, we also attenuated the signals at both ears in each interval by a common, random amount (0 - 10 dB) to confound any monaural intensity cues. A roving level over this range makes it impossible to use monaural intensity cues to perform interaural intensity discrimination for intensity differences less than 6.0 dB. The ear in which the lesser amplitude waveform is first presented is chosen at random with equal probability.

iii) Interaural Correlation Discrimination

Different interaural correlations were created by varying the relative amount of a common signal in one of the two intervals

$$x_L(t) = n_i(t) \qquad x_L(t) = n_j(t)$$

or

$$x_R(t) = \rho\,n_i(t) + \sqrt{1-\rho^2}\,n_j(t) \qquad x_R(t) = n_j(t)$$

where $n_i(t)$ and $n_j(t)$ are uncorrelated waveforms chosen from a set

of 64 uncorrelated waveforms and ρ is the test interaural correlation. Note that regardless of ρ, the average noise power in each ear is equal since all n_i's had the same ensemble average power. The interval in which the test correlation appears is chosen at random with equal probability.

iv) Binaural Detection

A tonal target signal was added to an in-phase noise masker in one of two signal interaural phase conditions. In the first configuration (NOSO), the tone was added to each ear (an interaural phase difference of 0 radians) in one of the two intervals as shown below

$$x_L(t) = n(t) + S(t) \qquad x_L(t) = n(t)$$

or

$$x_R(t) = n(t) + S(t) \qquad x_R(t) = n(t)$$

where s(t) is the tone target and n(t) is from the set of 64 uncorrelated waveforms used in the correlation and intensity discrimination experiments. In the second configuration (NOSπ), the tone was added to one ear and subtracted from the other (an interaural phase difference of π radians) in one of the two intervals

$$x_L(t) = n(t) + S(t) \qquad x_L(t) = n(t)$$

or

$$x_R(t) = n(t) - S(t) \qquad x_R(t) = n(t)$$

In both configurations, the interval which contained the target tone was chosen at random with equal probability.

C. Procedure

Subjects responded via push-button response boxes with no fixed response-interval duration in a two-interval, two-alternative-forced-choice (2I,2AFC) paradigm with feedback. In such a paradigm, temporally ordered pairs of stimuli are presented and the subject is asked to indicate in which interval an auditory "event" appeared. For discrimination experiments, such an event is the test difference along some dimension which must be distinguished from a reference difference. For detection experiments, such an event is the presence of a target sound which must be distinguished from a masking sound alone. Typical runs of such presentations lasted from 15 to 20 minutes.

Hence, for a particular stimulus attribute and reference condition, a plot of percent correct performance versus several different test conditions was obtained. Percent correct was plotted in logit units and a weighted, minimum-chi-square fit (see Appendix II) was used to characterize the curve. From such plots, a subject's discrimination ability was characterized by a just-noticeable difference (jnd), which was defined as the difference between the reference condition and test condition corresponding to 75% correct discrimination. Similarly, a subject's detection capability was characterized by a threshold signal-to-noise ratio, which was defined as the signal-to-noise ratio which corresponds to 75% correct detection.

Representative psychometric functions from both normal and impaired listeners are presented in Figures 3.5 - 3.6.

Sequential Testing Rule

The method outlined in this section and discussed in detail in Appendix II (a draft of a paper) was motivated by a desire to reduce the number of observations at extreme stimulus values (stimulus values corresponding to performance levels substantially different from a desired performance level) in a fixed-number-of-trials (FNOT) procedure.

The FNOT procedure is generally not efficient, particularly with hearing impaired listeners. A typical experiment with this method of testing requires estimation of performance level at several stimulus values. Performance estimates are usually obtained by selecting a particular stimulus value which is fixed throughout the run, presenting a specified, fixed number of trials, recording responses and calculating a percent correct at the end of the run. A pyschometric function is then constructed from 3 to 5 such estimates at several stimulus values bracketing the stimulus value corresponding to the desired performance level. It is not a priori clear to the experimenter what stimulus values will produce a suitably sampled psychometric function. Hence, in a FNOT procedure, there will necessarily be cases where a considerable number of trials are used to estimate performance at extreme stimulus values. This uncertainty about the range is especially important in the testing of hearing impaired listeners since the range of suitable

stimulus values can vary significantly from subject to subject, requiring a new stimulus range determination for each subject tested.

Extreme stimulus values correspond to nearly perfect or chance performance. In each case, after the first 5 to 10 trials it is usually apparent to both the subject and the experimenter that the stimulus value being used is either very easy or very hard to discern. Intuitively, in order to save time and preserve subject vitality, the experimenter should stop the run without presenting the remaining trials. However, the FNOT procedure requires the continued presentation of all the trials in the run. Practically, an experimenter often implements an arbitrary criterion (e.g., if a subject has 10 consecutive correct responses, then stop) in order to terminate such runs early.

In Appendix II, we formalize the above intuitive notions about reducing experimental data collection into a systematic, well-defined, objectively implemented rule.

CHAPTER 4

EXPERIMENTAL RESULTS

Results from the four binaural experiments are presented and discussed in relation to individual subject's hearing impairments and to normal binaural hearing.

A. Normal Listeners

i) Interaural Time Discrimination

Average results for the two listeners at 250, 1000 and 2000 Hz are presented in Figure 4.1, along with results from the studies reviewed in Chapter 2. Observed interaural time jnds (20 usecs at 250 Hz, 15 usecs at 1000 Hz and 70 usec at 2000 Hz) are in good agreement with results from previous work.

ii) Interaural Intensity Discrimination

Average interaural intensity jnds versus noise center frequency are presented for the two listeners in Figure 4.2 along with results from the studies reviewed in Chapter 2. For both subjects, the interaural intensity jnds obtained (0.8 dB at 250 Hz, 0.9 at 500 Hz, 0.8 at 1000 Hz, 0.7 at 2000 Hz and 0.6 at 4000 Hz) are consistent with values obtained by Hawkins (1977), as well as the frequency dependence observed (slightly smaller intensity jnds at high frequencies relative to intensity jnds at low frequencies).

iii) Interaural Correlation Discrimination

Figure 4.3 presents average interaural correlation jnds from a reference correlation of unity versus noise center frequency. Also plotted is the one point at 500 Hz obtained from the study by Gabriel and Colburn (1981). Interaural correlation jnds are best at low frequencies (approximately 0.01), increasing gradually to 0.05 at 4000 Hz.

iv) Binaural Detection

Figure 4.4 presents average NOSO and NOSπ detection thresholds versus target (or noise center) frequency, along with the results from the studies reviewed in chapter 2. Except at 500 Hz, where the NOSπ threshold reported for our normal listeners are approximately 5 dB higher than the threshold obtained in a previous study, our threshold measurements are consistent with previous binaural detection thresholds.

Generally, the normal data from this study is in agreement with results from past studies on narrowband, binaural discrimination and detection. It is important to note that due to constraints on time, the testing of normal listeners was not as extensive as the testing of the impaired listeners and was only intended to fill gaps in results from previous studies and provide a consistency check between past results and the results of this study.

B. Impaired Listeners

i) Interaural Time Discrimination

Results from the two high-frequency loss subjects are shown in Figures 4.5 and 4.6 . Despite their audiometric similarity (Figures 3.1 and 3.2), they had different sensitivities to interaural time differences. At low frequencies (250 - 1000 Hz) subject FG had time jnds ranging from 30 - 50 usecs (Figure 4.5), while subject DH had jnds on the order of 60 - 100 usecs (Figure 4.6). At higher frequencies (2000 and 4000 Hz), subject FG had time jnds of 80 and 100 usec while DH showed a marked loss of sensitivity with jnds equal 550 and 600 usecs.

Note that subject FG has near-normal (Figure 4.1) sensitivity to interaural time difference at high frequencies where his loss is most severe. In contrast to FG, subject DH has degraded interaural time sensitivity at both low an high frequencies.

Results from the subject with a flat hearing loss, subject VF, (Figure 4.7) show no sensitivity to interaural time differences (up to 1 msec, the largest time difference tested) except at 500 Hz where the jnd is 100 usec. Subsequent detailed measurements of this subject's thresholds near 500 Hz (at 10 Hz increments from 400 to 600 Hz) are consistent with her audiogram (Figure 3.3) and show no such region of good monaural hearing in either ear. This subject appears to have an "island" of sensitivity to interaural time differences at 500 Hz.

Finally, results from the MS listener, subject CS, showed no sensitivity (up to 1 msec) to interaural time differences at any frequency tested (Figure 4.8). Recall that this subject had a normal audiogram at all frequencies.

The time jnds obtained for the two high frequency loss listeners are in good agreement with the results of Hawkins (1977), except for subject DH at 4000 Hz. For his two high-frequency loss listeners, Hawkins reports time jnds ranging from 85 to 123 usec using the 4000 Hz centered noise. Subject DH has a time jnd of 600 usecs at 4000 Hz, a factor of 6 worse than the average time jnd reported by Hawkins at this frequency.

The time jnds of subject VF are similar to the time jnds of the two low-frequency loss listeners (no observable time jnds) tested by Hawkins. The two flat-loss listeners in Hawkins's study had smaller time jnds than those of subject VF (43 usecs at 500 Hz and 600 usec at 4000 Hz).

ii) Interaural Intensity Discrimination

Interaural intensity jnds measured from the two high-frequency loss subjects are shown in Figures 4.9 and 4.10. They indicate similar sensitivities to interaural intensity differences. Both subjects had larger than normal intensity jnds ranging from 2.5 - 3.0 dB at low frequencies (< 1000 Hz), decreasing to 2.0 - 2.5 dB at the higher frequencies. The low frequency intensity jnds are a factor of 3 - 4 worse than normals (Figure 4.2), even though both subjects had normal hearing at those frequencies. At higher frequencies, where both subjects have severe losses, the intensity jnds were a factor of 4 - 5 worse than normal.

Results from the flat-loss listener are shown in Figure 4.11. This subject's low-frequency intensity jnds are between 3.0 and 4.5 dB. At high frequencies, her intensity jnds increased to a maximum of 8 dB at 4 kHz. At all frequencies, this subject's intensity jnds were significantly worse (a factor of 6 - 10 larger) than normal.

Intensity discrimination results for the MS subject are shown in Figure 4.12. In contrast to interaural time discrimination, subject CS, the MS patient, showed some sensitivity to interaural intensity differences at 500 Hz and 1000 Hz. Since the jnds at other frequencies are near 6.0 dB, it is possible that this subject used monaural cues to perform interaural intensity discrimination (see below). Thus, despite a normal audiogram, subject CS has poor (a factor of 6 - 8 larger than normal) interaural intensity jnds.

The random, 10 dB roving level added to each interval of this experiment precluded the uses of monaural intensity information to effect performance up to an interaural intensity difference of approximately 6.0 dB (assuming a 2I, 2AFC paradigm). At and above this difference, it is possible to perform better than 75% correct using monaural intensity changes even with the 10 dB roving level. Thus, except at 4000 Hz for subject VF and at 250, 2000 and 4000 Hz for subject CS, interaural intensity discrimination could not have been mediated by monaural intensity cues.

Unfortunately, Hawkins did not measure the intensity jnds of his high-frequency loss listeners. However, he did measure the intensity jnd for one of his flat loss listeners and obtained a near-normal (0.8 dB) intensity jnd using the high-frequency noise waveform. This result is not consistent with our flat loss listener's 8 dB intensity jnd at 4000 Hz.

iii) Interaural Correlation Discrimination

Results from the two high-frequency loss listeners are shown in Figures 4.13 and 4.14. Despite their audiometric similarity, the two high-frequency loss subjects exhibited dissimilar sensitivities to interaural correlation differences. Subject FG has relatively constant jnds equal to approximately 0.25 (a factor of 5 - 10 larger than normal) at the middle frequencies (500, 1000 and 2000 Hz), decreasing to a near normal 0.05 at 250 Hz and to 0.1 at 4000 Hz. Subject DH has no sensitivity to interaural correlation (subject could not distinguish between correlated and uncorrelated noise) at

250 Hz (Figure 4.14). Moreover, this subject's sensitivity is worse at the low frequencies and best at the high frequencies, a result which does not seem to be consistent with either his audiogram or his time discrimination data.

As in the time discrimination experiment, subject VF showed no sensitivity to interaural correlation except at 500 Hz where we measured a jnd of 0.7 (Figure 4.15). This suggests that a common mechanism may be processing interaural time and correlation differences at low frequencies.

As in interaural time discrimination, subject CS showed no sensitivity to interaural correlation at any frequency (Figure 4.16). Recall that subject CS showed no sensitivity to interaural time differences at any frequency. The results from this subject further support the notion that interaural time and correlation processing are related.

In general correlation discrimination proved to be a difficult task for subjects to perform. The training for this task took longer than in other tasks and this task was reported as "annoying" and at times confusing by all of the subjects. This is consistent with reports of correlation discrimination by normal listeners as reported by Gabriel and Colburn (1981) and Widjadja (1982). It should be noted that in the latter study, one normal listener was unable to discriminate perfectly correlated noise from uncorrelated noise at 500 Hz even after a considerable amount of training.

vi) Binaural Detection

Detection thresholds for both the NOSO and NOSπ conditions are shown in Figure 4.17 and 4.18 for subjects FG and DH. Both show elevated (5 - 10 dB higher than normal) thresholds at all frequencies. Furthermore, both the NOSO and NOSπ thresholds are elevated by roughly equal amounts. More precisely, NOSO thresholds for subject FG are approximately 7 - 8 dB higher than normal and NOSπ thresholds are approximately 8 - 10 dB higher than normal---an unexpected result, particularly at low frequencies where this subject had normal, monaural thresholds. NOSO thresholds for subject DH are also approximately 8 - 10 dB higher than normal as are the NOSπ thresholds. As with subject FG, the elevated NOSO thresholds, particularly at the low frequencies, is surprising. Hence, subjects FG and DH have normal MLDs or, equivalently, a normal amount of advantage in listening to a target plus masker with interaural differences, even though they have elevated detection thresholds.

As shown in Figure 4.19, results from subject VF, the flat-loss listener, show a different pattern of threshold elevation. She had near normal NOSO thresholds (within 2 - 3 dB) but elevated (a 10 - 12 dB increase above normal) NOSπ thresholds at almost all frequencies (and hence, no MLDs). The one frequency which had the largest difference between the NOSO and NOSπ thresholds was 500 Hz, but this appears to be due to an elevated NOSO threshold rather than a reduced NOSπ threshold. If we had been measuring only the MLD, we might have incorrectly attributed the presence of the MLD to the

"island" of interaural time sensitivity this subject seems to have at 500 Hz.

The results from the above three subjects are in agreement with the results of Jerger (1982). Both subjects FG and DH have normal MLDs (albeit due to elevated NOSO thresholds) and near-normal hearing at 500 Hz (Figures 3.1 and 3.2), while subject VF has a abnormal MLDs and monaural threshold loss greater than 40 dB at all frequencies (Figure 3.3).

Finally, as is seen in Figure 4.20, subject CS has both elevated NOSO thresholds and NOSπ thresholds; furthermore, unlike the high-frequency loss listeners, subject CS showed almost no advantage in detecting out-of-phase signals relative to in-phase signals. Given the lack of any sensitivity to time and the degraded sensitivity to intensity differences, it is not surprising that the NOSπ configuration offers no listening advantage to subject CS.

C. Binaural Audiograms

In this section, we present a new method of displaying the results of interaural discrimination experiments on hearing impaired listeners. This method is similar to current audiometric descriptions and hence, we will refer to the new plots as binaural audiograms.

Binaural audiograms are plots of observed interaural jnds in decilog units re normal jnds. Figures 4.1 - 4.3 display the normal discrimination jnds used in the following development. We have chosen a log scale in order to conveniently plot the increased range (typically 1 to 2 orders of magnitude larger than normal) of time and correlation jnds encountered in testing hearing impaired listeners.

For interaural time discrimination, the binaural audiogram is constructed by plotting

$$10 \log \left[(\Delta\tau)_o / (\Delta\tau)_{o;\,\text{NORMAL}} \right]$$

versus the center frequency of the stimulus. Figure 4.21 plots the interaural time audiograms for all the subjects tested in our study. Note that the time audiogram clearly illustrates features which are not readily apparent in the previous plots. In particular, subject FG has a low-frequency time "loss" (in his region of normal, monaural hearing) and normal, high-frequency time discrimination (in the region of his loss). In contrast, subject DH (the other high-frequency loss subject) has an approximately constant time loss as a function of frequency, a characteristic not easily seen in Figure 4.6 .

Since interaural intensity jnds are already expressed in decibels and binaural audiograms are plots of "dB loss" re normal jnds, the intensity audiogram consistent with the time and monaural audiograms is a plot of

$$(\Delta\alpha)_o - (\Delta\alpha)_{o;\,\text{NORMAL}}$$

versus the stimulus center frequency. Figure 4.22 presents the intensity audiograms for the four subjects of this study. Note the

relatively constant intensity loss of the two high-frequency loss subjects. Furthermore, subjects VF and CS exhibit a high-frequency interaural intensity discrimination "loss", a pattern of loss highlighted by the intensity audiogram.

Finally, Figure 4.23 presents the correlation audiograms of the four subjects. Interaural correlation jnds were converted to dB re normal jnds by the transformation

$$10 \log \left[(\Delta\rho)_0 / (\Delta\rho)_{0;\,\text{NORMAL}} \right]$$

Note that subjects FG and DH show a low frequency correlation "loss" which resembles their time loss at low frequencies.

In summary, binaural audiograms (1) highlight patterns of loss which are not readily apparent in conventional displays, (2) incorporate the increased range of jnds observed in hearing impaired listeners and (3) provide a description of binaural performance which is similar to current audiometric descriptions of monaural hearing loss.

Clearly, binaural audiogram descriptions are dependent on what is termed "normal" data. However, the basic utility of the binaural audiograms in exposing patterns of impaired binaural hearing is independent of any specific set of normal data assumed. Hence, we feel that binaural audiograms are an informative display of binaural discrimination "loss" in hearing impaired listeners and should become a standardized method of reporting impaired discrimination results.

D. Relationships Among the Four Tasks

Scatter plots (Figures 4.24 - 4.29) of the results from the four binaural tests are presented for all possible combinations of pairs. Each scatter plot combines data from different frequencies and for the different subjects. Only measured data points (i.e., correlation jnds less than unity and time jnds less than 1000 usecs) are plotted and used in the calculation of the sample correlations.

The sample correlations, r, calculated for the various pairs are presented below :

$$r(\Delta\tau\ ,\ \Delta\alpha\ ) = -0.28\ ,\ n = 11$$
$$r(\Delta\tau\ ,\ \Delta\rho\ ) = -0.03\ ,\ n = 10$$
$$r(\Delta\tau\ ,10\log E/N_o) = 0.60\ ,\ n = 11$$
$$r(\Delta\alpha\ ,\ \Delta\rho\ ) = 0.41\ ,\ n = 10$$
$$r(\Delta\alpha\ ,10\log E/N_o) = -0.38\ ,\ n = 11$$
$$r(\Delta\rho\ ,10\log E/N_o) = -0.20\ ,\ n = 10$$

For n = 10, the critical values of r at 95% confidence levels are $r < -0.63$ and $r > 0.81$. For n = 11, they are $r < -0.60$ and $r > 0.60$. Thus, none of the sample correlations are significantly different from 0 at the 95% confidence level.

The low (and negative) sample correlation between correlation jnds and NOSπ detection thresholds is surprising in light of the believed dependence of binaural interaction on correlation processors (see Chapter 2). However, if we express $(\Delta\rho)_o$ in units

of a signal-to-noise ratio which causes an equivalent amount of decorrelation in a masker for an NOSπ signal configuration by the transformation :

$$(\Delta\rho)_o' = \log(WT) + 10\log \frac{\Delta\rho}{2-\Delta\rho},$$

we compute a new sample correlation equal to 0.67. This is still not significant, but it is larger than what it was before (and positive instead of negative).

The above analysis suggests that correlation values should be expressed in units similar to signal-to-noise ratios in detection experiments. This need is not only based on the increased correlation obtained above by such a transformation. In correlation discrimination experiments from a reference correlation of unity, one typically presents test correlation values ranging over two orders of magnitude (0.9 to 0.999) in order to sample a psychometric function. The range spanned by the transformed correlation value (see equation above), is less than a factor of three. Note that Pollack and Trittipoe (1959 a,b) plotted their results in terms of equivalent common-to-uncommon noise ratios rather than correlation.

Scatter plots of the results from the four binaural tests and monaural threshold losses are presented in Figures 4.30 - 4.33. Each scatter plot combines data from different frequencies and for different subjects. Only measured data points are plotted and used in the calculation of the sample correlations.

The sample correlations, r, calculated for the various tests are

$$r(\Delta\tau, HL) = 0.50, \quad n = 11$$

$$r(\Delta\alpha, HL) = -0.10, \quad n = 15$$

$$r(\Delta\rho, HL) = -0.08, \quad n = 10$$

$$r(10\log E/N_0, HL) = 0.29, \quad n = 20$$

For n = 15, the critical values of γ at the 95% confidence levels are $\gamma < -0.59$ and $\gamma > 0.45$. For n = 20, the critical values are $\gamma < -0.19$ and $\gamma > 0.66$. None of the results from the four binaural tests appear to be correlated with the measured monaural hearing losses.

CHAPTER 5

A MODEL OF BINAURAL INTERACTION

In this chapter we introduce a general model of binaural interaction in an attempt to : (1) unify interaural time and intensity discrimination phenomena with binaural detection phenomena in normal and impaired listeners; and (2) provide a simple characterization of binaural hearing on the basis of interaural time and interaural intensity processing. With this goal in mind, the model presented in this study is not a final model and is described in a way that allows alternate assumptions to be investigated. It is a working hypothesis that serves as basis for the development and modification of existing models of binaural interaction.

A. Outline of the Model

The basic thrust of the model is to characterize binaural interaction as decisions based on imperfect estimates of interaural time differences and interaural intensity differences. The estimation process is assumed to be intrinsically stochastic (or noisy) and limited in its temporal tracking capability. The use of these imperfect difference estimates is assumed to be ideal subject

to a specific combination rule.

The parameters of the model are estimated from the performance of the individual impaired subjects in interaural time and intensity discrimination experiments. Although the model can be formulated in either continuous time or discrete time, we have chosen a discrete time formulation in order to simplify the calculations. No attempt has been made to address bandwidth effects and individual frequency bands are assumed to be processed separately.

As discussed in Chapter 2, a general problem with models of binaural interaction is their inability to predict both lateralization and detection performance with the same set of parameter values. A possible resolution to this problem is an additional mechanism which reduces the variability of the binaural statistic without changing the mean value of the statistic. A mechanism which achieves this is an averager (or lowpass filter) of binaural differences. As will be seen in this chapter, the incorporation (or inclusion) of this mechanism in a general model of binaural interaction appears to make predicted NOSπ thresholds consistent with predictions based on observed discrimination jnds.

Evidence for such a mechanism is present in several studies (Blauert, 1972 ; Perrot and Musicant, 1977), most recently in a series of papers by Grantham (1980) and Grantham and Wightman (1980) concerned with the measurement of the binaural system's ability to follow time varying interaural differences. For interaural correlation differences about zero correlation, they measured cutoff frequencies of 5-8 Hz for a 500 Hz-centered narrowband noise. At a

noise center frequency of 1000 Hz, they measured an 8-15 Hz cutoff frequency, and at 2000 Hz, they measured a cutoff frequency of approximately 18-25 Hz. The increase in cutoff frequencies is roughly proportional to the center frequency of the noise and suggests a constant ratio of peripheral-filter bandwidth to low-pass filter cutoff frequency.

B. Elements of the Model

Figure 5.1 illustrates a block diagram of one frequency-band section of the binaural portion of the model. The assumptions of the model are:

1. The stimulus waveforms at each ear are filtered with a rectangular, 1/3-octave bandpass filter of width Wcb ;

2. The binaural system processes only a 300 msec segment of the signal for each decision. Equivalently, the effective duration of the stimulus is limited to 300 msec.

3. A temporal sequence of instantaneous interaural time and interaural intensity samples (τ_i and α_i) are obtained from the filtered stimuli at time intervals equal to the inverse of the peripheral filter bandwidth (Wcb^{-1}).

4. The interaural time and intensity estimates are corrupted by independent, zero-mean additive Gaussian noise terms of fixed level. The noise levels in each band and each interaural difference are specified by the standard deviations of the noise ($\sigma_{\tau I}$ and $\sigma_{\alpha I}$), and are the only free parameters of the model.

5. Both sequences of corrupted interaural estimates are separately averaged over K samples. Individual estimates of τ_i and α_i are not available nor are running averages. Each average estimate, $\bar{\tau}$ and $\bar{\alpha}$ (available every K samples) is independent of the others. Although K is a parameter of the model, it is not considered a free parameter in each frequency band. At most, we will consider different Ks for interaural time and intensity averaging.

6. The two averaged interaural estimates can be approximated as Gaussian random variables and are available as separate inputs to an ideal decision mechanism.

7. Two monaural channels are available to the ideal decision mechanism which, in the context of this study, serve to limit the predicted NOSπ thresholds to be no worse than the monaural thresholds.

C. Comments

The first four elements are not significantly different from the sort of assumptions included in most models of binaural interaction (Colburn and Durlach , 1978). The first two assumptions are irrelevant to the present study (we used only one-third-octave bands of noise and a duration of 300 msec), and are stated for completeness.

The third assumption is made on the basis of the characterization of a narrowband signal n(t) of bandwidth W by

$$n(t) = A(t) \cos [2\pi f_o t + \varphi(t)]$$

where A(t) is equal to the envelope function, $\varphi(t)$ is equal to the phase function and fo is the center frequency of the narrowband signal (Wozencraft and Jacobs, 1965). When n(t) is a Gaussian noise function, A(t) is a stochastic function with time samples which are Rayleigh distributed random variables and $\varphi(t)$ is a stochastic function with time samples which are uniformly distributed in the interval between 0 and 2π (Davenport and Root, 1958). Furthermore, independent time samples of both A(t) and $\varphi(t)$ occur every W^{-1} seconds (the first time instant when the autocorrelation functions of A(t) and $\varphi(t)$ equal zero) and completely describe the stochastic functions A(t) and $\varphi(t)$ (Van Trees, 1968). Thus, the samples of the interaural time (phase) difference

$$\tau_i \triangleq \frac{\varphi_R(t_i) - \varphi_L(t_i)}{2\pi f_o}$$

and interaural intensity difference

$$\alpha_i \triangleq 20 \log \frac{A_R(t_i)}{A_L(t_i)}$$

(where t_i = i/Wcb) are assumed to completely describe the interaural time and intensity difference functions (Footnote 1).

The fourth assumption is made in order to allow independent characterization of the imperfect interaural time and intensity processing. This assumption is both simple and applicable to various types of hearing impairments. Moreover, the additive noise term is presumed to characterize the combined noisy processing of the peripheral and central portions of the auditory system.

The fifth, key assumption is the additional mechanism argued for in Chapter 2, Section C. An averaging mechanism reduces the variability of the interaural difference statistics in binaural detection and correlation discrimination experiments without affecting the predictions of the interaural difference statistics in interaural time and intensity discrimination experiments. Initially, for ease of presentation calculation, we assume equal Ks (or equal temporal tracking capability) for both interaural time and interaural intensity processing. In chapter 8, we will show that different averaging Ks for the interaural time and intensity estimates provide a better fit to observed results.

The last assumption allows us to explore various combinations, including the optimal combination, of interaural time and intensity differences. This exploration is not only relevant to modelling in normal listeners, but is particularly important in modelling the binaural hearing of impaired listeners, where one of the interaural

difference measures may be so degraded as to be of little use in providing binaural information about the stimuli. Without a model which separates the interaural time and intensity processing and defines the combination of the two interaural differences, it is not clear from observed interaural time and intensity jnds what the relative usefulness of the two cues are in a given binaural task.

This model is similar to the one proposed by Ito et al., (1982) (1982) in a study of masked interaural time discrimination. Their model can be considered a special case of the model presented here in that they assumed no interaural intensity processing and a specific linear combination of the interaural phase observations. Moreover, the averaging of their interaural phase difference samples was explicitly performed since they assume that mean interaural phase differences are used in forming the decision variable.

Similarly, Hafter's lateralization model (described in Chapter 2) can also be considered a special case of the general model in that he assumed no temporal averaging of the interaural differences and a specific linear combination of the interaural time and intensity differences.

D. Estimation of the Model Parameters

As stated earlier, the averager reduces the number of independent interaural difference samples by averaging a fixed number, K, of these samples. From the Grantham studies, the number K seems to be constant across different center frequencies and is

approximately equal to 20. Thus the only free parameters of the single-critical-band model are the internal noise levels, $\sigma_{\tau I}$ and $\sigma_{\alpha I}$, in each of the binaural difference processors.

The most direct way of estimating these parameters is by matching model predictions to results from interaural intensity and interaural time discrimination experiments. In general, results from any two binaural experiments could be used to estimate the model parameters; however, other binaural experiments (e.g. correlation discrimination and detection) generally produce changes in both the interaural time and intensity differences (see chapter 6).

Further, using stimuli with fixed (non-random) interaural differences in interaural discrimination experiments of this type, τ_i and α_i can be considered as statistics with means equal to the stimulus interaural differences and variances equal to zero. Thus, the only limitations on performance are the additive internal noise terms.

In the following sections, using standard techniques of communication theory (Van Trees, 1968), we will relate $\sigma_{\tau I}$ and $\sigma_{\alpha I}$ to the interaural difference jnds, $(\Delta\tau)_0$ and $(\Delta\alpha)_0$. The form of this relationship depends on the way in which the interaural time and intensity difference estimates are combined prior to the decision mechanism.

i) Separate Time and Intensity Differences

With the assumption that each of the averaged interaural difference estimates ($\bar{\tau}$, $\bar{\alpha}$) is individually available to the ideal decision mechanism Figure 5.2 (a), it follows that (see Appendix III)

$$\sigma_{\alpha I} = \sqrt{\frac{2K}{\nu}} \, (\Delta\alpha)_0 \qquad (5.1\ a)$$

and

$$\sigma_{\tau I} = \sqrt{\frac{2K}{\nu}} \, (\Delta\tau)_0 \qquad (5.1\ b)$$

where ν = number of independent samples of $\bar{\alpha}$ or $\bar{\tau}$ obtained during the stimulus duration, T, (or 300 msec, whichever is shorter) and is given by

$$\nu = \frac{W_{CB}\,[\min(T,\ 300\ msec)]}{K}$$

ii) Weighted Sum of Interaural Differences (SID)

As an illustration of the way in which these relationships change for different mixing assumptions, one combination rule (which has been suggested as the variable underlying lateralization perception, see Chapter 2) is a fixed, weighted sum of the two interaural differences (Figure 5.2 (b)). The fixed weight is represented here by the parameter b and turns out to be $((\Delta\alpha)_0)/((\Delta\tau)_0)$, the inverse of the time-intensity trading ratio.

Given this assumption, there is effectively only one noise term, which is related to the interaural intensity jnd by

$$\sqrt{\sigma_{\alpha I}^2 + b^2 \sigma_{\tau I}^2} = \sqrt{\frac{2K}{\gamma}} \, (\Delta\alpha)_0$$

(5.2 a)

or, equivalently, from the interaural time jnd by

$$\sqrt{\sigma_{\alpha I}^2 + b^2 \sigma_{\tau I}^2} = \sqrt{\frac{2K}{\gamma}} \, b \, (\Delta\tau)_0$$

(5.2 b)

Since the left-hand-sides are the same in these equations, it is clear that b must be equal to $((\Delta\alpha)_0)/((\Delta\tau)_0)$, the ratio of the interaural intensity jnd to the interaural time jnd. Moreover, the values of $\sigma_{\alpha I}$ and $\sigma_{\tau I}$ in this sort of combination is less than the values of $\sigma_{\alpha I}$ and $\sigma_{\tau I}$ assuming no combination prior to the decision mechanism. This has consequences for the predictions of the two assumptions presented in chapter 8. In addition, note that the SID rule is still a two-parameter model. For each critical band, we must specify b and $\sqrt{\sigma_{\alpha I}^2 + b\sigma_{\tau I}^2}$.

The parameters of each narrowband portion of the model can be specified by predicting the noise level estimates from observed interaural time and intensity jnds at each of the five frequency bands tested. Thus, we now have a simple model of binaural interaction which allows us (1) to match the frequency dependence of interaural time and intensity jnds in normal and impaired listeners, and (2) to predict performance in other binaural hearing tasks with

no additional assumptions or parameter choices.

It is important to realize that the theoretical predictions are independent of (1) whether the averaging mechanism is placed before or after the noisy processing and (2) that in the case of equal Ks for interaural time and intensity averaging, predictions are independent of whether the combination of the two interaural differences occurs before or after the averaging. Although the values of the processing noise variances would change for different orders, the order of the operations is not important (because the operations following the extraction of the interaural difference estimates are linear).

CHAPTER 6

CHARACTERIZATION OF STIMULUS INTERAURAL DIFFERENCES

According to the model in Chapter 5, interaural time and intensity differences are extracted from the stimulus, corrupted, averaged, and then used as observations for an ideal decision mechanism. Thus, given a specification of the corruption (i.e., additive noise terms) and the averaging, the predictions of the model for a given binaural task can be calculated from the interaural intensity and time (or phase) differences present in the stimuli at the two ears.

In this chapter, we present the statistics of interaural intensity and interaural phase differences for the stimuli used in the correlation discrimination and binaural detection experiments. Using the method outlined by Domnitz and Colburn (1976), we obtained analytic expressions for the instantaneous interaural intensity and interaural phase differences. The expressions proved too intractable to evaluate analytically at intermediate values of correlation and signal-to-noise ratio; however, they were used in the numerical calculations and for characterizations of the differences at limiting values of correlation and signal-to-noise ratio.

A. Analytic Evaluation of Interaural Differences

i) Correlation Discrimination Stimuli

In the correlation discrimination experiments, the stimuli at the left ear, $\mathrm{Re}[\chi_L(t)]$, and at the right ear, $\mathrm{Re}[\chi_R(t)]$, can be described as complex waveforms of the form

$$\chi_L(t) = N_1(t)\, e^{j[2\pi f_0 t + \varphi_1(t)]} \qquad (6.1a)$$

$$\chi_R(t) = \rho\, \chi_L(t) + \sqrt{1-\rho^2}\, N_2(t)\, e^{j[2\pi f_0 t + \varphi_2(t)]} \qquad (6.1b)$$

where fo is the center frequency of the noise, $N_1(t)$ and $N_2(t)$ are Rayleigh stochastic time functions (i.e., functions with Rayleigh distributed sample values), and $\varphi_1(t)$ and $\varphi_2(t)$ are uniform stochastic time functions (i.e., functions with uniformly distributed sample values). The correlation time (i.e., the time instant at which the autocorrelation function first equals zero) for all the functions is equal to the inverse of the noise bandwidth.

Forming the interaural complex ratio of the two waveforms, we get

$$I(t) = \frac{x_R(t)}{x_L(t)}$$

$$= \rho + \sqrt{1-\rho^2}\,\frac{N_2(t)}{N_1(t)}\,e^{\,j\,[\varphi_2(t)-\varphi_1(t)]} \qquad (6.2)$$

Since $\varphi_1(t)$ and $\varphi_2(t)$ are both uniformly distributed in the interval from $-\pi$ to π and the phase is circular in 2π, we have that $\varphi_2(t) - \varphi_1(t) = \varphi(t)$, where $\varphi(t)$ is uniformly distributed from $-\pi$ to π.

Thus, at any time instant, I(ti) = I is a complex random variable given by

$$I = \rho + \sqrt{1-\rho^2}\,\frac{N_2}{N_1}\,e^{\,j\varphi} \qquad (6.3)$$

where N_1 and N_2 are independent, identically distributed Rayleigh random variables and φ is a uniformly distributed random variable in the interval $-\pi$ to π.

The magnitude of I, or equivalently the interaural magnitude ratio at any instant in time, is given by

$$|I| = \left[\rho^2 + 2\rho\sqrt{1-\rho^2}\,\frac{N_2}{N_1}\cos\varphi + (1-\rho^2)\,\frac{N_2^{\,2}}{N_1^{\,2}}\right]^{1/2} \qquad (6.4)$$

For $\rho = 1$, this magnitude ratio is identically unity and thus the interaural intensity difference in decibels is equal to zero. For $\rho = 0$,

$$|I| = \left[\frac{N_2^2}{N_1^2} \right]^{1/2}$$

$$\log|I| = \frac{1}{2} \log \left[\frac{N_2^2}{N_1^2} \right] \qquad (6.5)$$

Since N_1^2 and N_2^2 are identically distributed chi-squared random variables of degree 2, their ratio is an F-distributed random variable, usually represented by $F(\nu_1, \nu_2)$ with $\nu_1 = \nu_2 = 2$ degrees of freedom. Thus,

$$\log|I| = \frac{1}{2} \log F = 0.4343 \left[\frac{1}{2} \ln F \right] \qquad (6.6)$$

From Johnson and Katz (1970), we have

$$E\left\{ \frac{1}{2} \ln F \right\} = 0 \qquad (6.7a)$$

$$Var\left\{ \frac{1}{2} \ln F \right\} = 0.822 \qquad (6.7b)$$

It then follows that,

$$E\{ 20 \log|I| \} = 0 \qquad (6.8)$$

and

$$\mathrm{Var}\{20\log|I|\} \cong 62.0 \qquad (6.9)$$

Therefore, the interaural intensity difference ($20\log|I|$) in dB at $\rho = 0$ has an expected value of zero and a standard deviation equal to approximately 7.9 dB. Furthermore, as is shown in Eqn. 6.3, the amount of variability in I (and in $|I|$) is modulated by $\sqrt{1-\rho^2}$. Clearly, the maximum variability occurs at $\rho = 0$, and hence, 7.9 dB is the maximum amount of interaural intensity difference fluctuations possible for the correlated waveforms of Eqn. 6.1 .

The phase of I, the interaural phase difference at any instant in time, is given by the expression

$$\measuredangle I = \tan^{-1}\left[\frac{\sqrt{1-\rho^2}\,\frac{N_2}{N_1}\sin\varphi}{\rho + \sqrt{1-\rho^2}\,\frac{N_2}{N_1}\cos\varphi}\right] \qquad (6.10)$$

Since the above equation (the angle of a vector in the complex plane) is satisfied by an infinite set of $\measuredangle I$ values differing in multiples of 2π, we restrict the values $\measuredangle I$ in our development to be in the principal-value range of $-\pi < \measuredangle I < \pi$.

Although any continuous range of length 2π could serve as a principle-range, we have chosen the above range because it is symmetric about zero, and hence, for near diotic stimuli (small

interaural differences), the phase distribution clusters about zero phase. Since the stimulus conditions of interest in this study are near diotic (near-zero interaural intensity and phase differences), the above principal-value range is appropriate.

For $\rho = 1$, we have $\measuredangle I = 0$, and hence, no interaural phase difference. For $\rho = 0$,

$$\measuredangle I = \tan^{-1}\left[\frac{\sin\varphi}{\cos\varphi}\right] = \varphi \qquad (6.11)$$

As in the case of $|I|$, the amount of variability in the phase distributions is modulated by $\sqrt{1-\rho^2}$ and the variablility at $\rho = 0$ represents the maximum amount of variability in the stimulus phase difference. To realize that this represents the maximum variability, it is helpful to consider the probability distribution of the phase difference to be defined over a circular abscissa, with $-\pi$ and π being the same point on the circle. For values of ρ near 1, all the probability is clustered around the 0 point. As ρ decreases to 0 , the probability becomes distributed uniformly around the circle.

Finally, it is important to note that $|I|$ and $\measuredangle I$ are functions of the random variables, N_2/N_1 and φ . The statistics of both these variables are independent of the power in the stimulus waveforms. Thus, for correlated waveforms of the form in Eqn. 6.1, the interaural difference statistics depend only on ρ .

ii) Binaural Detection Stimuli

Just as in the correlation discrimination experiments, the stimulus waveforms in the binaural detection experiments can be described as complex waveforms. For the NOSO detection configuration (in-phase noise added to an in-phase signal) we have

$$\chi_L(t) = N(t)e^{j[2\pi f_o t + \varphi(t)]} + Ae^{j2\pi f_o t} \qquad (6.13a)$$

$$\chi_R(t) = N(t)e^{j[2\pi f_o t + \varphi(t)]} + Ae^{j2\pi f_o t} \qquad (6.13b)$$

where N(t) is a Rayleigh stochastic time function, $\varphi(t)$ is a uniform stochastic time function, fo is the center frequency of the noise as well as the frequency of the target signal, and A is equal to the signal amplitude. Hence, for all signal-to-noise ratios, I(t) = 1 which implies $20\log|I| = 0$ and $\angle I = 0$.

For the NOSπ detection configuration (in-phase noise added to an out-of-phase signal) we have,

$$\chi_L(t) = N(t)e^{j[2\pi f_o t + \varphi(t)]} + Ae^{j2\pi f_o t} \qquad (6.13c)$$

$$\chi_R(t) = N(t)e^{j[2\pi f_o t + \varphi(t)]} - Ae^{j2\pi f_o t} \qquad (6.13d)$$

where N(t), $\varphi(t)$, fo and A are as defined above.

Forming the interaural complex ratio, we get

$$I(t) = \frac{N(t)e^{j\varphi(t)} - A}{N(t)e^{j\varphi(t)} + A}$$

(6.14)

Hence, at any instant of time, I(ti) = I is a random variable given by

$$I = \frac{Ne^{j\varphi} - A}{Ne^{j\varphi} + A} \qquad (6.15)$$

The magnitude of the interaural intensity ratio is given by

$$|I| = \left[\frac{1 - \frac{2A}{N}\cos\varphi + \frac{A^2}{N^2}}{1 + \frac{2A}{N}\cos\varphi + \frac{A^2}{N^2}} \right] \qquad (6.16)$$

For the case of no signal present (A/N = 0), we have |I| = 1 which implies 20log|I| = 0. In the limit as the signal-to-noise ratio approaches infinity, |I| again approaches 1 and 20log|I| approaches 0.

The phase of I is given by

$$\measuredangle I = \tan^{-1}\left[\frac{N\sin\varphi}{N\cos\varphi - A}\right] - \tan^{-1}\left[\frac{N\sin\varphi}{N\cos\varphi + A}\right]$$

$$= \tan^{-1}\left[\frac{\sin\varphi}{\cos\varphi - A/N}\right] - \tan^{-1}\left[\frac{\sin\varphi}{\cos\varphi + A/N}\right] \quad (6.17)$$

For A/N = 0, we have $\angle I = 0$, and hence, no interaural phase difference. In the limit as the signal-to-noise ratio approaches infinity, the argument of the first term of Eqn. 6.17 approaches 0 from a negative value while the argument of the second term approaches 0 from a positive value. Therefore, we have

$$\angle I = \tan^{-1}[\to -0] - \tan^{-1}[\to +0]$$

$$= \pi - 0 = \pi$$

B. Numerical Computation of Interaural Differences

At intermediate values of ρ and signal-to-noise ratio, the distributions of $20\log|I|$ and $\angle I$ were empirically obtained through computer simulations. Rayleigh amplitude and uniform phase random variables were generated by inverse cumulative distribution techniques and a pseudo-random number generator (Dahlquist and Bjork, 1974).

Using equations 6.4, 6.10, 6.16, and 6.17, density histograms and second-order statistics of interaural intensity and interaural phase differences were obtained from 10,000 samples of φ (chosen from a uniform distribution in $-\pi$ to π) and N_1, N_2 (chosen from a Rayleigh distribution corresponding to a unit-normal Gaussian, i.e.

$\sigma^2_{N_i} = (2 - \frac{\pi}{2})$) at each value of ρ and signal-to-noise ratio.

Example distributions of intensity differences and phase differences at intermediate values of ρ and signal-to-noise ratio are illustrated in Figures 6.1 through 6.12. In each figure, probability density is plotted versus interaural intensity or phase difference. Figures 6.1 - 6.3 illustrate probability density functions (PDFs) for interaural intensity differences at ρ = 0.995, 0.80 and 0.0. Figures 6.4 - 6.6 illustrate PDFs for interaural phase differences at ρ = 0.995, 0.80 and 0.0. Figures 6.7 - 6.9 illustrate PDFs for interaural intensity differences at signal-to-noise ratios of -26.0, -21.5 and 0 dB. Figures 6.10 - 6.12 illustrate PDFs for interaural phase differences at signal-to-noise ratios of -26.0, -21.5 and 0 dB.

In the correlation case for values of ρ equal to 0.995 (Figures 6.1 and 6.4), 0.8 (Figures 6.2 and 6.5) and 0 (Figures 6.3 and 6.6) both difference distributions are unimodal and zero mean. Note that as ρ approaches zero, both distributions retain their unimodal, zero-mean characteristics with the phase difference distribution becoming increasingly uniform (as predicted by Eqn. 6.11) and the intensity distribution reaching its maximum width.

For the detection case at signal-to-noise ratios -26 dB (Figures 6.7 and 6.10), -21.5 dB (Figures 6.8 and 6.11) and 0 dB (Figures 6.9 and 6.12) both difference distributions are also zero mean. Although it is not apparent in each figure, the distributions of both differences are also bimodal. The bimodal structure of the phase distributions (Figures 6.10, 6.11, and 6.12) is more apparent

than that of the intensity distributions, particularly at the higher signal-to-noise ratios where the double peaks are more pronounced and separate.

The detailed functional forms of these difference distributions are not important from the modelling point of view but are presented here for completeness. Since the model presented in chapter 5 averages approximately 20 such difference estimates, the resulting averaged samples can be approximated by Gaussian random variables (see Chapter 7). Such averaging must be carefully defined for the interaural phase estimates since phase is a circular function. In this study, we assume that (as a result of the averaging), the PDFs of the phase distributions are circularly convolved to obtain the resultant, average distribution. In the case of uniformly distributed phase (ρ and 10log(S/N) equal to zero), averaging the phase does not result in convergence to a Gaussian distribution. However, since most of the predicted correlation jnds in the next chapter are less than 0.7 (correlation values greater than 0.3), the uniform phase distribution does not appear in our predictions.

Given the Gaussian assumption, a sufficient characterization of the stimuli which is useful for the modelling predictions is a second order description of the difference estimates. Thus, the dependence of the standard deviations of 20log|I| and Δ I versus and signal-to-noise ratio are plotted in figures 6.13 through 6.16. For all values of and signal-to-noise ratio, the expected value of both 20log|I| and Δ I were equal to zero. In addition, for all values of ρ and signal-to-noise ratio, the interaural phase and intensity measures appeared to be uncorrelated (numerically

calculated correlations were always a factor of 10^{-3} less than the product of the individual standard deviations).

In the correlation case, for both difference variables, there is a monotonic increase in standard deviations as ρ decreases from unity to zero. Specifically, the intensity difference standard deviation rises sharply at values of ρ near 1, a normalized slope of 5.6 (ordinate values divided by the maximum ordinate value), reaching a constant value of approximately 7.0 dB at $\rho = 0.6$. The phase difference standard deviation showed a relatively shallower rise near unity (a normalized slope of 3.7) and increased at a linear rate of 1.25 radians per unit decrease in ρ for ρ less than 0.9 .

In the detection case, as with the correlation waveforms, there is a monotonic increase in standard deviations as signal-to-noise ratio increases up to approximately 0 dB. However, unlike the correlation waveforms, the intensity difference and phase difference standard deviations rise at approximately the same normalized rate (0.018 for intensity and 0.013 for phase) for small signal-to-noise ratios. Moreover, at higher signal-to-noise ratios (up to approximatly 0 dB), both difference standard deviations increase at a linear rate of 0.4 dB intensity difference per dB signal-to-noise ratio and 0.07 radians of phase difference per dB signal-to-noise ratio.

CHAPTER 7

BINAURAL PERFORMANCE BASED ON STIMULUS VARIABILITY

We have presented experimental results from normal and impaired listeners in four binaural experiments at several different narrowband noise center frequencies. In chapter 5, we presented a simple, narrowband model of binaural interaction which facilitates the exploration of relationships between the four different binaural tasks. The major goal of this model is to unify the relationship between interaural time and intensity discrimination and the ability to discriminate interaural correlation and detect targets in binaural signal configurations.

In chapter 6, we characterized the interaural intensity and time (phase) differences for the stimuli used in the correlation discrimination and binaural detection experiments of this study. In this chapter, we derive the equations for predicting performance in the correlation discrimination and binaural detection experiments. These predictions are obtained from the model presented in chapter 5 in conjunction with the stimulus characterization discussed chapter 6.

Depending on the interaural differences combination rule assumed, the model predicts performance from a particular relationship between the time and intensity jnds (the internal noise parameters of the model) and the time and intensity variability in the stimulus (the "information" available to the model). Thus, given the characterization of the correlation discrimination and binaural detection stimuli in terms of their interaural time and intensity difference distributions, we can estimate performance in these two tasks under various combination assumptions. The results of the formulations which are derived in this chapter are presented and discussed in chapter 8.

A. Distribution of Averaged Interaural Differences

In the derivations that follow, we assume that the averaged interaural difference observations, $\bar{\tau}$ and $\bar{\alpha}$, are Gaussian random variables with means equal to the mean of the corresponding stimulus interaural differences and variances proportional to the variances of the corresponding stimulus interaural differences plus the processing noise variances (see Figure 5.1).

Figures 7.1 through 7.8 illustrate plots of the log-probability distributions for twenty (20) averaged values of φ_i and α_i along with Gaussian distributions which have the same means and variances. Averaged interaural intensity distributions (Figures 7.1 and 7.2) and phase distributions (Figures 7.3 and 7.4) are presented for correlation values of 0.995 and 0.80. Averaged interaural intensity distributions (Figures 7.5 and 7.6) and phase distributions (Figures

7.7 and 7.8) are also presented for for NOSπ detection stimuli at signal-to-noise ratios of -26.0 dB and -21.5 dB. Note that for both differences, the variability seen in these figures comes completely from the external variability of the stimulus; the Gaussian, internal noise is not included.

As can be seen in these figures, for both the correlation discrimination and binaural detection waveform statistics, the Gaussian assumption is supported out to more than 2 or 3 standard deviations.

Furthermore, because the variance of these estimates is critical to the predictions presented in this chapter, we were concerned about the effect of a small number of very large samples on the variances computed in chapter 6. This is particularly important for the interaural intensity differences where no "natural" limiting occurs as in the case of interaural phase differences (the natural limiting being the circularity of the phase in 2π). Therefore, we symmetrically hard-limited or clipped the interaural intensity difference samples at maximum, absolute values of 5, 10, 15, 20 and 30 dB. From Figures 6.5 - 6.8 it is clear that the variance of the interaural intensity difference is largest at a correlation and signal-to-noise ratio of zero. Hence, clipping would have the largest effect on the computed variances near this correlation and signal-to-noise value. Therefore, in the following discussion, the differences in the computed variances at the various clipping maxima are presented for a correlation and signal-to-noise ratio equal to zero. The reported differences decrease to zero as the correlation increases to unity

and the signal-to-noise ratio decreases.

We found that for clipping bounds greater than or equal to 15 dB, the decrease in the computed variances was at worst 5% of the unclipped noise. For clipping bounds less than 15 dB, the variances were decreased by more than 5% ; however, for bounds of 10 dB, this decrease was at most 10% of the unclipped value. The effect of a 5 - 10 % decrease in the variance on the predictions proved to be less than the variability of the predictions due to the observed variability in the measured time and intensity jnds. Thus, the predictions in this chapter are based on the unclipped variances computed before averaging in chapter 6.

The above results suggest that processing of interaural intensity differences greater than approximately 15 dB does not provide any significant, additional information about the variance or width of the interaural intensity distribution in the correlation and detections tasks. It is interesting to note that the "critical" value of the hard limiting of the intensity difference ($\sim$ 15 dB) is close to the value observed which results in a completely lateralized image (Durlach and Colburn, 1978).

B. Model Predictor Equations

For a correlation discrimination or an NOSπ detection configuration, the mean values of the stimulus interaural differences are zero and the variances are functions of the interaural correlation or the signal-to-noise ratio. Therefore, in

these experiments, the only aspect of the binaural difference observations ($\bar{\tau}$ and $\bar{\alpha}$) which changes between the test and reference stimulus conditions is the variance of the two, averaged interaural differnces.

The just-noticeable change in variance will correspond to that stimulus parameter value (ρ or signal-to-noise ratio) which produces just enough additional stimulus variability so as to be just noticeable from the variance of the noisy processing. Given the stimulus presentation structure of the form described in chapter 3,

	Interval		
	1	2	
S1	R	T	R = reference stimulus
S2	T	R	T = test stimulus

and assuming a reference condition with no interaural difference variability (reference correlation of unity or masker alone in an NOSπ paradigm), we obtain prediction equations under the following combination rules.

i) Separate Time and Intensity Difference Observations

In this section, we assume that interaural time and intensity differences are separately available to an ideal decision mechanism (Figure 5.2 a). Given this assumption, we can investigate the predictions for four possible combinations of the interaural

differences : (1) intensity differences alone, (2) time differences alone, (3) a weighted, linear sum of the interaural differences , and (4) the optimal combination of the two interaural differences. By testing the predictions of these four combinations, we are able to explore : (1) how the optimal combination rule of interaural time and intensity compares to a lateralization-like, linear combination rule of interaural time and intensity, and (2), which interaural difference cue is important in effecting performance at different frequency regions.

It is important to note that for all four combination rules, the processing noise estimates are made on the assumption of separately available differences (Equations 5.1 a and b). As such, the linear sum considered in this section is not the same as the weighted, fixed linear sum considered in the next section (Figure 5.2 b). The linear combinations are different in two ways : (1) the processing noise estimates are different (Equations 5.1 and 5.2) and (2) the combination weight in section B-i is assumed to be the ratio of the interaural difference jnds (consistent with lateralization-type models) whereas in section B-ii of this chapter, the weighting is constrained to be the ratio of interaural difference jnds.

a) Interaural Intensity Difference Alone

Assuming the use of interaural intensity differences alone and performing a likelihood ratio test, the optimal decision test (based on a minimum probability-of-error criterion, Van Trees, 1968)

results in a decision rule of the form (see Appendix IV)

$$\bar{\alpha}_1^2 - \bar{\alpha}_2^2 \underset{S_1}{\overset{S_2}{\gtrless}} 0$$

or equivalently

$$\frac{\bar{\alpha}_1^2}{\bar{\alpha}_2^2} \underset{S_1}{\overset{S_2}{\gtrless}} 1$$

where $\bar{\alpha}_i$ is the interaural intensity observation in the ith interval. Combined with the processing noise estimate of equation 5.1 a, the above equation implies the just-noticeable change in the test stimulus interaural variability ($\sigma_{\alpha T}$) is satisfied by the equation

$$\frac{\sigma_{\alpha T}}{(\Delta\alpha)_0} = \sqrt{\frac{2K}{\nu}\left[F_{.25}(\nu,\nu) - 1\right]} \qquad (7.1)$$

where K = 20 and ν is equal to

$$\nu = \frac{W_{cB} \min [T, 300 \text{ msec}]}{K}$$

and $F_{.25}(\nu, \nu)$ is the critical value for an F-distribution at a probabililty of 0.25 with $\nu_1 = \nu_2 = \nu$ degrees of freedom. Hence, the test-stimulus value corresponding to $\sigma_{\alpha T}$ which satisfies the right-hand side of equation 7.1 is the just-noticeable test stimulus.

b) Interaural Time Differences Alone

Similarly, using interaural time alone, we obtain a decision rule

$$\bar{\tau}_1^{\,2} - \bar{\tau}_2^{\,2} \underset{S_1}{\overset{S_2}{\gtrless}} 0$$

Combining the above decision rule with the processing noise estimate of equation 5.1 b, we get that the just-noticeable change in the stimulus interaural phase variability ($\sigma_{\varphi T}$) is satisfied by

$$\frac{\sigma_{\varphi T}\, C_\varphi}{(\Delta\tau)_0} = \sqrt{\frac{2K}{\gamma}\left[F_{.125}(\gamma,\nu) - 1\right]} \quad (7.2)$$

where $C_\varphi = 10^6/2\pi f_0$ usec/radian (fo is the center frequency of the critical band filters), a conversion factor from interaural phase difference to an interaural time difference.

To compute the prediction at any one frequency, we use the time and intensity jnds measured for that critical band and scale the interaural differences standard deviations (Figures 6.13 - 6.16) by $1/(\Delta\alpha)_0$ and $C_\varphi/(\Delta\tau)_0$. We then find the scaled standard deviation equal to the expression on the right appropriate for that frequency. The stimulus value which corresponds to that scaled standard deviation is the just-noticeable stimulus value.

Because the rate of independent difference samples is equal to the bandwith of the stimulus and the bandwidth of the critical band is proportional to the center frequency, the rate at which independent stimulus differences samples are available is higher at high frequencies than at low frequencies. Hence, there are more independent averaged difference samples available to the processor and therefore, a larger γ . This increase is reflected in a

smaller "threshold" for the stimulus variability as seen in the expression to the right of the equality in Equations 7.1 and 7.2 .

Since this threshold expression will appear once again and is of importance in the predictions to follow, we have tabulated values of the expression in Table 7.1 for the different narrowband center frequencies tested in this study.

c) Linear Sum of Differences

Assuming a linear combination of the form,

$$1 = \frac{\bar{\alpha}}{(\Delta\alpha)_o} + \frac{\bar{\tau}}{(\Delta\tau)_o}$$

forming an LRT and using the processing noise estimates of equations 5.1 a and b, we find that the just-noticeable test stimulus value corresponds to interaural difference variances which satisfy (see Appendix IV)

$$(7.3)\quad \sqrt{\frac{1}{2}\left[\frac{\sigma_{\alpha T}^2}{(\Delta\alpha)_o^2} + \frac{\sigma_{\varphi T}^2 C_\varphi^2}{(\Delta\tau)_o^2}\right]} = \sqrt{\frac{2K}{\gamma}\left[F_{.25}(\gamma,\nu) - 1\right]}$$

Note that the above variance expression has elements of the interaural-intensity-alone expression (Equation 7.1) and the interaural-time-alone expression (Equation 7.2). Moreover, if time or intensity processing is severely degraded ($(\Delta\alpha)_o$ or $(\Delta\tau)_o$ much greater than $\sigma_{\varphi T} C_\varphi$ or $\sigma_{\alpha T}$), then the left-hand side of

equation 7.3 reduces to the left hand side of equation 7.1 or 7.2 reduced by a factor of $1/\sqrt{2}$. Clearly, the linear-sum combination is sub-optimal if the interaural differences are separately available.

d) Optimal Combination of Interaural Differences

With no a priori combination assumptions, i.e, assuming both interaural time and intensity difference observations are separately available, we form an LRT and obtain a decision rule of the form (see Appendix IV)

$$(\bar{\alpha}_1^2 - \bar{\alpha}_2^2) + d^2(\bar{\tau}_1^2 - \bar{\tau}_2^2) \underset{S_1}{\overset{S_2}{\gtrless}} 0$$

where

$$d = \frac{\sigma_{\phi T} C_\phi}{\sigma_{\alpha T}} \quad \frac{(\Delta\alpha)_0}{(\Delta\tau)_0} \left[\frac{\sigma_{\alpha T}^2/K + \frac{2(\Delta\alpha)_0^2}{\nu}}{C_\phi^2 \sigma_{\phi T}^2/K + \frac{2(\Delta\tau)_0^2}{\gamma}} \right]^{1/2}$$

is a variable binaural mixing coefficient dependent on the processing noise terms and the stimulus interaural difference variances.

There seems to be no tractable or enlightening analytic expression for the performance of this rule. Hence, the predictions of this rule were numerically obtained by Monte Carlo simulations of the decision rule. One thousand sample values of $\bar{\alpha}_1^2$, $\bar{\alpha}_2^2$, $\bar{\tau}_1^2$, and

$\bar{\tau}_2^2$ were generated (as detailed in chapter 6) at each value of ρ and 10log(S/N), and used to calculate a percent correct based on the above decision rule. Jnds and detection thresholds were then estimated from the correlation value and signal-to-noise ratio which corresponded to 75% correct. Predictions of this rule will be discussed in chapter 8.

ii) Fixed Sum of Interaural Differences

We know from the review of chapter 2 that lateralization phenomena suggest the binaural processor weights and sums the two interaural differences and forms a single binaural difference variable. Moreover, from the analysis of chapter 5, a fixed weighting coefficient, b, must equal the ratio of the interaural difference jnds.

Thus, assuming the model is forced to use a fixed, linear combination of the form (see Figure 5.2 b)

$$B = \bar{\alpha} + \frac{(\Delta\alpha)_0}{(\Delta\tau)_0}\,\bar{\tau}$$

and performing an LRT , we obtain a decision rule of the form (Appendix IV)

$$B_1^2 - B_2^2 \underset{S_1}{\overset{S_2}{\gtrless}} 0$$

Combined with the processing noise estimate of equation 5.2 (recall that under the fixed, linear sum assumption there is essentially only one noise term in the model) we find that the just-noticeable test stimulus value corresponds to interaural difference variations

which satisfy

$$\sqrt{\frac{\sigma_{\alpha T}^2}{(\Delta\alpha)_0^2} + \frac{\sigma_{\phi T}^2 C_\phi^2}{(\Delta\tau)_0^2}} = \sqrt{\frac{2k}{\gamma}\left[F_{.125}(\gamma,\gamma)-1\right]} \quad (7.4)$$

Note that the prediction equation of the fixed, sum of interaural differences (SID) combination is related to the expressions obtained for either interaural difference alone. Specifically, if the processing of either interaural intensity or time differences is severely degraded ($(\Delta\alpha)_0$ or $(\Delta\tau)_0$ much larger than the stimulus difference variations), the fixed linear sum predictions approaches the predictions of the separate, non-impaired interaural difference (Equations 7.1 and 7.2). Furthermore, in contrast to the development in section B-i-c, Equation 7.4 predicts optimal performance given the assumption of the fixed, SID combination rule (see Figure 5.2 b).

In the next chapter, we present the values predicted by these equations for both normal listeners and the hearing impaired listeners in this study. Not only do we investigate the predictions of different interaural difference combinations, but in addition, by comparing the values of the time and intensity components of the stimulus variability to the other expressions at threshold, we assess the relative importance of the two interaural differences in effecting performance for a given binaural task and a given hearing impairment.

CHAPTER 8

COMPARISONS OF PREDICTIONS WITH OBSERVATIONS

The equations of chapter 7 were used in conjunction with the stimulus characteristics obtained in chapter 6 to predict performance in the interaural correlation discrimination and binaural detection experiments. Below, we present the predictions of the four combination rules investigated in the previous chapter and compare them with the observed correlation jnds and NOS detection thresholds of chapter 4.

For the graphs presented in this chapter, observed correlation jnds and detections thresholds are plotted with dashed connecting-lines along with the predictions of the model which are connected by solid lines. In addition, vertical bars representing the range of predicted values obtained due to the variability of the observed time and intensity jnds (approximately 10 - 15 % of the observed jnds and thresholds) are included with the predictions.

A. Separate Time and Intensity Difference Observations

None of the four combination rules considered under this assumption, including the optimal, non-linear combination rule, were able to predict correlation jnds and NOSπ detection thresholds at all frequencies. Specifically, both the weighted linear sum and optimal combination rules predicted correlation thresholds and NOSπ detection thresholds that were larger than the observed jnds and detection thresholds (Figures 8.1 and 8.2).

Moreover, the predictions of the model using the linear sum (Chapter 7, section B-i-c) of interaural time and intensity differences is not significantly different than the predictions of the optimal combination rule. As can be seen in Figures 8.1 and 8.2, the difference between the predictions of the two rules are within the range of predictions due to the observed variability of the observed time and intensity jnds.

Thus, in the remainder of this chapter, we will present predictions of the weighted, sum-of-interaural differences (SID) model. The time alone component of the SID rule and the intensity alone component of the SID rule are presented for comparison and to show the relative usefulness of the interaural difference cues at the different frequency bands.

B. Normal Listeners

i) Interaural Correlation Predictions

Predictions of the SID rule for normal listeners is presented in Figure 8.3. The functional form of the observed jnd versus frequency curve is correctly predicted and, from the time alone (Figure 8.4) and intensity alone (Figure 8.5) predictions, it is apparent that the SID rule predictions are effected by interaural time differences at low frequencies and interaural intensity differences at high frequencies. However, note that the high frequency (2000 and 4000 Hz) jnds are significantly smaller than the observed jnds.

ii) NOSπ Detection Thresholds

Figure 8.6 presents the predictions of the SID rule for normal listeners along with observed average data. The predicted values are close to the observed thresholds at 250 and 1000 Hz, but are significantly different (> 5 dB) at 500 Hz, 2000 Hz and 4000 Hz. As in the correlation jnd predictions, the threshold predictions are mediated by interaural time differences at low frequencies (Figure 8.7) and interaural intensity differences at high frequencies (Figure 8.8).

Part of the discrepancy between the predicted and observed jnds and thresholds is almost certainly due to not having interaural time, interaural intensity, interaural correlation discrimination and binaural detection results from the same set of normal listeners. For example, at 500 Hz, if a 20 usec time jnd were used rather than a 10 usec jnd, the predicted threshold would be -7 dB rather than -10 dB -- which is only 1 dB lower than the observed value and well within experimental variability.

However, the SID rule appears to consistently predict lower than observed correlation discrimination jnds and detection thresholds at high frequencies (2000 and 4000 Hz). Predictions of the model at high frequencies could be improved by assuming different averaging K's at different frequency bands. Larger K's would increase the value of the variance "threshold" terms derived in chapter 7, and hence, the model would predict larger correlation jnds and higher thresholds. Figure 8.9 plots the value of this threshold (the expression tabulated in Tabel 7.1) versus frequency, with K as a parameter. Note the relatively large effect of increasing K on the threshold values at low frequencies as compared to the threshold values at high frequencies. In addition, Figures 8.10 - 8.13 plot the correlation discrimination and detection threshold predictions for time alone (Figures 8.10 and 8.12) and intensity alone (Figure 8.11 and 8.13) for the corresponding values of K.

In terms of the model's complexity, allowing different K's at high frequencies begins to detract from its simplicity and trivializes the predictions. A modification of the model which would have an equivalent effect of increasing the predicted correlation jnds and detection thresholds at high frequencies is to have different K's for the interaural time and intensity estimates averaging. Since the predictions of the model appear to be mediated by interaural time processing at low frequencies (frequencies less than or equal to 1000 Hz) and interaural intensity processing at high frequencies, a larger K for intensity estimate averaging will not affect predictions of the model at low frequencies, but it will

increase the predictions at high frequencies. The assumption of equal K's for both interaural time and intensity samples was originaly made to simplify calculations.

The value for interaural intensity averaging (to be denoted by K_α) which best fit both the correlation jnds and the detection thresholds at 2000 and 4000 Hz was found to be a $K_\alpha = 40$. Predictions of the different-K's SID rule, Figure 8.14 (henceforth refered to as simply the SID rule), are presented in Figures 8.15 and 8.16. As expected, the predictions at low frequencies are unaffected by the increased K_α for intensity sample averaging. More importantly, the predictions of the SID rule at high frequencies are in good agreement with observed results for both correlation discrimination and NOSπ detection.

Note that by assuming a different K for interaural intensity averaging, γ_α, the number of independent estimate averages ($\bar{\tau}$ and $\bar{\alpha}$) is now different for time and intensity. Specifically, for time estimates we have

$$\gamma_\tau = \frac{W_{CB} \min [T, 300 \text{ msec}]}{K_\tau}$$

and for intensity estimates we have

$$\gamma_\alpha = \frac{W_{CB} \min [T, 300 \text{ msec}]}{K_\alpha}$$

Thus for the predictions presented in Figure 8.15 and 8.16, at low frequencies (frequencies less than or equal to 1000 Hz) where the predictions of the model are predominately due to interaural time

processing, we used a threshold value computed from a K = 20. At high frequencies (2000 and 4000 Hz) we used a threshold value as computed from a K = 40 (see Figure 8.9).

The analysis above suggests that different K's for interaural time and intensity processing result in predictions which are closer to the observed results. Specifically, high-frequency correlation jnd and NOSπ detection predictions (both predominantly due to interaural intensity processing in this model) are closer to the observed, normal results. Hence, we now compare the different K's rule to observed results from the hearing impaired listeners.

C. Impaired Listeners

In this section, we present the predictions of the SID rule with the different averaging K's for time and intensity samples. Consistent with the assumptions of the model as presented in chapter 5, the total effect of the hearing impairment on binaural hearing is presumed to be described by an increased variance in the time and intensity processing noise (Figure 5.1). In the following predictions, we have assumed the same "normal" K's (K_{τ} = 20 and K_{α} = 40) for all of the impaired subjects.

i) Interaural Correlation Predictions

Predictions of the SID rule for subject FG is shown in Figure 8.17. Note that the functional form of the observed frequency dependence is correctly predicted and that predicted jnds are , at most, a factor of 2 - 3 different from the observed values. Moreover, from Figures 8.18 and 8.19 (plots of time alone and intensity alone predictions), it is clear that the predictions of the SID model is essentially due to interaural time processing at low frequencies and interaural intensity processing at high frequencies.

Predictions of the SID rule for subject DH are presented in Figure 8.20. The observed frequency dependence is generally predicted and the predicted jnds are within a factor of 2 or better at all frequencies except 500 Hz. From the time alone and intensity alone predictions (Figures 8.21 and 8.22), it seems as if subject DH is predominately using interaural intensity information at all the frequencies, even at 500 Hz where there is useful information in the interaural time difference.

Predictions of the SID rule for subject VF is presented in Figure 8.23. The observed frequency dependence is correctly predicted as is the jnd at 500 Hz where she was able to discriminate correlation. It is interesting to note that neither time alone (Figure 8.24) nor intensity alone (Figure 8.25) were able to correctly predict this point. From VF's interaural time and intensity jnds, one would have incorrectly attributed her correlation sensitivity solely to her time sensitivity at 500 Hz.

For subject CS (the MS patient) the SID rule, time alone and intensity alone all predicted jnds greater than 1 at all frequencies. As such, the predictions of all three rules are presented in Figure 8.26 for this subject.

ii) NOSπ Threshold Predictions

Figure 8.27 shows the predictions of the SID rule for subject FG. The predicted thresholds are close to the observed thresholds except at 2000 Hz. As in the case of the correlation jnd predictions for this subject, the SID predictions are primarily due to time processing at low frequencies (Figure 8.28) and intensity processing at high frequencies (Figure 8.29).

Predictions of the SID rule for subject DH (Figure 8.30) show a reasonable fit to the observed thresholds at 500 Hz and 1000 Hz but are too high at 250 Hz and too low at 2 and 4 kHz. From the time alone and intensity alone predictions (Figures 8.31 and 8.32) neither time nor intensity seems to dominate the predictions, although the functional form of the frequency dependence (except at 250 Hz) is close to that observed in the time alone predictions.

For subjects VF and CS, the SID rule predicted NOSπ thresholds higher than their observed NOSO thresholds at all frequencies except at 500 Hz. Hence, except at 500 Hz for subject VF, the SID rule (Figure 8.33 and 8.34) predicted NOSπ thresholds equal to the NOSO thresholds, i.e. no binaural advantage between the two interaural signal configurations. At 500 Hz, the SID rule predicted a

threshold of 10 dB when the observed threshold is about 6 dB. Once again, as in the correlation discrimination predictions for subject VF, neither time nor intensity alone was individually sufficient to predict the 10 dB threshold.

D. Relative Use of Interaural Difference Cues

While the ratio of the time and intensity jnds provides a measure of the relative sensitivity to interaural time and intensity differences, it does not provide a description of their relative importance in effecting performance for a given binaural task. By plotting the ratio of the intensity-alone variance component (Equation 7.1) to the time-alone variance component of (Equation 7.2) the SID rule at threshold values of $\sigma_{\alpha T}^2$ and $C_\zeta^2 \sigma_{\zeta T}^2$, we obtain a measure of the relative usefulness of the two interaural differences.

For normal listeners, Figure 8.35 shows the expected dependence of this ratio (plotted on a dB scale) for both correlation discrimination and NOSπ-signal detection. At low frequencies, (< 1000 Hz), interaural time differences account for more than 90% of the SID rule predictions (a ratio of approximately -10 dB). At 1000 Hz, both differences contribute equally to the SID rule predictions (a ratio of 0 dB). At higher frequencies, interaural intensity differences account for more than 95% of the predictions (ratios greater than 20 dB).

Subject FG, despite his low-frequency time loss, shows a near-normal dependence interaural time differences (Figure 8.36).

Interestingly, subject DH shows a close to normal dependence on the two interaural differnces (Figure 8.37) despite a significant amount of loss in both time and intensity. Moreover, although the predicted and observed correlation jnds and NOSπ-signal thresholds for subjects FG and DH were quite different, the ratios of relative usefulness are very similar except at 2 kHz.

Plots for the remaining two subjects were not presented since no thresholds were predicted except at 500 Hz, where subject VF had a ratio of 7.2 dB, which is approximately 17 dB higher than normal. Hence, time differences account for only 10% of the SID rule predictions for this subject, whereas for normal listeners, interaural time differences account for more than 90% of the SID rule predictions.

It is generally accepted that the binaural system is unable to make use of interaural time (fine structure) differences for narrowband signals at frequencies above approximately 1500 Hz (Durlach and Colburn, 1978). Performance in interaural time (fine structure) discrimination tasks with complex, high frequency waveforms is believed to be mediated by processing of low frequency differences in the envelopes of the waveforms. Since the interaural time processor of the model being considered in this study is assumed to be processing fine-structure time differences, we are technically incorrect in using the stimulus interaural phase differences in the predictions of the model at the higher

frequencies (2000 and 4000 Hz). However, the predictions at these frequencies are essentially due to the interaural intensity differences in the stimuli (see Figures 8.25 - 8.27). Hence, making the time jnds larger at 2000 and 4000 Hz (effectively making the model have no sensitivity to fine-structure time differences) has a negligible effect on the predictions of the model.

CHAPTER 9

CONCLUSIONS AND REMARKS

The discussion in this chapter is divided into two parts. First, we evaluate the impaired binaural phenomena with attention to directions for future clinical and academic investigations of binaural hearing in impaired listeners. Second, we evaluate the essential features of the augmented model of binaural interaction introduced in chapter 5, not only as a predictive tool, but as a generally applicable modification to existing models of binaural interaction.

A. Conclusions from the Psychophysical Results

The conclusions we draw from the observed binaural phenomena are :

1. The audiogram tells us very little about the impairments in binaural hearing. This is true for both describing the frequency regions in which impaired binaural hearing occur and the extent or amount of binaural impairment.

2. Noise-induced, high-frequency loss subjects with similar audiograms and presumed etiologies can have significant differences between their binaural hearing abilities. This includes differences in the frequency regions of their impaired binaural hearing and the extent of the impairments in their binaural hearing.

3. Impairments in interaural time discrimination are independent of impairments in interaural intensity discrimination. Except for one subject at one frequency (subject VF at 500 Hz), there was no clear correlation between the impairments in the two tasks.

4. Interaural correlation discrimination, although it proved to be difficult for subjects to discriminate, provides a direct and simple measure of interaural time sensitivity (at low frequencies) and interaural intensity sensitivity (at high frequencies). Moreover, unlike interaural intensity discrimination and NOSπ-signal detection, it cannot be mediated by monaural cues.

5. The MLD alone is not a good indicator of binaural hearing loss in hearing impaired listeners. Although the absence of an MLD implies a loss in binaural hearing (see results for subject VF and CS), the presence of a normal MLD does not necessarily imply normal binaural hearing (subjects FG and DH). Future investigations of the MLD in impaired listeners should report the NOSO and NOSπ thresholds along with the MLD.

6. Our results also suggest that studies with large numbers of hearing impaired listeners are not as useful in modelling hearing impairments as as series of complimentary tests on a few impaired listeners. Our two, matched high-frequency loss listeners (FG and DH) had significantly different time loss. This is almost certainly due to the detailed differences in their physiological loss not exposed by the monaural audiogram. Thus, while an average can be useful as a descriptive measure of binaural hearing impairment, it is of little value in assessing the loss of any one individual listener within that class.

7. A useful representation of impaired binaural discrimination jnds is the binaural audiogram. These plots of dB loss re normal jnds are similar to monaural audiograms in structure and are capable of displaying patterns of binaural hearing loss not readily apparent in the traditional methods of representation.

8. Finally, studies on large groups of impaired listeners may find it useful to classify listeners on the basis of their binaural audiograms and look for similarities within a "binaural" categorization. Thus, subjects FG and DH would both be classified as flat, intensity-loss listeners but subject FG would be a low-frequency time-loss listener while subject DH would be a flat time-loss listener. This should not be viewed as a conflicting set of data, but rather as a verification of the need for an increase in the number of dimensions which fully characterize a hearing

impairment.

Given the importance of measuring results from all the tests on each impaired subject in a study, we feel the most critical problem in testing hearing impaired listeners is the duration of the testing program. Even with the development of our sequential testing routines (which reduced our testing time by approximately 40%), each subject in our study was tested approximately 16 hrs per week for almost four months. The problem is further compounded by the fact that, unlike normal listeners, impaired listeners must be individually tested. Not only is it difficult to obtain impaired subjects willing to participate in studies of the type presented in this report (particularly at academic institutions), but such programs are also a drain on the experimenter.

A resolution to this problem would be the development of quick, simple and robust binaural tests analogous to Bekesy audiometry. Standard audiometry can easily be modified (Jerger et al, 1982) to perform binaural detection tasks, but as yet, there exists no equally easy was to test interaural time, interaural intensity or interaural correlation discrimination.

In chapter 1, we argued for the use of narrowband noise as an appropriate stimulus for the frequency analysis of binaural hearing impairments. In addition, we introduced the binaural audiogram in chapter 4, a new description of impaired discrimination jnds. This definition of impaired binaural hearing is dependent on an accurate description of normal binaural hearing in these discrimination tasks. Thus, given the paucity of data on the frequency dependence

impairment.

Given the importance of measuring results from all the tests on each impaired subject in a study, we feel the most critical problem in testing hearing impaired listeners is the duration of the testing program. Even with the development of our sequential testing routines (which reduced our testing time by approximately 40%), each subject in our study was tested approximately 16 hrs per week for almost four months. The problem is further compounded by the fact that, unlike normal listeners, impaired listeners must be individually tested. Not only is it difficult to obtain impaired subjects willing to participate in studies of the type presented in this report (particularly at academic institutions), but such programs are also a drain on the experimenter.

A resolution to this problem would be the development of quick, simple and robust binaural tests analogous to Bekesy audiometry. Standard audiometry can easily be modified (Jerger et al, 1982) to perform binaural detection tasks, but as yet, there exists no equally easy was to test interaural time, interaural intensity or interaural correlation discrimination.

In chapter 1, we argued for the use of narrowband noise as an appropriate stimulus for the frequency analysis of binaural hearing impairments. In addition, we introduced the binaural audiogram in chapter 4, a new description of impaired discrimination jnds. This definition of impaired binaural hearing is dependent on an accurate description of normal binaural hearing in these discrimination tasks. Thus, given the paucity of data on the frequency dependence

of narrowband noise binaural phenomena (particularly for interaural intensity and interaural correlation discrimination), we see a need for an extensive study of normal listeners in the binaural tests of this study to measure the mean and limits of normal performance. Ideally, such a study should include older, normal hearing listeners to reduce differences in ability due to age differences.

Finally, given the apparent independence of interaural time and intensity sensitivity, we feel it critical to measure both interaural time and interaural intensity discrimination in any future binaural studies of impaired listeners. Based on the modelling results, the inclusion of interaural intensity processing appears to be particularly important to the understanding of high frequency binaural interaction.

B. Conclusions from the Modelling Results

The conclusions we draw from the modelling portion of this study are

1. A mechanism which low-pass filters (averages) interaural time and intensity differences unifies lateralization and detection predictions of current binaural interaction models under the same set of model parameters. For models which extract interaural time and intensity estimates directly, the averaging can be included as presented in this study. For models which do not explicitly extract time and intensity estimates, a similar type of

modification would be the inclusion of a correlation window which temporally averages the computation of the cross-correlation (Sayers and Cherry, 1957 ; Stern and Bachorski, 1983)

2. Different averaging durations (different averaging Ks) for interaural time and interaural intensity differences appears to be needed to predict observed correlation jnds and NOSπ detection thresholds at high frequencies. Without a relatively larger K (a slower, temporal tracking ability) for interaural intensity averaging as compared to interaural time averaging, high frequency predictions are better than observed performance.

3. Given an augmented model of this sort, it is possible to characterize binaural hearing in correlation and NOSπ detection tasks from a description of sensitivity to interaural time and intensity differences.

4. The predictions of the model using the weighted, linear sum of interaural time and intensity differences is not significantly worse than the predictions using the ideal combination of interaural time and intensity differences. The difference between the predictions of the two combination rules are within observed experimental variability.

5. The general model presented in this study enabled us to simply characterize impaired binaural hearing in four hearing impaired subjects with different types of hearing loss. Although the model is purely functional and includes only a gross description of the impairment, it is a useful investigative tool and can expose the essential character of relationships between various binaural phenomena without getting involved in the detailed computations typically encountered in physiologically based models of binaural interaction.

6. By having a model with simple and separate descriptions of interaural time and intensity processing, we can assess the relative importance of interaural time and intensity differences at a given frequency for a particular binaural task. Although a ratio of observed time and intensity jnds is a necessary component of such an assessment, it can only describe how well each difference is processed and not the consequences of that degraded processing for a given binaural task. A complete assessment requires an integration of the amount of information present in the stimuli along with a description of how well such information is processed.

We emphasize the fact that we have not developed a new model of binaural interaction in this study. Rather, we have proposed a general, additional mechanism to the models presented in chapter 2, which allow those models to make predictions consistent with both

lateralization and detection data. For example, inclusion of an averager of binaural differences in Hafter's (1971) lateralization model would enable that model to predict both detection and lateralization data. Recall that without the averager, the predicted value of $\overline{\Delta}$ at signal-to-noise threshold was approximately 90 usecs. With an added averaging mechanism, the variance of the stimulus interaural time differences would be reduced by a factor of $1/K_\tau$ or the value of $\overline{\Delta}$ would be reduced by a factor of $1/\sqrt{K_\tau} = 1/\sqrt{20} \simeq 0{,}22$. Thus, Hafter's lateralization model would predict a new threshold value for $\overline{\Delta}$ approximately equal to 20 usec, a value consistent with his assumed time-intensity trading ratio and observed time jnds at low frequencies.

Since the temporal averaging mechanism plays such a critical role in enabling the model to predict discrimination and detections data with the same set of parameter values, further study of the temporal tracking ability of the binaural system is needed. The work of Grantham (1980) and Grantham and Wightman (1982) was an essential first step, but more work is needed. Specifically, a comparison of the temporal tracking capability of interaural correlations near unity (recall that they tested fluctuation about zero) with interaural time and intensity tracking capability about a diotic reference, would help to further identify the relationships between the three binaural phenomena.

The main deficiency of the current model is that it is essentially a narrowband model. One possible modification of the model so as to include wideband stimuli would be to incorporate an additional averager which averages the $\overline{\tau}$'s and $\overline{\alpha}$'s (the time

averaged estimates of interaural time and intensity) from each stimulated narrowband section across the different frequency bands. Such an averaging processor would necessarily have to be noisy or else it would predict increasingly better interaural time and intensity jnds with increasing bandwidth. Zurek and Leshowitz (1975) report less than a factor of two difference between narrowband (100 Hz centered at 500 Hz) noise intensity jnds and wideband noise intensity jnds. A similar result between narrowband time jnds and wideband time jnds has also been reported (Durlach and Colburn, 1978).

Given such a frequency-band averager, a resulting question would be how to average the different number of independent $\bar{\tau}'s$ and $\bar{\alpha}'s$ available from the different frequency channels. Recall that due to the larger peripheral bandwidths at the higher frequencies, there were more independent averages available at high frequencies than at low frequencies.

We feel that the main contribution of the model presented in this study has been to demonstrate the need for an interaural-differences averager or lowpass filter. Future modelling efforts would be better expended at refining existing models of binaural interaction to include such an averaging mechanism.

The simple model presented in this study may be useful in situations where a quick, rough estimate of the relative usefulness of interaural time and interaural intensity cues are needed. The ability to predict which interaural difference is important at a given frequency for a particular binaural task can help in the

fitting and development of binaural hearing aids. The binaural hearing aid could be adjusted so as to match residual binaural hearing. For example, subject VF might be fitted with hearing aids designed to preserve the interaural time characteristics of the stimuli near 500 Hz in order to match her residual time sensitivity. Moreover, one could also enhance the stimulus interaural differences in order to compensate for impaired sensitivities. It may be possible to magnify the interaural intensity differences through differential interaural scaling and match an impaired subject's residual intensity sensitivity.

In addition, although the model was developed with a certain set of stimuli and experiments in mind, there is no reason why it cannot be applied to other binaural experiments. All that is needed is a characterization of the stimuli used in the experiments in terms of the stimulus interaural time (phase) and intensity differences. Specifically, a model of this type will be able to correctly predict masked time discrimination results (Ito et al., 1982 ; Stern et al., 1983).

Moreover, although only bilaterlly symmetric hearing-loss subjects were tested in this study, the model developed in this study should also be useful in relating interaural time and intensity discrimination to correlation discrimination and binaural detection tasks for other types of hearing impairments.

Appendix I

Waveform Generation

Our waveforms are sample functions from zero mean, Gaussian process which is periodic in some interval T. The sample function n(t) of bandwidth W and center frequency fo can be decomposed into a finite Fourier series in the interval 0 < t < T as shown below ;

$$n(t) = \sum_{n=-N/2}^{N/2} |A_n| \cos[2\pi(f_c + nf_o)t + \varphi_{A_n}]$$

where

$$A_n = \frac{2}{T}\int_0^T n(t)\, e^{-j2\pi(f_c + nf_o)t}\, dt \quad ; \quad f_o = \frac{1}{T} \;,\; Nf_o = W$$

It can be shown (Davenport and Root, 1958) that the $|A_n|$ are random variables with a Rayleigh probability density distribution and the φ_{A_n} are uniformly distributed in the interval from $-\pi$ to π . Below is a Fortran listing of the program used to generate the noise waveforms used in both the experimental portion of this study and in the waveform analysis section.

```
!       Program  NOISE.FOR
!
!       Generates Gaussian noise waveforms of any given
!       bandwidth and level (< 110 dB SPL) by using sums of
!       random amplitude, random phase cosines.  The program
!       also generates the Hilbert transforms of the noise
!       waveforms by creating corresponding sums of
!       sines waveforms.

        real*4 uniform,rayleigh,freq,amp,pha,temp,pi,magsq
        real*4 array(0:1023),A,P,F,comp
        integer*2 cnoise(0:1023),snoise(0:1023),tbuff(0:1023),fileid
        integer*4 lo_freq,hi_freq,in_freq,ncomp
        integer*4 seed,idbn,creabn,putbn,index,i
        character*13 fulnam
        character*9 filnam
        character*4 ext


        pi=3.14159265
        temp=seconds(0.0)
        seed=jint(temp)

        call clear_screen
        type *,'Enter low, high and incremental freq; level and'
        type *,'       waveform family file name and number'

        accept *,lo_freq,hi_freq,in_freq,level,filnam,fileid


        ncomp=((hi_freq - lo_freq)/in_freq) + 1
        comp =10*alog10(floatj(ncomp))
        power=2.62*exp(.2303*(level - comp - 30.0))

        do i = lo_freq,hi_freq,in_freq


           uniform=ran(seed)              ! Generate random amplitude
           A=rayleigh(uniform,power)      !
           P=2.*pi*ran(seed)              ! and random phase
           F=floatj(i)

           call wavcos(F,A,P,tbuff,1024)! Generate cos component wave


           do j=0,1023
              cnoise(j)=cnoise(j)+tbuff(j)
           enddo


           call wavsin(F,A,P,tbuff,1024)! Generate sin component wave


           do j=0,1023
              snoise(j)=snoise(j)+tbuff(j)
           enddo


        enddo


        write(ext,10) fileid                        ! Store cos component
10      format('.',I3)                              ! wave as filnam.#
```

```
call closbn(idbn)

write(ext,10) (fileid+64)                    ! Store sin component
fulnam = filnam//ext                         ! wave as filnam.(#+64)
idbn = creabn(fulnam,2048,0)
call putbn(idbn,snoise,2048)
call closbn(idbn)

end
```

```
      subroutine get_files(buff,nfiles)

      real*2 time,nfiles
      integer*2 buff(2,0:1023),n(2)
      integer*4 idbn,creabn,openbn,getbn,putbn,nbyts,seed
      character*9 filnam
      character*4 ext
      character*13 fulnam

      time = secnds(0.0)                          ! Get seed for the
      seed = jint(time)                           ! random # generator

10    n(1) = iint(nfiles*ran(seed)+0.5)           ! Pick two uncorrelated
      n(2) = iint(nfiles*ran(seed)+0.5)           ! noise files from 1-nfiles
      if ( n(1) .eq. n(2) ) go to 10

      do i = 1,2                                  ! Put file contents into
                                                  ! buff(1) and buff(2)
         write(ext,20) n(i)
20       format('.',I3)

         fulnam = filnam//ext

         idbn   = openbn(fulnam,1)
         nbyts  = getbn(idbn,buff(i),2048)

         call closbn(idbn)

      enddo

      return
      end
```

```
real*4 amp,freq,level,phase
integer*2 buff(0:1023),bufflen
integer*4 idbn,creabn,openbn,getbn,putbn,nbyts,closbn
character*30 filnam
parameter pi=3.141592654

data bufflen /1024/

call clear_screen
type *,'Enter tone level (dB SPL), frequency and starting phase'

accept *,level,freq,phase,filnam

amp = 1.414*5.12*EXP(0.115*(level - 40))

call wavcos(freq,amp,phase,buff,bufflen)



idbn = creabn(filnam,2048,0)

call putbn(idbn,cnoise,2048)

call closbn(idbn)

end
```

Appendix II

Sequential Testing Methods

An essential element of certain psychophysical experiments is the construction of psychometric functions and concomitantly, the determination of thresholds. Typical experimental methods of testing require estimation of performance at several stimulus values which span the full range of performance (chance to correct response on every stimulus presentation). Prior to the experiment, it is not clear to the experimenter what stimulus values will produce a suitably sampled psychometric function over the desired range of performance. Hence, the experimenter initially selects stimulus values to provide a coarse partitioning of the stimulus range followed by successively finer grain divisions until the final psychometric function is completed. This can require substantial amounts of time, effort and cost to the experimenter. Thus, it is not surprising that a considerable amount of effort has been directed towards the development of efficient procedures for the estimation of psychophysical performance (Taylor and Creelman, 1966; Levitt, 1971).

A. Previous Work

To date, the procedures developed to reduce the amount of data collection have been varieties of stimulus-adaptive methods. Details of these procedures vary across specific implementations,

but, in general, the adaptive methods converge at a single specified level of performance by using several of the most recently presented stimulus values and the corresponding subject responses to modify the stimulus value for the next presentation.

These methods have been and are being used extensively with considerable success. In general, measurements made by these procedures are repeatable, efficient and significantly reduce experimentation time. However, there are a number of critical issues relevant to all adaptive procedures which restrict their generality.

Pollack (1968) in his review of PEST by Taylor and Creelman (1966) identifies at least six parameters of the procedure which must be specified by the experimenter. Of these, three are applicable to most adaptive procedures; the exit criterion, the initial stimulus value, and the step size. Thus, in addition to the assumptions all experimenters need to make concerning the selection of intial stimulus values, the specification of the above parameters requires the experimenter to make arbitrary assumptions about the shape and slope of a subject's psychometric function.

Although the efficiency of the stimulus-adaptive methods is not critically dependent on <u>all</u> of the parameters examined by Pollack, the three mentioned above have a substantial effect on the efficiency of the methods if chosen incorrectly (or, equivalently, if the initial assumptions concerning the subject's psychometric function are false). For instance, a too fine exit criterion or step sizes which are too small (i.e., changes in the stimulus value

have a small effect on performance) increase the number of trials required until convergence, thus reducing the speed and efficiency of the methods.

The above discussion becomes even more critical when applied to testing of hearing impaired subjects. Depending on the particular experiment being performed and the type of hearing impairment, a hearing impaired subject's psychometric function may be (1) normal, (2) shifted ,(3) have a different slope, (4) both (2) and (3), or (5) have a different shape (possibly non-monotonic). Furthermore, it is not clear that stimulus-adaptive methods provide the right kind of training for hearing impaired subjects. In adaptive procedures, a single stimulus value is rarely presented consecutively for more than four trials, hence providing little opportunity for a subject to get acquainted to the task (perception of stimuli near threshold may be radically different at values different than threshold).

B. Sequential Decision and Estimation Procedures

The method presented in this study was motivated by a desire to reduce the number of observations at extremal stimulus values (stimulus values corresponding to performance levels substantially different from a desired performance level) in a fixed-number-of-trials (FNOT) procedure. A typical experiment with this method of testing requires estimation of performance level at several stimulus values. Performance estimates are usually obtained by selecting a particular stimulus value which is fixed throughout the run, presenting a specified, fixed number of trials, recording responses and calculating a percent correct at the end of the run. A pyschometric function is then constructed from 3 to 5 such estimates at each of several stimulus values near and at the stimulus value corresponding to the desired performance level. As stated in the introduction, it is not a priori clear to the experimenter what stimulus values will produce a suitably sampled psychometric function. Hence, in a FNOT procedure, there will necessarily be cases where a considerable number of trials are used to estimate performance at extremal stimulus values.

Most extremal stimulus values correspond to near perfect or chance performance. In each case, after the first 5 to 10 trials it is usually apparent to both the subject and the experimenter that the stimulus value being used is either very easy or very hard to discern. Intuitively, in order to save time and preserve subject

vitality, the experimenter should stop the run without presenting the remaining trials. However, the FNOT procedure requires the continued presentation of all the trials in the run. Practically, an experimenter often implements an arbitrary criterion (e.g., if a subject has 10 consecutive correct responses, then stop) in order to terminate such runs early. In the following sections, we formalize the above intuitive notions about reducing experimental data collection into a systematic, well-defined, objectively implemented rule.

i) Theoretical Development of Sequential Testing

A detailed description and development of sequential analysis can be found in Wald (1945, 1947) and Bernard (1946). In this section, we present the results for a family of sequential tests and apply them to psychophysical procedures.

The general form of the sequential test is similar to the classical hypothesis test. In a conventional, binary hypothesis test, one typically obtains a fixed number of observations, computes the value of a statistic and based on whether this value lies in the acceptance or rejection region, decides to accept or reject the null hypothesis. The acceptance and rejection regions are delineated by a single criterion or several criteria depending on the form of the statistic's conditional density functions, the a priori probabilities of the two hypotheses and the conditional probablities of error.

The sequential tests described here involve the same sort of operations on a statistic, but with three decision regions; (I) stop testing and accept the null hypothesis, (II) stop testing and reject the null hypothesis, or (III) take another observation and repeat the test (until the maximum number of observations have been taken). Moreover, the value of the statistic is updated and compared to the criterion at the end of each observation. Hence, sequential testing affords an opportunity of making an early decision when the null hypothesis is either clearly wrong or clearly right.

Furthermore, unlike the conventional hypothesis tests with constant criteria, the criteria in the sequential tests are also updated at the end of each observation. For the family of sequential tests considered in this paper, the criteria delineating the three decision regions are linear functions of the form (Wald, 1945)

$$C_A(m) = I_A + Sm \qquad (II.1)$$

$$C_R(m) = I + Sm \qquad (II.2)$$

where

$C_A(m)$, $C_R(m)$ = acceptance and rejection criteria

I_A, I_R = acceptance and rejection intercepts

S = slope of the decision lines

m = number of observations

As in classical hypothesis testing, the criteria are functions of the conditional probabilities and the form of the statistic's conditional density functions.

ii) Application to Psychophysical Testing

For the application presented in this study, the decision statistic (the total number of correct responses) can be considered a sum of Bernoulli random variables and the observations are the trials presented in a run. The null "hypothesis" in the psychophysical test is that the subject's performance level (P_S), is greater than or equal to the upper value of the desired performance range (R), about the target level of performance (P_T), i.e., ($P_S \geq P_T + R/2$). The alternative hypothesis is that the subject's performance is less than or equal to the lower value of the range ($P_S < P_T - R/2$). Hence, the total number of correct responses at the end of the mth trial (k(m)) is compared to the values of $C_A(m)$ and $C_R(m)$ and one of the three decisions is made:

if $k(m) > C_A(m)$	; accept the null hypothesis ($P_S > P_T + R/2$)
if $k(m) < C_R(m)$	; reject the null hypothesis ($P_S < P_T + R/2$)
if $C_R(m) < k(m) < C_A(m)$	; present another trial and repeat the test (until the maximum number of trials have been presented) ($\|P_S - P_T\| < R/2$)

The sequential test illustrated in Figure II.1 has been designed for a symmetric, 2I,2AFC experiment. The targeted level was P_T = 75% correct, R = 10% with conditional error probabilities of α (the probability of rejecting the null hypothesis given the null hypothesis is true) and β (the probability of accepting the null hypothesis given the alternative hypothesis is true) equal to 0.05.

Note that the slope of the decision lines, S, is equal to 0.75, the probability of a correct answer at the target performance level. Furthermore, if R is decreased, the two decision lines would be pulled farther apart (but still maintain the same slope and their parallelness), thus making an early termination decision less likely. Finally, by increasing the conditional error probabilities (the testing decision is more prone to error), the lines will come closer together (again with the same slope and parallelness) thereby making an early termination decision more likely.

C. Implementation of the Test

The incorporation of the sequential decision rule is extremely simple. Most psychophysical test keep track of the number of trials presented and the corresponding number of correct responses. If the test is to be implemented on a computer, it is a simple matter to write a subroutine to inspect subject performance at the end of each trial.

If the experiment is being performed without the use of automated equipment, a piece of graph paper (with decision regions drawn on the graph with axes of total number correct (ordinate) versus number of trials presented (abcissa)) can be used to track subject performance and stop the test when the subject's "path" enters one of the two decision regions (see Figure II.1).

As stated in section B-ii, the "null" hypothesis is $|P_S - P_T| < R/2$, i.e. subject performance is inside the desired range about the target performance level. For most psychophysical tests, there is no preference for the type of error made in reaching a decision about the null hypothesis. Hence, α (the probability of incorrectly deciding P_S is outside R) will usually be equal to β (the probability of incorrectly deciding P_S is inside R). Note that the general sequential decision rule does <u>not</u> require these assumptions. The author has made these assumptions (which are valid for most psychophysical experiments) in order to simplify the application of the decision rule. Henceforth, a sequential test with $\alpha = \beta$ will be

referred to as a symmetric sequential test.

For symmetric tests, the acceptance and rejection intercepts, I_A and I_R, are negatives of each other. In addition, the slope of the decision lines is just equal to the probability of a correct response at the target performance level. For example, in the test of Figure II.1, P_T =75 percent correct which implies S = 0.75.

Thus, by specifying P_T, R and γ (the value of both α and β), the experimenter obtains S, I_A and I_R. Figure 4.2 is calculated from the equations below for S and I_A (Wald, 1945)

$$S = \log \frac{1 - (P_T + R/2)}{1 - (P_T - R/2)} \Big/ D$$

$$I_A = -I_R = \log (1-\gamma)/\gamma \Big/ D$$

$$D = \log \frac{P_T + R/2}{P_T - R/2} - \log \frac{1 - (P_T + R/2)}{1 - (P_T - R/2)}$$

and is intended as a graphical, symmetric-sequential-decision-rule parameter computer. Having decided on P_T, one moves vertically until one intersects the desired R curve. The value of I_A (or equivalently, $-I_R$) is the value of the intersection point plotted on the ordinate for three values of γ. The slope S (at the top of the figure, directly opposite the P_T abcissa), although equal to the target P, is provided for completeness.

To provide an illustration of this figure's use, suppose an experimenter wants to apply a symmetric decision rule to an experiment where P_T = 75 percent correct, R = 10 percent (i.e. the interval between 70 and 80 percent correct) and γ = 0.05. From Figure II.2, S is seen to be 0.75 and I_A equal to approximatley 5.5.

D. Statistics of the Test

Recall that the sequential decision rule was motivated by a desire to reduce the number of observations at extremal stimulus values. Thus, a reasonable measure of the sequential test's performance is how well it allocates the number of trials to the desired range of stimulus values.

Figure .3 shows theoretical plots of the average number of trials presented versus subject performance level, P_S , for a symmetric sequential test with P_T = 75 percent correct, R = 10% and γ = 0.05, 0.10 and 0.15 . Note that for the conditional error probabilities considered, the maximum number of trials is always within the range of desired performance levels R. In addition, note that the farther P_S is away form P_T , the less trials are presented at that level.

One way to interpret the advantages of sequential testing over FNOT procedures is that for a fixed number of trials allocated to the measurement of a psychometric function, sequential testing provides better estimates (smaller standard deviations) of subject performance at stimulus values corresponding to and near the threshold. Quantitatively, the amount of the advantage can be illustrated by a graph of the type shown in Figure II.4. As in Figure II.3, the same sample symmetric sequential test is used.

Alternatively, the advantage of a sequential decision rule over an FNOT procedure is that for fixed estimate errors (standard deviations) at stimulus values corresponding to performance levels in R, the sequential test requires approximately 40 % less trial than the FNOT procedure.

The early termination, besides reducing the number of trials, causes a bias in the predicted thresholds at termination. In general, for the tests considered in this study, this bias is negligible, particularly within the desired range of probabilities. Figure II.5 plots the sequential estimate of P_S versus the true P_S. As is evident from the graph, values of P_S greater than $P_T + R/2$ have positive, increasing biases while values of P_S less than $P_T - R/2$ have negative, increasing biases.

All of the above statements remain essentially true for any P chosen, the only major difference being in the place of the maximum, i.e. as stated earlier, the maximum number of trials is always within R. By choosing different Rs and s, one can increase or decrease the degree to which sequential testing provides an improvement over an FNOT procedure, but not the basic advantage of the sequential decision rule.

Finally, an advantage of the sequential decision rule which is hard to quantify is the salutary effect it has on subjects. During the course of using the sequential test in psychophysical tests, the author has found subjects to be more alert during experimental sessions and has found that they maintain a higher level of interest compared to a FNOT procedure.

E. Data Analysis

The above statistical advantages of sequential testing are based on an important assumption. The number correct and the number of trials presented are retained at the end of each run and not just the estimated percent correct. There are two reasons for this : (1) since the number of trials presented during a run is not always the same, different estimates of percent correct at each stimulus value are based on different total number of trials, hence, it is not correct to calculate percent correct estimates from individual runs and average those estimates to obtain a grand average, and (2) the variance of the estimates (due to the random nature of the total number of trials) which are obtained at the end of the run are sufficiently large to negate the reduction in variance usually obtained by averaging percent correct estimates across runs. Hence, at the end of the experimental session, a subject performance at a particular stimulus value is computed from the ratio of the cumulative number correct to the cumulative number of trials presented at that stimulus value.

This is not to say that estimates of percent correct at the end of individual runs are not useful. Estimates should be calculated and used to help the experimenter in deciding where to place the next set of observations.

i) Computation of Percent Correct

We now show an example of how data from a hypothetical sequential experimental session should be analyzed in order to (1) use local estimates for placement of succeeding observations and (2) guarantee reduction in estimate variances. Let

$K_j(X_i)$ = number of correct responses obtained during the jth run using stimulus vaule X_i .

$N_j(X_i)$ = number of trials presented during the jth run using stimulus value X_i .

Suppose we perform an experiment using the sample, sequential decision rule presented in section D. Thus, we are interested in the stimulus value (which for the purposes of this example, will be in some arbitrary units) corresponding to P_T = 75 percent correct. Let us say we initially choose three stimulus values which we believe (either through past experience or through reasonable assumptions regarding the physical nature of the stimulus) to encompass the stimulus threshold. A possible result of testing at these values could be as follows,

$$P(0) = \frac{K1(0)}{N1(0)} \times 100 = 52$$

$$P(1) = \frac{K1(1)}{N1(1)} \times 100 = 64$$

$$P(5) = \frac{K1(5)}{N1(5)} \times 100 = 95$$

We now choose another three stimulus values based on these results. A reasonable set to test next would be any three stimulus values in the interval (1,5). Hence, after the seconds set, we may have

$$P(2) = \frac{K1(2)}{N1(2)} \times 100 = 70$$

$$P(3) = \frac{K1(3)}{N1(3)} \times 100 = 76$$

$$P(4) = \frac{K1(4)}{N1(4)} \times 100 = 84$$

We would continue in this manner, presenting new stimulus values or possibly returning to previously presented stimulus values until our alloted time (or equivalently, the alloted number of trials) had been reached. At the end of the session, we would collect the total number correct and the total number of trials and compute collective, percent correct estimates of subject performance at all the stimulus values presented.

F. Estimation of Thresholds

By plotting the probabilities, P(Xi) versus the stimulus values, Xi, we obtain a psychometric function with constituent points calculated from unequal numbers of observations. As stated in earlier sections, we are interested in extracting that value of the stimulus corresponding to some desired level of performance.

There exist several methods for extracting threshold stimulus values (Ashton, 1972). A method which takes into account the unequal number of observations and at the same time, provides a measure of the statistical goodness of the analysis is the method of Minimum Logit χ^2 (ML χ^2).

As is evinced by the name, this method assumes a quasi-sigmoidal psychometric function which can be described by the logistic curve

$$P(x_i) = \frac{1}{N} + \frac{\frac{N-1}{N}}{1 + e^{-(a+bx)}} \qquad (II.3)$$

where N is equal to the number of alternatives in a forced-choice experimental paradigm.

In most psychophysical experiments, threshold is defined as the stimulus value corresponding to a performance level equal to the geometric mean between the worst possible performance and the best possible performance. Thus, the stimulus value at threshold, X_T, is that value of Xi which satisfies

$$P(X_T) = \frac{N+1}{N} \qquad (II.4)$$

or

$$e^{-(a+bx)} = 1 \qquad (II.5)$$

Therefore,

$$X_T = -\frac{a}{b} \qquad (II.6)$$

Ashton gives formulas for estimating a and b, as well as the cumulative χ^2 score. These formula were used in an analysis program, which took the $K_j(X_i)$s and the $N_j(X_i)$s as input and calculated the stimulus threshold value along with a plot of the psychometric function. Even in cases where the psychometric functions were considerably non-sigmoidal (but still monotonic), the estimate of threshold was close to the visually estimated threshold. However, the estimates for the spread of the psychometric functions deteriorated rapidly for non-sigmoidal functions and were generally not as robust as the threshold estimates.

APPENDIX III

Estimation of Model Parameters

For the development which follows in this appendix we will assume

1. (1) the $\bar{\alpha}$ s and $\bar{\tau}$ s are Gaussian random variables

2. (2) the stimuli used in the interaural time and interaural intensity experiments are perfectly correlated (hence no variability in the interaural differences present in the stimuli)

3. (3) a symmetric, 2I-2AFC experimental paradigm.

We can represent the interaural differences present in each interval of a given presentation by

	Interval 1	Interval 2
Stimulus 1 (S1)	$\Delta\theta/2$	$-\Delta\theta/2$
Stimulus 2 (S2)	$-\Delta\theta/2$	$\Delta\theta/2$

where $\Delta\theta$ = interaural difference, either intensity (α) or time (τ).

I. Separate Differences Assumption

For a single observation of either interaural difference alone, we form a likelihood-ratio-test (LRT) as shown below

$$\frac{f(\bar{\theta}_1 : S2)\, f(\bar{\theta}_2 : S2)}{f(\bar{\theta}_1 : S1)\, f(\bar{\theta}_2 : S1)} \begin{matrix} \text{decide S2} \\ \geq \\ \gamma \\ < \\ \text{decide S1} \end{matrix} \qquad \text{(III.1)}$$

where

$f(\bar{\theta}_i)$ = probability density function of the interaural difference

$\bar{\theta}_i$ = interaural difference observation in the ith interval

γ = decision threshold .

For S1 and S2 equally likely and a minimum probability of error constraint, we have $\gamma = 1$ and hence

$$\frac{e^{-\frac{(\bar{\theta}_1 + \frac{\Delta\theta}{2})^2}{2\sigma^2_{-\frac{\Delta\theta}{2}}}} \; e^{-\frac{(\bar{\theta}_2 - \frac{\Delta\theta}{2})^2}{2\sigma^2_{\frac{\Delta\theta}{2}}}}}{e^{-\frac{(\bar{\theta}_1 - \frac{\Delta\theta}{2})^2}{2\sigma^2_{\frac{\Delta\theta}{2}}}} \; e^{-\frac{(\bar{\theta}_2 + \frac{\Delta\theta}{2})^2}{2\sigma^2_{-\frac{\Delta\theta}{2}}}}} \begin{matrix} S_2 \\ \geq \\ 1 \\ < \\ S_1 \end{matrix} \qquad \text{(III.2)}$$

Taking the ln of both sides and collecting like terms, we get a decision rule of the form

$$l = \bar{\theta}_2 - \bar{\theta}_1 \;\underset{\text{decide S1}}{\overset{\text{decide S2}}{\gtrless}}\; 0 \qquad \text{(III.3)}$$

where l is usually refered to as a sufficient statistic.

Since l is a Gaussian random variable, we can characterize the performance of this test by a quantity known as d (Van Trees, 1968) given by the expression

$$d = \frac{E[\, l : S2 \,] - E[\, l : S1 \,]}{\sqrt{Var[\, l : S2 \,]}} \qquad \text{(III.4)}$$

From equation III.3 and the stimulus presentation structure, we have

$$E[\, l : S2 \,] = \frac{\Delta\theta}{2} - \left(-\frac{\Delta\theta}{2} \right) = \Delta\theta ,$$

$$E[\, l : S1 \,] = -\frac{\Delta\theta}{2} - \left(\frac{\Delta\theta}{2} \right) = -\Delta\theta ,$$

and

$$Var[\, l : S1 \,] = Var[\, l : S2 \,]$$

$$= \mathrm{Var}[\bar{\theta}_2 : S2] + \mathrm{Var}[\bar{\theta}_1 : S2] \; ;$$

but since there is no stimulus difference variability,

$$\mathrm{Var}[\bar{\theta}_2 : S2] = \mathrm{Var}[\bar{\theta}_1 : S2] = \sigma^2_{\theta I}/K$$

where $\sigma^2_{\theta I} = \sigma^2_{\alpha I}$ or $\sigma^2_{\tau I}$.

Therefore,

$$d = \frac{2\,\Delta\theta}{\sqrt{\sigma^2_{\theta I}/K}} = \sqrt{2K}\,\frac{\Delta\theta}{\sigma_{\theta I}} \qquad \text{(III.5)}$$

At threshold, d (for a single observation) is equal to 1 and hence

$$\sigma_{\theta I} = \sqrt{2K}\,(\Delta\theta)_o$$

where $(\Delta\theta)_o$ = threshold interaural difference value. For γ observations,

we have that d increases by a factor of $\sqrt{\gamma}$ and hence

$$\sigma_{\theta I} = \sqrt{\frac{2K}{\gamma}}\,(\Delta\theta)_o$$

Thus for $\sigma_{\theta I} = \sigma_{\alpha I}$ we have

$$\sigma_{\alpha I} = \sqrt{\frac{2K}{\gamma}}\,(\Delta\alpha)_o \qquad \text{(III.6 a)}$$

and similarly for time

$$\sigma_{\tau I} = \sqrt{\frac{2K}{\nu}}\ (\Delta\tau)_0 \qquad \text{(III.6 b)}$$

II. Fixed, Weighted Linear Sum Assumption

We now assume a single, compound binaural difference variable of the form

$$B = \bar{\alpha} + b\,\bar{\tau}\ .$$

Assuming a single observation of the combined differences, we can perform a LRT and obtain a decision rule identical to the one in equation III.3 . Unlike the development in section I however,

$$E[\ 1 : S2\ ] = \Delta\Theta\ ,$$

$$E[\ 1 : S1\ ] = -\Delta\Theta\ ,$$

and

$$Var[\ 1 : S2\ ] = Var[\ 1 : S1\ ] = (\sigma^2_{\alpha I} + b\,\sigma^2_{\tau I})\ /\ K$$

Thus,

$$d = \frac{2\,\Delta\Theta}{\sqrt{(\sigma^2_{\alpha I} + b^2\sigma^2_{\tau I})/K}}$$

or at threshold

$$\sqrt{\sigma_{\alpha I}^2 + b^2\sigma_{\tau I}^2} = \sqrt{2K}\,(\Delta\theta)_o .$$

For intensity discrimination experiments, $(\Delta\theta) = (\Delta\alpha)$ or

$$\sqrt{\sigma_{\alpha I}^2 + b^2\sigma_{\tau I}^2} = \sqrt{2K}\,(\Delta\alpha)_o ,$$

and

$$\sqrt{\sigma_{\alpha I}^2 + b^2\sigma_{\tau I}^2} = \sqrt{2K}\; b\,(\Delta\tau)_o .$$

For γ independent observations of the compound variable, we have

$$\sqrt{\sigma_{\alpha I}^2 + b^2\sigma_{\tau I}^2} = \sqrt{2K/\gamma}\,(\Delta\alpha)_o , \qquad \text{(III.7a)}$$

and

$$\sqrt{\sigma_{\alpha I}^2 + b^2\sigma_{\tau I}^2} = \sqrt{2K/\gamma}\; b\,(\Delta\tau)_o \qquad \text{(III.7b)}$$

Note that with the fixed, weighted sum assumption, there is effectively only one source of processing noise in the system. Therfore, Equations III.7a,b imply that b must equal $(\Delta\alpha)_o/(\Delta\tau)_o$. In addition, note that the values of $\sigma_{\alpha I}$ and $\sigma_{\tau I}$ will be smaller (even though we cannot estimate them) under the fixed-sum assumption than in the separate differences assumption.

Appendix IV

Predictor Equations for Correlation Discrimination and Binaural Detection

For the development which follows in this appendix, we will assume

1. (1) the $\bar{\alpha}$ s and $\bar{\tau}$ s are Gaussian random variables

2. (2) the means of the $\bar{\alpha}$ s and $\bar{\tau}$ s are equal to zero

3. (3) the variances of the $\bar{\alpha}$ s and $\bar{\tau}$ s are equal to the scaled sum of the processing noise variance and the variance in the stimulus differences

4. (4) a symmetric, 2I-2AFC experimental paradigm

We can represent the stimulus parameters in each interval of a given presentation by

	Interval 1	2
Stimulus 1 (S1)	R	T
Stimulus 2 (S2)	T	R

where

R = reference stimulus value

T = test stimulus value

A. Separate Differences Assumption

As in Appendix III, for a single observation of either interaural difference alone, we can form a LRT of the

$$\frac{e^{-\frac{\bar{\theta}_1^2}{2\sigma^2_{\bar{\theta},T}}} \; e^{-\frac{\bar{\theta}_2^2}{2\sigma^2_{\bar{\theta},R}}}}{e^{-\frac{\bar{\theta}_1^2}{2\sigma^2_{\bar{\theta},R}}} \; e^{-\frac{\bar{\theta}_2^2}{2\sigma^2_{\bar{\theta},T}}}} \begin{matrix} S_2 \\ \geq \\ < \\ S_1 \end{matrix}$$

where

$$\sigma^2_{\bar{\theta},R} = (1/K)[\sigma^2_{\theta R} + \sigma^2_{\theta I}]$$

$$\sigma^2_{\bar{\theta},T} = (1/K)[\sigma^2_{\theta T} + \sigma^2_{\theta I}]$$

$\sigma^2_{\theta R}$ = stimulus interaural difference

variance for the reference value

$\sigma^2_{\theta T}$ = stimulus interaural difference

variance for the test value

where the subscript I denotes internal.

Taking the ln of both sides and collecting terms, we get a decision rule of the form

$$l = \bar{\theta}_1^{\,2} - \bar{\theta}_2^{\,2} \;\underset{\text{decide S1}}{\overset{\text{decide S2}}{\gtrless}}\; 0 \qquad \text{(IV.1)}$$

Alternatively, we can express this rule as

$$\frac{\bar{\theta}_1^{\,2}}{\bar{\theta}_2^{\,2}} \;\underset{\text{decide S1}}{\overset{\text{decide S2}}{\gtrless}}\; 1 \; .$$

Dividing each of the $\bar{\theta}_i^{\,2}$ by $\sigma^2_{\bar{\theta}_i}$ we get

$$\frac{\bar{\theta}_1^{\,2}/\sigma^2_{\bar{\theta}_1}}{\bar{\theta}_2^{\,2}/\sigma^2_{\bar{\theta}_2}} \;\underset{S_1}{\overset{S_2}{\gtrless}}\; \frac{\sigma^2_{\bar{\theta}_2}}{\sigma^2_{\bar{\theta}_1}}$$

Thus, our test is now equivalent to

$$F(1,1) \underset{S_1}{\overset{S_2}{\gtrless}} \sigma^2_{\bar{\theta}_2} / \sigma^2_{\bar{\theta}_1}$$

where F(1,1) is an F-distributed random variable with $\gamma_1 = \gamma_2 = 1$ degree of freedom. For γ independent observations, we have

$$F(\gamma,\gamma) \underset{S_1}{\overset{S_2}{\gtrless}} \sigma^2_{\bar{\theta}_2} / \sigma^2_{\bar{\theta}_1}$$

We can characterize the performance in such a test by directly computing the probability of a correct decision. Since the test is symmetric (S1 is equally as likely as S2) we have

$$P(\text{correct}) = \frac{1}{2}\left[P\left(F(\gamma,\gamma) > \frac{\sigma^2_{\bar{\theta}_2}}{\sigma^2_{\bar{\theta}_1}} \mid S_2 \right) + P\left(F(\gamma,\gamma) < \frac{\sigma^2_{\bar{\theta}_2}}{\sigma^2_{\bar{\theta}_1}} \mid S_1 \right) \right]$$

Furthermore, from the reciprocity rules of the F-distribution

$$P(\text{correct}) = P\left[F(\gamma,\gamma) > \frac{\sigma^2_{\bar{\theta}_2}}{\sigma^2_{\bar{\theta}_1}} \mid S_2 \right]$$

For P(correct) = 0.75 (threshold level of performance), we have that

$$\frac{\sigma^2_{\bar{\theta}_2}}{\sigma^2_{\bar{\theta}_1}} = \frac{\sigma^2_{\theta,R}}{\sigma^2_{\theta,T}} = \frac{1}{F_{.25}(\gamma,\gamma)}$$

where $F_{.25}(\gamma;\gamma)$ = the value of an $F(\gamma,\gamma)$ distributed random variable such that the cumulative is evaluated at this value is equal to 0.25 . Therefore, at threshold, we must have the following relationship hold for the ratio of the variances

$$\frac{1/K\left[\sigma^2_{\theta I} + \sigma^2_{\theta R}\right]}{1/K\left[\sigma^2_{\theta I} + \sigma^2_{\theta T}\right]} = \frac{1}{F_{.25}(\gamma,\nu)}$$

or

$$\frac{\sigma^2_{\theta I} + \sigma^2_{\theta T}}{\sigma^2_{\theta I} + \sigma^2_{\theta R}} = F_{.25}(\gamma,\nu) \qquad \text{(IV.3)}$$

For reference stimuli values with no stimulus interaural difference variability, $\sigma^2_{\theta R} = 0$, equation iV.3 reduces to

$$1 + \frac{\sigma^2_{\theta T}}{\sigma^2_{\theta I}} = F_{.25}(\gamma,\nu) \qquad \text{(IV.4)}$$

From Appendix III, we have

$$\sigma^2_{\theta I} = \frac{2K}{\nu}(\Delta\theta)_0^2$$

thus,

$$\frac{\sigma^2_{\theta T}}{\frac{2K}{\nu}(\Delta\theta)_0^2} = F_{.25}(\gamma,\nu) - 1$$

or

$$\frac{\sigma^2_{\theta T}}{(\Delta\theta)_0^2} = \frac{2K}{\nu}\left[F_{.25}(\gamma,\nu) - 1\right] \qquad \text{(IV.5)}$$

i) Intensity Alone

For $\theta = \alpha$ alone, we get

$$\frac{\sigma_{\alpha T}}{(\Delta\alpha)_0} = \sqrt{\frac{2K}{\nu}\left[F_{1,25}(\gamma,\nu)-1\right]}$$

ii) Time Alone

For $\theta = \tau$ alone, we get

$$\frac{\sigma_{\epsilon T}\, C_\varphi}{(\Delta\tau)_0} = \sqrt{\frac{2K}{\nu}\left[F_{1,25}(\gamma,\nu)-1\right]}$$

where $C_\varphi = 10^6/2\pi f_0$ usec/rad, a conversion factor from phase to time in usecs.

iii) Weighted Linear Sum

For

$\bar{\theta} = \bar{\alpha} + \frac{(\Delta\alpha)_0}{(\Delta\tau)_0}\bar{\tau}$, we have

$$\sigma^2_{\theta I} = \frac{4k}{\gamma}(\Delta\alpha)_0^2$$

and hence, at threshold

$$\sqrt{\frac{1}{2}\left[\frac{\sigma_{\alpha T}^2}{(\Delta\alpha)_0^2} + \frac{\sigma_{\varphi T}^2 C_\varphi^2}{(\Delta\tau)_0^2}\right]} = \sqrt{\frac{2K}{\gamma}\left[F_{1,25}(\gamma,\nu)-1\right]}$$

iv) Optimal Combination Rule

For a single observation of both interaural differences, we have

$$\frac{e^{-\frac{\bar{\alpha}_1^2}{2\sigma_{\alpha,T}^2}} e^{-\frac{\bar{\tau}_1^2}{2\sigma_{\tau,T}^2}} e^{-\frac{\bar{\alpha}_2^2}{2\sigma_{\alpha,R}^2}} e^{-\frac{\bar{\tau}_2^2}{2\sigma_{\tau,R}^2}}}{e^{-\frac{\bar{\alpha}_1^2}{2\sigma_{\alpha,R}^2}} e^{-\frac{\bar{\tau}_1^2}{2\sigma_{\tau,R}^2}} e^{-\frac{\bar{\alpha}_2^2}{2\sigma_{\alpha,T}^2}} e^{-\frac{\bar{\tau}_2^2}{2\sigma_{\tau,T}^2}}} \quad \begin{matrix} \text{decide S2} \\ \geq \\ 1 \\ < \\ \text{decide S1} \end{matrix}$$

Taking the log of both sides and collecting terms we have,

$$(\bar{\alpha}_1^2 - \bar{\alpha}_2^2)\left[\frac{1}{\sigma_{\alpha,R}^2} - \frac{1}{\sigma_{\alpha,T}^2}\right] + (\bar{\tau}_1^2 - \bar{\tau}_2^2)\left[\frac{1}{\sigma_{\tau,R}^2} - \frac{1}{\sigma_{\tau,T}^2}\right] \begin{matrix} S_2 \\ \geq \\ < \\ S_1 \end{matrix} 0$$

or

$$(\bar{\alpha}_1^2 - \bar{\alpha}_2^2) + d^2(\bar{\tau}_1^2 - \bar{\tau}_2^2) \begin{matrix} S_2 \\ \geq \\ < \\ S_1 \end{matrix} 0$$

where

$$d^2 = \frac{\sigma_{\alpha,R}^2 \sigma_{\alpha,T}^2}{\sigma_{\tau,R}^2 \sigma_{\tau,T}^2} \frac{\sigma_{\tau,T}^2 - \sigma_{\tau,R}^2}{\sigma_{\alpha,T}^2 - \sigma_{\alpha,R}^2}$$

B. Sum of Interaural Differences (SID)

For a composite interaural difference of the form

$$B = \bar{\alpha} + \frac{(\Delta\alpha)_0}{(\Delta\tau)_0}\bar{\tau},$$

the calculations of performance up to a critical variance ratio are identical to the calculations of section I. Hence, we can begin our analysis at equation IV.3 or

$$\frac{\sigma_{BI}^2 + \sigma_{BT}^2}{\sigma_{BI}^2 + \sigma_{BR}^2} = F_{.25}(\gamma,\nu) \qquad (IV.6)$$

where

$$\sigma_{BT}^2 = \sigma_{\alpha T}^2 + \frac{(\Delta\alpha)_0^2}{(\Delta\tau)_0^2}\sigma_{\tau T}^2$$

and from appendix III,

$$\sigma_{BI}^2 = \frac{2K}{\gamma}\cdot(\Delta\alpha)_0^2$$

Therefore, combining the above equation with equation IV.6,

$$1 + \frac{\sigma_{BT}^2}{\sigma_{BI}^2} = F_{.25}(\gamma,\nu)$$

or

$$\frac{\sigma_{BT}^2}{(\Delta\alpha)_0^2} = \frac{2K}{\gamma}\left[F_{.25}(\gamma,\nu) - 1\right]$$

Finally,

$$\sqrt{\frac{\sigma_{\alpha T}^2}{(\Delta\alpha)_0^2} + \frac{C_\phi^2 \sigma_{\phi T}^2}{(\Delta\tau)_0^2}} = \sqrt{\frac{2K}{\nu}\left[F_{.125}(\nu,\nu) - 1\right]}$$

FOOTNOTES

(1) Although both A(t) and φ(t) are bandlimited functions, it is not clear that the interaural intensity difference ($20\log\left|\frac{A_R(t)}{A_L(t)}\right|$) and the interaural phase difference ($\varphi_R(t) - \varphi_L(t)$) are necessarily bandlimited. Clearly, since the phase difference is a linear operation on the right and left phase terms, it is bandlimited. The interaural intensity difference is not as easy to analyze, but the log transformation has been observed (Braida, private communications) to not significantly alter the spectral properties of bandlimited speech waveforms.

(2) In order for the average of the phase terms to converge to a Gaussian, one must be careful in defining what is meant by the average. When phase estimates are averaged, their distributions are convolved. For non-circular functions, this succesive averaging, and concomitantly the successive convolving of the distributions, produces estimate average distributions which approach that of a Gaussian. However, for a circular function such as the phase, succesive averaging may not necessarily result in an increasingly Gaussian average estimate distribution. This is primarily due to the fact that succesive <u>circular convolutions</u> do not converge under certain conditions. Such a condition occurs when the phase is uniformly distributed between $-\pi$ and π (e.g, corresponding to $\rho = 0$). Regardless of the number of phase sample estimates averaged, the resulting average estimate distribution will still be a uniform distribution.

Table 3.1

Presentation Levels Of Noise Waveforms
(dB SPL, total noise power)

	Noise Center Frequency				
	250	500	1000	2000	4000
High-Frequency Loss Listeners	50	50	60	75	90
Flat Loss Listener	90	90	90	90	90
MS Listener	50	50	50	50	30

Table 7.1

Noise Center Frequency	$\sqrt{\frac{2k}{\nu}\left[F_{.125}(\nu,\nu)-1\right]}$
250	14.0
500	6.3
1000	4.3
2000	2.0
4000	1.5

FIGURE CAPTIONS

Figure 2.1 Interaural time jnds as a function of the noise center frequency for normal listeners. (▽) Klump and Eady, (△) Hawkins, (□) McFadden and Pasanen, (+) Henning, and (o) Bernstein and Trahiotis.

Figure 2.2 Interaural intensity jnds as a function of the noise center frequency for normal listeners. (△) Hawkins, (▽) Zurek and Leshowitz and (▷–□) Durlach and Colburn.

Figure 2.3 NOSO and NOSπ detection thresholds as a function of the noise center frequency for normal listeners. (▽) Hirsch and Webster, (□) Bourbon, (△) Wightman and (o) Zurek.

Figure 2.4 Block-box description of a general model of binaural interaction (from Colburn and Durlach, 1978).

Figure 3.1 Audiogram of subject FG, a high-frequency loss listener.

Figure 3.2 Audiogram of subject DH, a high-frequency loss listener.

Figure 3.3 Audiogram of subject VF, a flat-loss listener.

Figure 3.4 Audiogram of subject CS, an MS patient.

Figure 3.5 Representative psychometric function for one of the normal subjects in the NOSπ detection task at 2000 Hz.

Figure 3.6 Representative psychometric function for one of the impaired listeners in the NOSπ detection task at 4000 Hz.

Figure 4.1 Average interaural time jnds for normal subjects in an ancillary experiment of this study (▼—▼), along with results of Figure 2.1.

Figure 4.2 Average interaural intensity jnds for normal subjects in an ancillary experiment of this study (▼—▼), along with results of Figure 2.2.

Figure 4.3 Average interaural correlation jnds for normal subjects in an ancillary experiment of this study (▼—▼), along with a result from Gabriel and Colburn (1981).

Figure 4.4 Average NOSO and NOSπ detection thresholds for normal subjects in an ancillary experiment of this study (▼—▼), along with results of Figure 2.3.

Figure 4.5 Interaural time jnds for subject FG as a function of the noise center frequency.

Figure 4.6 Interaural time jnds for subject DH as a function of the noise center frequency.

Figure 4.7 Interaural time jnds for subject VF as a function of the noise center frequency.

Figure 4.8 Interaural time jnds for subject CS as a function of the noise center frequency.

Figure 4.9 Interaural intensity jnds for subject FG as a function of the noise center frequency.

Figure 4.10 Interaural intensity jnds for subject DH as a function of the noise center frequency.

Figure 4.11 Interaural intensity jnds for subject VF as a function of the noise center frequency.

Figure 4.12 Interaural intensity jnds for subject CS as a function of the noise center frequency.

Figure 4.13 Interaural correlation jnds for subject FG as a function of the noise center frequency.

Figure 4.14 Interaural correlation jnds for subject DH as a function of the noise center frequency.

Figure 4.15 Interaural correlation jnds for subject VF as a function of the noise center frequency.

Figure 4.16 Interaural correlation jnds for subject CS as a function of the noise center frequency.

Figure 4.17 NOSO (Δ—Δ) and NOSπ (∇--∇) detection thresholds for subject FG as a function of the noise center frequency.

Figure 4.18 NOSO (Δ--Δ) and NOSπ (∇--∇) detection thresholds for subject DH as a function of the noise center frequency.

Figure 4.19 NOSO (Δ--Δ) and NOSπ (▽--▽) detection thresholds for subject VF as a function of the noise center frequency.

Figure 4.20 NOSO (Δ--Δ) and NOSπ (▽--▽) detection thresholds for subject CS as a function of the noise center frequency.

Figure 4.21 Binaural Time Audiograms for subjects FG (▽), DH (Δ), VF (+), and CS (◇).

Figure 4.22 Binaural Intensity Audiograms for subjects FG (▽), DH (Δ), VF (+), and CS (◇).

Figure 4.23 Binaural Correlation Audiograms for subjects FG (▽), DH (Δ), VF (+), and CS (◇).

Figure 4.24 Scatter plot of interaural time jnds versus interaural intensity jnds.

Figure 4.25 Scatter plot of interaural time jnds versus interaural correlation jnds.

Figure 4.26 Scatter plot of interaural time jnds versus NOSπ thresholds.

Figure 4.27 Scatter plot of interaural intensity jnds versus interaural correlation jnds.

Figure 4.28 Scatter plot of interaural intensity jnds versus NOSπ thresholds.

Figure 4.29 Scatter plot of interaural correlation jnds versus NOS thresholds.

Figure 4.30 Scatter plot of interaural time jnds versus hearing loss.

Figure 4.31 Scatter plot of interaural intensity jnds versus hearing loss.

Figure 4.32 Scatter plot of interaural correlation jnds versus hearing loss.

Figure 4.33 Scatter plot of NOSπ detection threshold versus hearing loss.

Figure 5.1 Block-box description of the general model of binaural interaction used in this study.

Figure 5.2 The separate-interaural-differences assumption (a) and the Sum of Interaural Differences (SID) assumption (b).

Figure 6.1 Probability density distribution of interaural intensity differences for ρ = 0.995.

Figure 6.2 Probability density distribution of interaural intensity differences for ρ = 0.8.

Figure 6.3 Probability density distribution of interaural intensity differences for ρ = 0.0

Figure 6.4 Probability density distribution of interaural phase differences for $\rho = 0.995$

Figure 6.5 Probability density distribution of interaural phase differences for $\rho = 0.8$

Figure 6.6 Probability density distribution of interaural phase differences for $\rho = 0.0$

Figure 6.7 Probability density distribution of interaural intensity differences for 10log(S/N) = -26.0 dB.

Figure 6.8 Probability density distribution of interaural intensity differences for 10log(S/N) = -22.0 dB.

Figure 6.9 Probability density distribution of interaural intensity differences for 10log(S/N) = 0.0 dB.

Figure 6.10 Probability density distribution of interaural phase differences for 10log(S/N) = -26.0 dB.

Figure 6.11 Probability density distribution of interaural phase differences for 10log(S/N) = -22.0 dB.

Figure 6.12 Probability density distribution of interaural phase differences for 10log(S/N) = 0.0 dB.

Figure 6.13 Plot of interaural intensity variance as a function of the waveform correlation.

Figure 6.14 Plot of interaural phase variance as a function of the waveform correlation.

Figure 6.15 Plot of interaural intensity variance as a function of signal-to-noise ratio in an NOSπ paradigm.

Figure 6.16 Plot of interaural phase variance as a function of signal-to-noise ration in an NOSπ paradigm.

Figure 7.1 Probability density distribution of averaged interaural intensity differences for $\rho = 0.995$. Solid curve is distribution obtained by numerical simulation, dashed curve is Gaussian distribution with the same mean and variance.

Figure 7.2 Probability density distribution of averaged interaural intensity differences for $\rho = 0.8$. Solid curve is distribution obtained by numerical simulation, dashed curve is Gaussian distribution with the same mean and variance.

Figure 7.3 Probability density distribution of averaged interaural phase differences for $\rho = 0.995$. Solid curve is distribution obtained by numerical simulation, dashed curve is Gaussian distribution with the same mean and variance.

Figure 7.4 Probability density distribution of averaged interaural phase differences for $\rho = 0.8$. Solid curve is distribution obtained by numerical simulation, dashed curve is Gaussian distribution with the same mean and variance.

Figure 7.5 Probability density distribution of averaged interaural intensity differences for 10log(S/N) = -26.0 dB. Solid curve is distribution obtained by numerical simulation, dashed curve is Gaussian distribution with the same mean and variance.

Figure 7.6 Probability density distribution of averaged interaural intensity differences for 10log(S/N) = -22.0 dB. Solid curve is distribution obtained by numerical simulation, dashed curve is Gaussian distribution with the same mean and variance.

Figure 7.7 Probability density distribution of averaged interaural phase differences for 10log(S/N) = -26.0 dB. Solid curve is distribution obtained by numerical simulation, dashed curve is Gaussian distribution with the same mean and variance.

Figure 7.8 Probability density distribution of averaged interaural phase differences for 10log(S/N) = -22.0 dB. Solid curve is distribution obtained by numerical simulation, dashed curve is Gaussian distribution with the same mean and variance.

Figure 8.1 Correlation predictions of the optimal combination (▽) and a linear combination rule (△) along with observed, normal performance (▽--▽).

Figure 8.2 NOS π detection threshold predictions of the optimal combination (▽) and a linear combination rule (△) along with observed, normal performance (▽--▽).

Figure 8.3 Correlation jnd predictions of the SID rule using equal Ks for time and intensity averaging (Δ——Δ), along with observed correlation jnds (∇- - -∇) for normal listeners.

Figure 8.4 Correlation jnd prediction of time alone rule (Δ——Δ) along with observed correlation jnds (∇- - -∇) for normal listeners.

Figure 8.5 Correlation jnd predictions using intensity alone (Δ——Δ)) along with observed correlation jnds for normal listeners(∇--∇)

Figure 8.6 NOSπ detection threshold predictions using the SID (Δ——Δ) , along with observed thresholds (∇--∇) for normal listeners.

Figure 8.7 NOSπ detection threshold predictions usning time alone (Δ——Δ) along with observed thresholds (∇--∇) for normal listeners.

Figure 8.8 NOSπ detection thresholds using intensity alone (Δ——Δ) along with observed thresholds (∇- - -∇) for normal listeners.

Figure 8.9 Variance threshold values as a function of noise center frequency for four values of K.

Figure 8.10 Correlation predictions using time alone versus noise center frequency for K = 10 (∇), K = 20 (Δ), K = 40 (□) and K = 80 (o).

Figure 8.11 Correlation predictions using intensity alone versus noise center frequency for K = 10 (∇), K = 20 (Δ), K = 40 (□) and K = 80 (o).

Figure 8.12 NOSπ threshold predictions using time alone versus noise center frequency for K = 10 (∇), K = 20 (Δ), K = 40 ($\square$) and K = 80 (o).

Figure 8.13 NOSπ threshold predictions using intensity alone versus noise center frequency for K = 10 (∇), K = 20 (Δ), K = 40 ($\square$) and K = 80 (o).

Figure 8.14 Modified SID rule model with different averaging lengths (Ks) for interaural time and intensity estimates.

Figure 8.15 Correlation jnd predictions using the SID rule (Δ—Δ) along with observed correlation jnds for normal listeners (∇--∇).

Figure 8.16 NOSπ detection threshold predictions using the SID rule (Δ—Δ) along with observed thresholds for normal listeners (∇--∇).

Figure 8.17 Correlation jnd prediction of the SID rule (Δ——Δ) along with observed correlation jnds (∇--∇) for subject FG.

Figure 8.18 Correlation jnd prediction using time alone (Δ——Δ) along with observed correlation jnds (∇--∇) for subject FG.

Figure 8.19 Correlation jnd predictions using interaural intensity differences alone (Δ——Δ) along with observed correlation jnds (∇--∇) for subject FG.

Figure 8.20 Correlation jnd prediction of the SID rule (Δ——Δ) along with observed correlation jnds (∇--∇) for subject DH.

Figure 8.21 Correlation jnd prediction using time alone (Δ——Δ) along with observed correlation jnds (▽--▽) for subject DH.

Figure 8.22 Correlation jnd predictions using interaural intensity differences alone (Δ——Δ) along with observed correlation jnds (▽--▽) for subject DH.

Figure 8.23 Correlation jnd prediction of the SID rule (Δ——Δ) along with observed correlation jnds (▽--▽) for subject VF.

Figure 8.24 Correlation jnd prediction using time alone (Δ——Δ) along with observed correlation jnds (▽--▽) for subject VF.

Figure 8.25 Correlation jnd predictions using interaural intensity differences alone (Δ——Δ) along with observed correlation jnds (▽--▽) for subject VF.

Figure 8.26 Correlation jnd predictions (Δ——Δ) along with observed correlation jnds (▽--▽) for subject CS.

Figure 8.27 NOSπ threshold predictions of the SID rule (Δ——Δ) along with the observed NOSπ thresholds (▽--▽) for subject FG.

Figure 8.28 NOSπ threshold predictions using interaural time differences alone (Δ——Δ) along with the observed NOSπ thresholds for subject FG(▽--▽).

Figure 8.29 NOSπ threshold predictions using interaural intensity differences alone (Δ——Δ) along with the observed NOSπ thresholds for subject FG(▽--▽).

Figure 8.30 NOSπ threshold predictions of the SID rule (Δ——Δ) along with the observed NOSπ thresholds (∇--∇) for subject DH.

Figure 8.31 NOSπ threshold predictions using interaural time differences alone (Δ—Δ) along with the observed NOSπ thresholds for subject DH(∇--∇)

Figure 8.32 NOSπ threshold predictions using interaural intensity differences alone (Δ——Δ) along with the observed NOSπ thresholds for subject DH(∇--∇

Figure 8.33 NOSπ threshold predictions of the SID rule (Δ——Δ) along with the observed NOSπ thresholds (∇--∇) for subject VF.

Figure 8.34 NOSπ threshold predictions of the SID rule (Δ——Δ) along with the observed NOSπ thresholds (∇--∇) for subject CS.

Figure 8.35 Plot of relative usefulness (in dB) of interaural intensity differences to interaural time differences in correlation discrimination (∇—∇) and NOSπ detection (Δ—Δ) versus center frequency of the noise for normal listeners.

Figure 8.36 Plot of relative usefulness (in dB) of interaural intensity differences to interaural time differences in correlation discrimination (∇——∇) and NOSπ detection (Δ——Δ) versus center frequency of the noise for subject FG.

Figure 8.37 Plot of relative usefulness (in dB) of interaural intensity differences to interaural time differences in correlation discrimination (∇——∇) and NOSπ detection (Δ——Δ) versus center frequency of the noise for subject DH.

Figure A-II.1 Sample performance tracks for Ps = 1.00, 0.75 and 0.5 (———) along with the decision lines (— — —) of the test discussed in the text.

Figure A-II.2 Plot of the decision line intercepts (Ia and Ir) for R = 5, 10, and 15%, and γ = 0.05, 0.10 and 0.15 as a function of P_T.

Figure A-II.3 Plot of the expected value and standard deviations of the number of trials for the sequential test described in the text versus Ps.

Figure A-II.4 Plot of the ratio between the FNOT-estimate standard deviation and the sequential-estimate standard deviation versus Ps.

Figure A-II.5 Plot of the sequentially estimated Ps versus true Ps for the test described in the text.

REFERENCES

Ashton, J. The Logit Transformation 1972 Metheun Monograph on Applied Probability and Statistics. Chapman and Hall, London.

Bernstein, L.R., and Trahiotis, C. Detection of Interaural Delay in High-Frequency Noise, 1982 J. Acoust. Soc. Am. 71, 147-152

Blauert, J. On the Lag of Lateralization Caused by Interaural Time and Intensity Differences, 1972 Audiology 11, 265-270.

Bourbon, W.T. Effect of Bandwidth of Masking Noise on Detection of Homophasic and Antiphasic Tonal Signals, 1966 Unpublished Thesis.

Colburn H.S. Theory of Binaural Interaction Based on Auditory Nerve Data I. General Strategy and preliminary results on interaural discrimination J. Acoust. Soc. Am. 1973, 54, 1458-1470

Colburn H.S., Durlach N.I. Models of Binaural Interaction in Carterette and Friedman, Handbook of Perception, vol. 4, Hearing, pp. 467-518 (Academic Press, New York 1978)

Dahlquist, J. and Bjork, A. Numerical Methods Prentice-Hall 1974 Englewood Cliffs, New Jersey.

Davenport W.B. and Root, W.L. Random Signals and Noise 1958 McGraw-Hill Book Company. New York, N.Y.

Davis, H., and Silverman, S.R. Hearing and Deafness, Holt Rinehart, New York, NY, 1970.

Domnitz R.H., Colburn, H.S. Lateral Position and Interaural Discrimination J. Acoust. Soc. Am. 1977, 61, 1586-1598

Domnitz R.H., Colburn, H.S. Analysis of Binaural Detection Models for Dependence on Interaural Target Parameters. J. Acoust. Soc. Am. 1976, 59, 598-601

Durlach, N.I. Equalization and Cancellation Theory of Binaural Masking-Level Differences 1963 J. Acoust. Soc. Am. 35, 1206-1218.

Durlach N.I., Colburn H.S. Binaural Phenomena in Carterette and Friedman, Handbook of Perception, vol. 4, Hearing, pp. 360-466 (Academic Press, New York 1978)

Durlach N.I., Thompson C.L. and Colburn H.S. Binaural Interaction in Impaired Listeners - A Review of Past Research Audiology 1981, 20 181-211

Gabriel K.J., Colburn H.S. Interaural Correlation Discrimination: I. Bandwidth and Level Dependence J. Acoust. Soc. Am. 1981, 69, 1394-1401

Grantham, D.W. Detectability of Time-Varying Interaural Correlation in Narrowband Stimuli 1982 74, 1185-1194.

Grantham, D.W. Detectability of Time-Varying Interaural Intensity Differences with Narrowband Stimuli 1980 Abstract (S100).

Guinan, J. J., Jr., Norris, B.E., and Guinan, S.S, Single Auditory Units in the Superior Olivary Complex. II. Locations of Unit Categories and Tonotopic Organization, Intern. J. Neuroscience 4: 147-166

Hafter, E.R., Quantitative Evaluation of a Lateralization Model of Masking Level Differences, 1971 50, 1116-1122.

Hausler R., Colburn, H.S. and Marr, E. Sound Localization in Subjects with Impaired Hearing Acta. Otolaryngology. 1983, In press.

Hausler R., Levine R. Brain Stem Auditory Evoked Potentials are Related to Interaural Time Discrimination in Patients with Multiple Sclerosis. Brain Res. July, 1980.

Hawkins, D.B., Interaural Time Discrimination in Hearing-Impaired Listeners, Unpublished Dissertation, Northwestern University, 1977.

Hawkins D.B., Wightman F.F. Interaural Time Discrimination Ability of Listeners with Sensorineural Hearing Loss. Audiology 19, 495-507 (1980)

Henning, G.B., Detectability of Interaural Delay in High-Frequency Complex Waveforms, 1974 J. Acoust. Soc. Am. 55, 84-90.

Hirsch, I.J. and Webster, F.A. Some Determinants of Interaural Phase Effects, 1949 J. Acoust. Soc. Am. 21, 496-501.

Ito, Y. and Colburn, H.S. and Thompson, C.L., Masked Discrimination of Interaural Time Delays with Narrow-Band Signal 1982 J. Acoust. Soc. Am. 72, 1821-1826

Jefferess, L.A. A Place Theory of Sound Localization, 1949 J. of Comparative and Physiological Psychology 41, 35-39.

Jeffress, L.A., Blodgett, H.C., Sandel, T.T. and Wood, C.L., III. Masking of Tonal Signals 1956 J. Acoust. Soc. Am. 28, 416-426.

Jerger J., Jerger S. Critical Evaluation of SAL Audiometry J. Speech and Hearing Res. 8, 103-127 (1965)

Jerger J., Brown, D. and Smith, S., Effect of Peripheral Hearing Loss on the Masking Level Difference, Submitted to Archives of Otolaryngology, 1982.

Johnson and Katz Distributions in Statistics: Continuous Univariate Distributions, Vol. 2. (1970) John Wiley and Sons, Inc. New York, N.Y.

Kearney, J.K. Binaural Intensity Discrimination, M.A. Thesis, University of Texas, 1979.

Kiang, N.Y.S., Watanabe, T., Thomas, E.C., and Clark, L.F. Discharge Patterns of Single Fibers in the Cat's Auditory Nerve M.I.T. Monograph No. 35 (M.I.T. Press: Cambridge, MA) 1965.

Klump, R.G., and Eady, H.R. Some Measurements of Interaural Time Difference Thresholds, J. Acoust. Soc. Am. 28, 859-860

Levine, R.A. Binaural Interaction in Brainstem Potentials of Human Subjects. Ann. Neurol. 9:384-393, 1981

Levitt, H. Transformed Up-Down Methods in Psychoacoustics, 1971 J. Acoust. Soc. Am. 49, 467-477.

Lindemann, W. Evaluation of Interaural Signal Differences, 1982

from Binaural Effects in Normal and Impaired Hearing Scan. Audio. Suppl. 15, 1982.

Lynn G., Gilroy J., Taylor P., Leiser R. Binaural Masking-Level Differences in Neurological Disorders. Acta. Otolaryngol 107, 1981

McFadden D., and Pasanen, E.G. Lateralization at High Frequencies Based on Interaural Time Differences, 1976, J. Acoust. Soc. Am. 59, 634-639.

Mills, A.W. Lateralization of High-Frequency Tones J. Acoust. Soc. Am., 1960, 32, 132-134

Noffsinger D., Olsen W., Carhart R., Hart C., Sahgal V. Auditory and Vestibular Aberrations in Multiple Sclerosis Acta oto-lar, suppl. 303 (1972)

Noffsinger, D. Clinical Application of Selected Binaural Effects from Binaural Effects in Normal and Impaired Hearing Scan. Audio. Suppl. 15, 1982.

Olsen, W., Noffsinger, D. Masking Level Differences For Cochlear and Brain Stem Lesions, 1976 Ann. Otol. Rhino. Lar. 85 820-826.

Osman, E. A Correlation Model of Binaural Masking Level Differences. 1971 J. Acoust. Soc. Am. 50, 1494-1511.

Perrot, D.R. and Musicant, A.D. Rotating Tones and Binaural Beats, J. Acoust. Soc. Am. 1977 61, 1288-1292.

Pollack I., Trittipoe W.J. Binaural Listening and Interaural Noise Cross Correlation J. Acoust. Soc. Am. 1959, 31, 1250-1252 (a)

Pollack I., Trittipoe W.J. Interaural Cross Correlations : Examination of Variables J. Acoust. Soc. Am. 1959, 31, 1616-1618 (b)

Sayers, B. McA., and Cherry, E.C. Mechanism of Binaural Fusion in the Hearing of Speech. 1957 29, 973-987.

Schuknecht, H.F., Presbycusis, Pathology of the Ear, 1974 Harvard University Press, pp. 338-403.

Stern, R.M. and Colburn, H.S. Theory of Binaural Interaction Based on Auditory Nerve Data : IV. A model for subjective lateral position. 1978, J. Acoust. Soc. Am. 64(1), 127-140

Stern, R.M. and, Bachorski, S.J. Dynamic Cues in Binaural Perception 1983 Submitted to J. Acoust. Soc. Am.

Taylor, W. and Creelman, C.D. PEST: Efficient Estimates on Probability Functions, J. Acoust. Soc. Am. 41, 782-787.

Van Trees, H.L., Detection, Estimation and Modulation Theory 1968 John Wiley and Sons, Inc. New York, N.Y.

Wald, A. Sequential Analysis John Wiley and Sons, 1947, New York, N.Y.

Webster, F.A. The Influence of Interaural Phase on Masked Thresholds. I. The Role of Interaural Time-Deviation 1951 J. Acoust. Soc. Am. 23, 452-462.

Widjaja, R.W. The Relationship between Interaural Correlation Discrimination and Binaural Detection Unpublished Report, Feb. 1982

Wightman, F.L. Detection of Binaural Tones as a Function of Masker Bandwidth, 1971 50, 623-636.

Wozencraft, J.M. and Jacobs, I.M. Principles of Communication Engineering 1965 John Wiley and Sons, Inc. New York, N.Y.

Zurek, P.M., and Leshowitz, B. Interaural Amplitude JNDs and Frequency Selectivity, Talk presented at the 91st Acoustical Society Meeting in Austin, Texas (1975).

Zurek, P.M., Durlach, N.I. , Colburn, H.S. and Gabriel, K.J. Masker Bandwidth and the MLD 1983, Abstract presented at the 105th Meeting of the Acoustical Soc. of America.

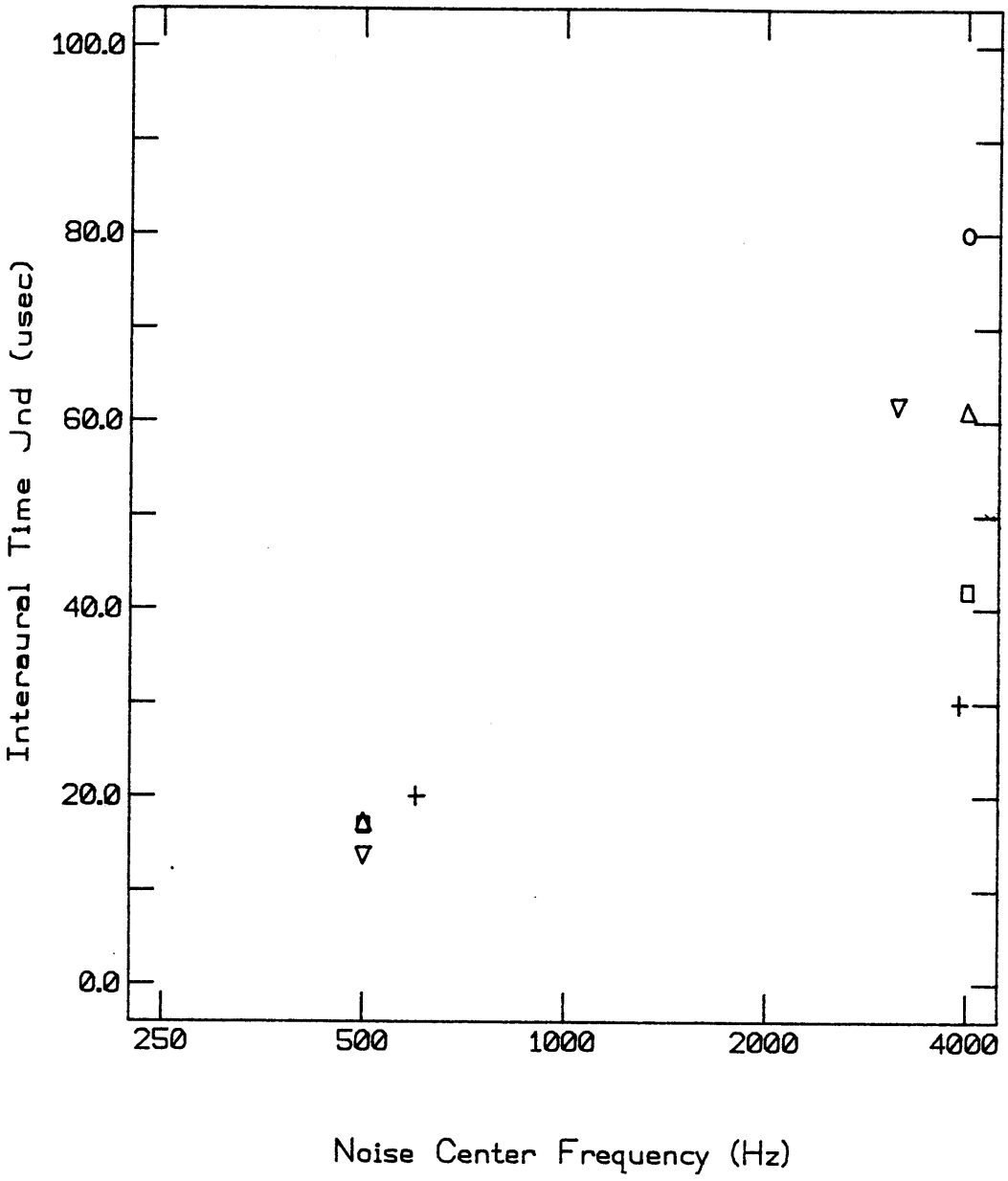
100.0
80.0
60.0
40.0
20.0
0.0
Interaural Time Jnd (usec)
250
500
1000
2000
4000
Noise Center Frequency (Hz)

Figure 2.1

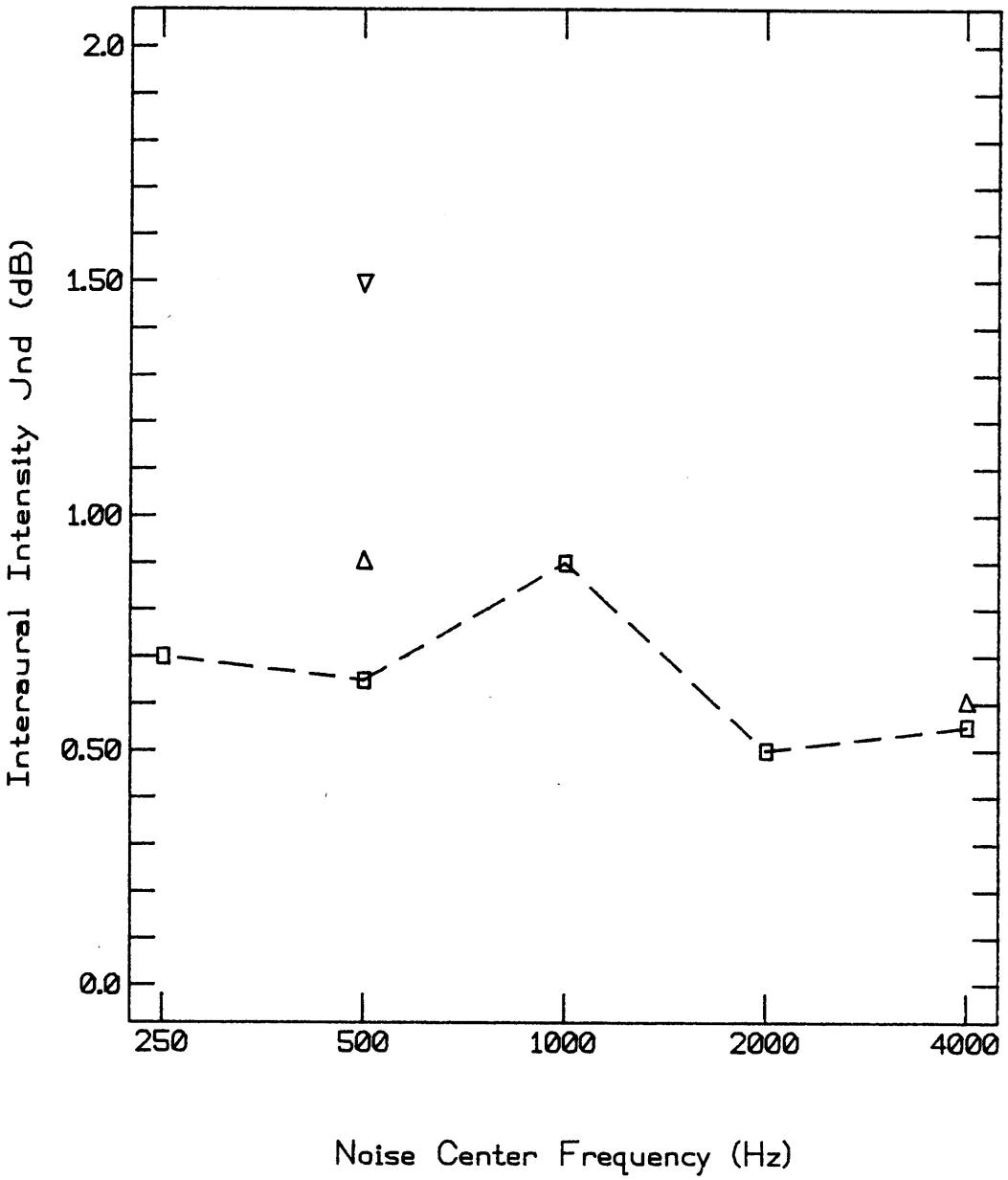
2.0
1.50
1.00
0.50
0.0
Interaural Intensity Jnd (dB)
250
500
1000
2000
4000
Noise Center Frequency (Hz)

Figure 2.2

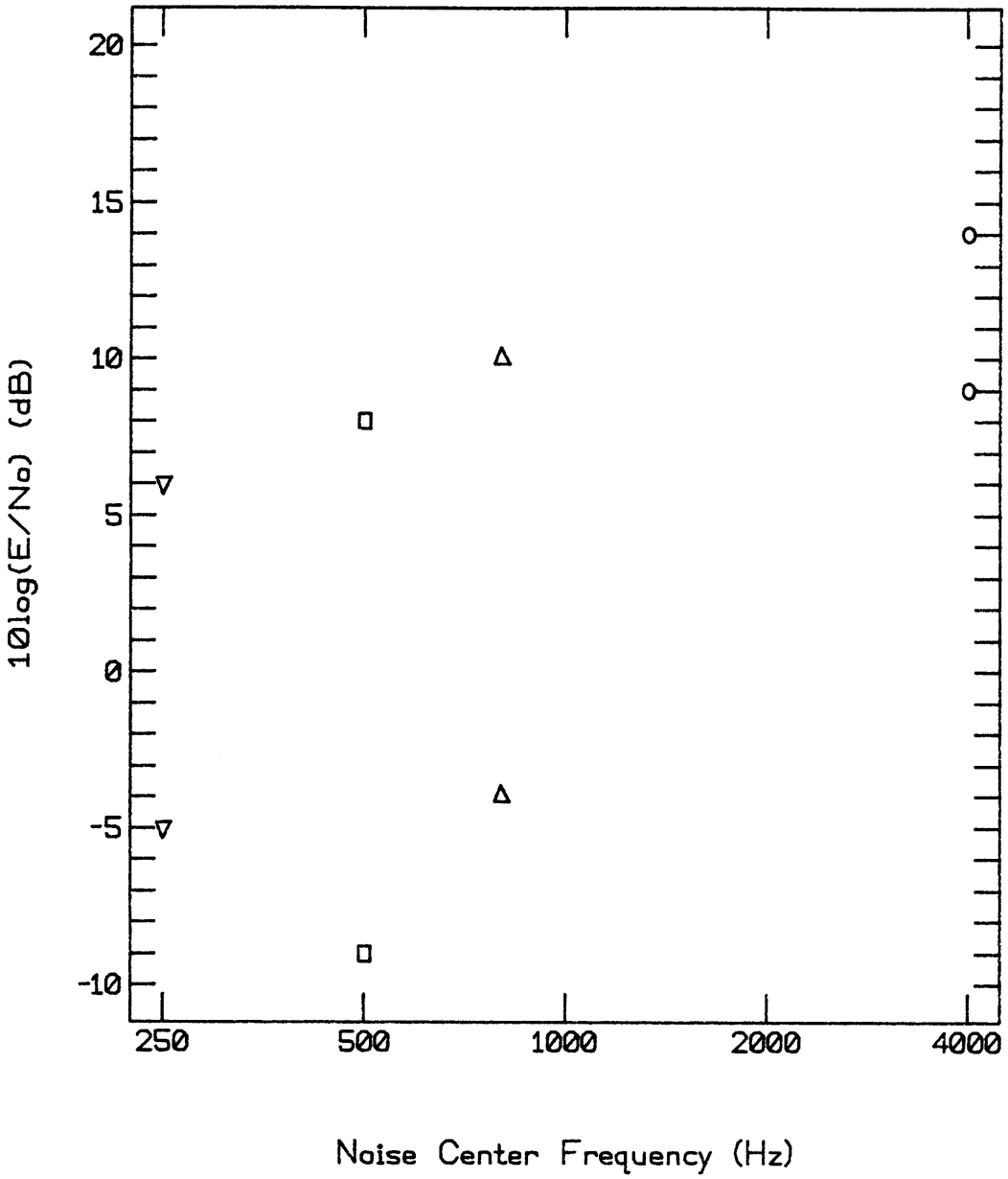
20
15
10
5
0
-5
-10
10log(E/No) (dB)
250
500
1000
2000
4000
Noise Center Frequency (Hz)

Figure 2.3

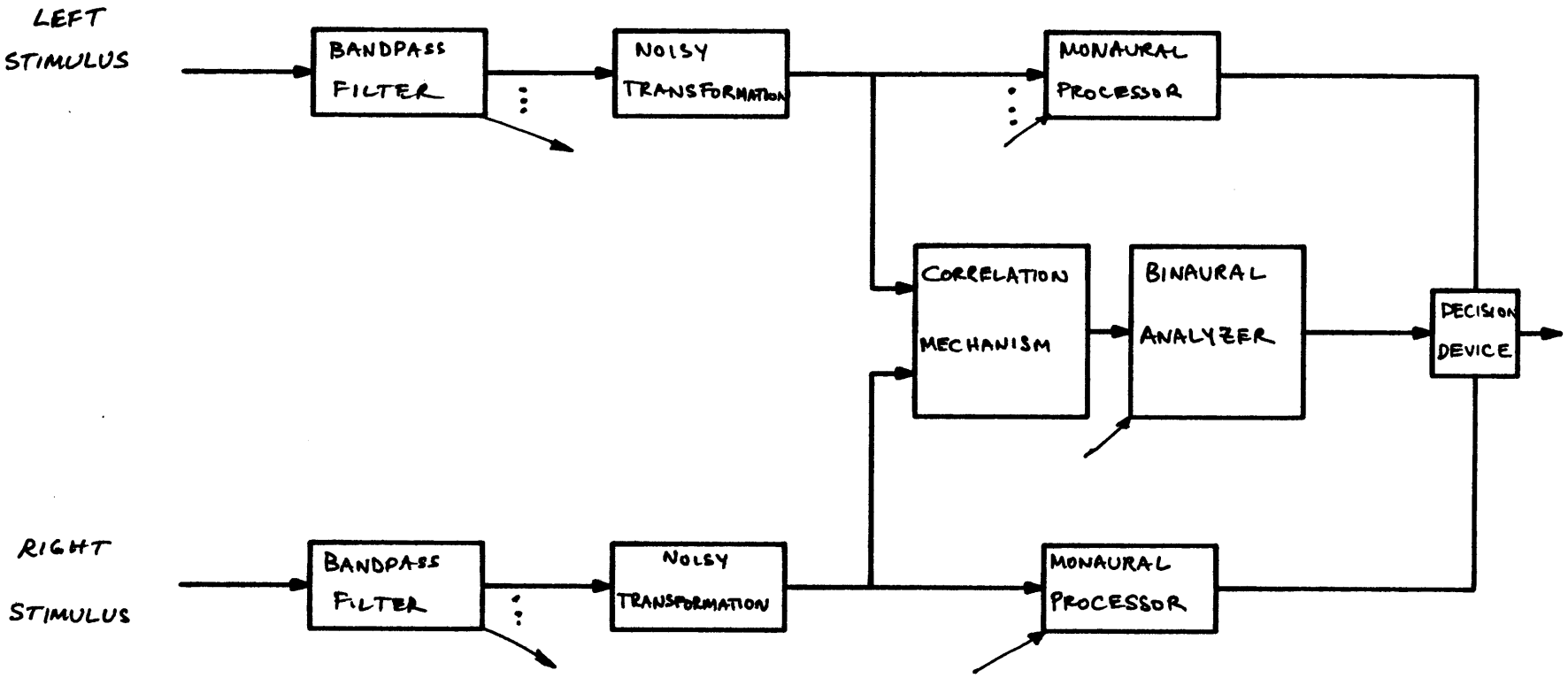
LEFT
STIMULUS
BANDPASS
FILTER
NOISY
TRANSFORMATION
MONAURAL
PROCESSOR
CORRELATION
MECHANISM
BINAURAL
ANALYZER
DECISION
DEVICE
RIGHT
STIMULUS
BANDPASS
FILTER
NOISY
TRANSFORMATION
MONAURAL
PROCESSOR

Figure 2.4

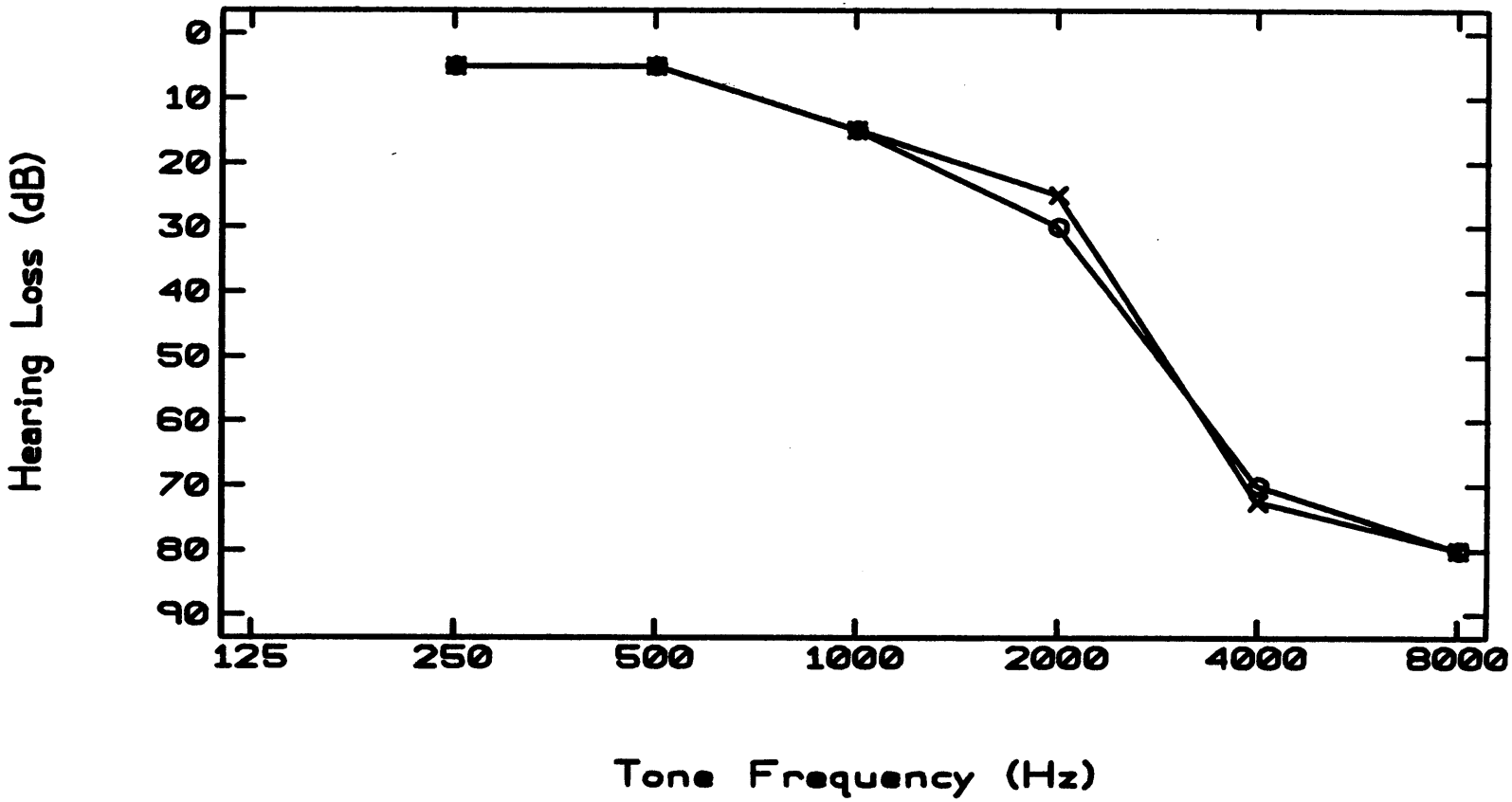
Hearing Loss (dB)
0
10
20
30
40
50
60
70
80
90
125
250
500
1000
2000
4000
8000
Tone Frequency (Hz)

Figure 3.f

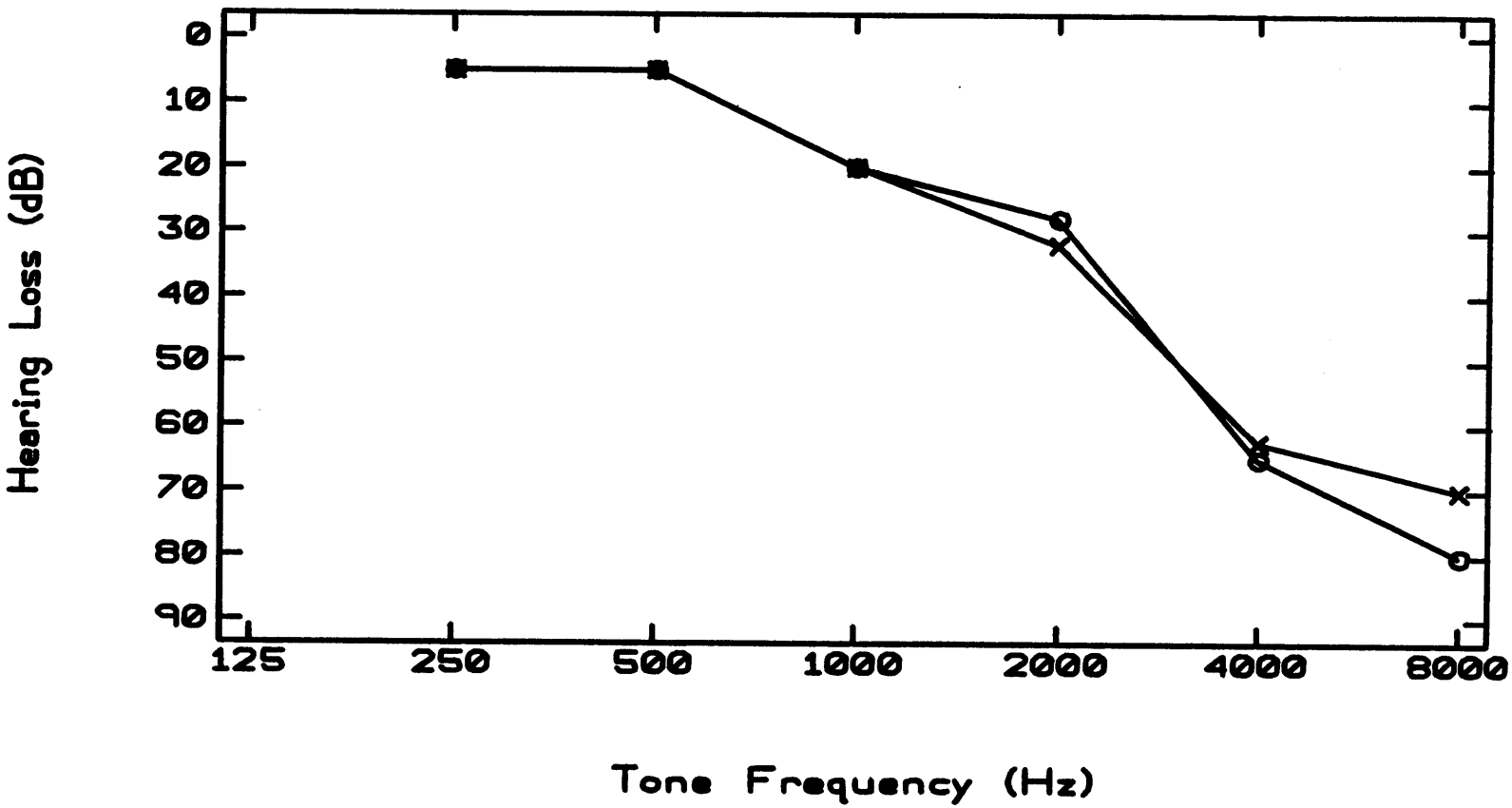
Hearing Loss (dB)
0
10
20
30
40
50
60
70
80
90
125
250
500
1000
2000
4000
8000
Tone Frequency (Hz)

Figure 3.2

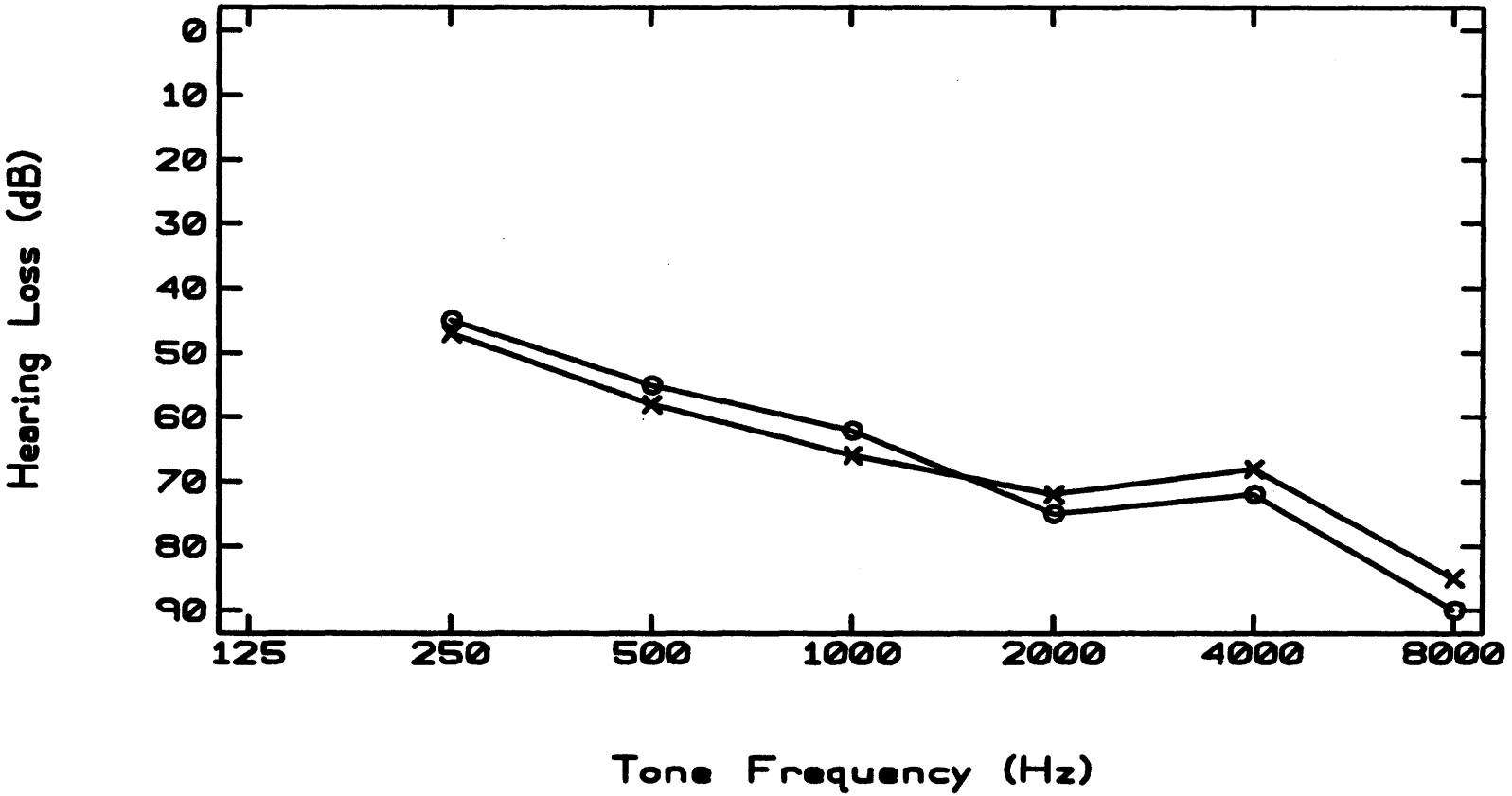
Hearing Loss (dB)
0
10
20
30
40
50
60
70
80
90
125
250
500
1000
2000
4000
8000
Tone Frequency (Hz)

Figure 3.3

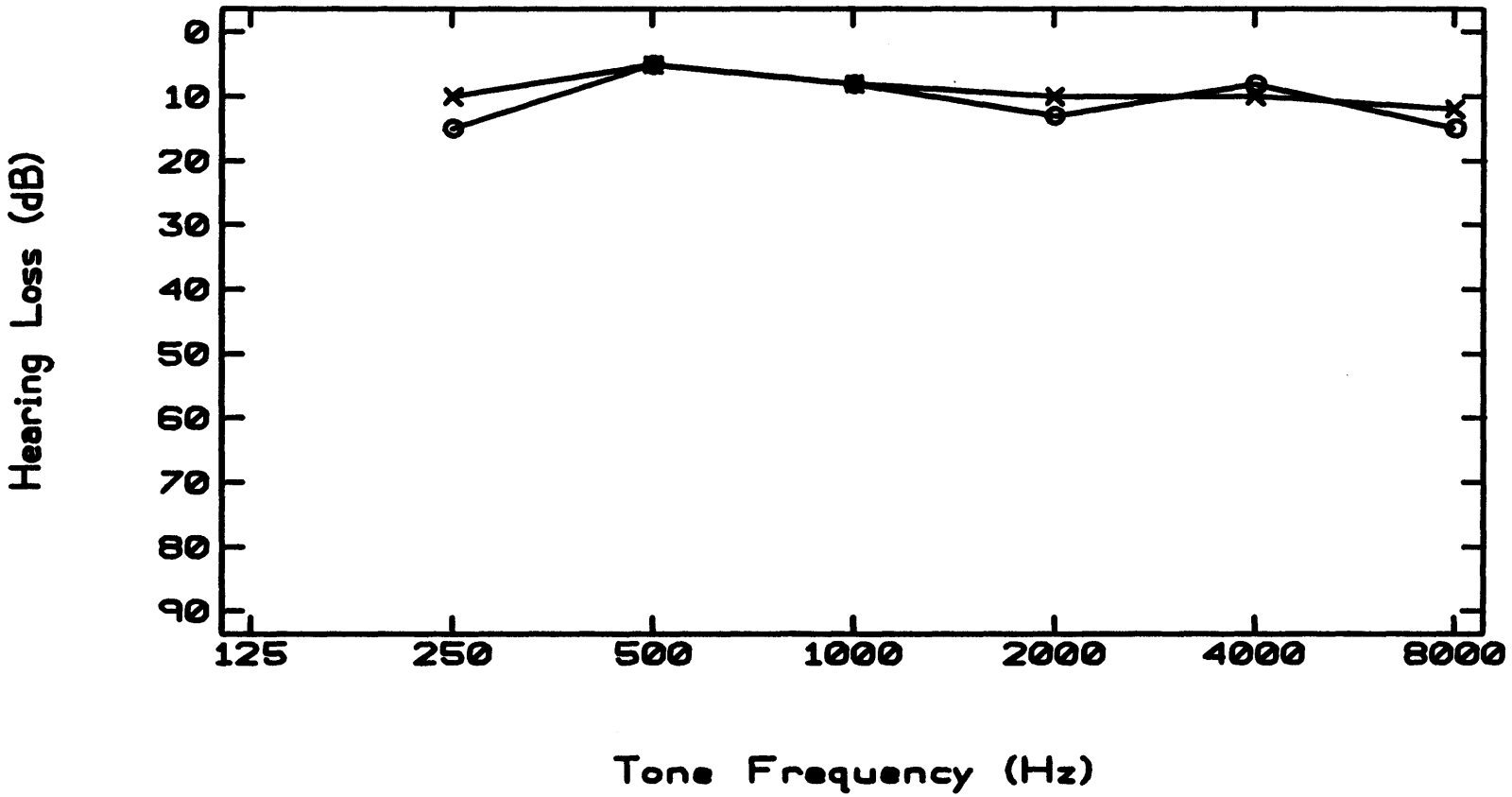
Hearing Loss (dB)
0
10
20
30
40
50
60
70
80
90
125
250
500
1000
2000
4000
8000
Tone Frequency (Hz)

Figure 3.4

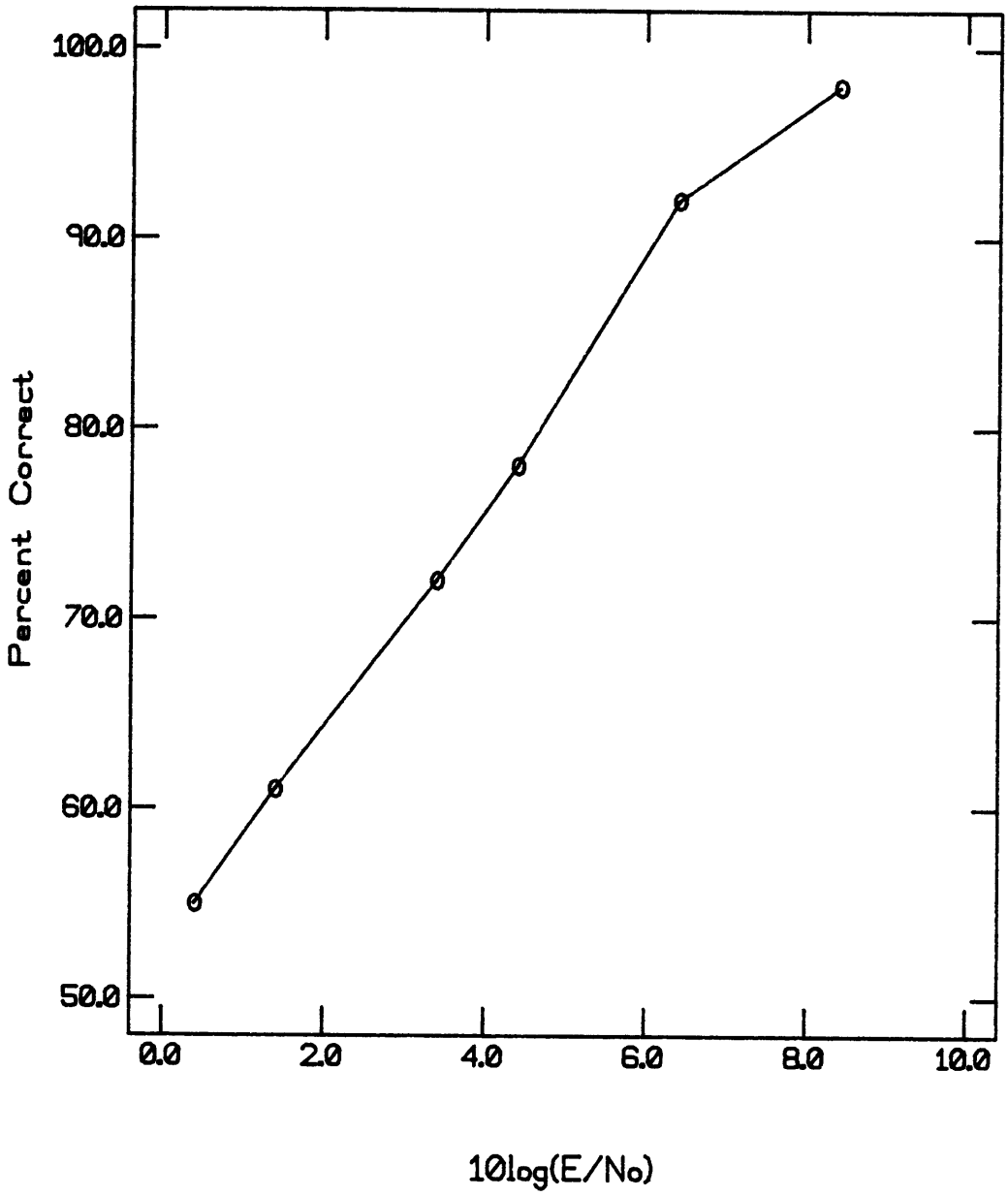
100.0
90.0
80.0
70.0
60.0
50.0
Percent Correct
0.0
2.0
4.0
6.0
8.0
10.0
10log(E/No)

Figure 3.5

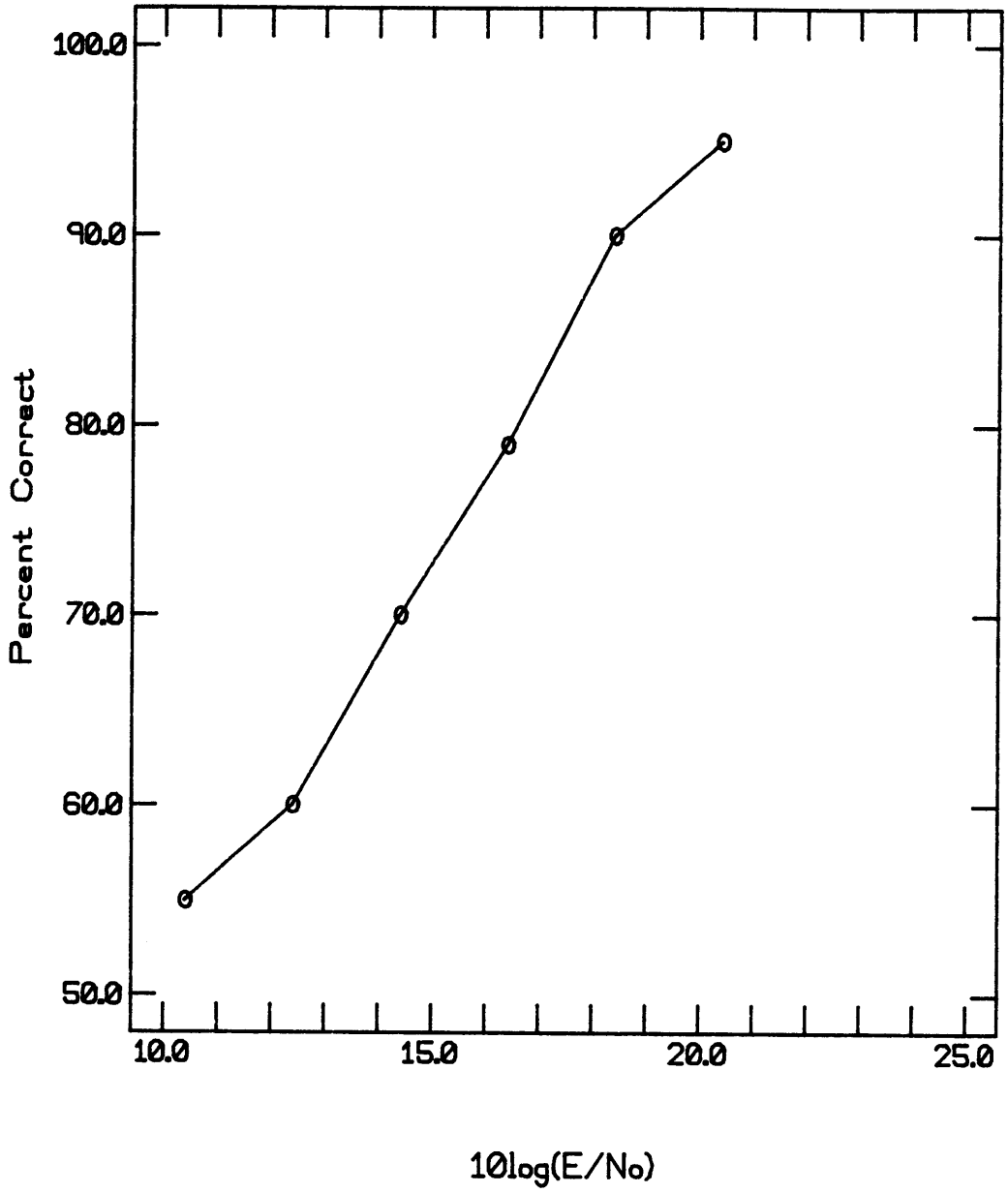
100.0
90.0
80.0
70.0
60.0
50.0
Percent Correct
10.0
15.0
20.0
25.0
10log(E/No)

Figure 3.6

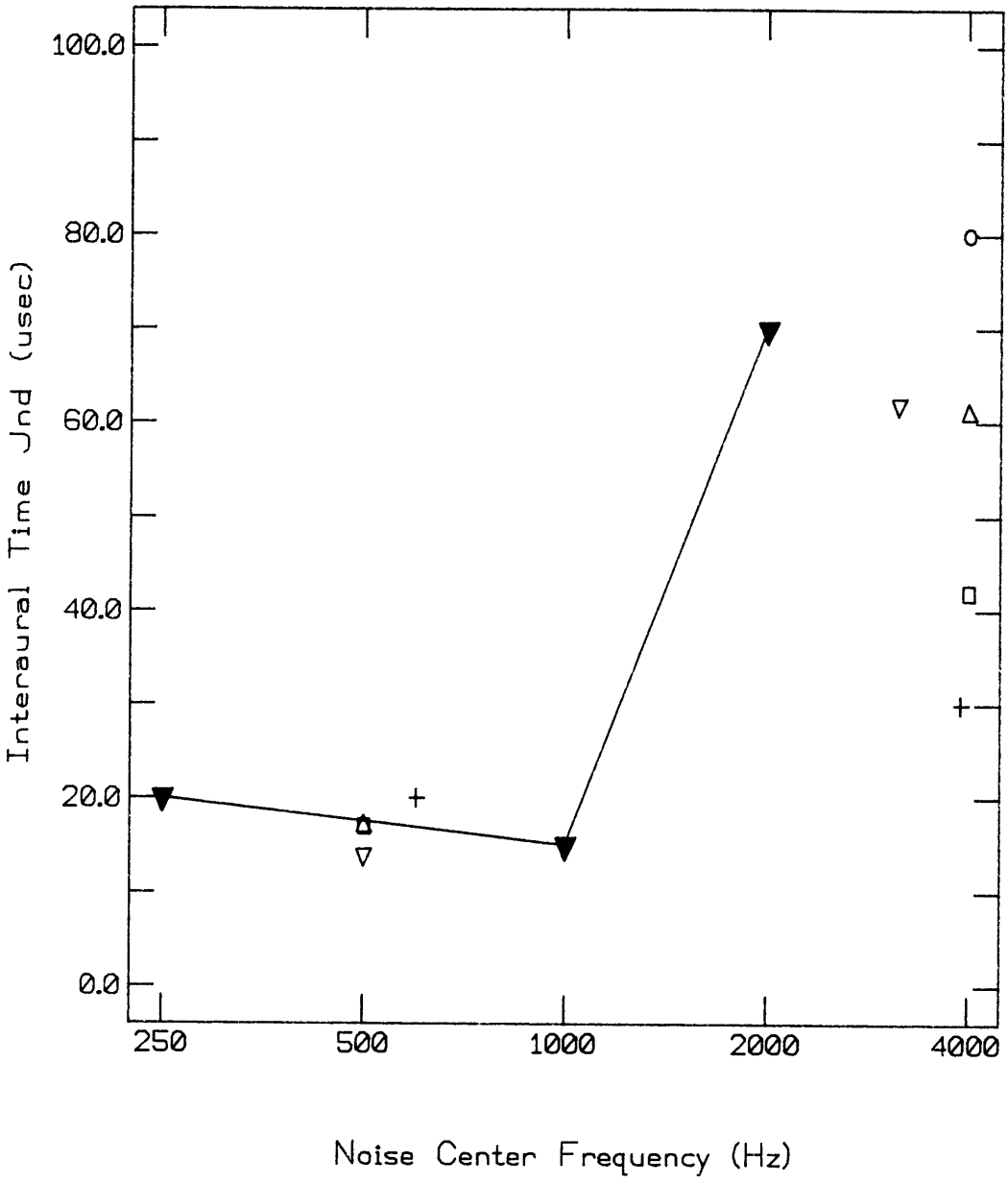
100.0
80.0
60.0
40.0
20.0
0.0
Interaural Time Jnd (usec)
250
500
1000
2000
4000
Noise Center Frequency (Hz)

Figure 4.1

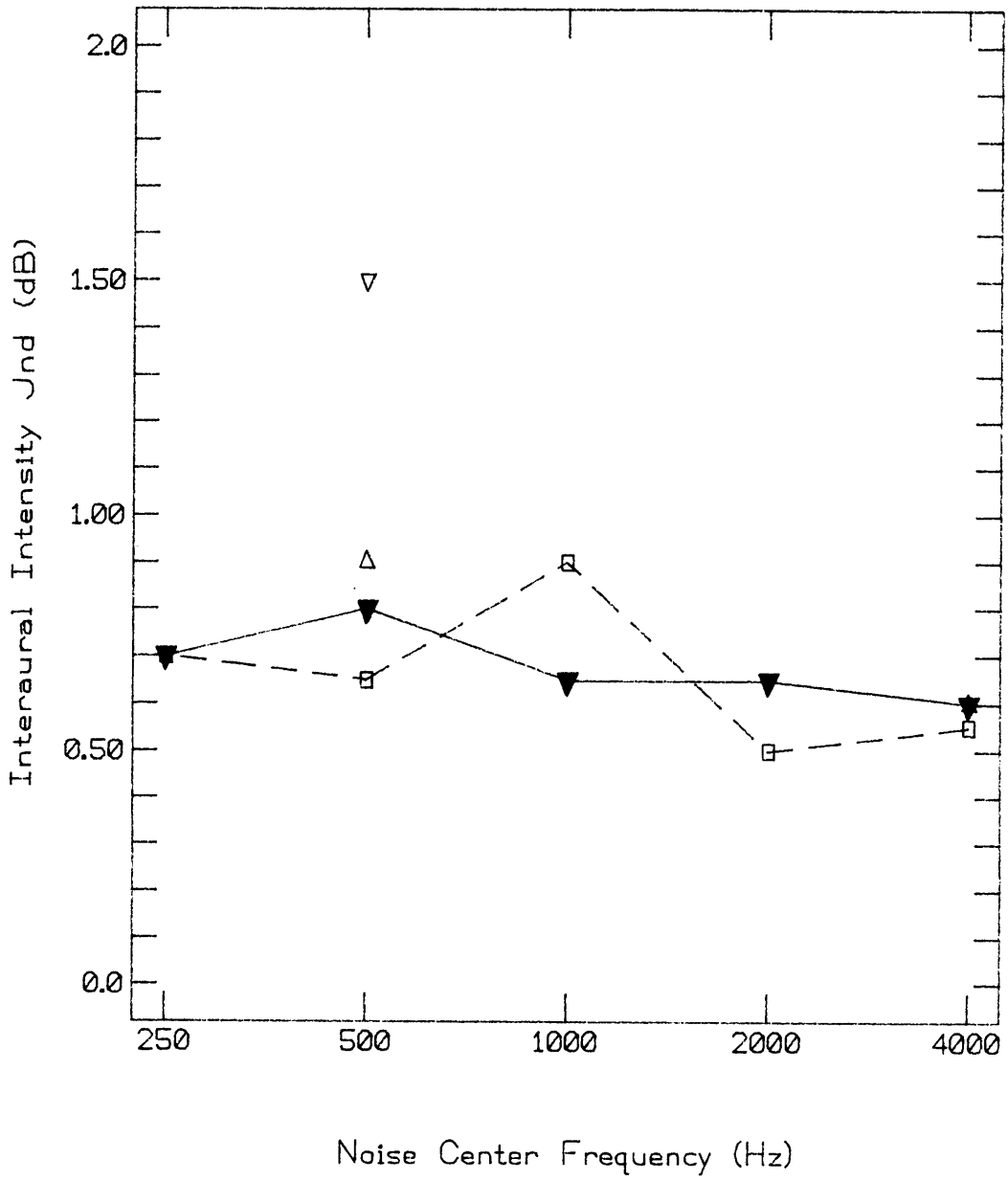
2.0
1.50
1.00
0.50
0.0
Interaural Intensity Jnd (dB)
250
500
1000
2000
4000
Noise Center Frequency (Hz)

Figure 4.2

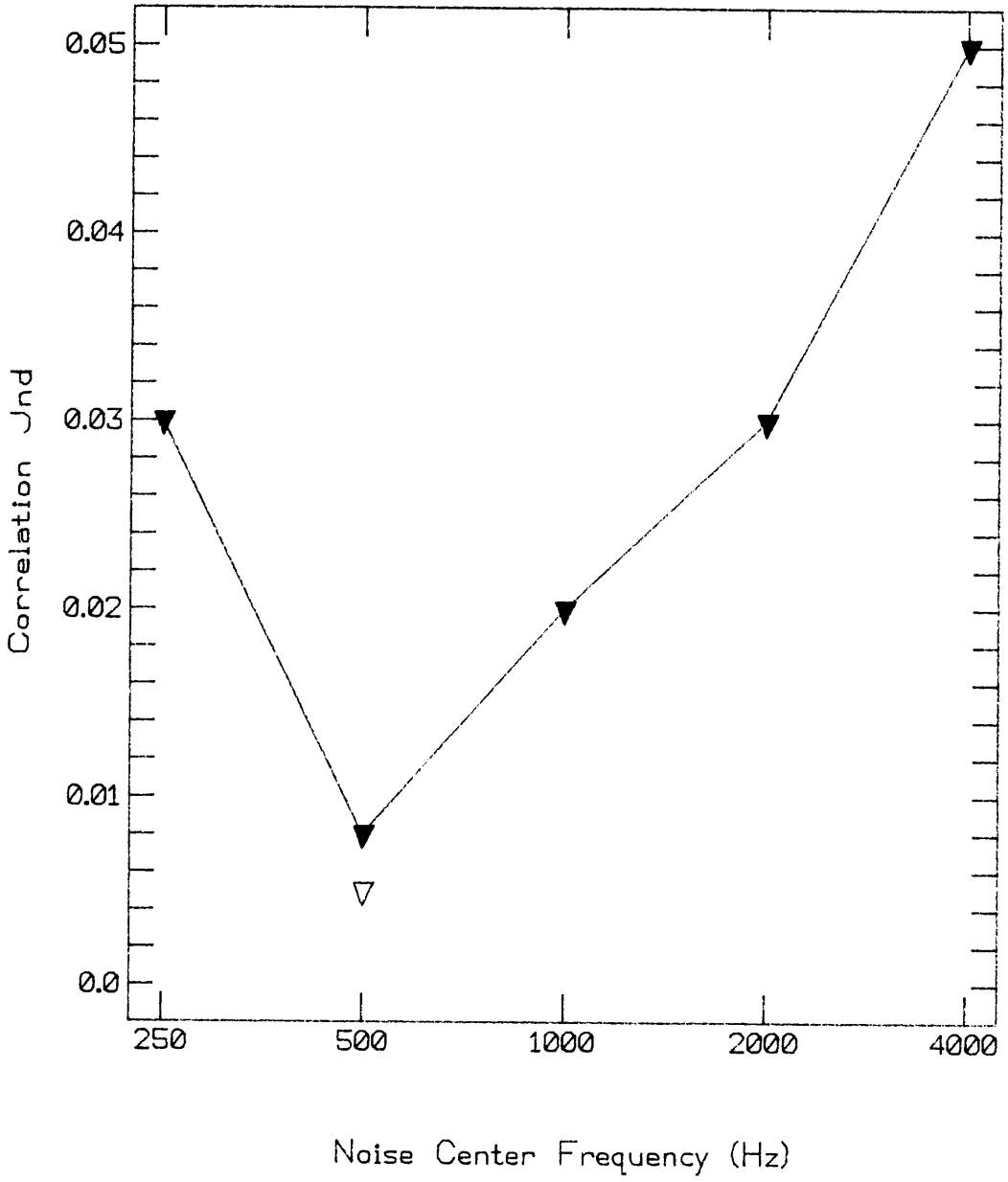
0.05
0.04
0.03
0.02
0.01
0.0
Correlation Jnd
250
500
1000
2000
4000
Noise Center Frequency (Hz)

Figure 4.3

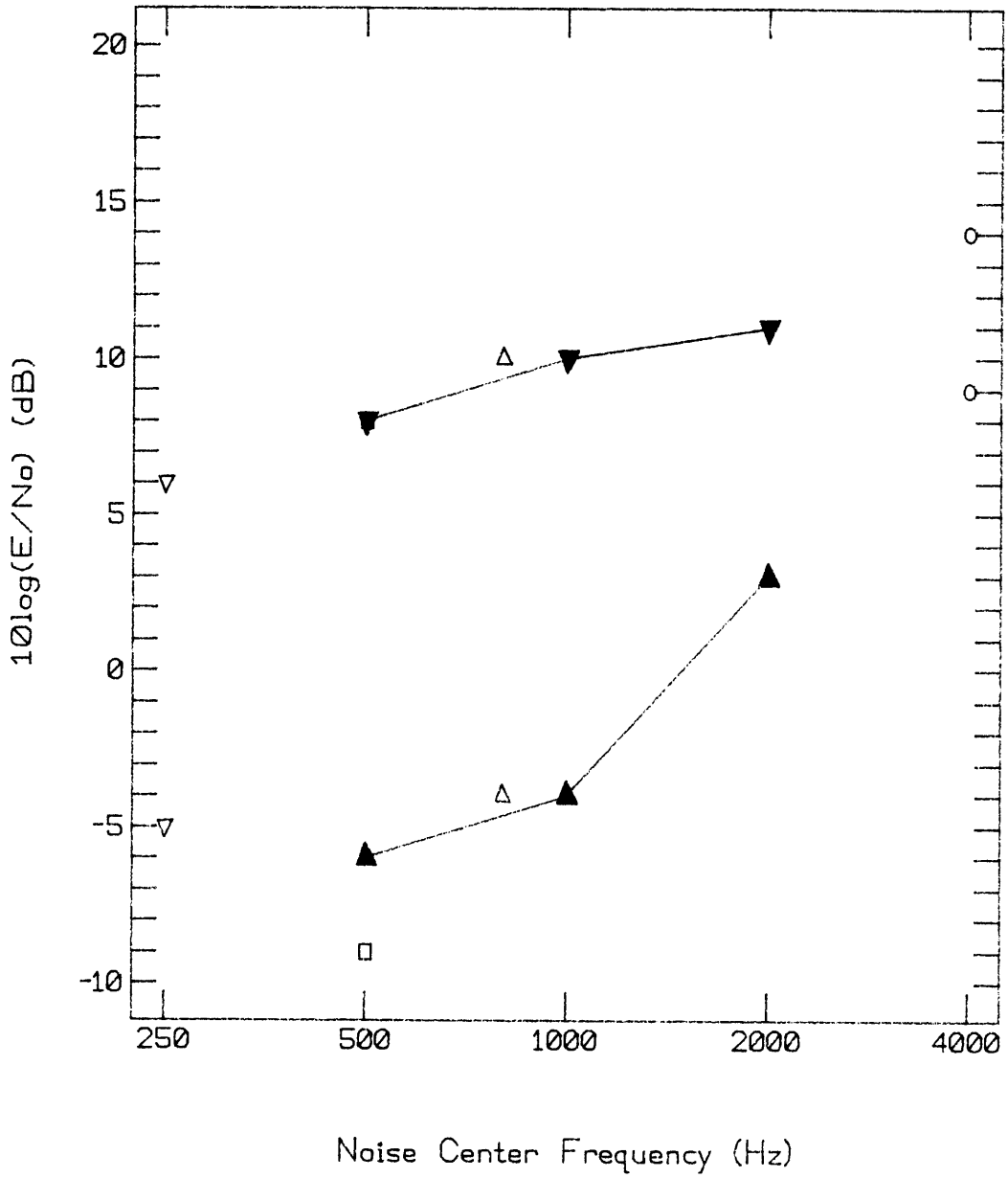
20
15
10
5
0
-5
-10
10log(E/No) (dB)
250
500
1000
2000
4000
Noise Center Frequency (Hz)

Figure 4.4

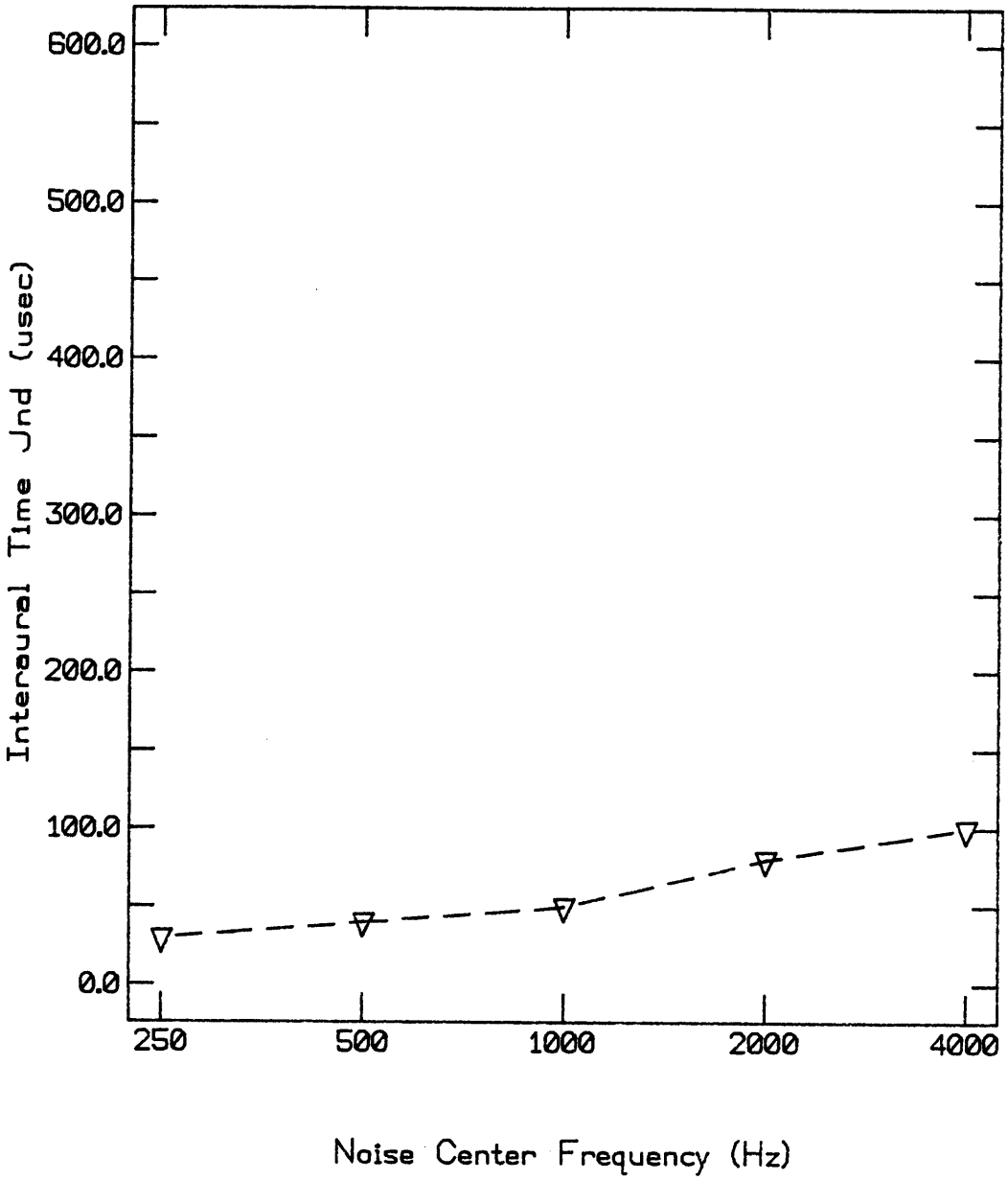
600.0
500.0
400.0
300.0
200.0
100.0
0.0
Interaural Time Jnd (usec)
250
500
1000
2000
4000
Noise Center Frequency (Hz)

Figure 4.5

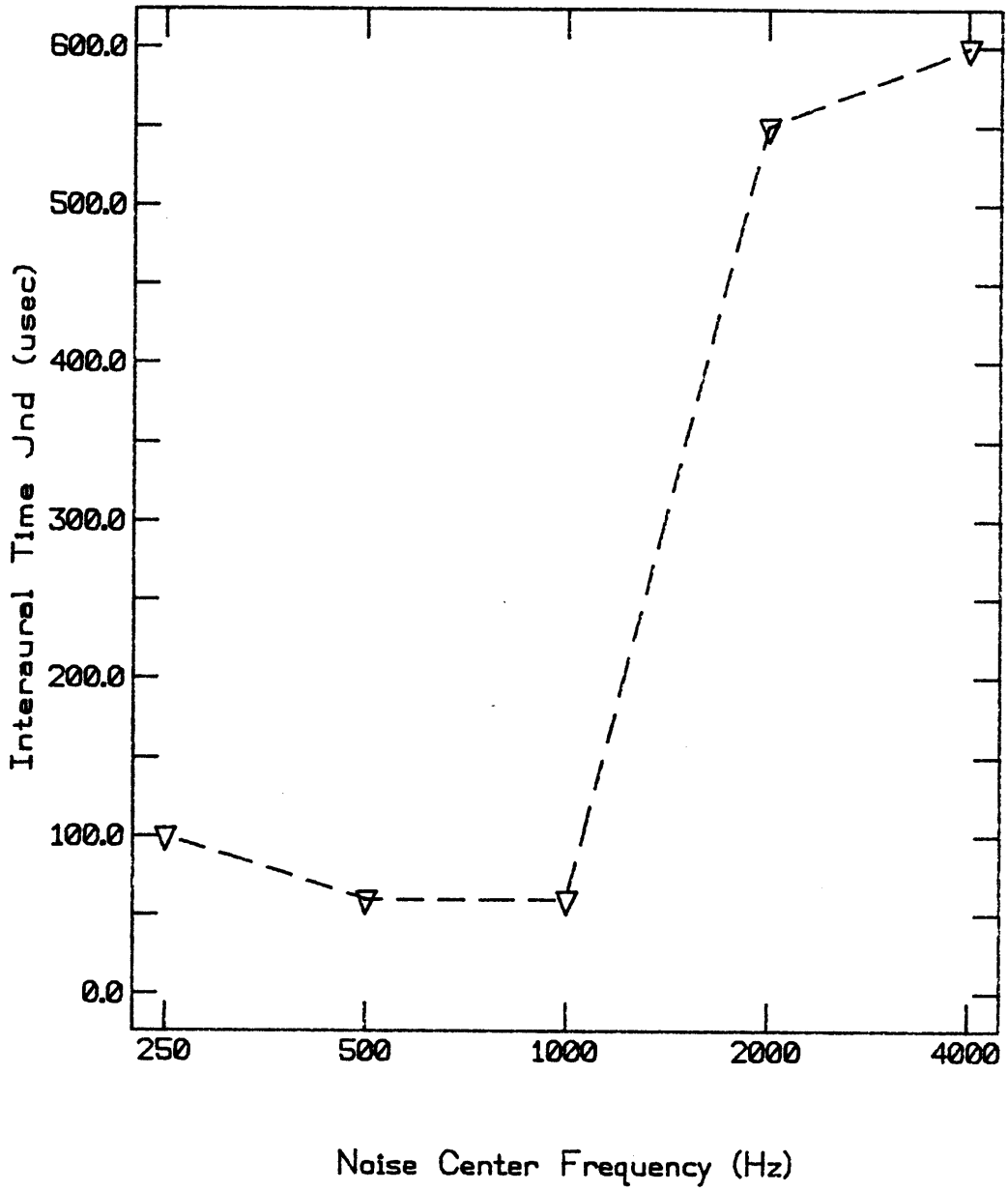
600.0
500.0
400.0
300.0
200.0
100.0
0.0
Interaural Time Jnd (usec)
250
500
1000
2000
4000
Noise Center Frequency (Hz)

Figure 4.6

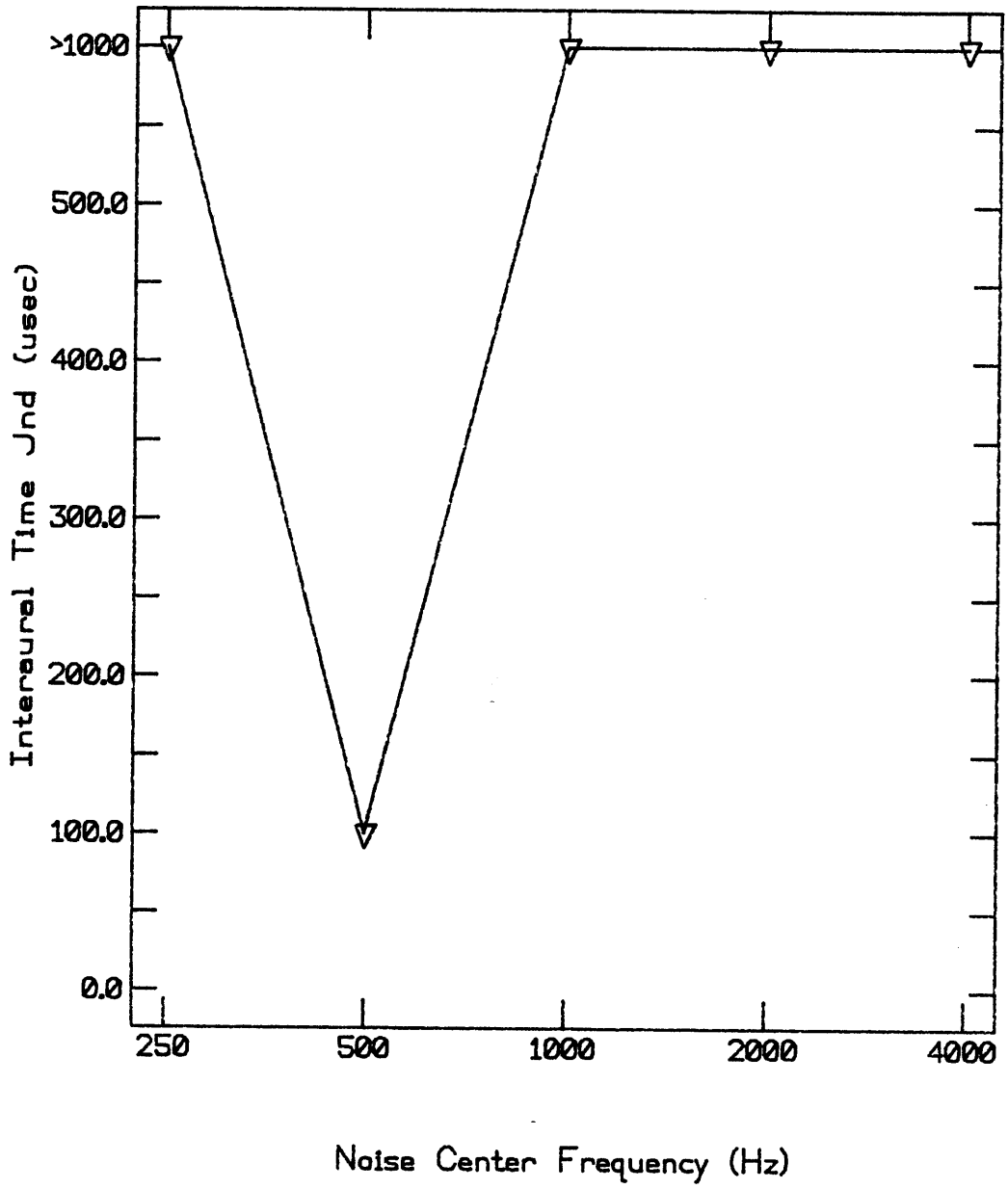
>1000
500.0
400.0
300.0
200.0
100.0
0.0
Interaural Time Jnd (usec)
250
500
1000
2000
4000
Noise Center Frequency (Hz)

Figure 4.7

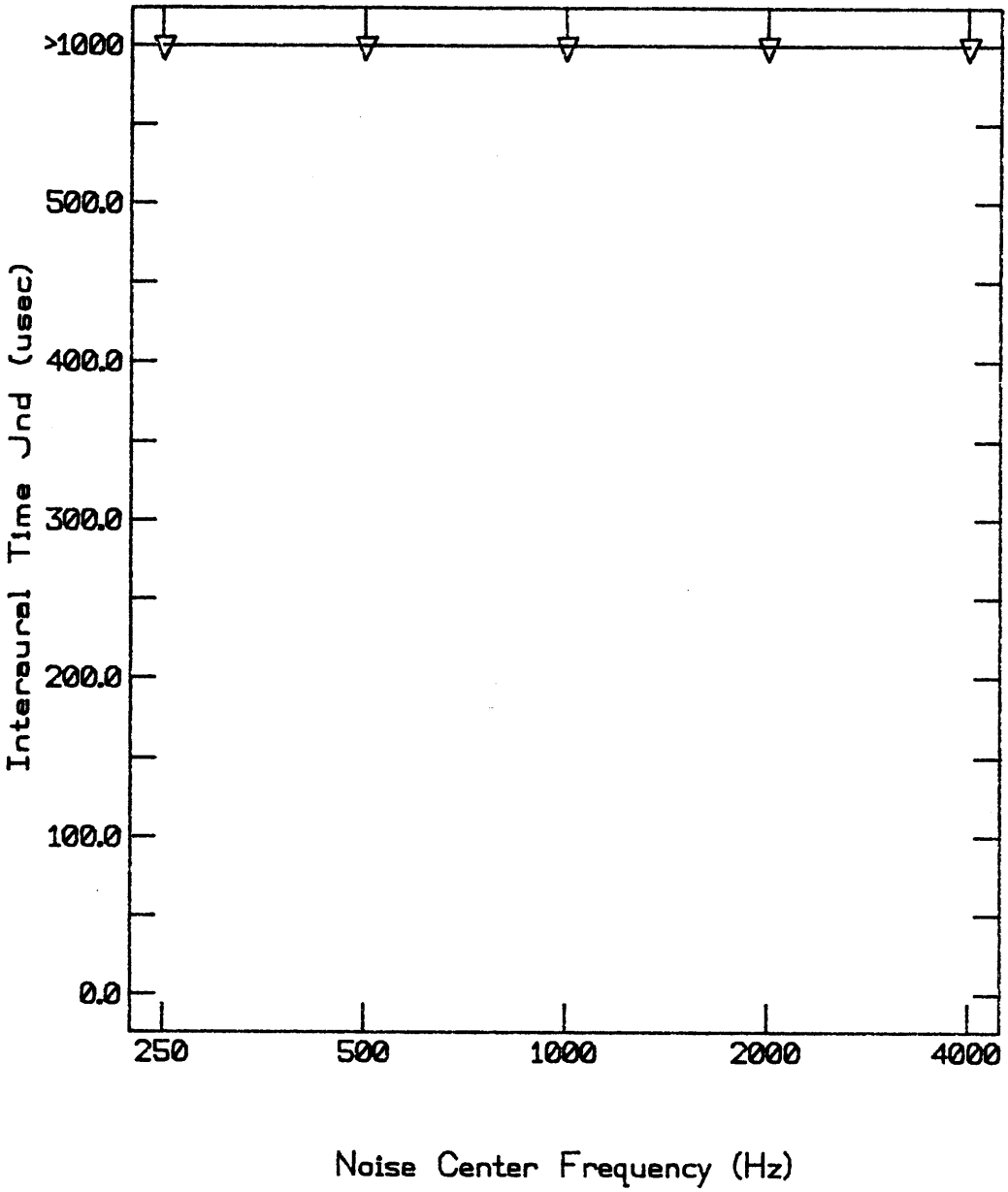
>1000
500.0
400.0
300.0
200.0
100.0
0.0
Interaural Time Jnd (usec)
250
500
1000
2000
4000
Noise Center Frequency (Hz)

Figure 4.8

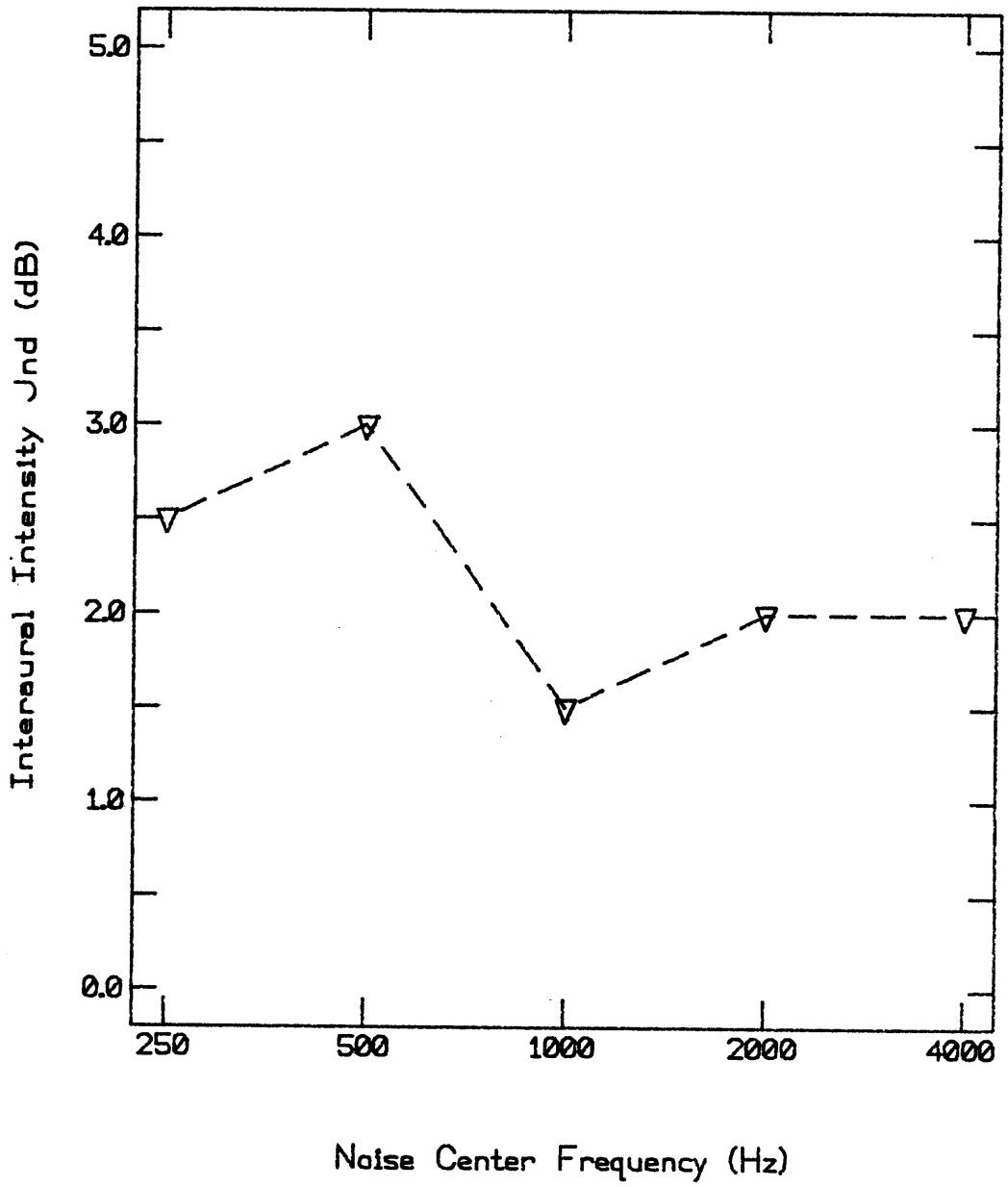
5.0
4.0
3.0
2.0
1.0
0.0
Interaural Intensity Jnd (dB)
250
500
1000
2000
4000
Noise Center Frequency (Hz)

Figure 4.9

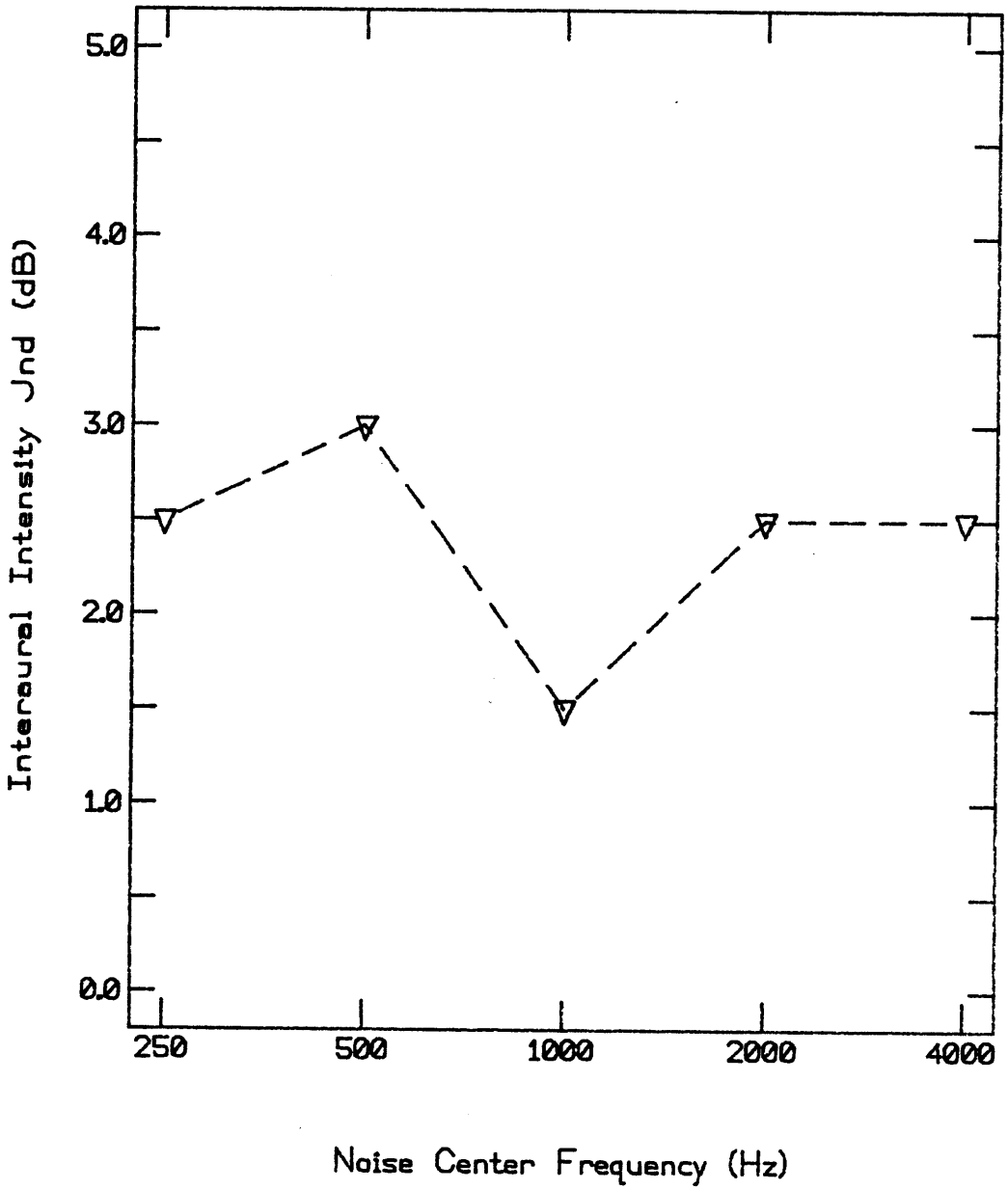
5.0
4.0
3.0
2.0
1.0
0.0
Interaural Intensity Jnd (dB)
250
500
1000
2000
4000
Noise Center Frequency (Hz)

Figure 4.10

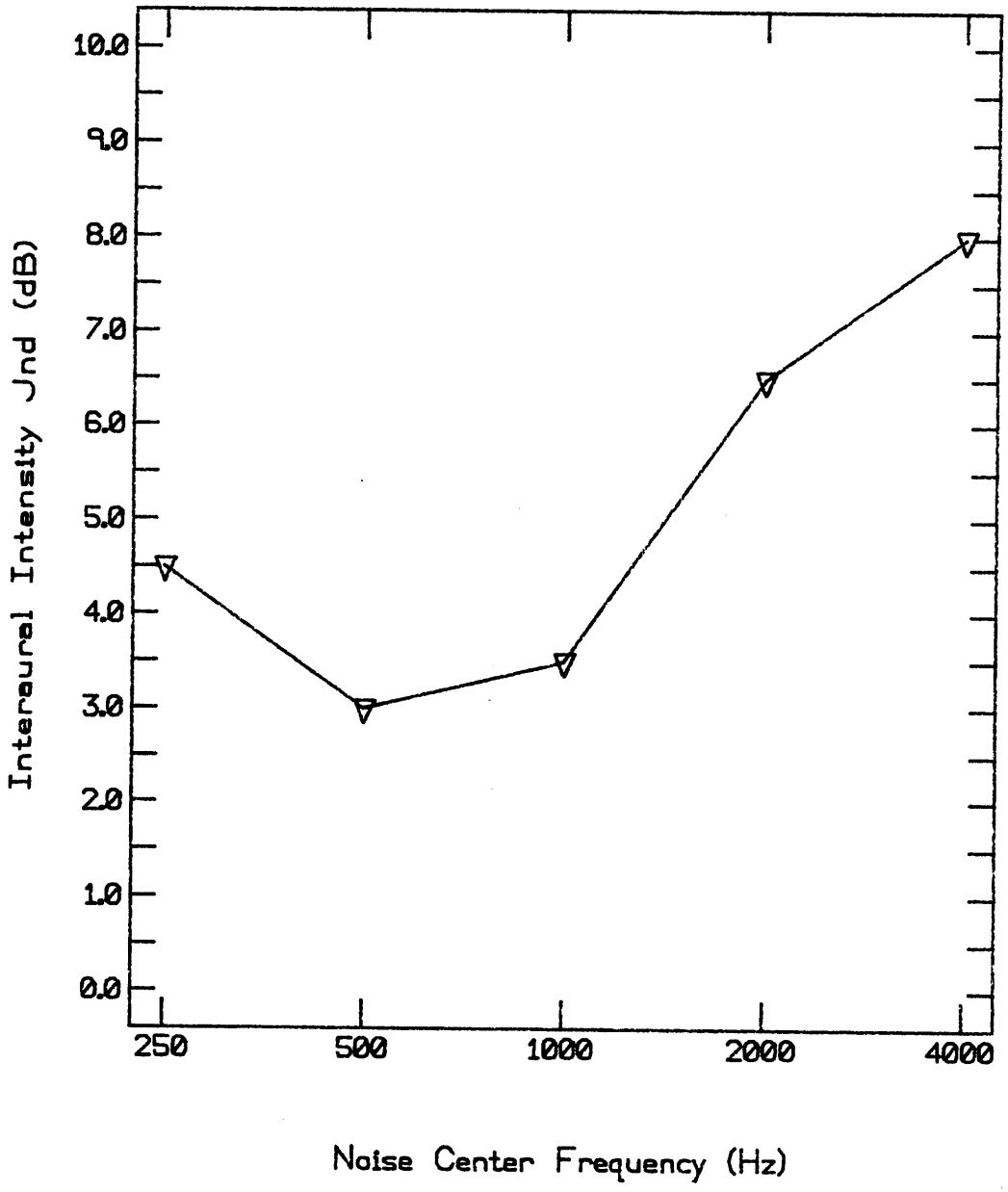
Interaural Intensity Jnd (dB)
10.0
9.0
8.0
7.0
6.0
5.0
4.0
3.0
2.0
1.0
0.0
250
500
1000
2000
4000
Noise Center Frequency (Hz)

Figure 4.11

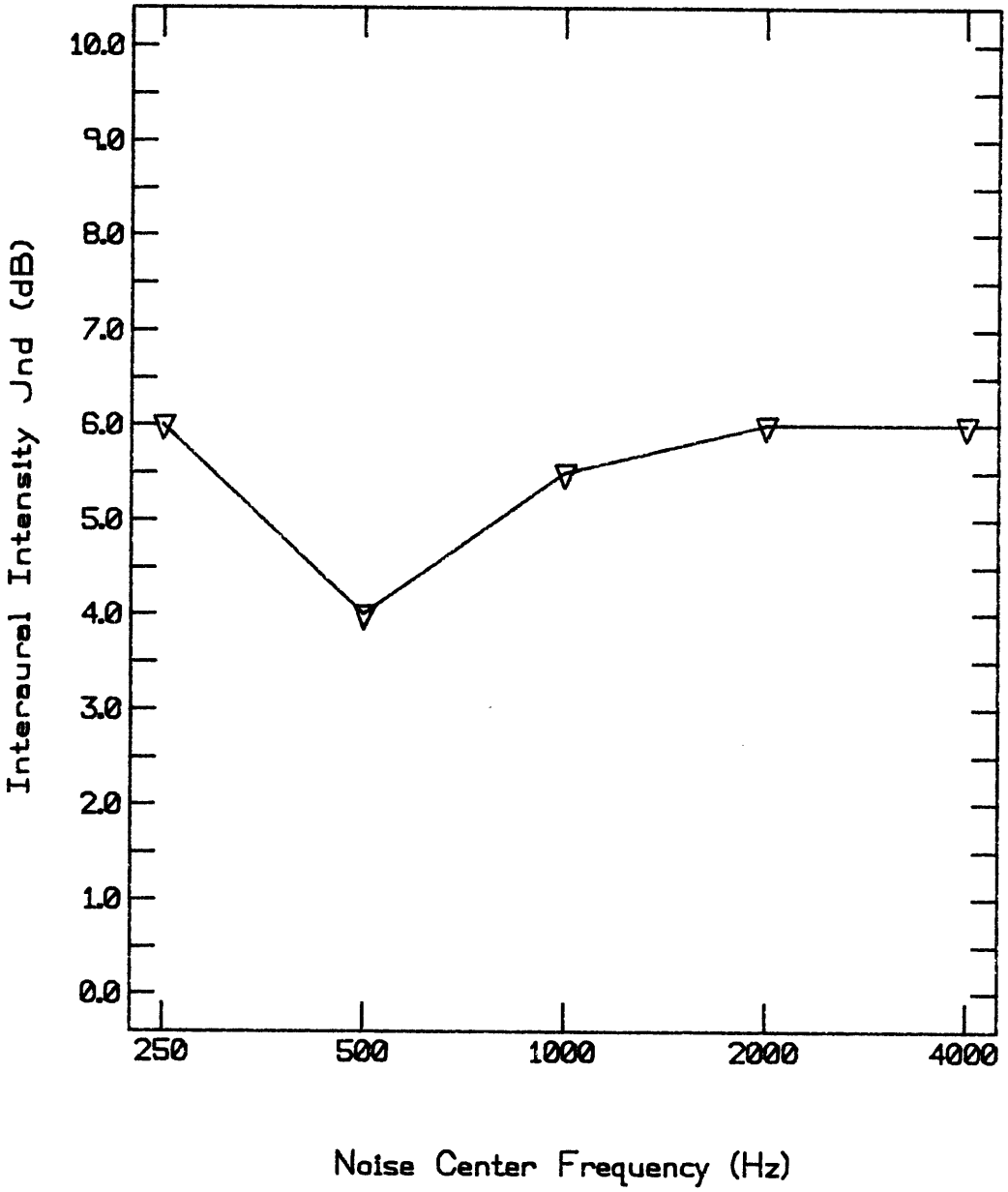
10.0
9.0
8.0
7.0
6.0
5.0
4.0
3.0
2.0
1.0
0.0
Interaural Intensity Jnd (dB)
250
500
1000
2000
4000
Noise Center Frequency (Hz)

Figure 4.12

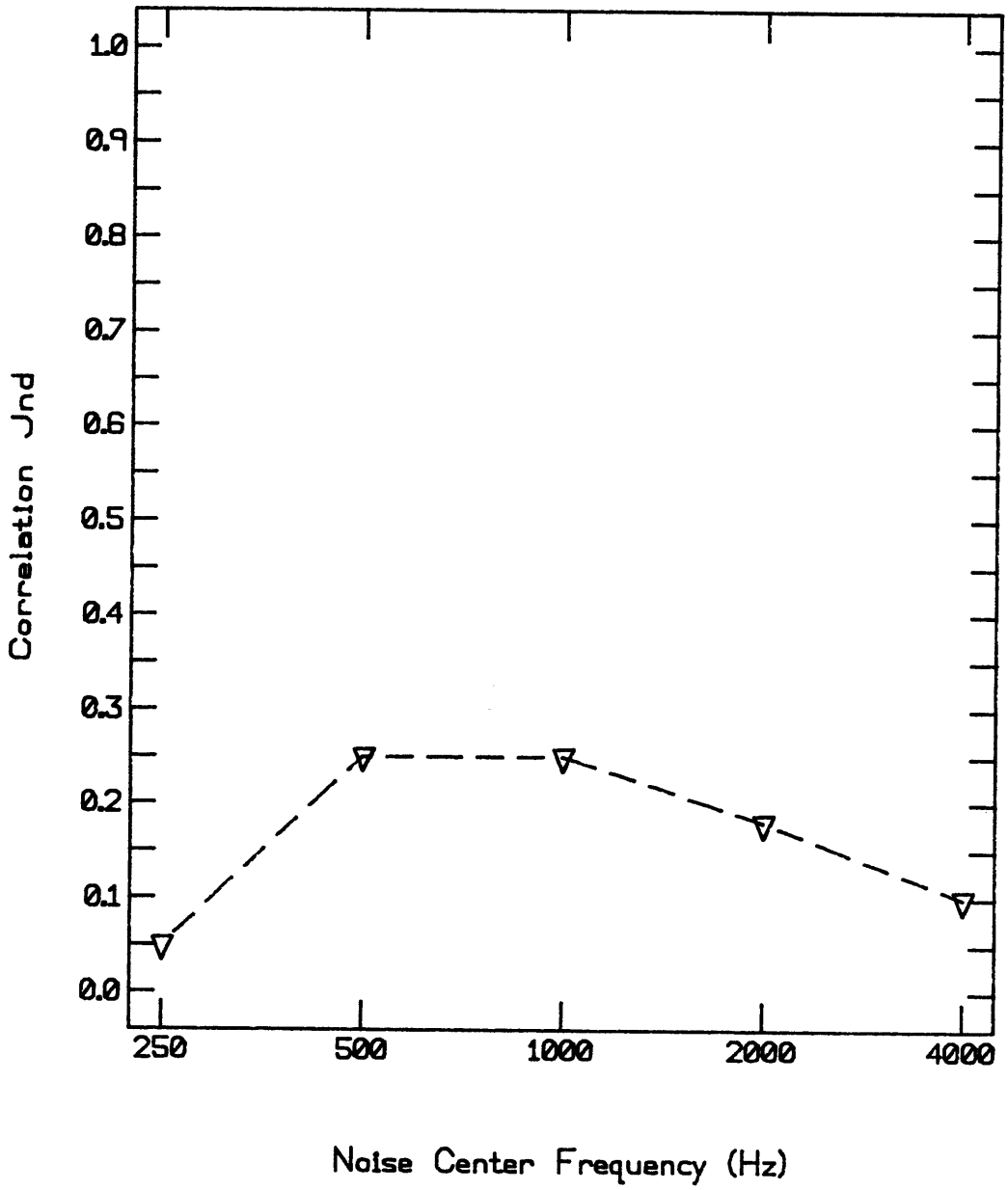
1.0
0.9
0.8
0.7
0.6
0.5
0.4
0.3
0.2
0.1
0.0
Correlation Jnd
250
500
1000
2000
4000
Noise Center Frequency (Hz)

Figure 4.13

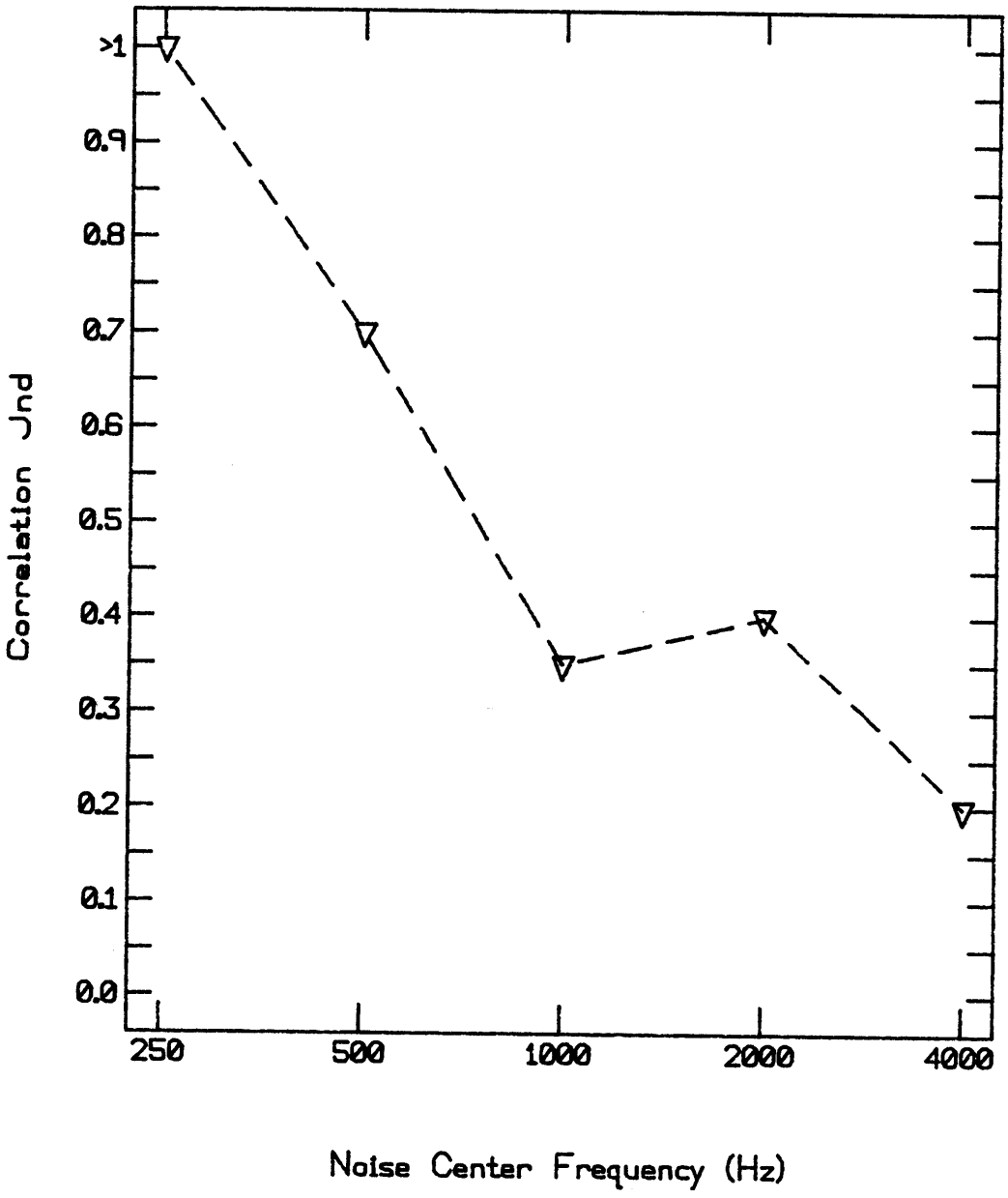
Correlation Jnd
>1
0.9
0.8
0.7
0.6
0.5
0.4
0.3
0.2
0.1
0.0
250
500
1000
2000
4000
Noise Center Frequency (Hz)

Figure 4.14

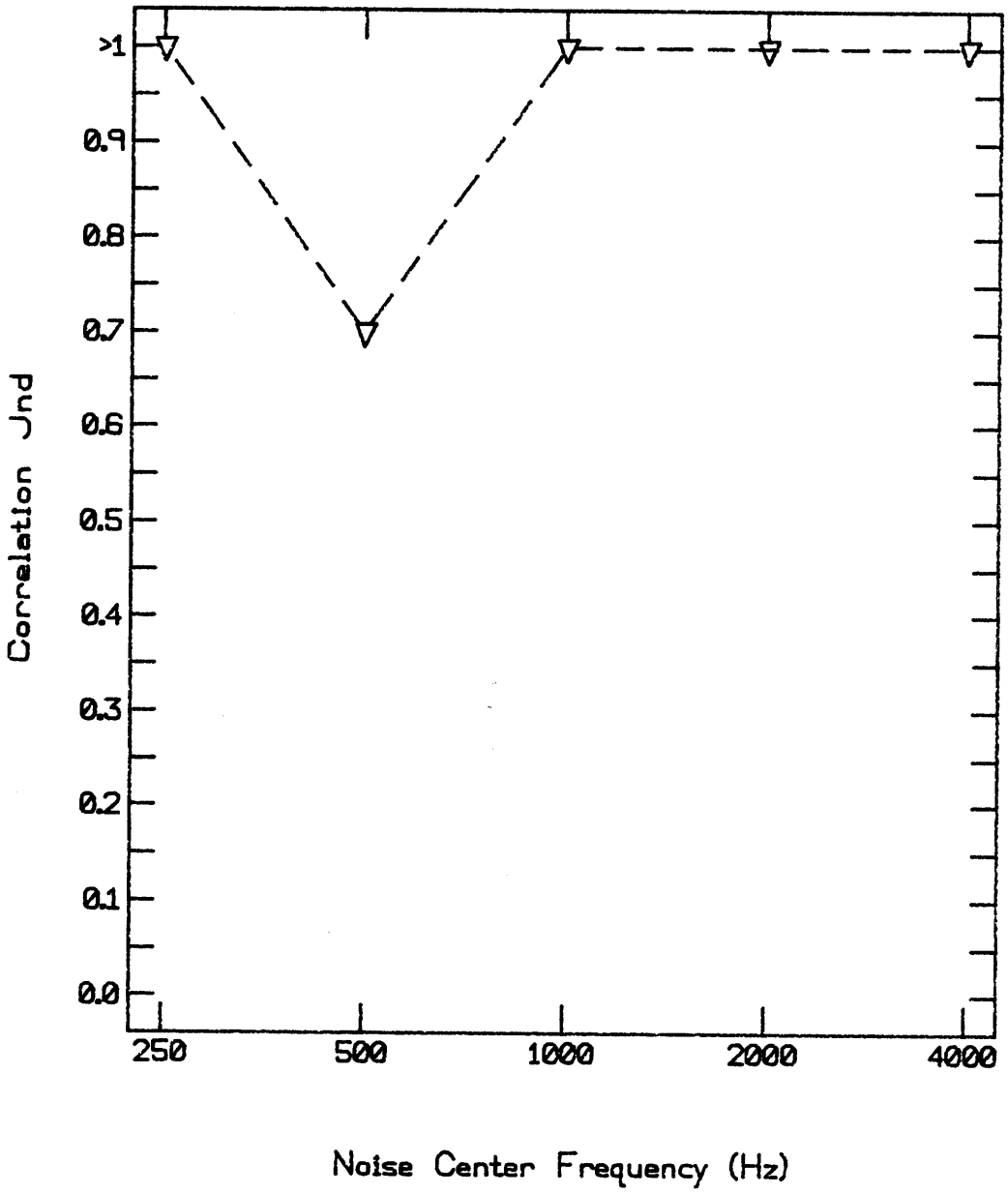
>1
0.9
0.8
0.7
0.6
0.5
0.4
0.3
0.2
0.1
0.0
Correlation Jnd
250
500
1000
2000
4000
Noise Center Frequency (Hz)

Figure 4.15

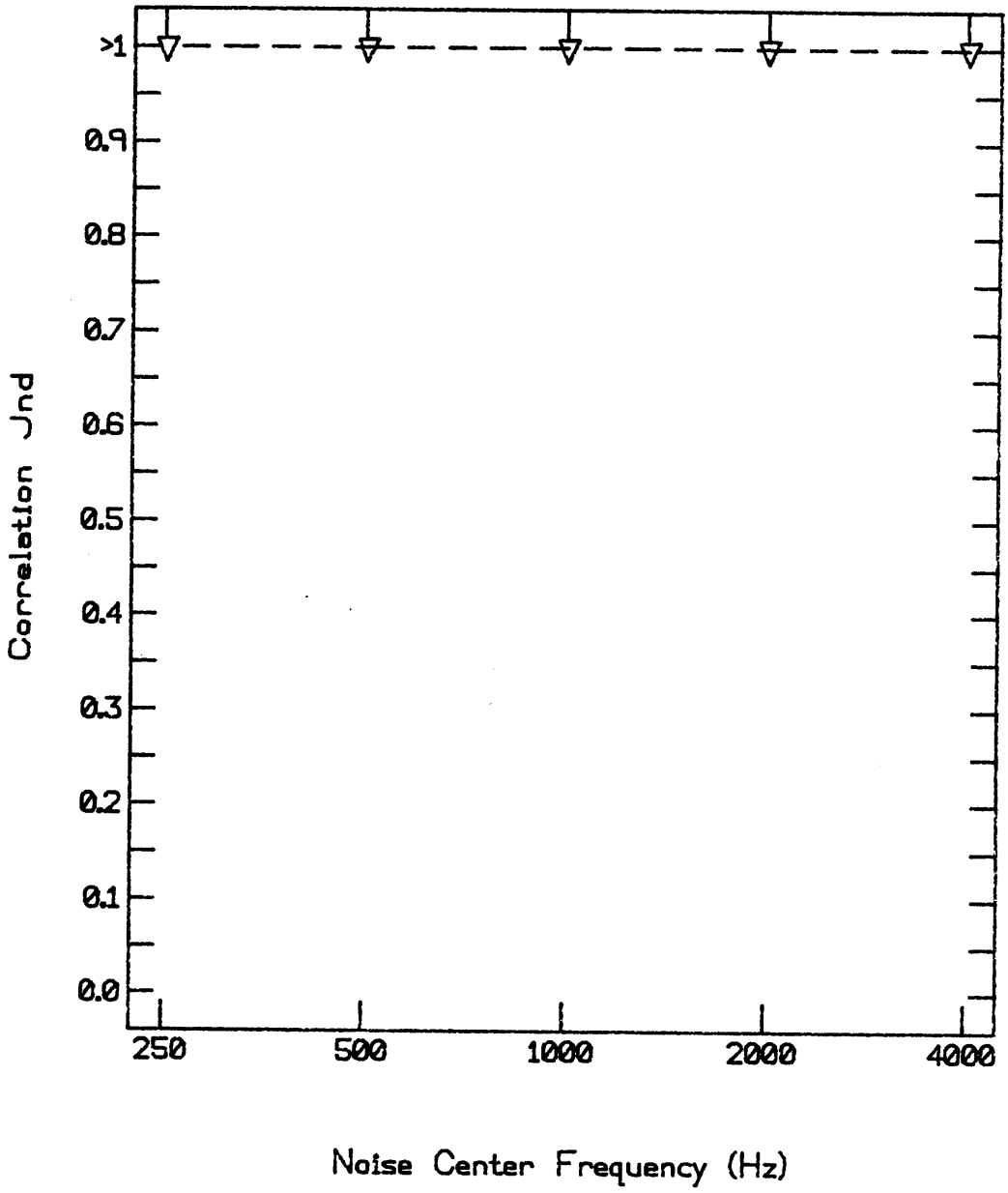
>1
0.9
0.8
0.7
0.6
0.5
0.4
0.3
0.2
0.1
0.0
Correlation Jnd
250
500
1000
2000
4000
Noise Center Frequency (Hz)

Figure 4.16

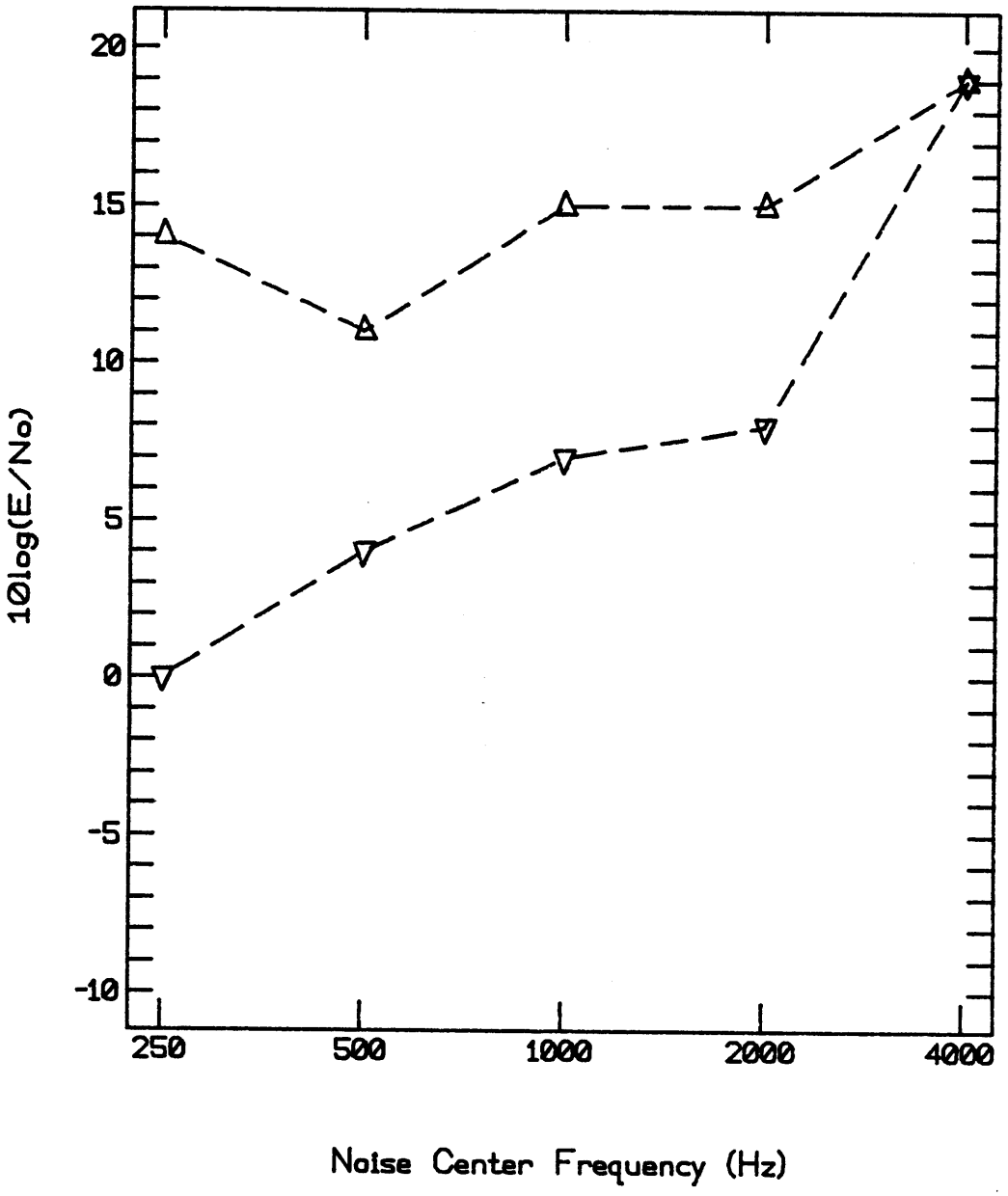
20
15
10
5
0
-5
-10
10log(E/No)
250
500
1000
2000
4000
Noise Center Frequency (Hz)

Figure 4.17

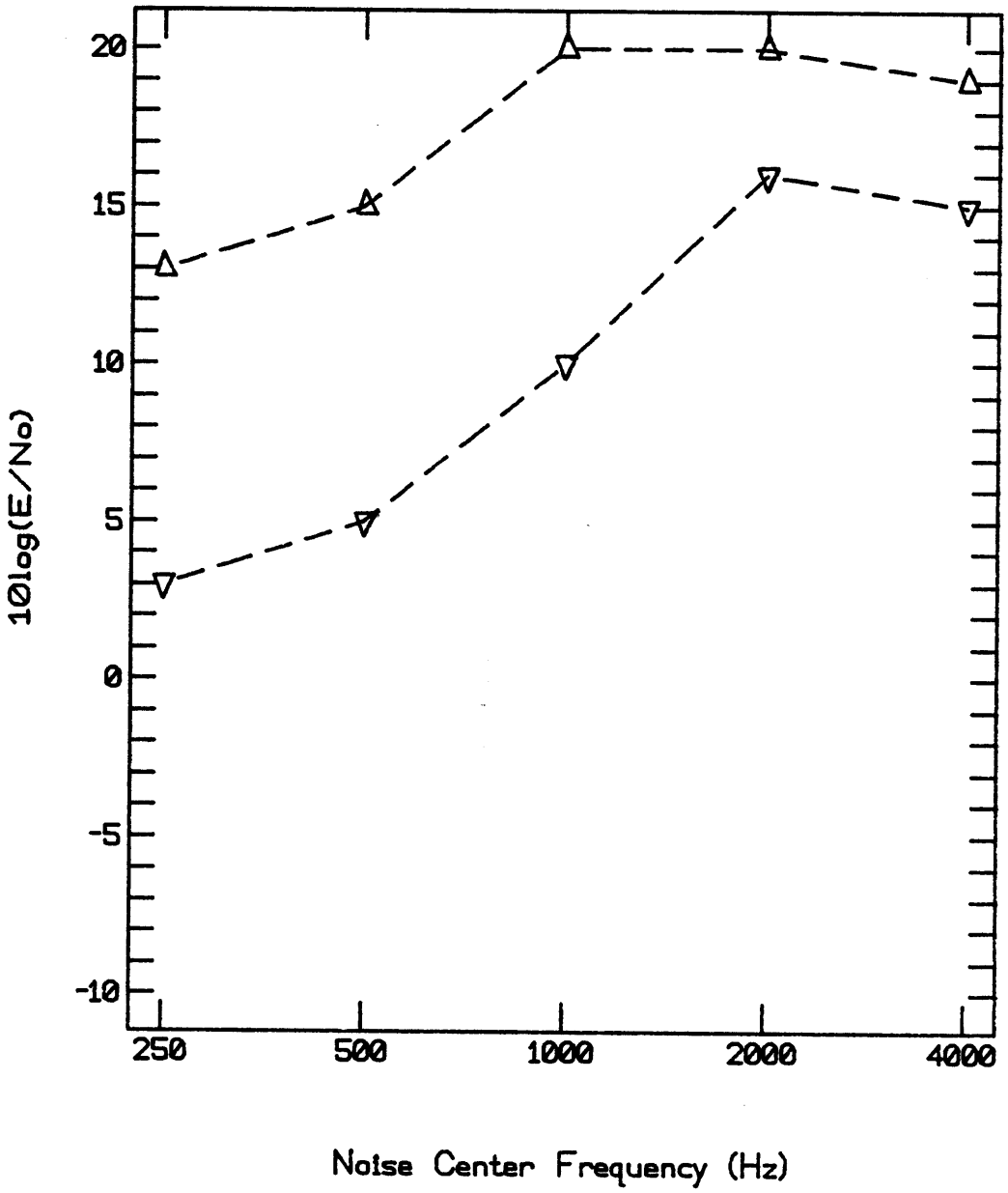
20
15
10
5
0
-5
-10
10log(E/No)
250
500
1000
2000
4000
Noise Center Frequency (Hz)

Figure 4.18

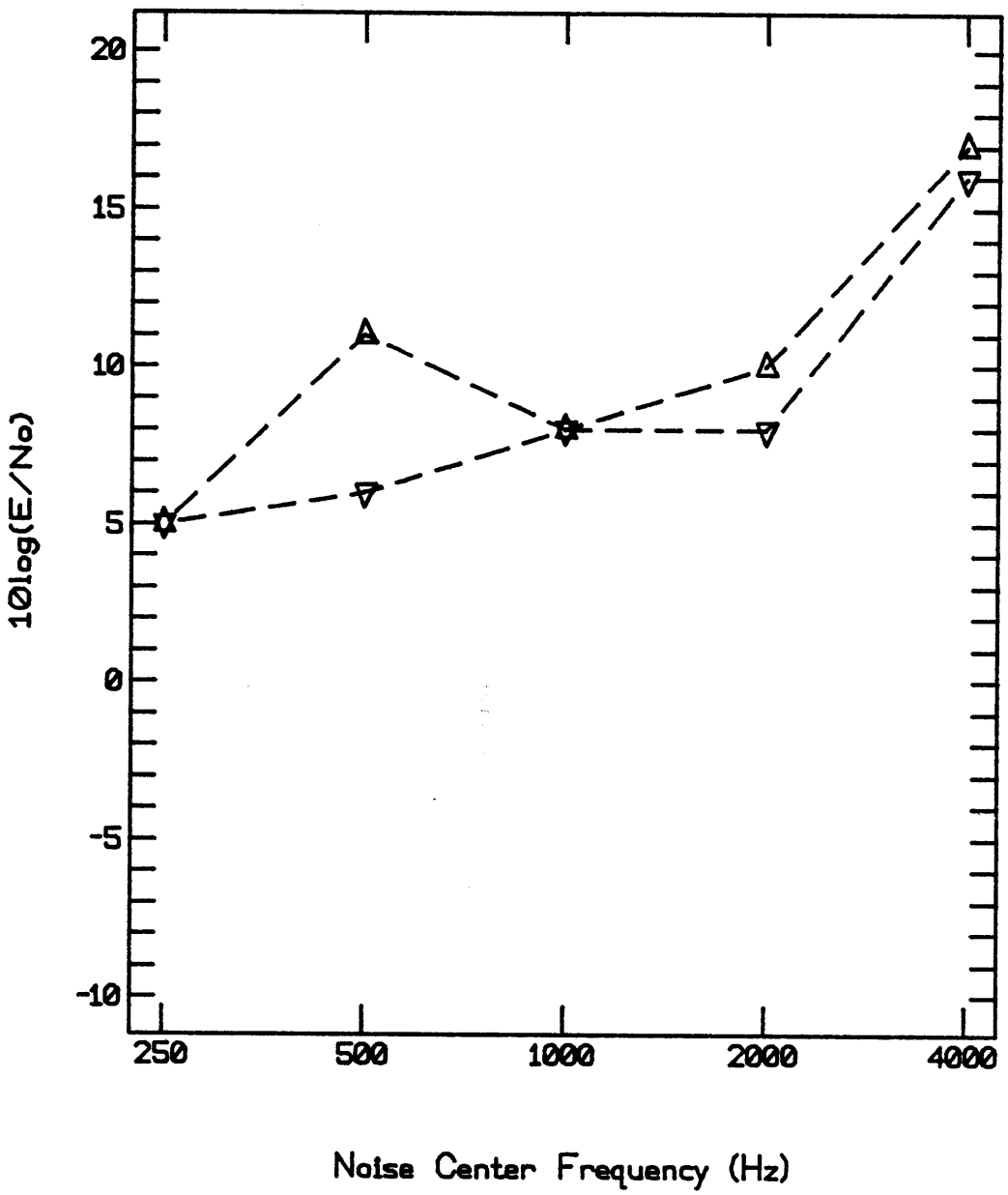
20
15
10
5
0
-5
-10
10log(E/No)
250
500
1000
2000
4000
Noise Center Frequency (Hz)

Figure 4.19

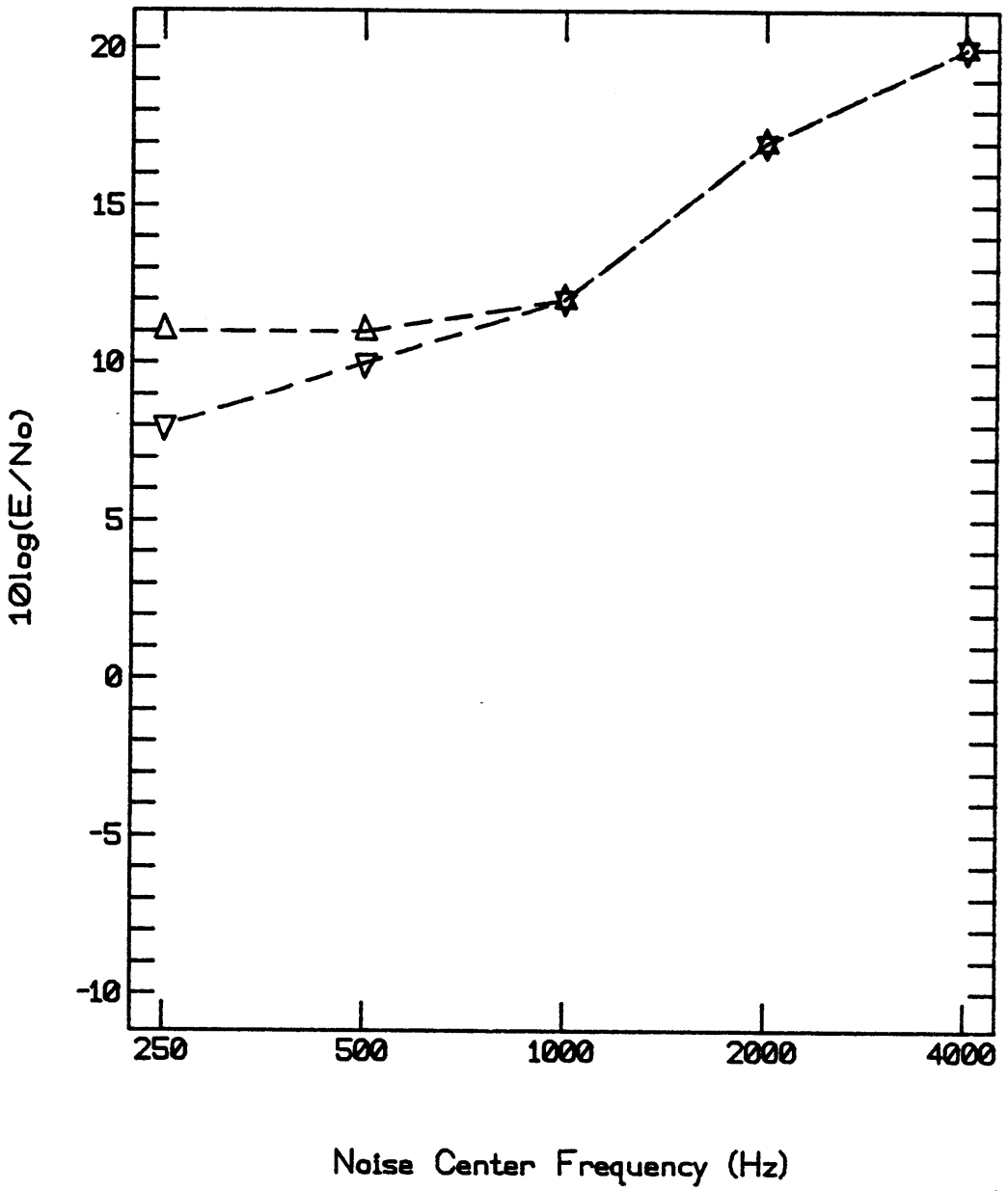
20
15
10
5
0
-5
-10
10log(E/No)
250
500
1000
2000
4000
Noise Center Frequency (Hz)

Figure 4.20

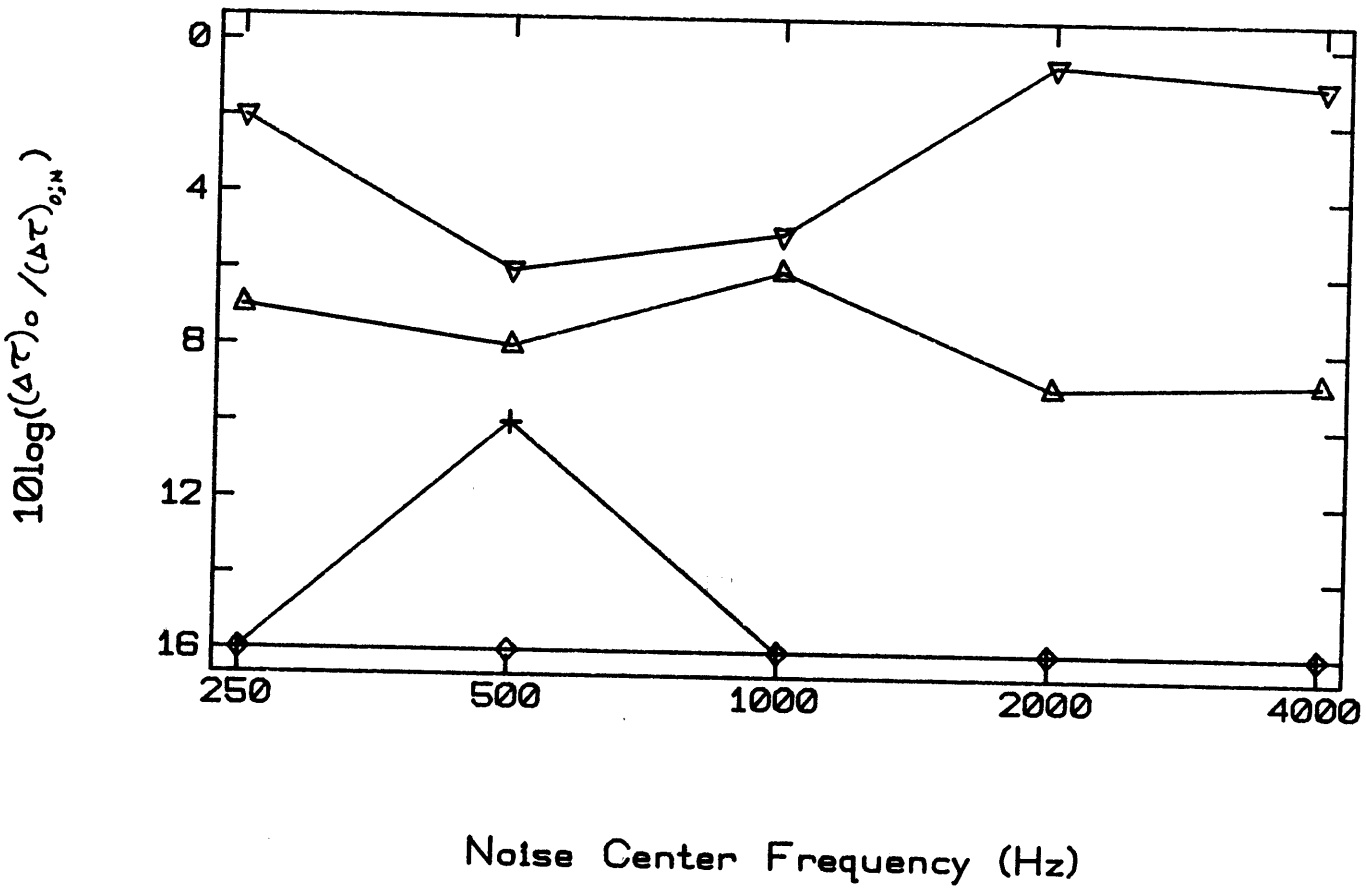
10log((Δτ)o /(Δτ)o;N)
0
4
8
12
16
250
500
1000
2000
4000
Noise Center Frequency (Hz)

Figure 4.21

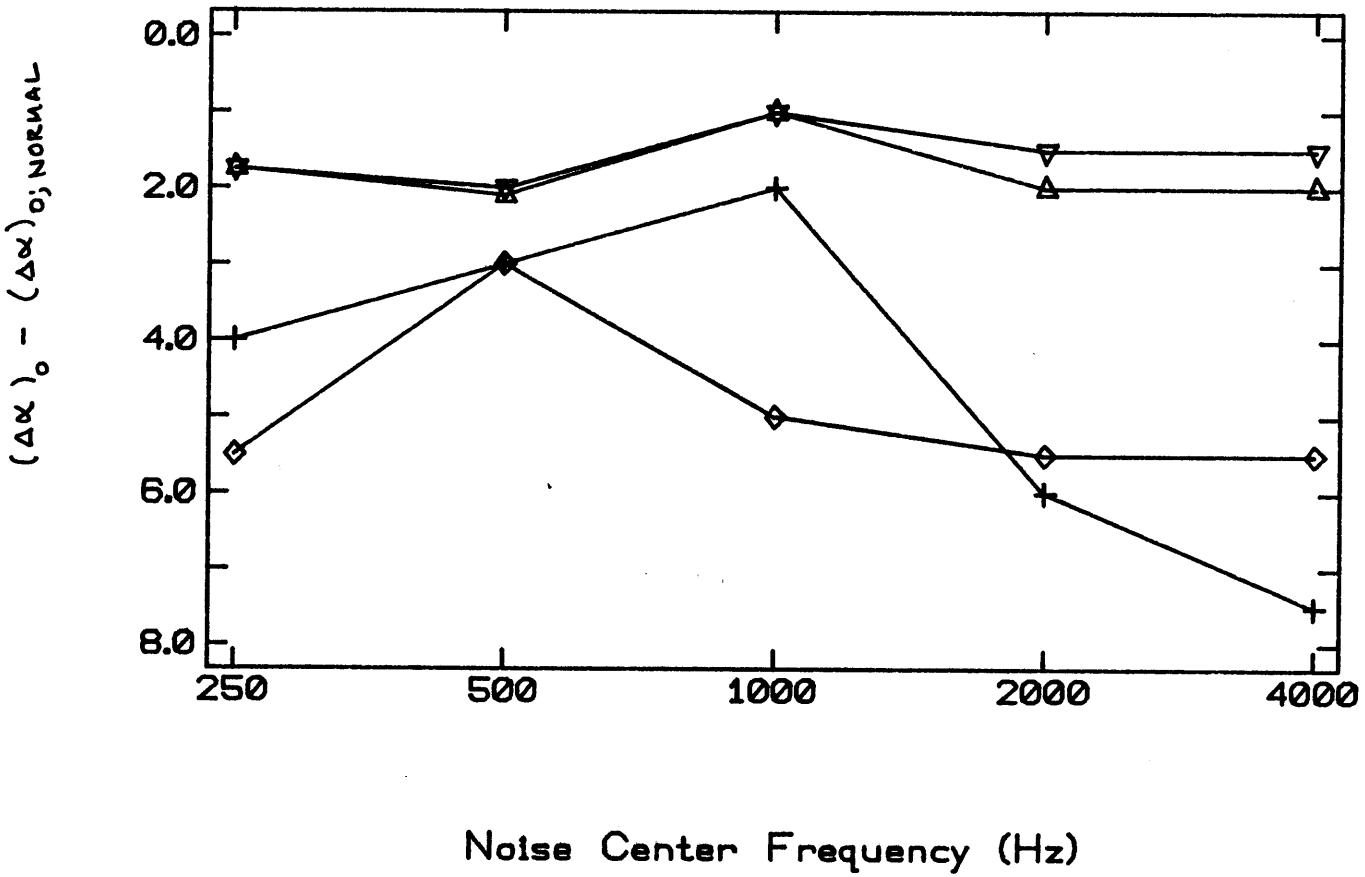
$(\Delta\alpha)_o - (\Delta\alpha)_{o;NORMAL}$
0.0
2.0
4.0
6.0
8.0
250
500
1000
2000
4000
Noise Center Frequency (Hz)

Figure 4.22

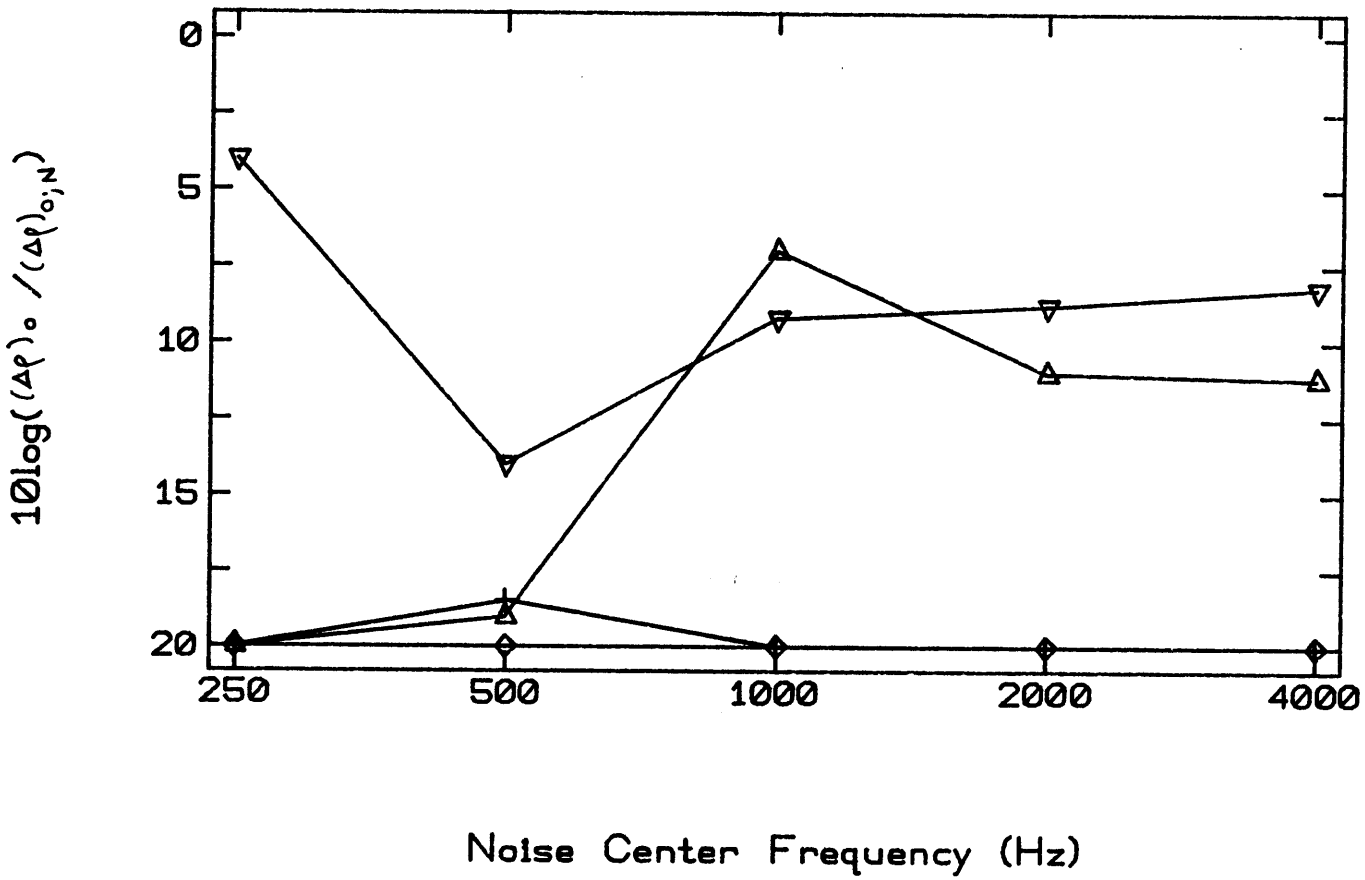
0
5
10
15
20
250
500
1000
2000
4000
10log((Δρ)o /(Δρ)o;N)
Noise Center Frequency (Hz)

Figure 4.23

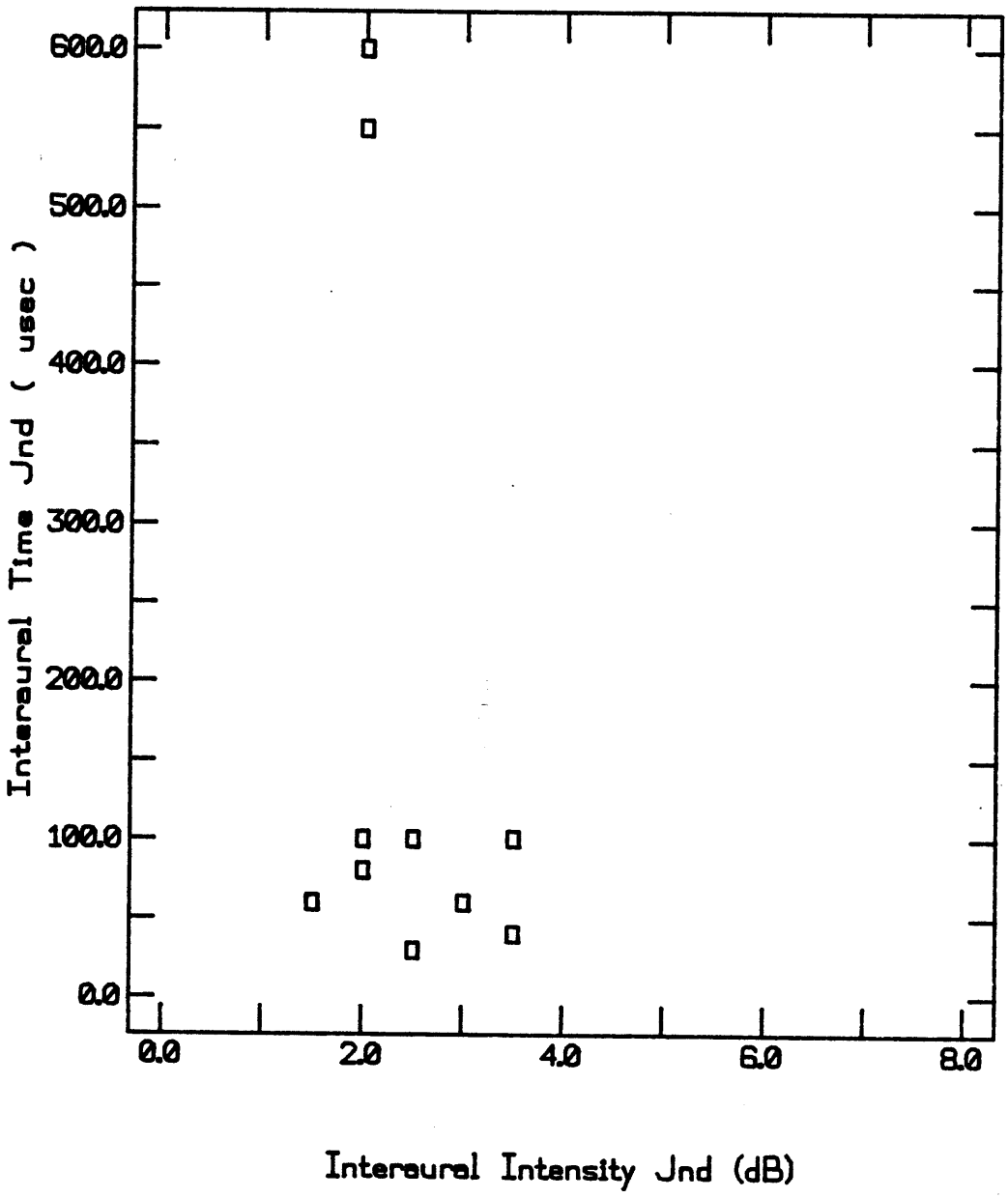
600.0
500.0
400.0
300.0
200.0
100.0
0.0
Interaural Time Jnd (usec)
0.0
2.0
4.0
6.0
8.0
Interaural Intensity Jnd (dB)

Figure 4.24

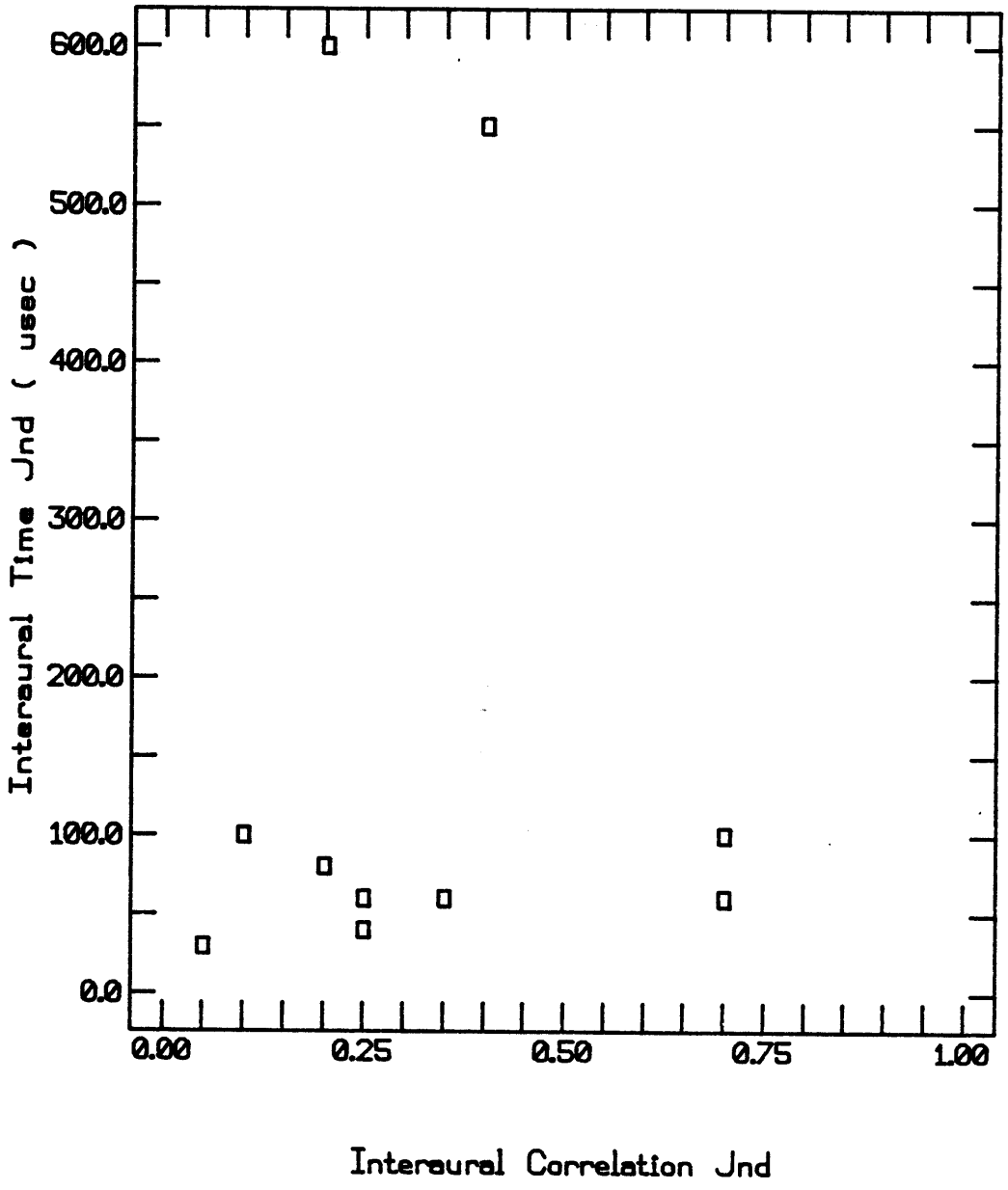
600.0
500.0
400.0
300.0
200.0
100.0
0.0
Interaural Time Jnd (usec)
0.00
0.25
0.50
0.75
1.00
Interaural Correlation Jnd

Figure 4.25

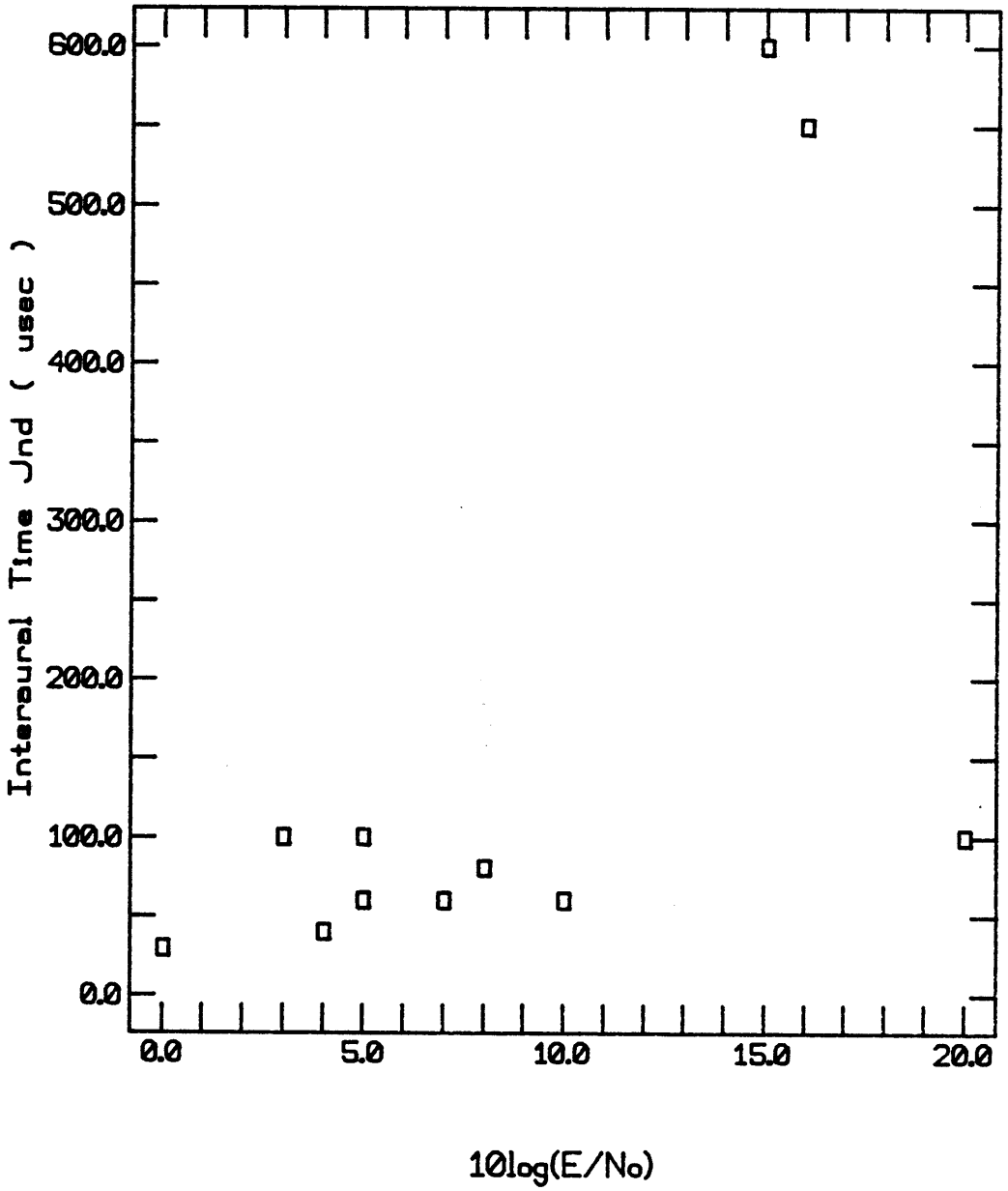
600.0
500.0
400.0
300.0
200.0
100.0
0.0
Interaural Time Jnd (usec)
0.0
5.0
10.0
15.0
20.0
10log(E/No)

Figure 4.26

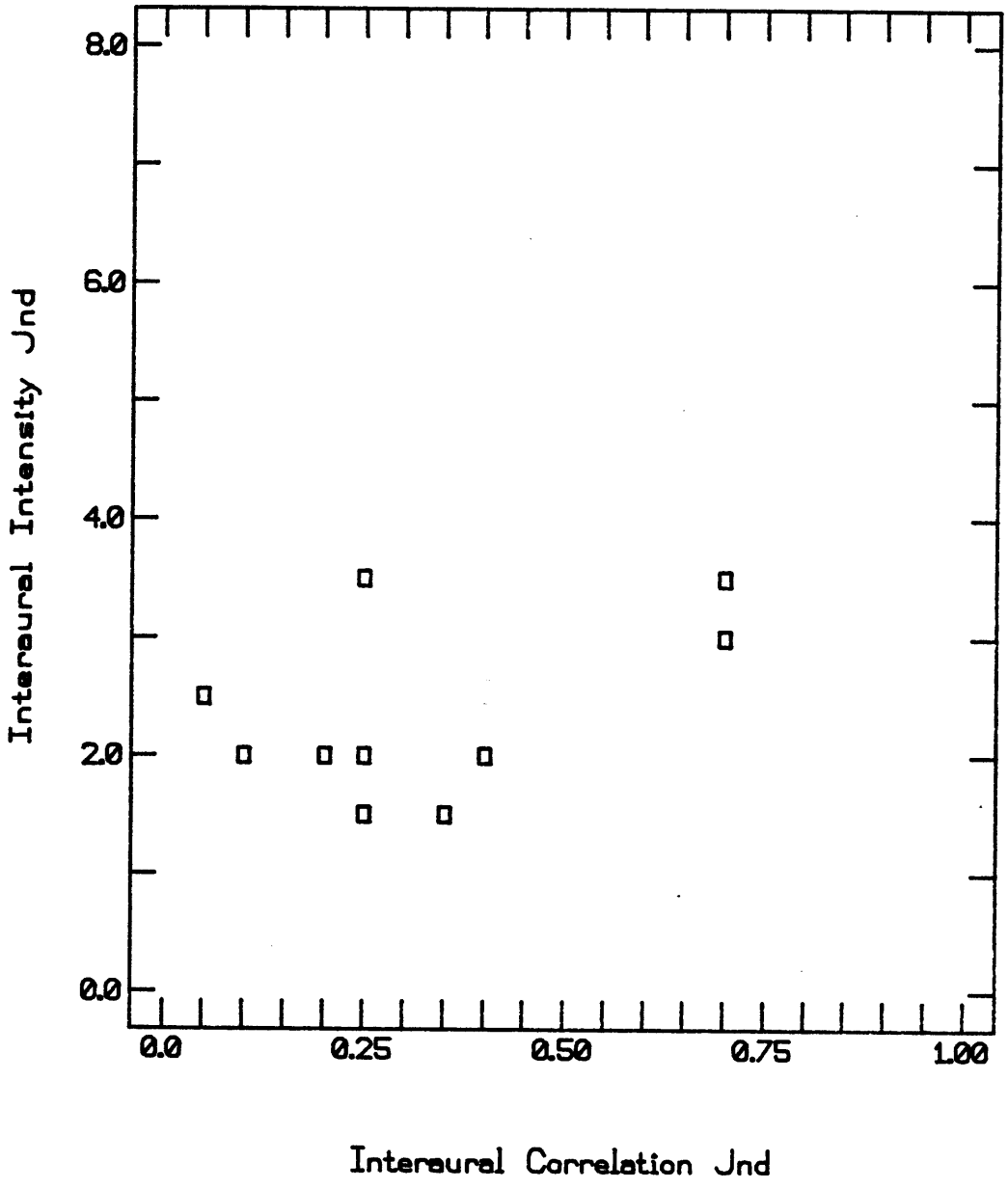
8.0
6.0
4.0
2.0
0.0
Interaural Intensity Jnd
0.0
0.25
0.50
0.75
1.00
Interaural Correlation Jnd

Figure 4.27

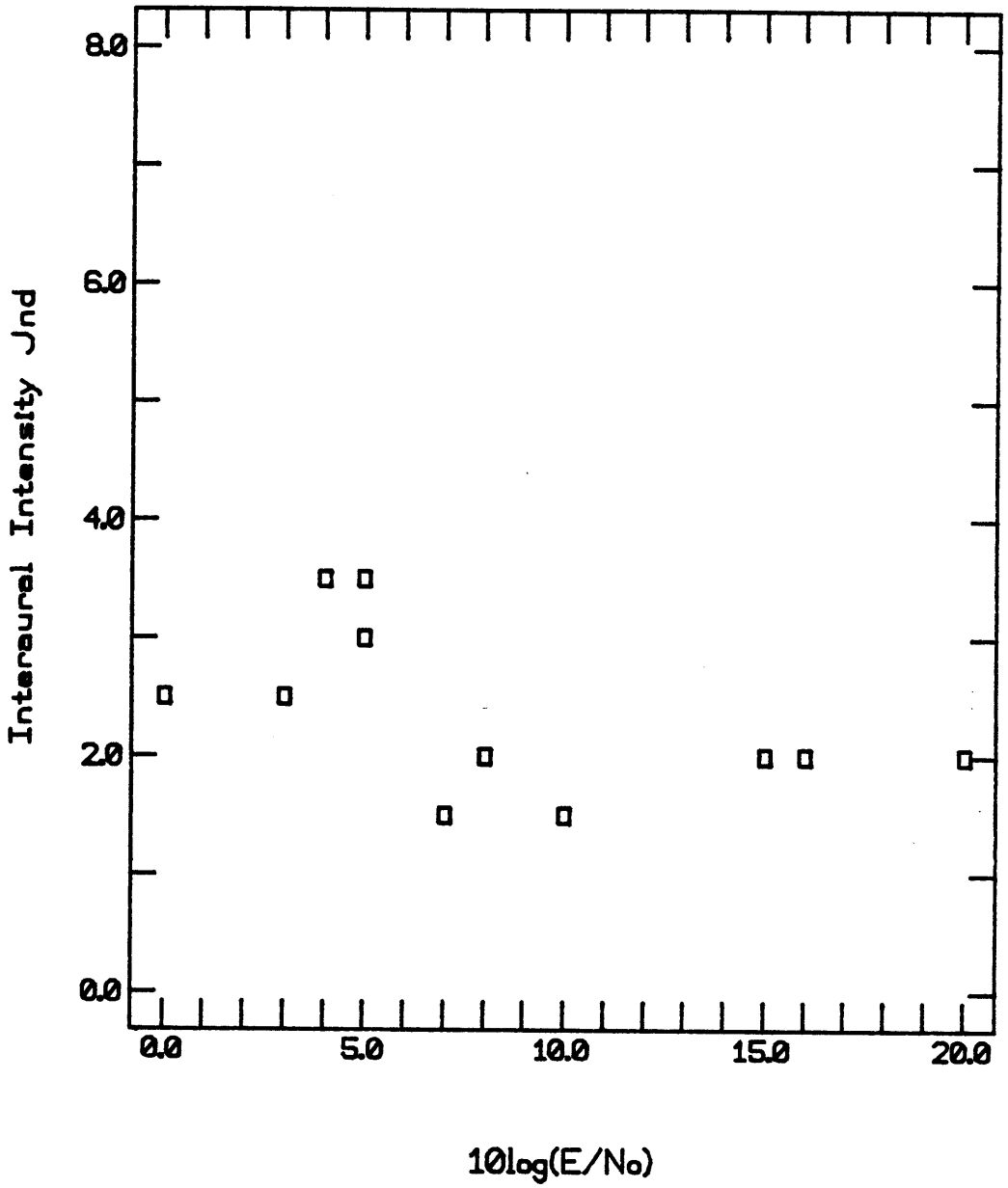
8.0
6.0
4.0
2.0
0.0
Interaural Intensity Jnd
0.0
5.0
10.0
15.0
20.0
10log(E/No)

Figure 4.28

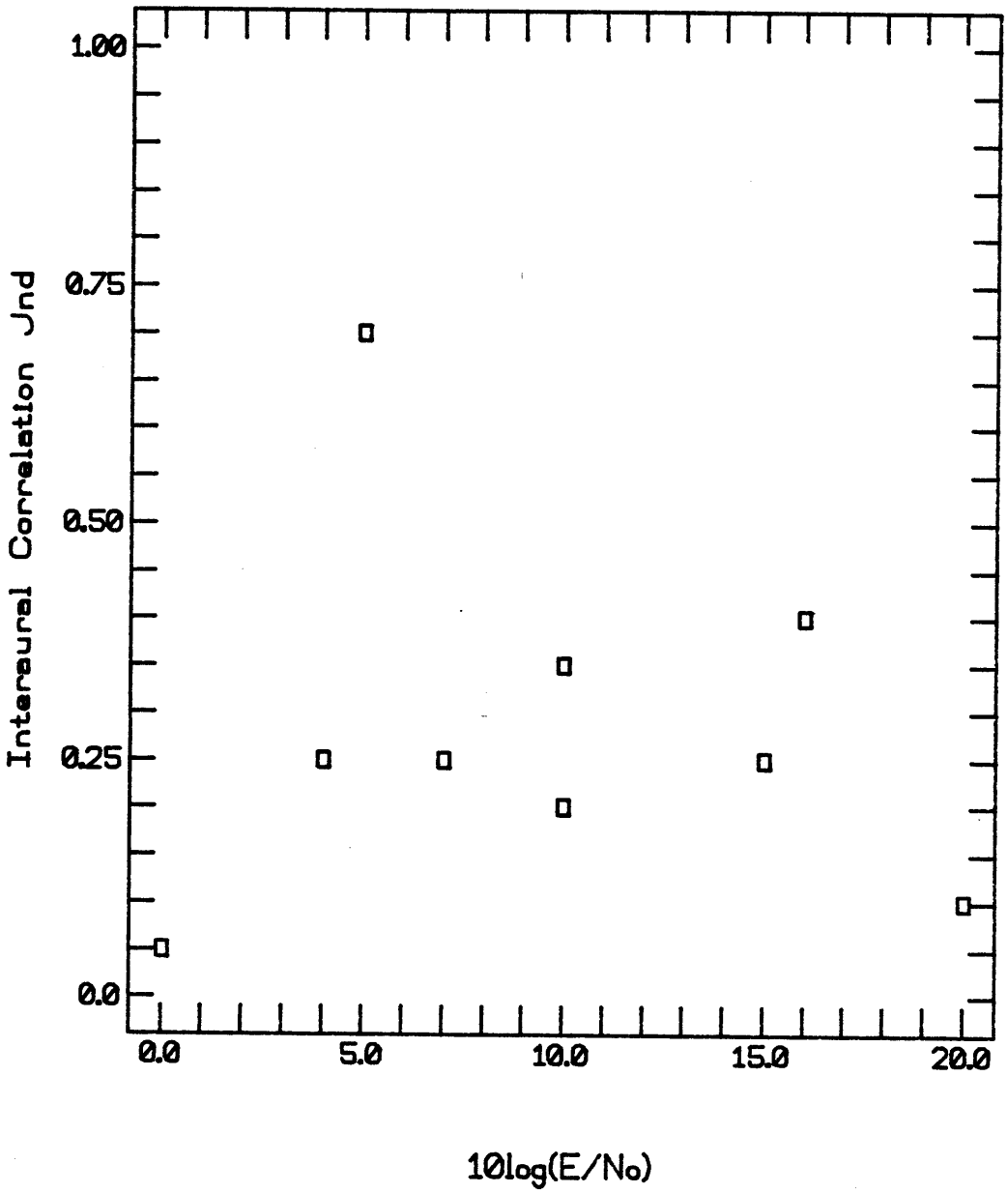
1.00
0.75
0.50
0.25
0.0
Interaural Correlation Jnd
0.0
5.0
10.0
15.0
20.0
10log(E/No)

Figure 4.29

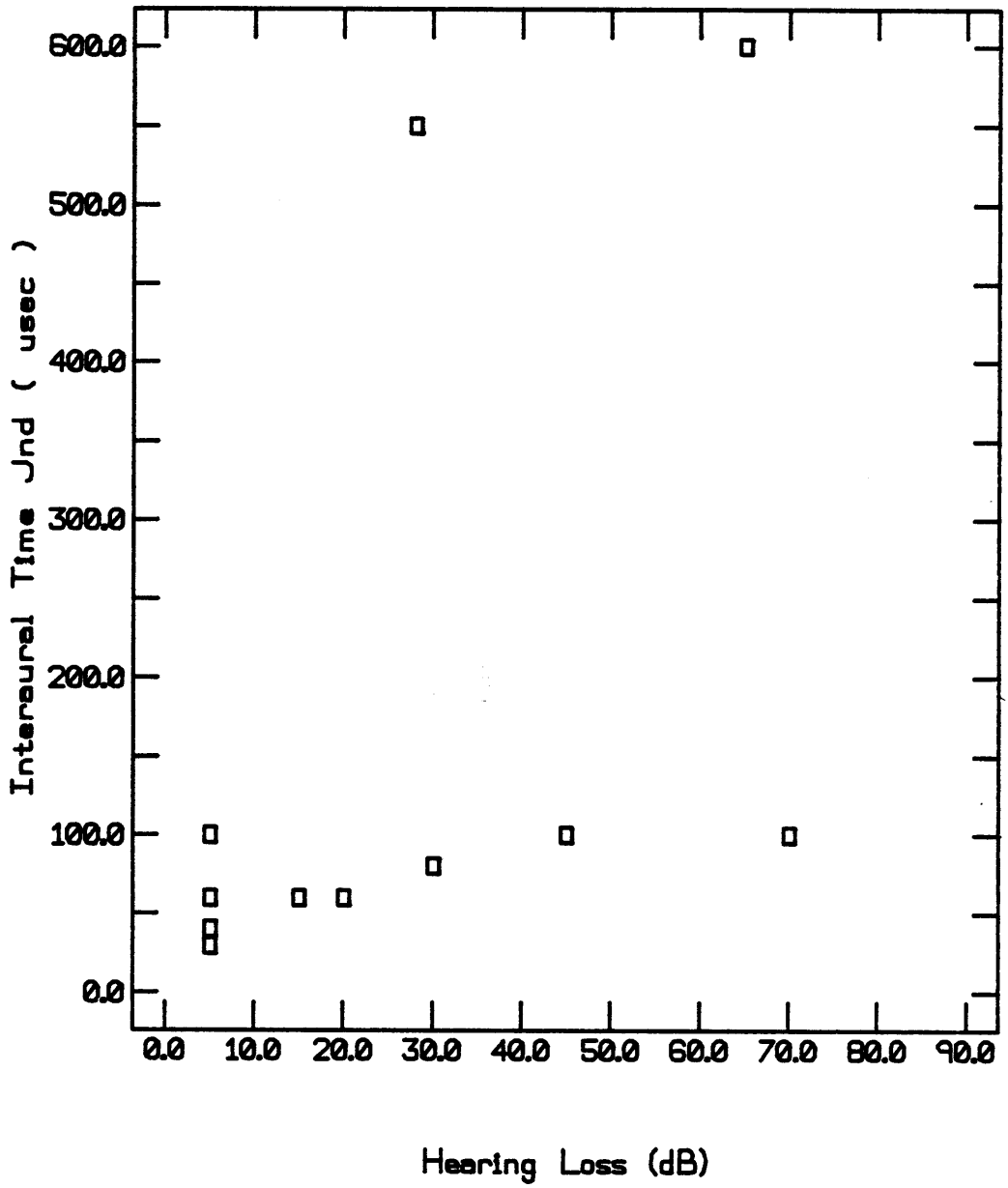
600.0
500.0
400.0
300.0
200.0
100.0
0.0
Interaural Time Jnd (usec)
0.0
10.0
20.0
30.0
40.0
50.0
60.0
70.0
80.0
90.0
Hearing Loss (dB)

Figure 4.30

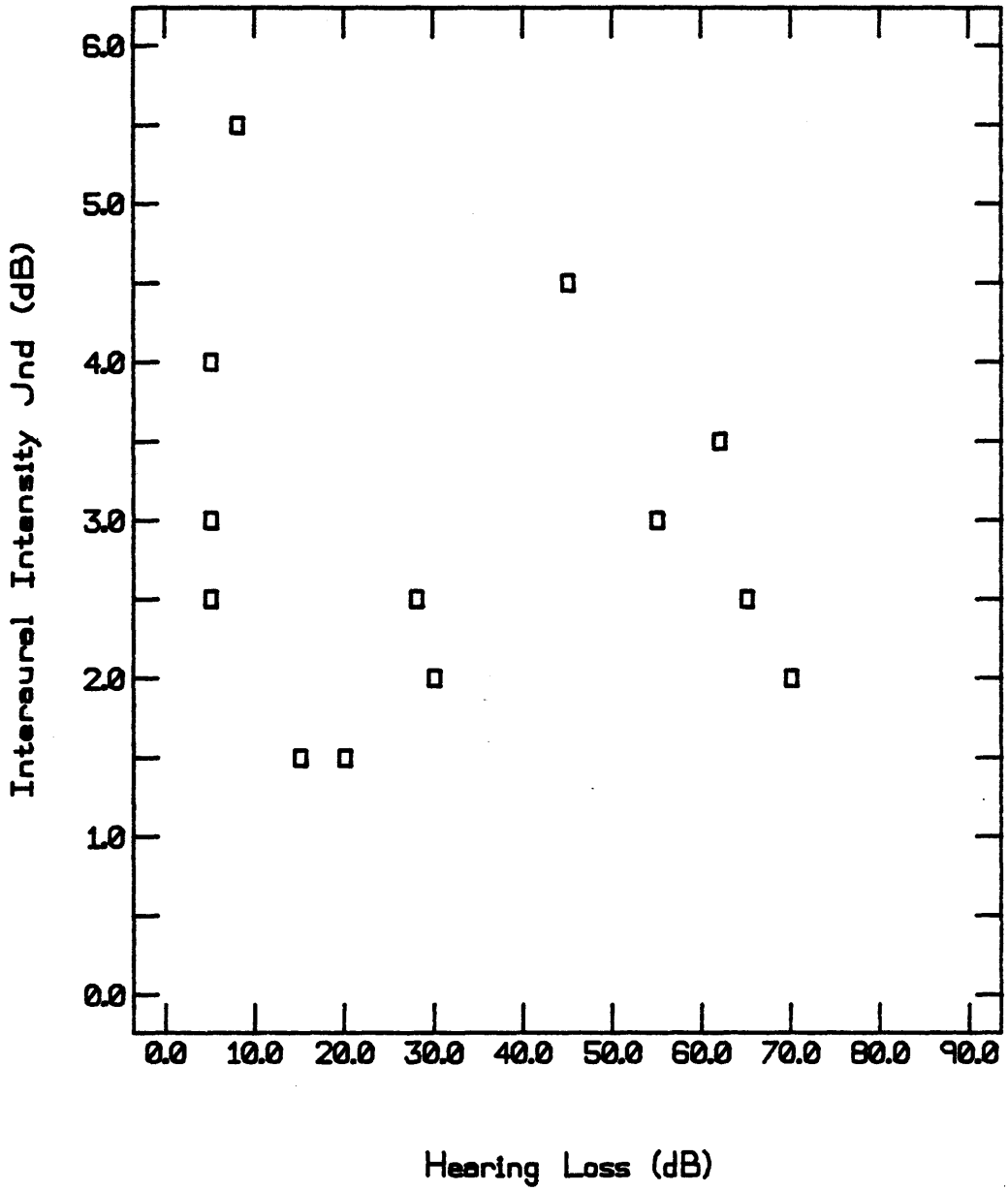
Interaural Intensity Jnd (dB)
6.0
5.0
4.0
3.0
2.0
1.0
0.0
0.0
10.0
20.0
30.0
40.0
50.0
60.0
70.0
80.0
90.0
Hearing Loss (dB)

Figure 4.31

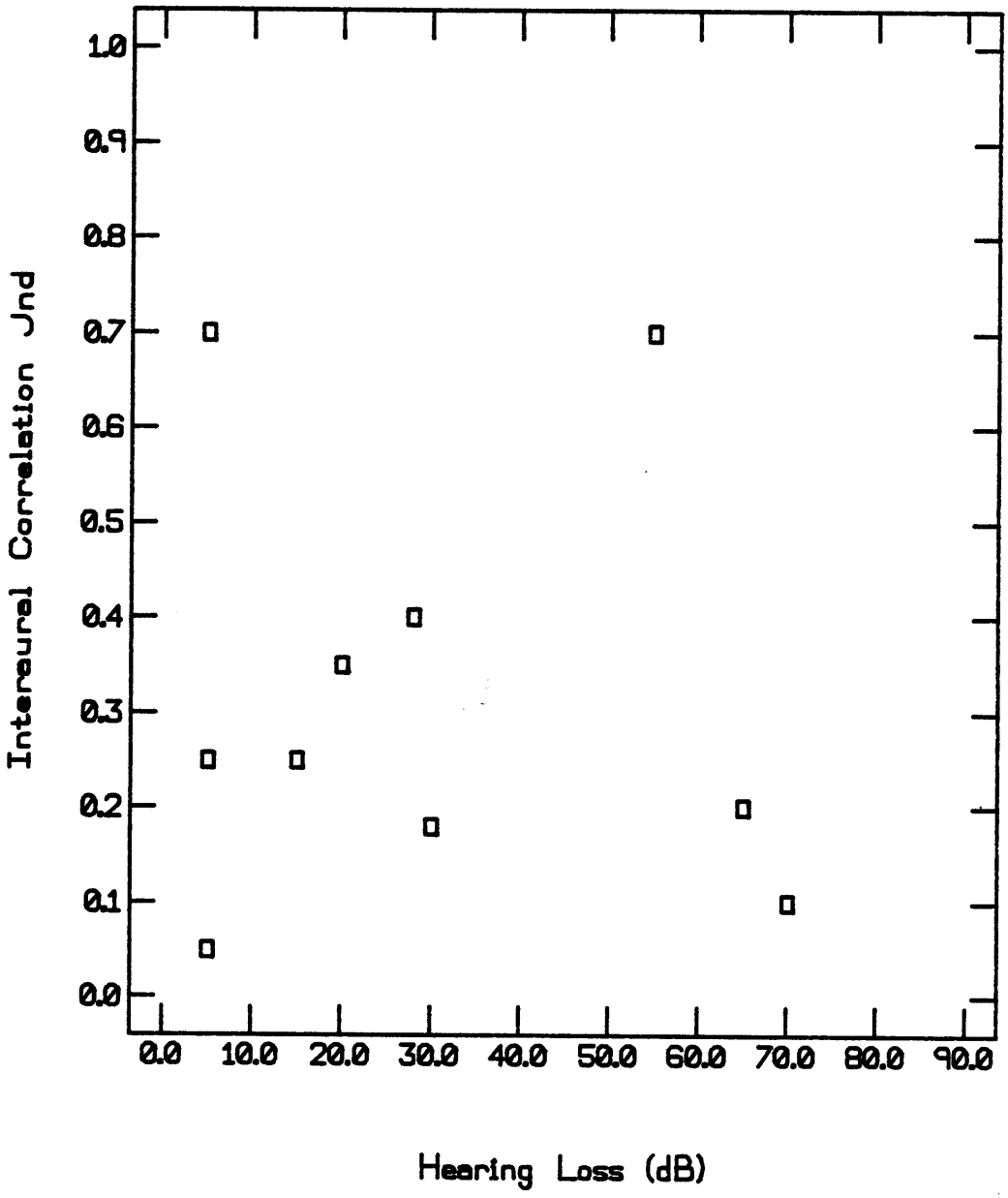
Interaural Correlation Jnd
1.0
0.9
0.8
0.7
0.6
0.5
0.4
0.3
0.2
0.1
0.0
0.0
10.0
20.0
30.0
40.0
50.0
60.0
70.0
80.0
90.0
Hearing Loss (dB)

Figure 4.32

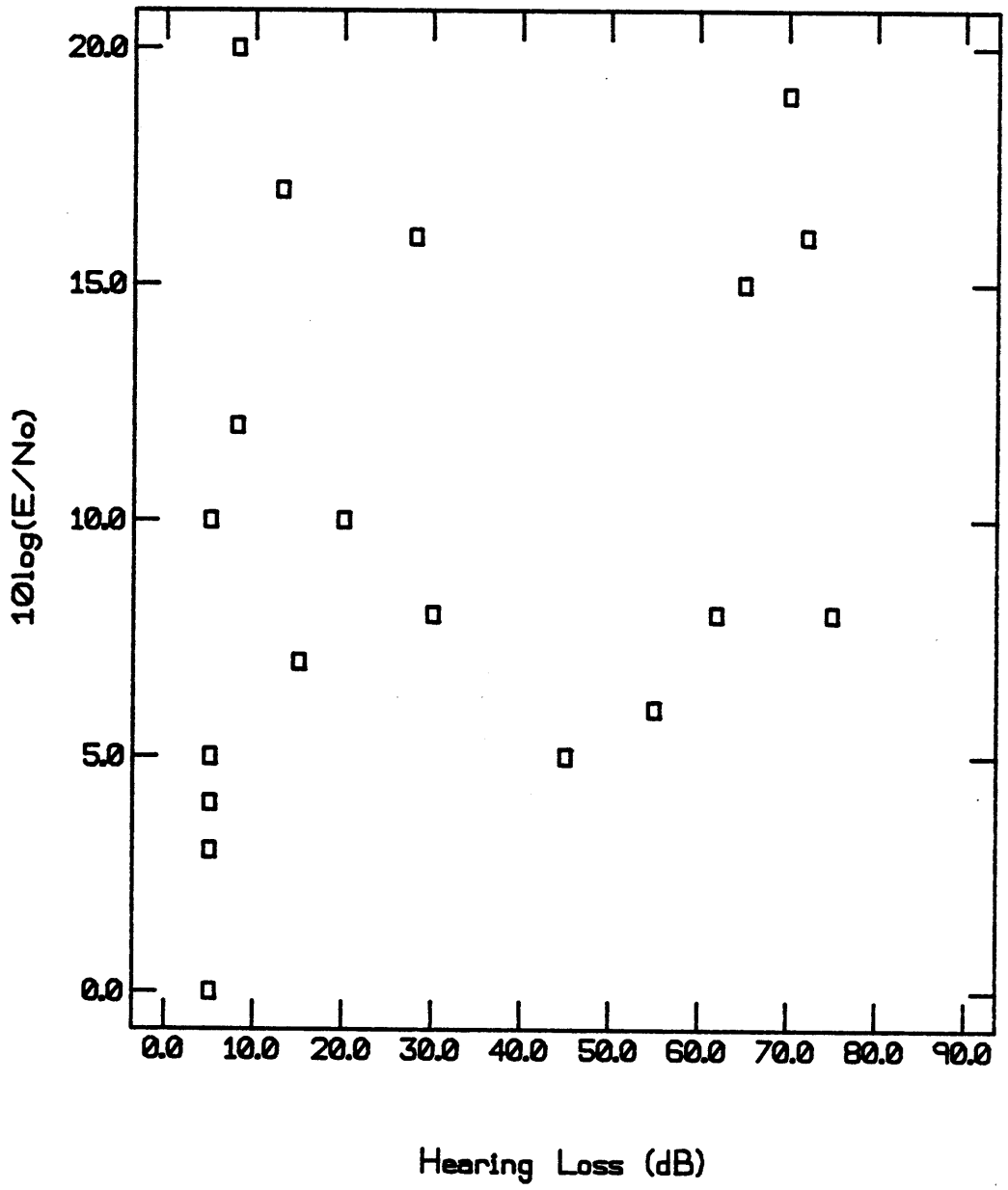
20.0
15.0
10.0
5.0
0.0
10log(E/No)
0.0
10.0
20.0
30.0
40.0
50.0
60.0
70.0
80.0
90.0
Hearing Loss (dB)

Figure 4.33

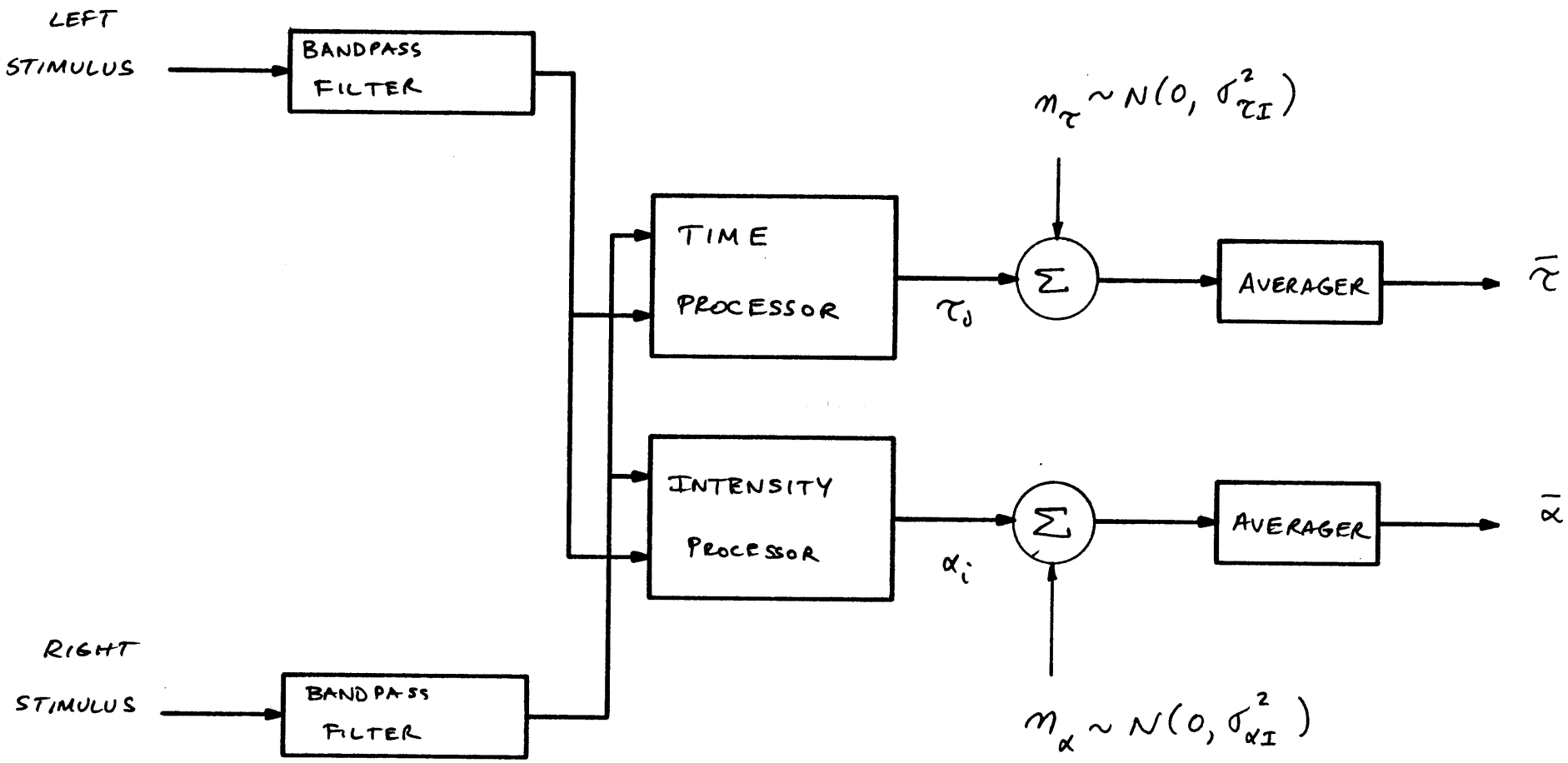
LEFT
STIMULUS
BANDPASS
FILTER
RIGHT
STIMULUS
BANDPASS
FILTER
TIME
PROCESSOR
INTENSITY
PROCESSOR
τ_i
α_i
Σ
Σ
$n_\tau \sim N(0, \sigma^2_{\tau I})$
$n_\alpha \sim N(0, \sigma^2_{\alpha I})$
AVERAGER
AVERAGER
$\bar{\tau}$
$\bar{\alpha}$

Figure 5.1

$\bar{\tau}$
$\bar{\alpha}$
IDEAL
PROCESSOR
(a)
$\bar{\tau}$
$\frac{(\Delta\alpha)_o}{(\Delta\tau)_o}$
Σ
$\bar{\alpha}$
IDEAL
PROCESSOR
(b)

Figure 5.2

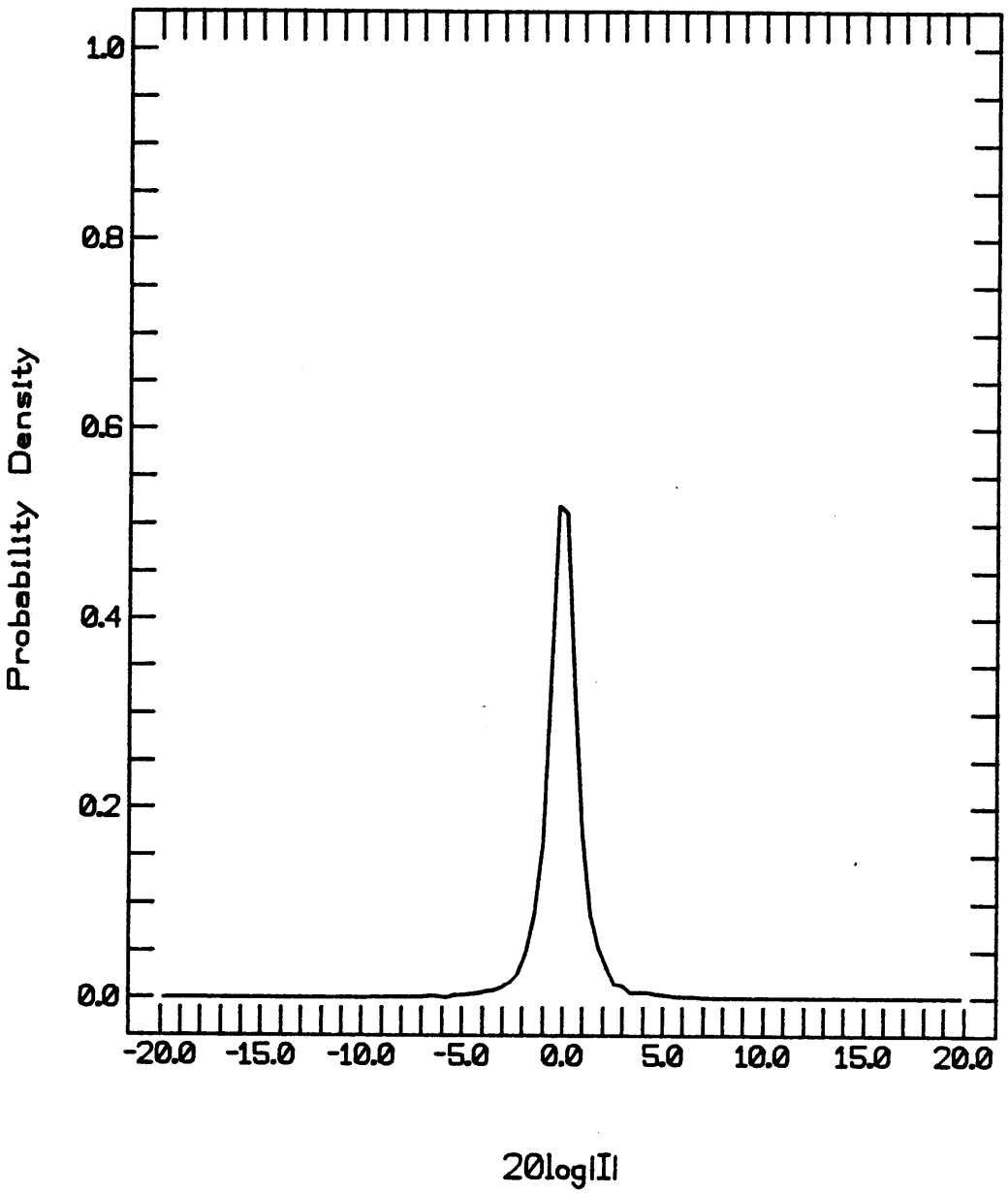
1.0
0.8
0.6
0.4
0.2
0.0
Probability Density
-20.0
-15.0
-10.0
-5.0
0.0
5.0
10.0
15.0
20.0
20log|I|

Figure 6.1

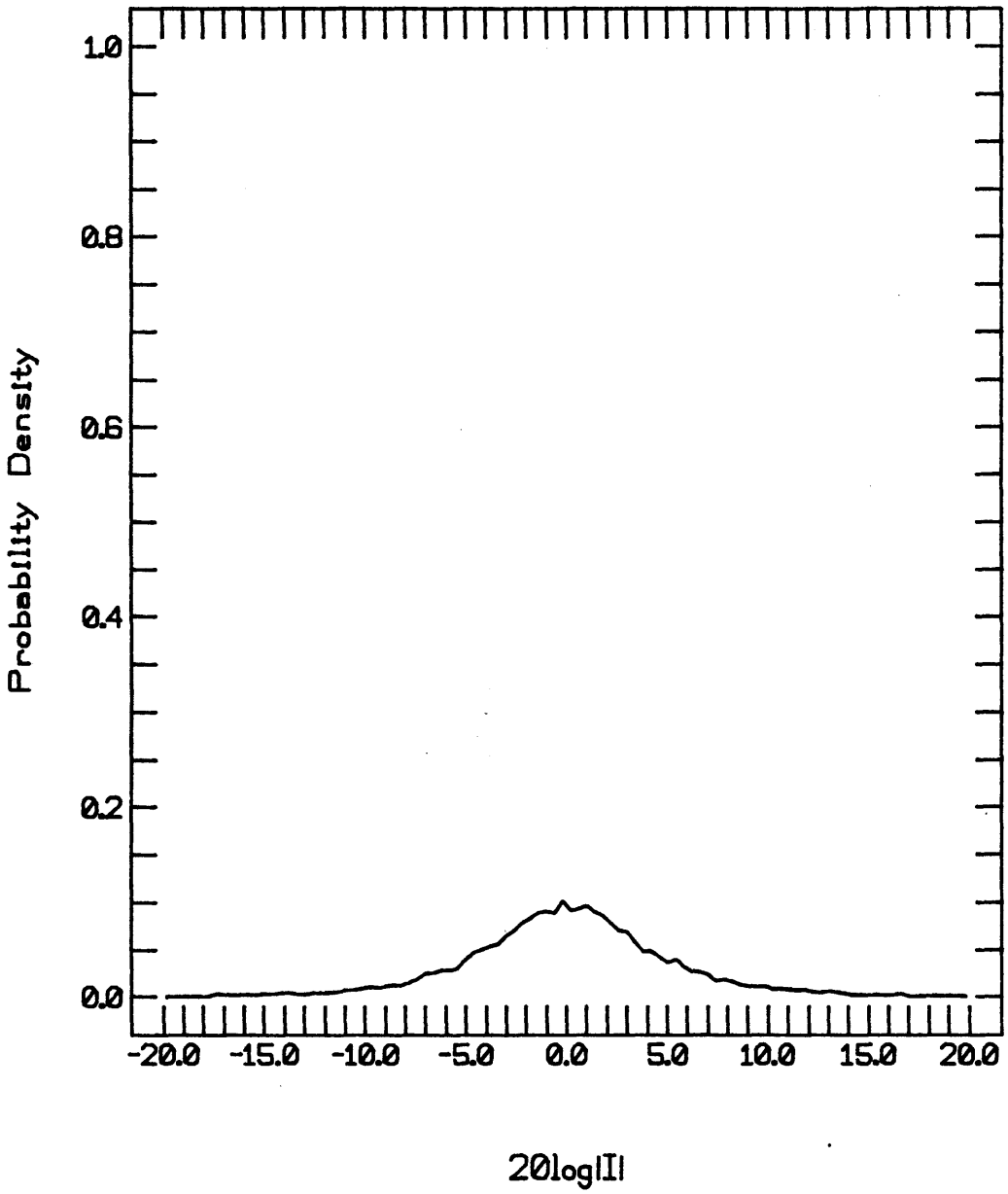
1.0
0.8
0.6
0.4
0.2
0.0
Probability Density
-20.0
-15.0
-10.0
-5.0
0.0
5.0
10.0
15.0
20.0
20log|I|

Figure 6.2

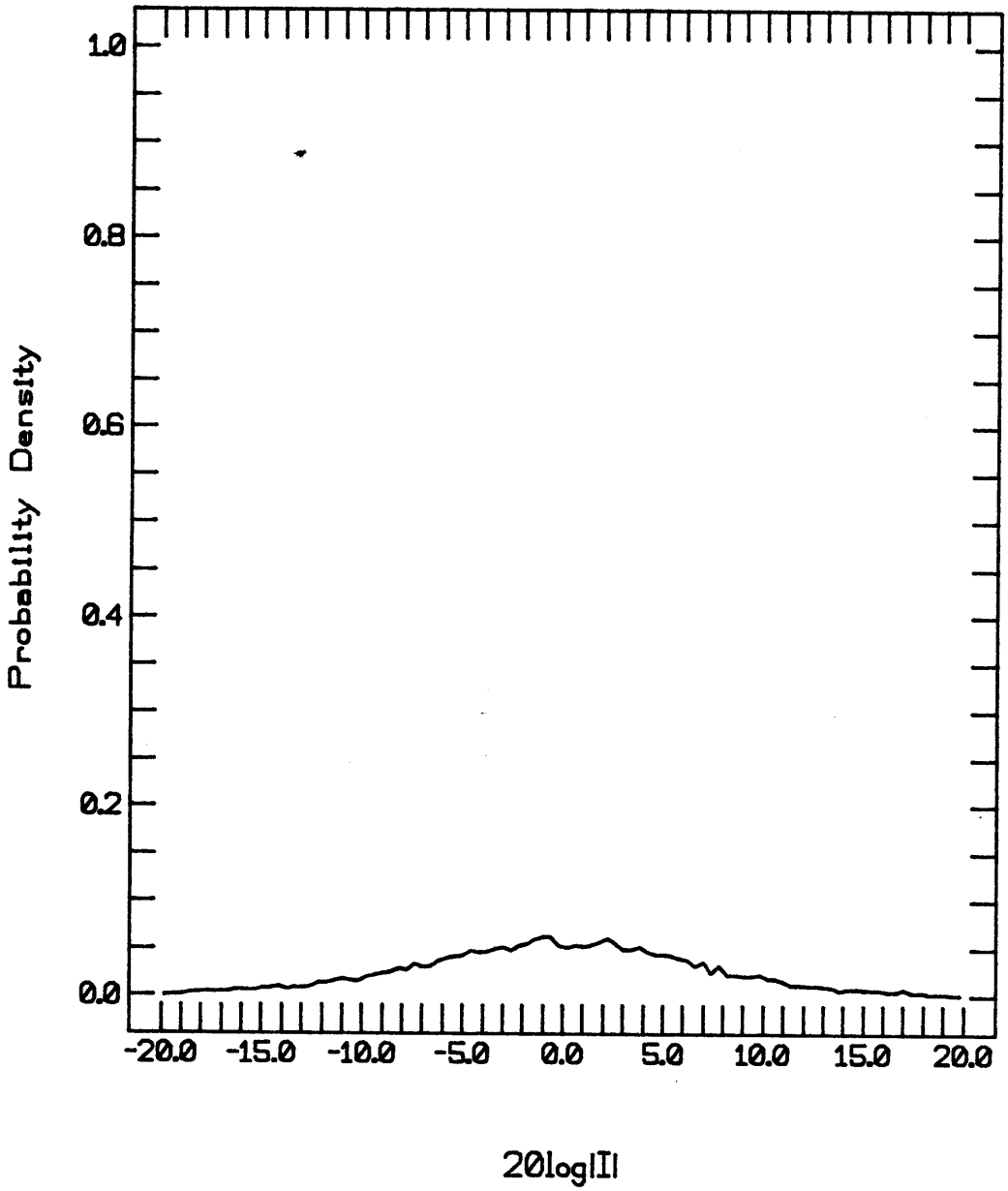
1.0
0.8
0.6
0.4
0.2
0.0
Probability Density
-20.0
-15.0
-10.0
-5.0
0.0
5.0
10.0
15.0
20.0
20log|I|

Figure 6.3

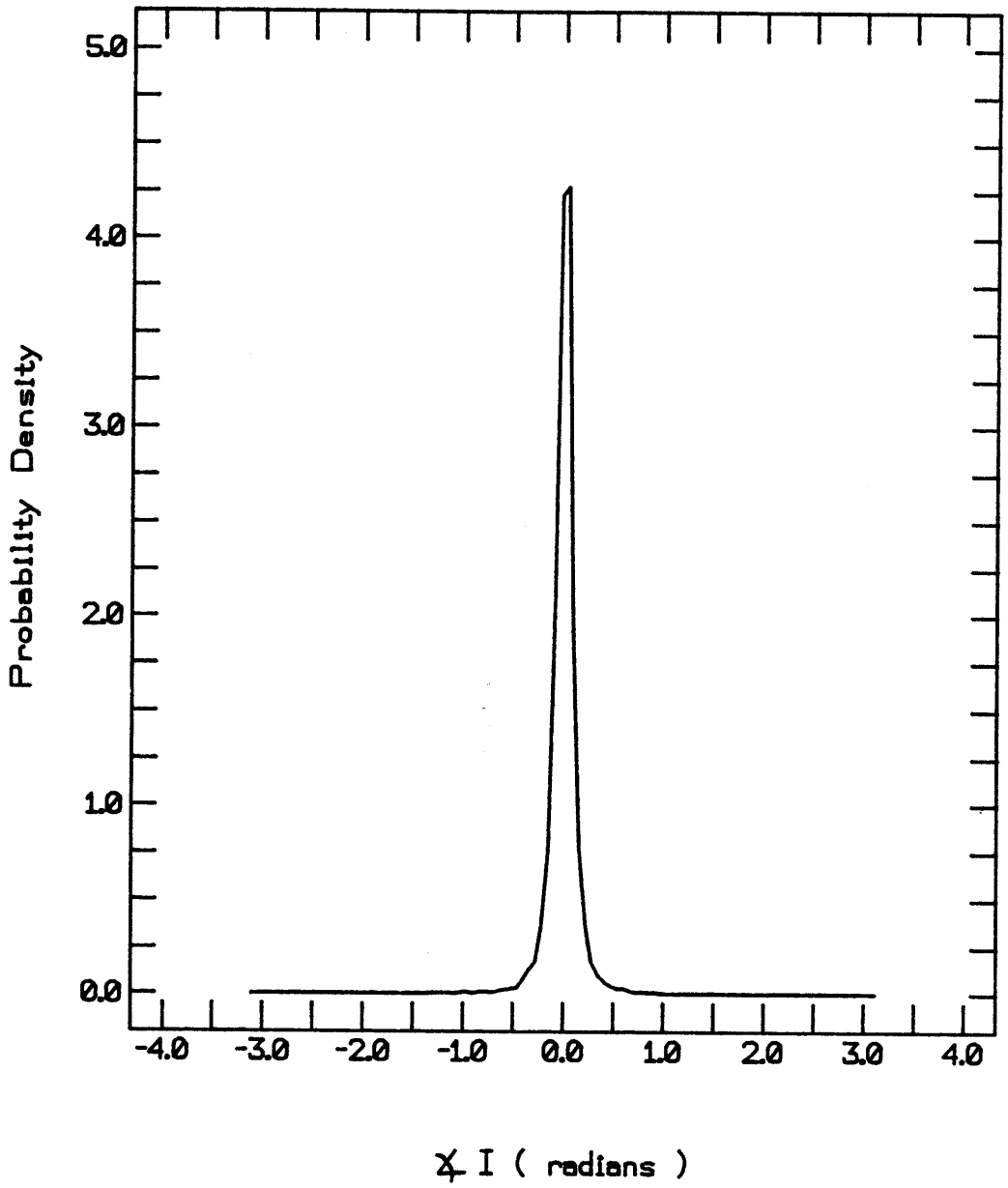
5.0
4.0
3.0
2.0
1.0
0.0
Probability Density
-4.0
-3.0
-2.0
-1.0
0.0
1.0
2.0
3.0
4.0
X I (radians)

Figure 6.4

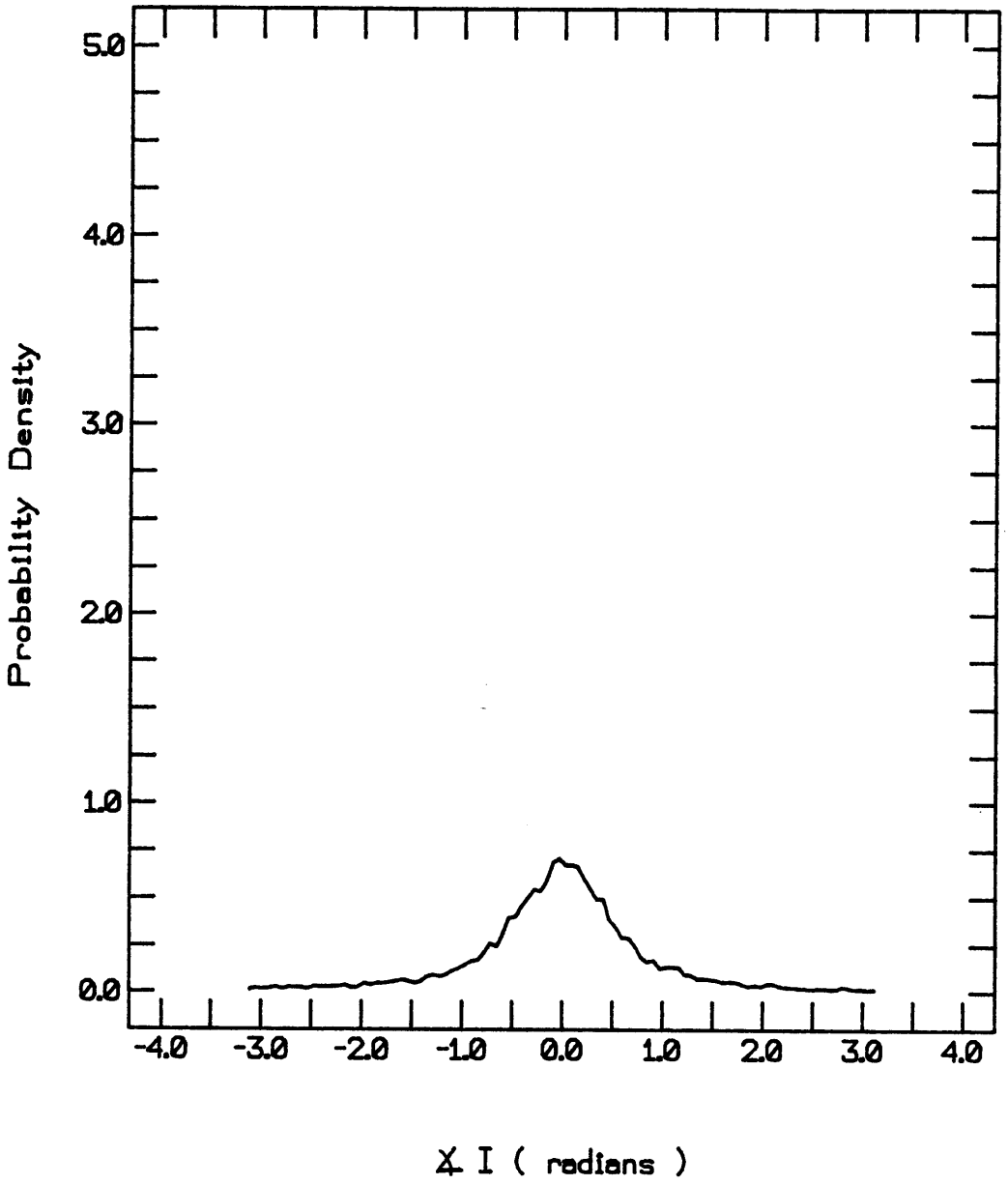
5.0
4.0
3.0
2.0
1.0
0.0
Probability Density
-4.0
-3.0
-2.0
-1.0
0.0
1.0
2.0
3.0
4.0
X I (radians)

Figure 6.5

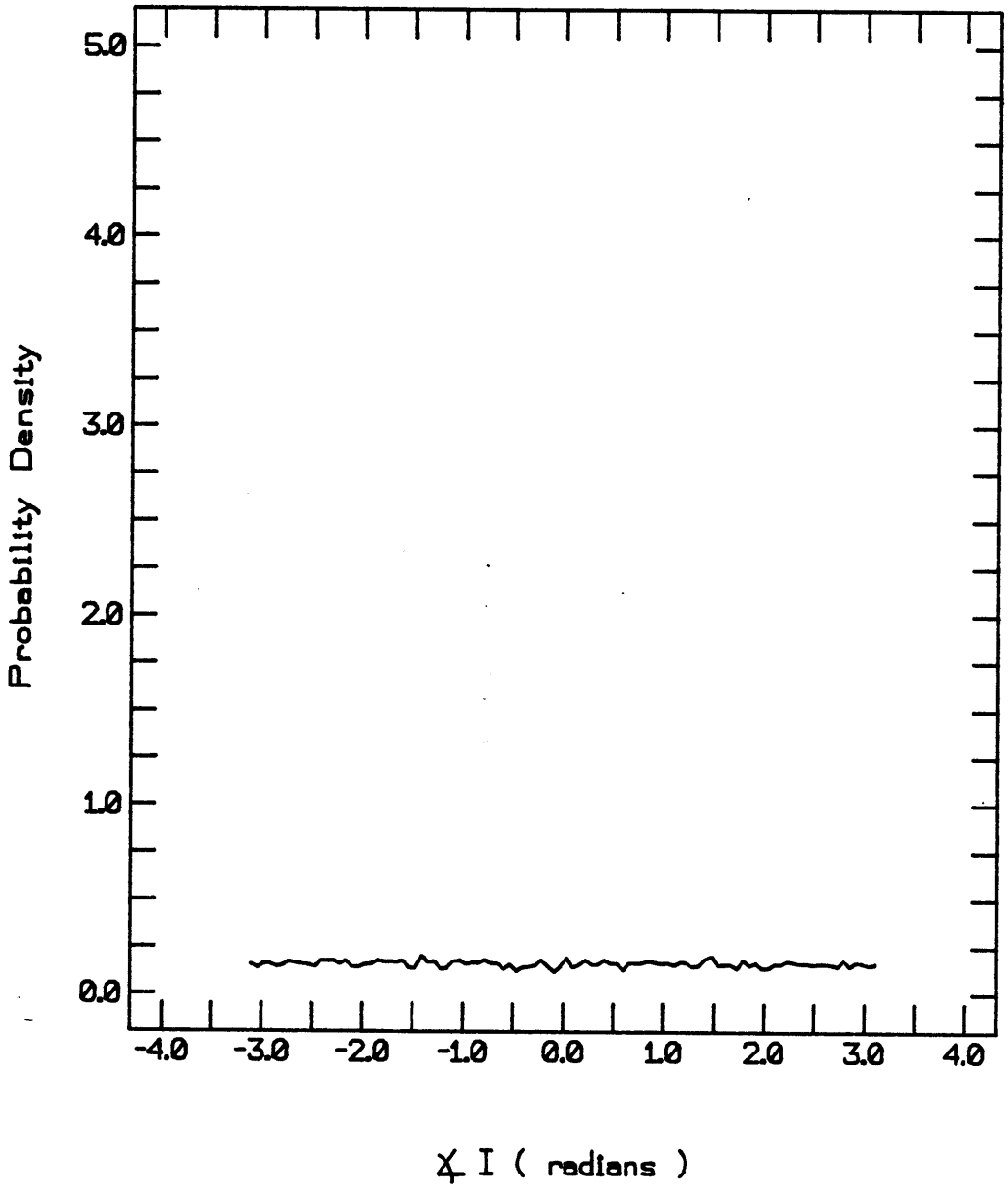
5.0
4.0
3.0
2.0
1.0
0.0
Probability Density
-4.0
-3.0
-2.0
-1.0
0.0
1.0
2.0
3.0
4.0
χ I (radians)

Figure 6.6

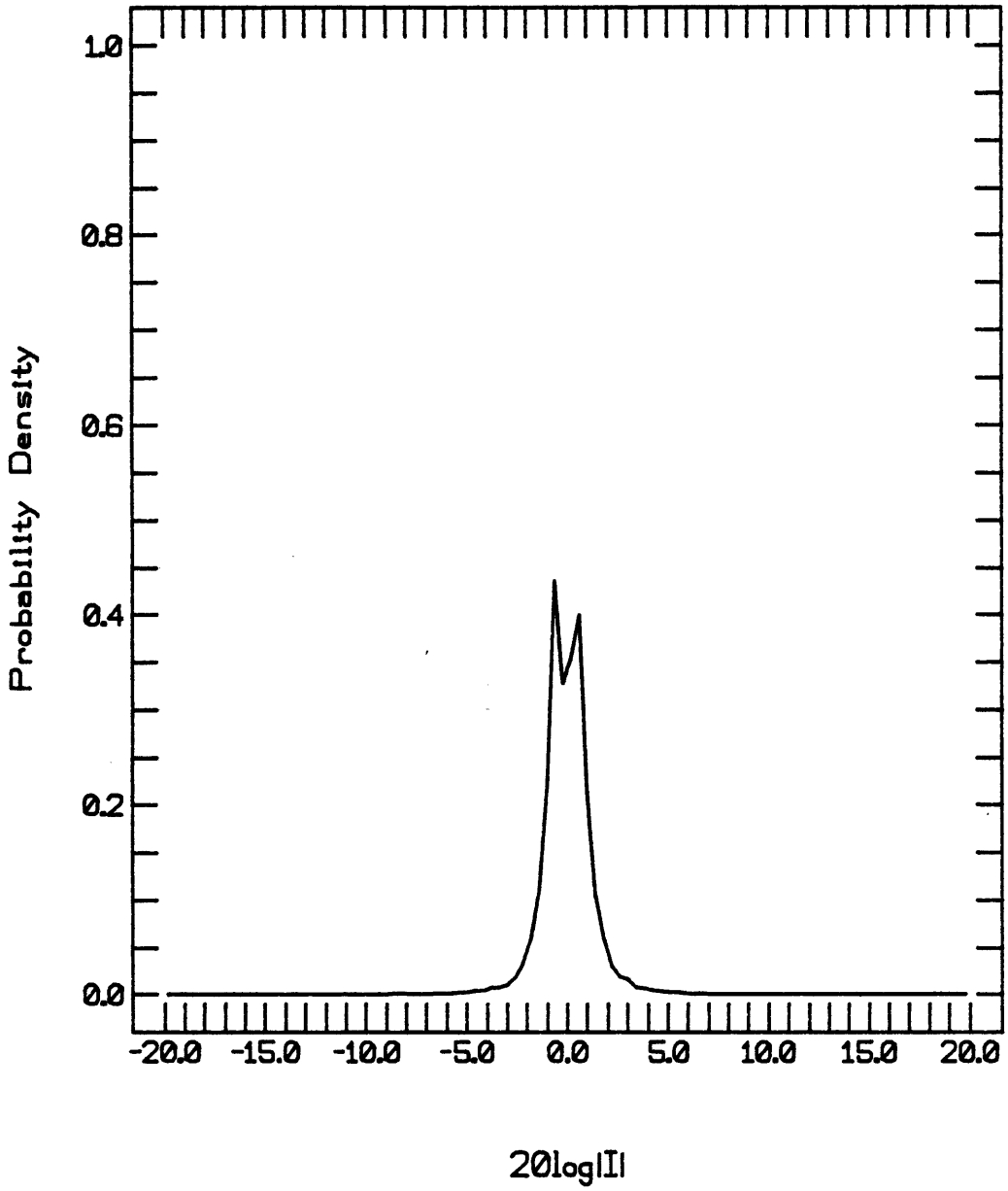
1.0
0.8
0.6
0.4
0.2
0.0
Probability Density
-20.0
-15.0
-10.0
-5.0
0.0
5.0
10.0
15.0
20.0
20log|I|

Figure 6.7

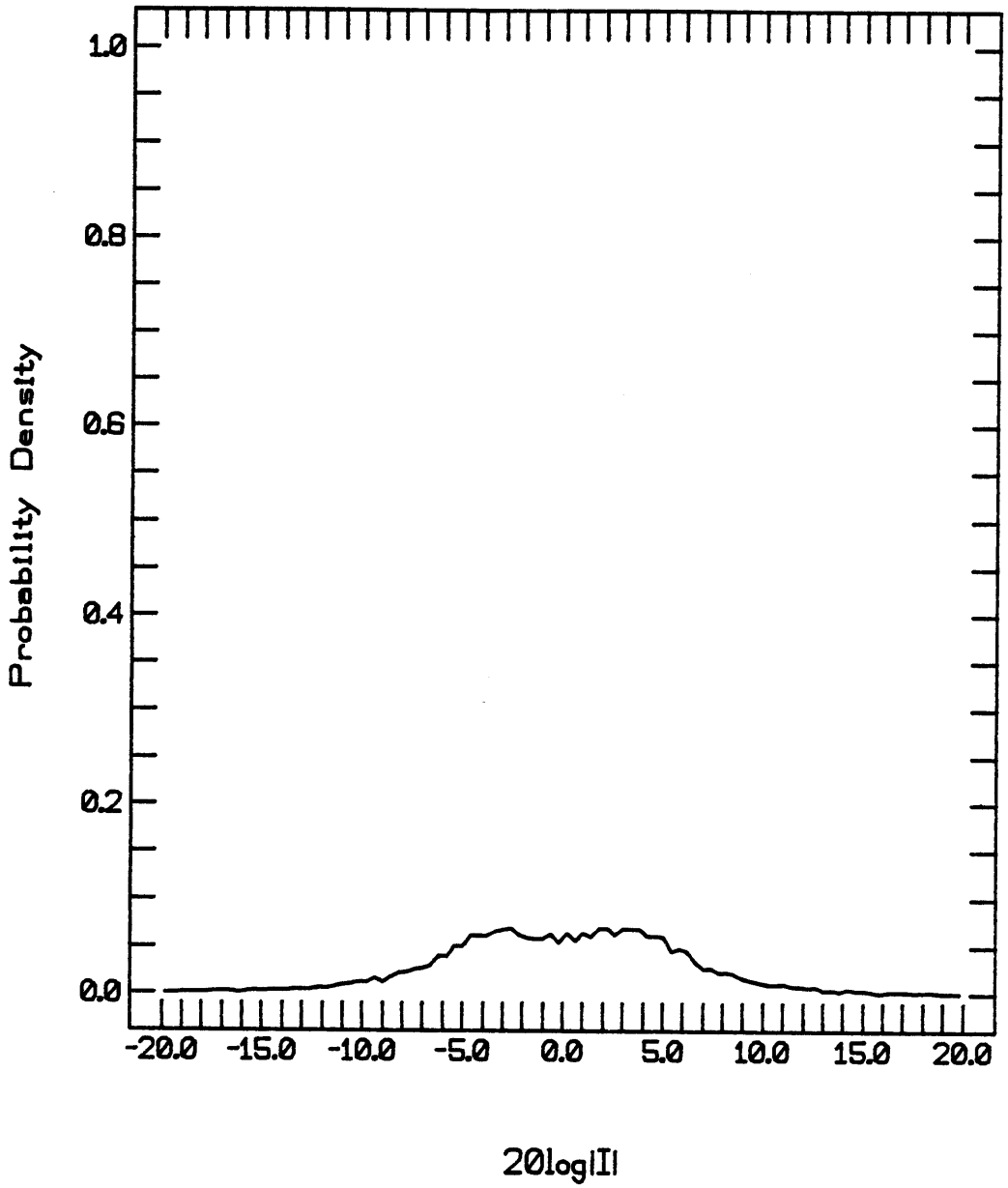
1.0
0.8
0.6
0.4
0.2
0.0
Probability Density
-20.0
-15.0
-10.0
-5.0
0.0
5.0
10.0
15.0
20.0
20log|I|

Figure 6.8

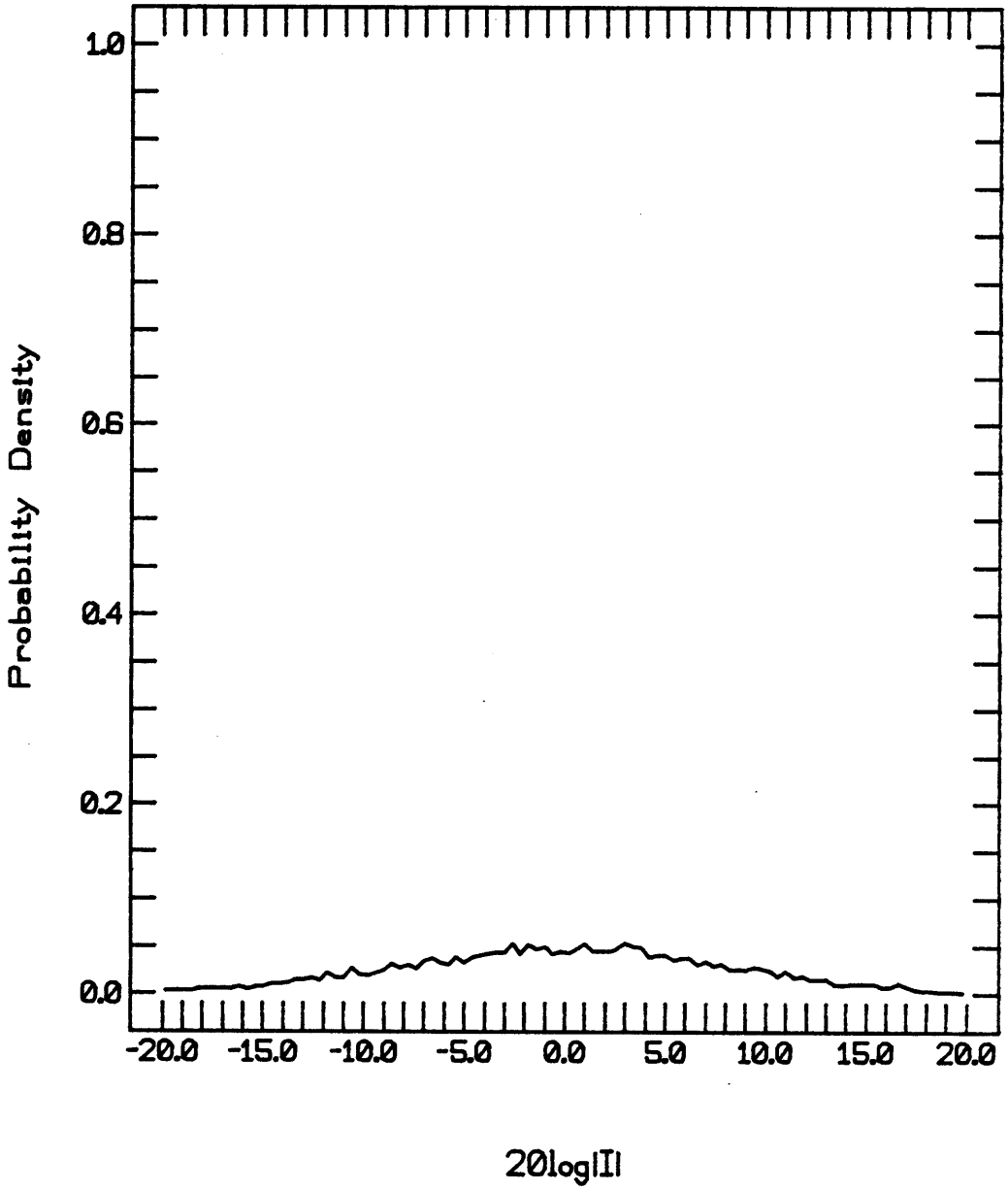
1.0
0.8
0.6
0.4
0.2
0.0
Probability Density
-20.0
-15.0
-10.0
-5.0
0.0
5.0
10.0
15.0
20.0
20log|I|

Figure 6.9

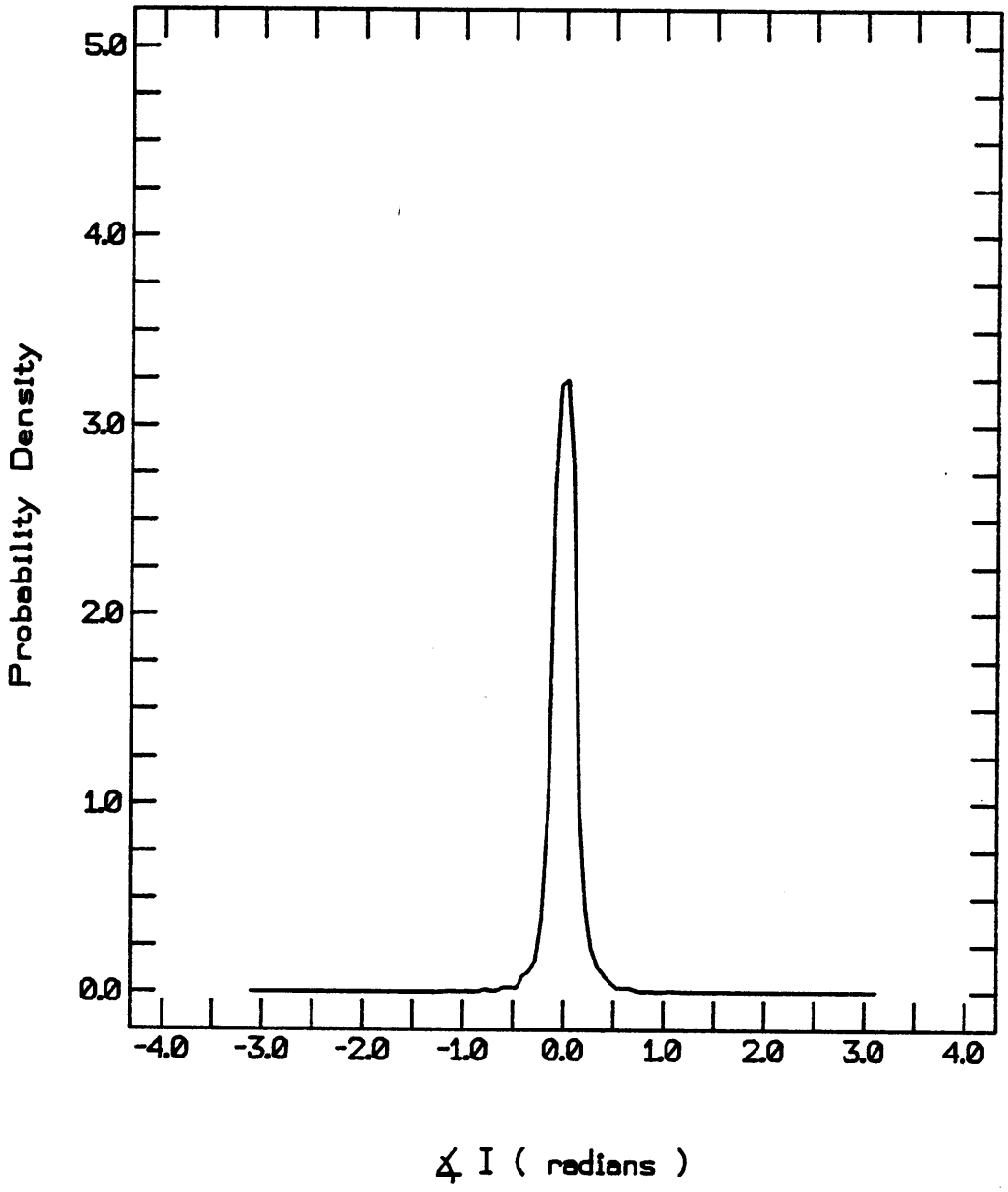
Probability Density
5.0
4.0
3.0
2.0
1.0
0.0
-4.0
-3.0
-2.0
-1.0
0.0
1.0
2.0
3.0
4.0
∠ I (radians)

Figure 6.10

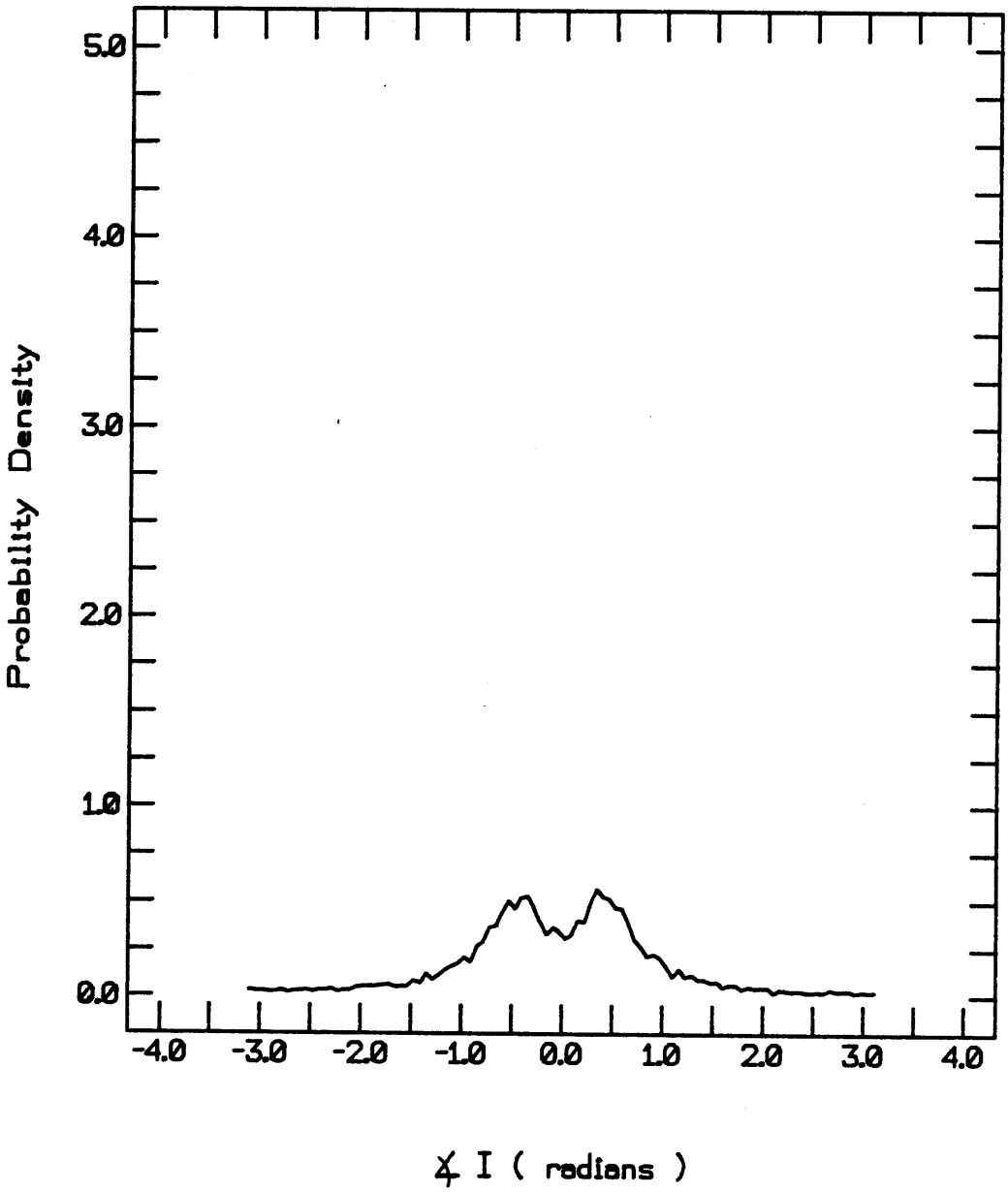
5.0
4.0
3.0
2.0
1.0
0.0
Probability Density
-4.0
-3.0
-2.0
-1.0
0.0
1.0
2.0
3.0
4.0
∠ I (radians)

Figure 6.11

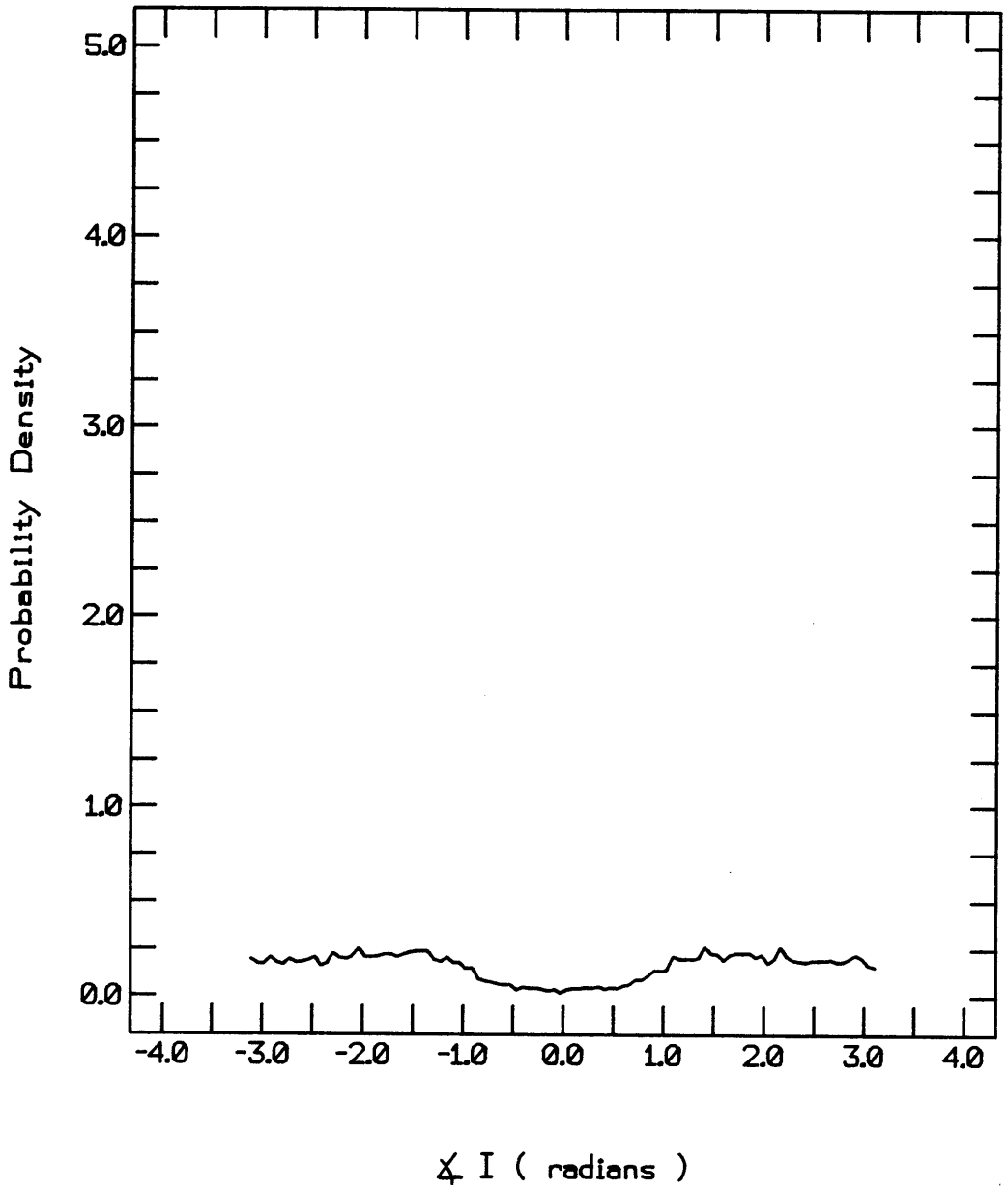
5.0
4.0
3.0
2.0
1.0
0.0
Probability Density
-4.0
-3.0
-2.0
-1.0
0.0
1.0
2.0
3.0
4.0
∡ I (radians)

Figure 6.12

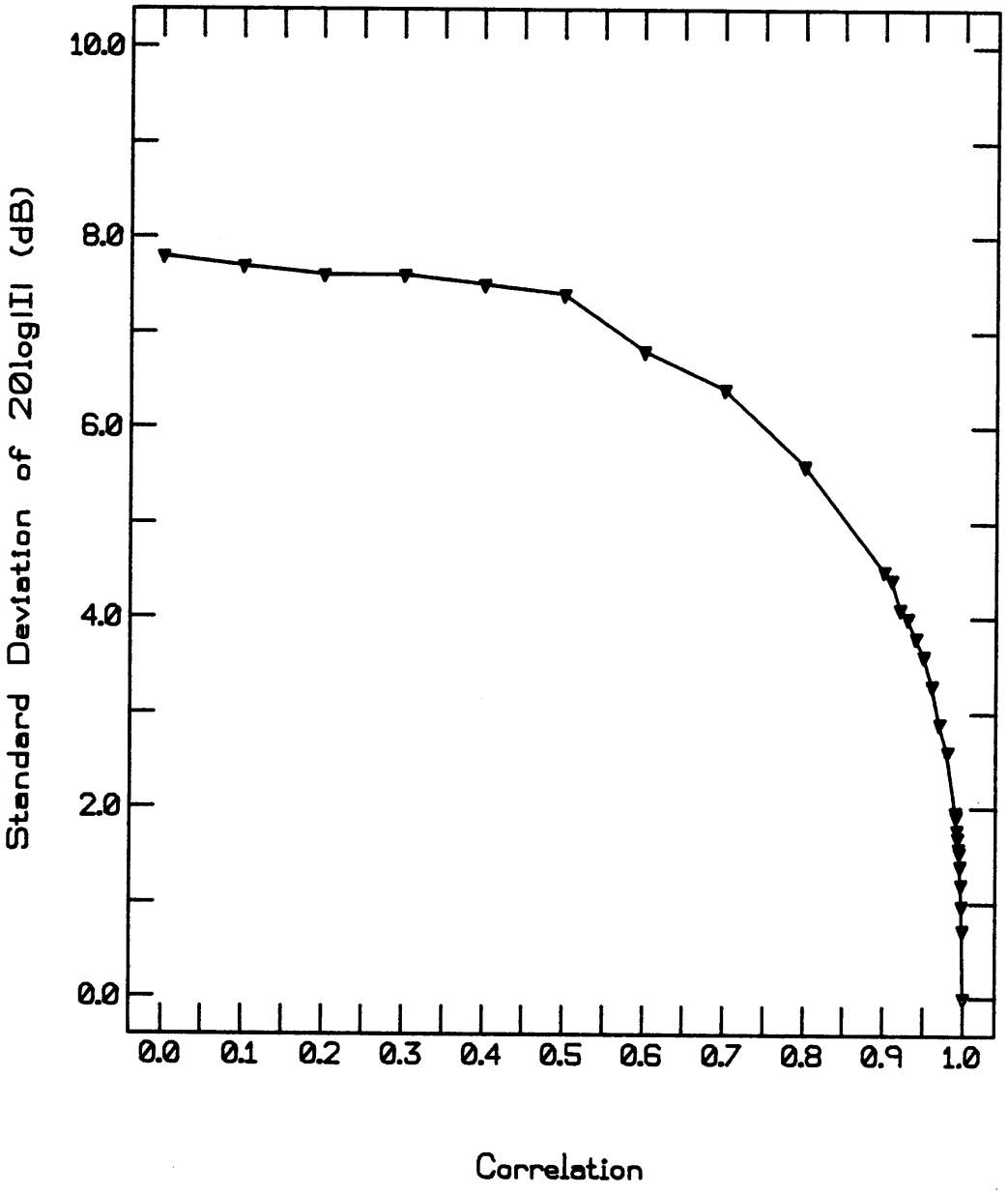
Standard Deviation of 20log|I| (dB)
10.0
8.0
6.0
4.0
2.0
0.0
0.0
0.1
0.2
0.3
0.4
0.5
0.6
0.7
0.8
0.9
1.0
Correlation

Figure 6.13

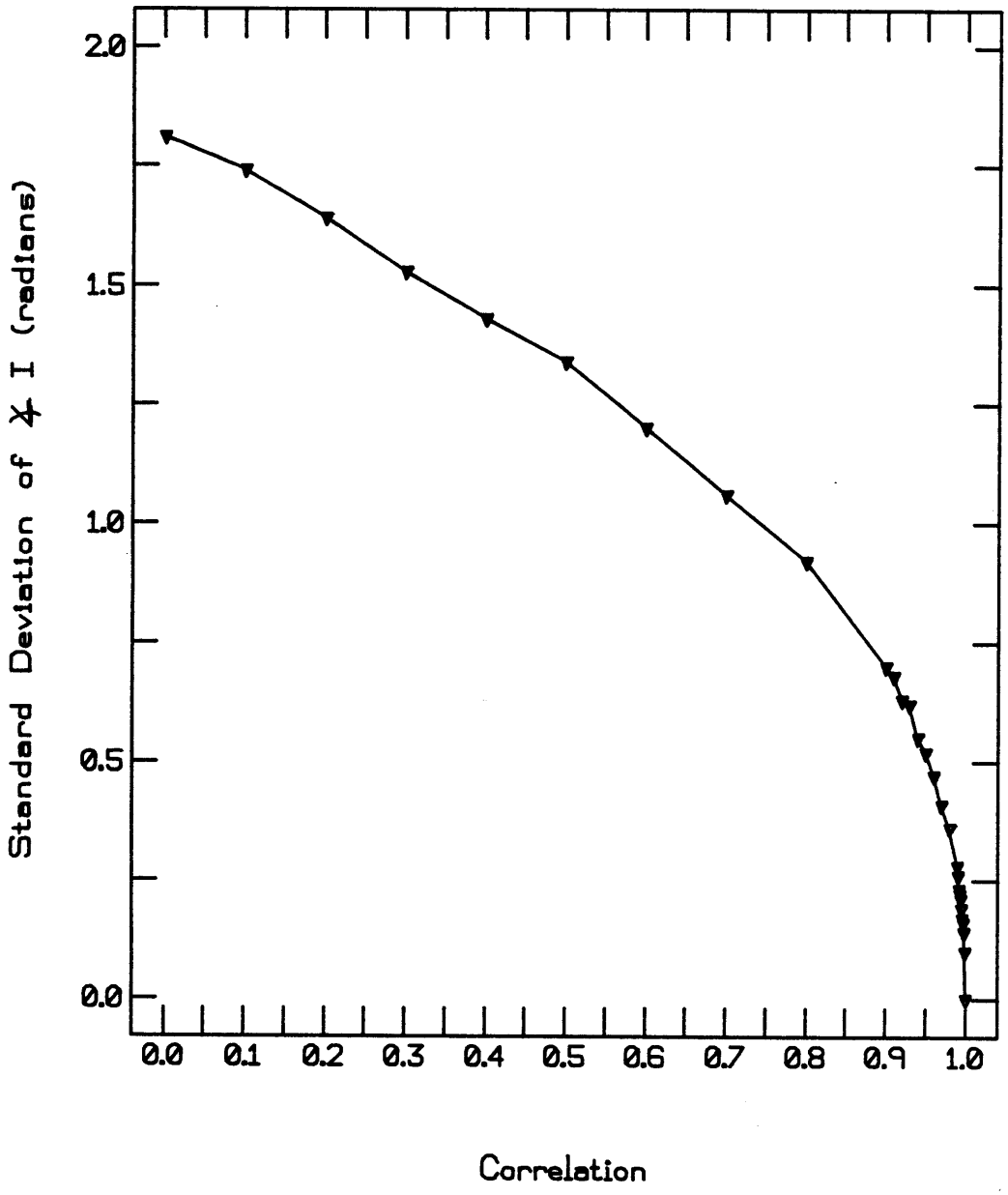
Standard Deviation of ∠ I (radians)
2.0
1.5
1.0
0.5
0.0
0.0
0.1
0.2
0.3
0.4
0.5
0.6
0.7
0.8
0.9
1.0
Correlation

Figure 6.14

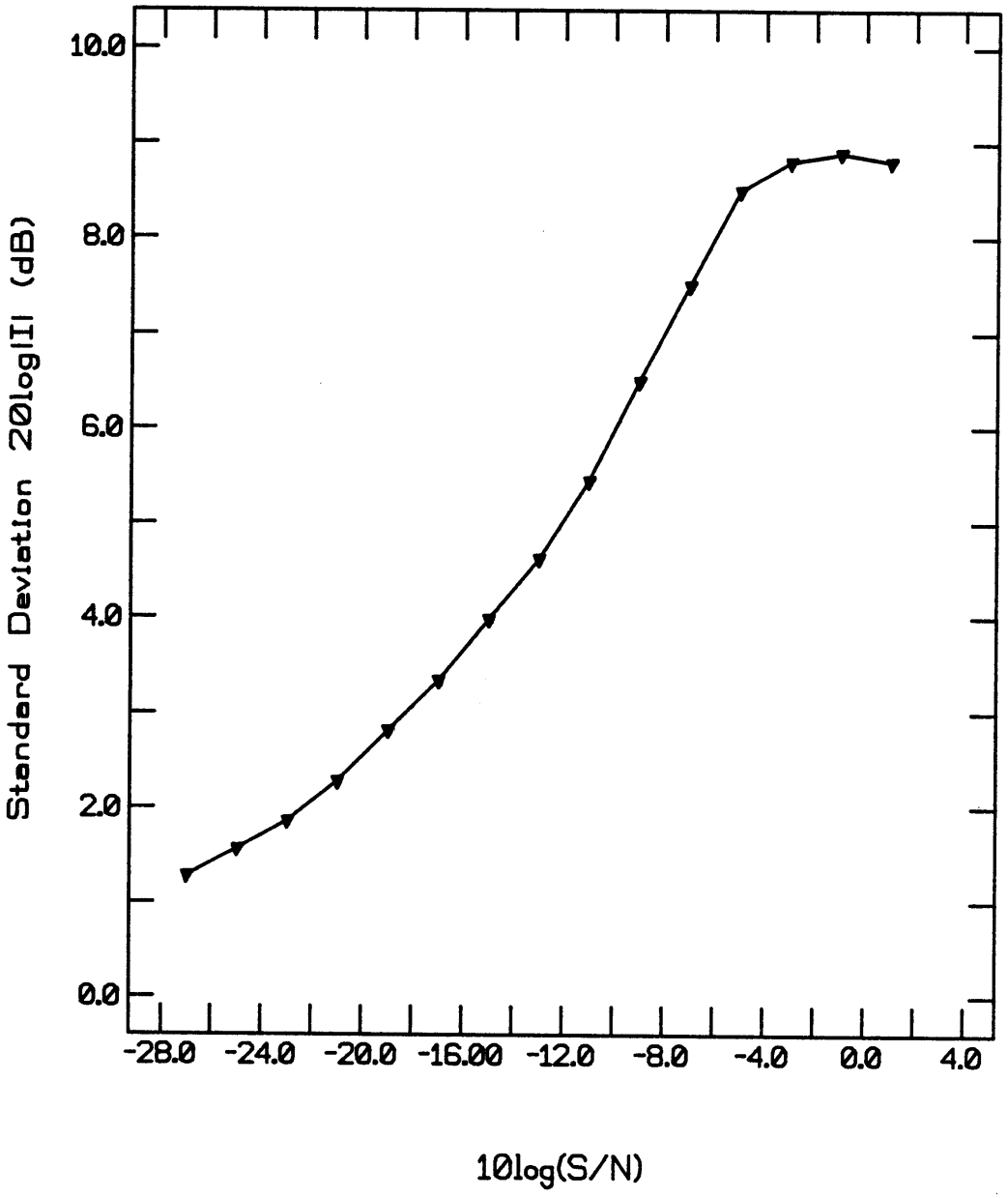
Standard Deviation 20log|I| (dB)
10.0
8.0
6.0
4.0
2.0
0.0
-28.0
-24.0
-20.0
-16.00
-12.0
-8.0
-4.0
0.0
4.0
10log(S/N)

Figure 6.15

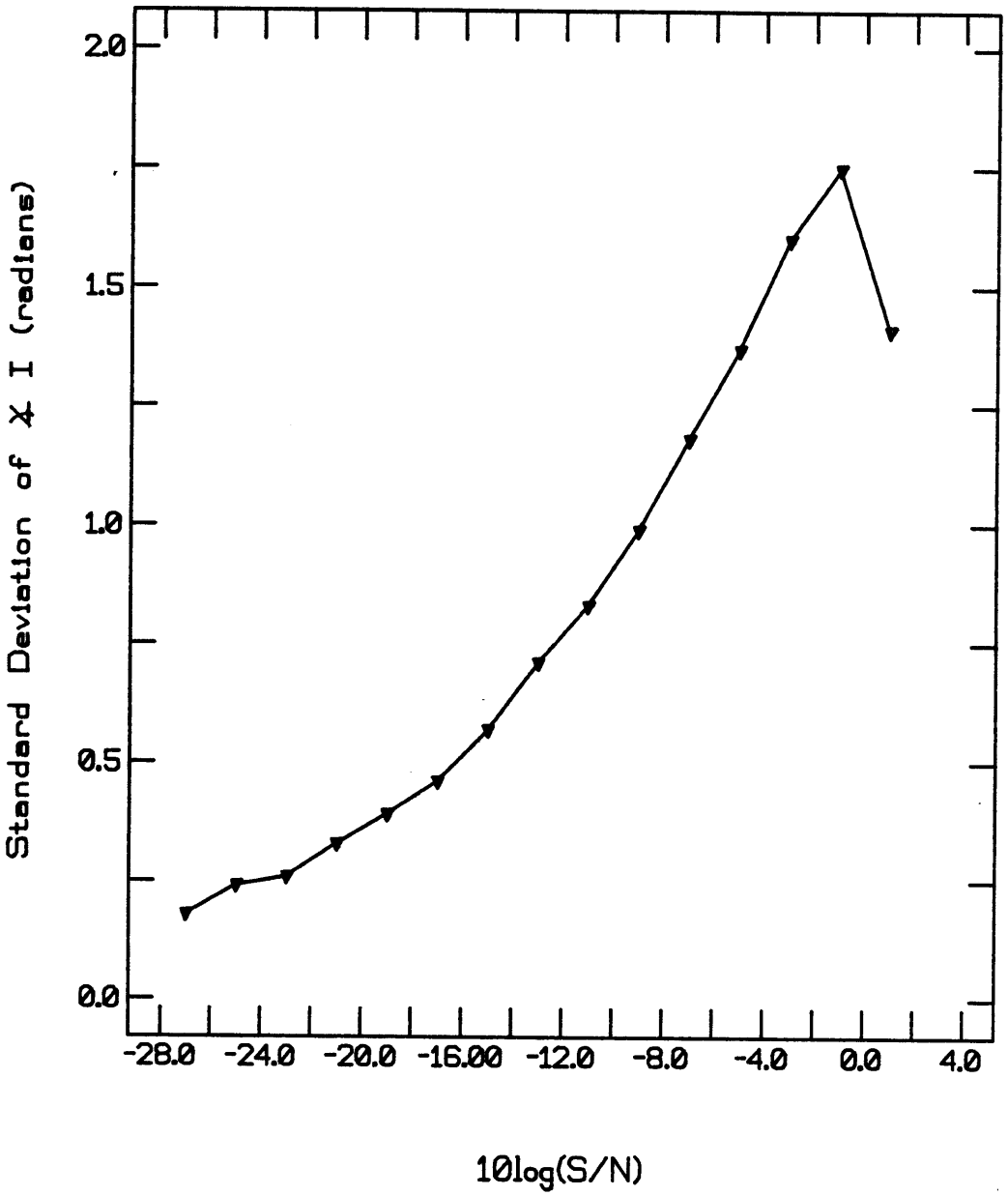
Standard Deviation of χ I (radians)
2.0
1.5
1.0
0.5
0.0
-28.0
-24.0
-20.0
-16.00
-12.0
-8.0
-4.0
0.0
4.0
10log(S/N)

Figure 6.16

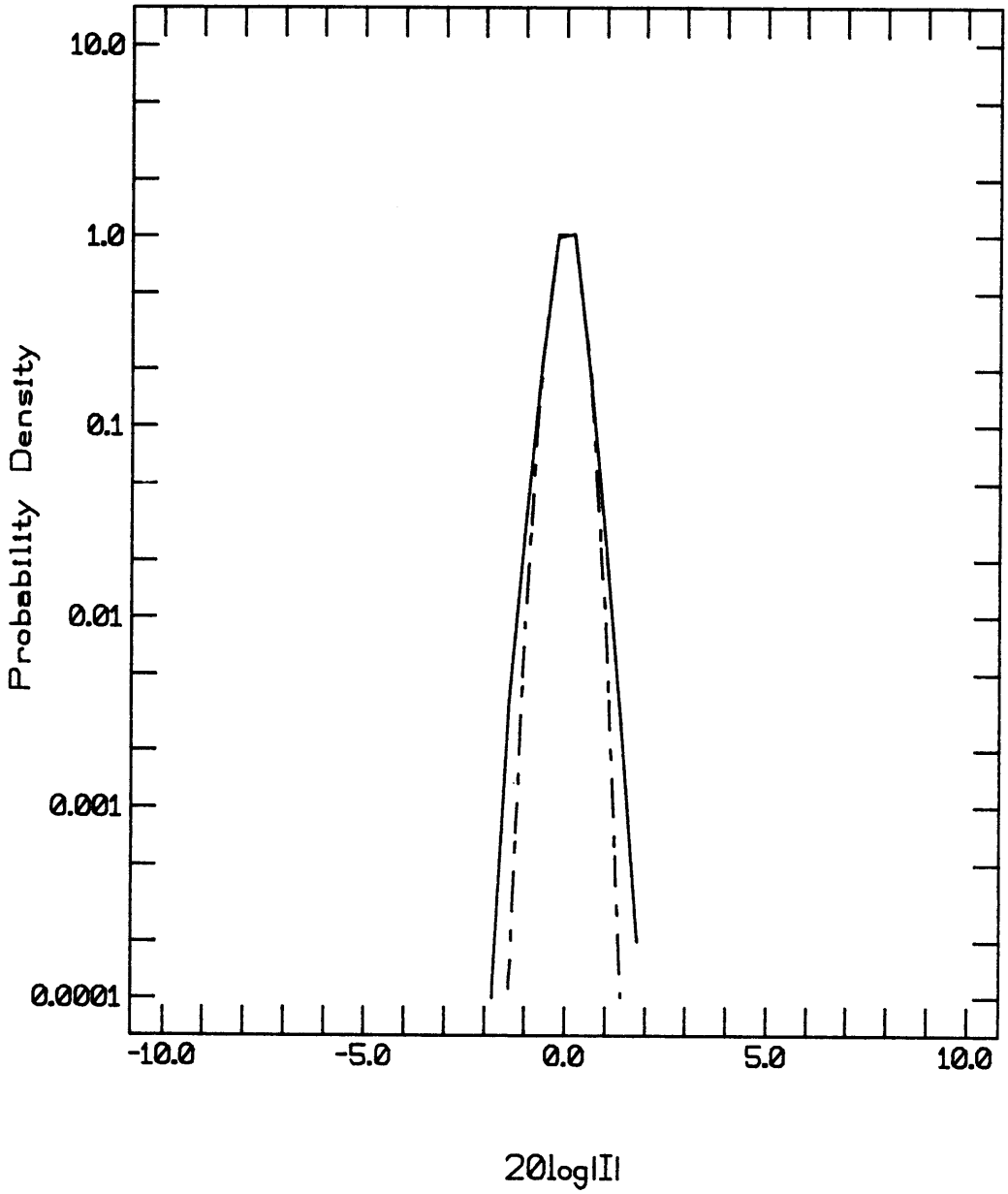
10.0
1.0
0.1
0.01
0.001
0.0001
Probability Density
-10.0
-5.0
0.0
5.0
10.0
20log|I|

Figure 7.1

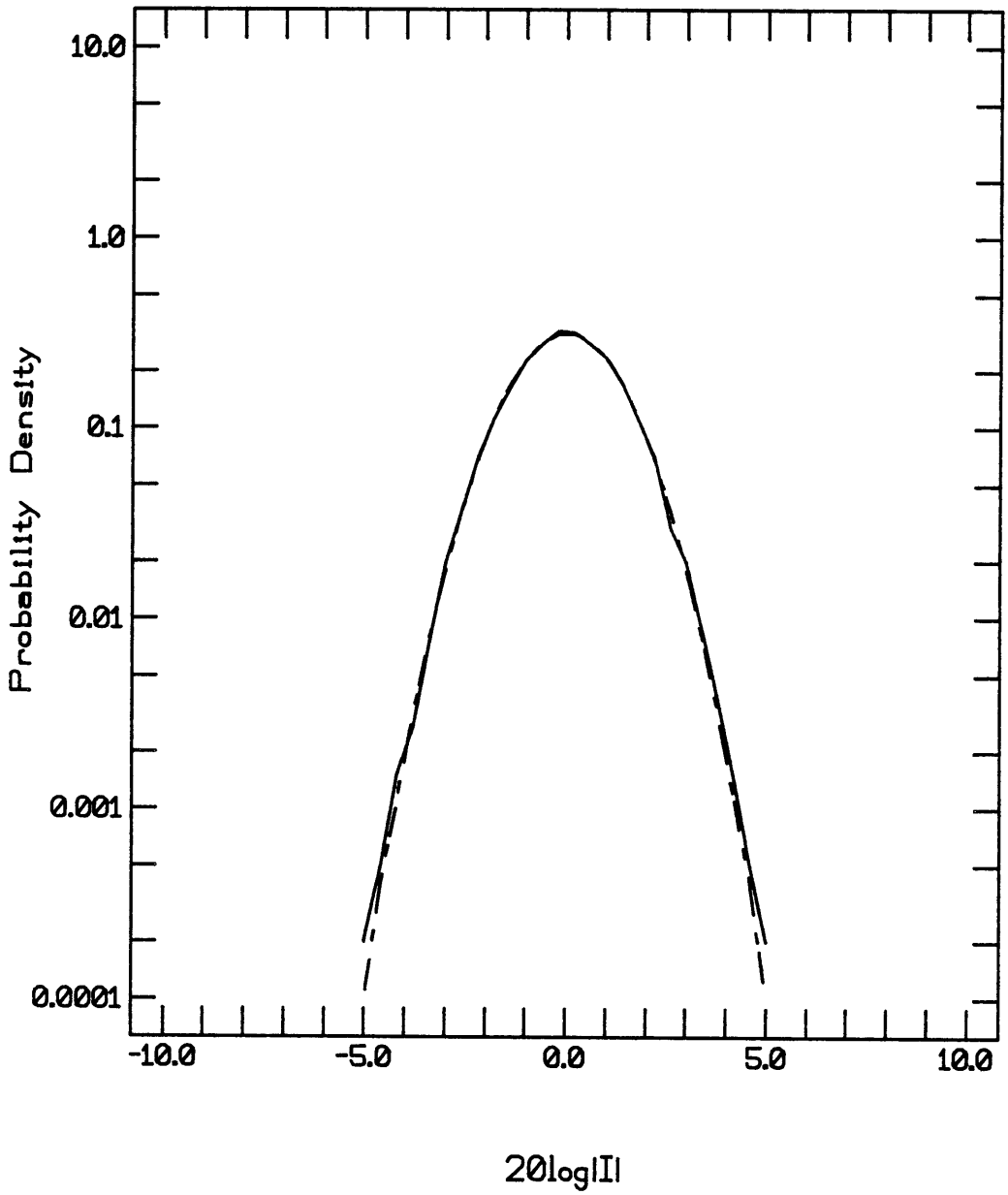
10.0
1.0
0.1
0.01
0.001
0.0001
Probability Density
-10.0
-5.0
0.0
5.0
10.0
20log|I|

Figure 7.2

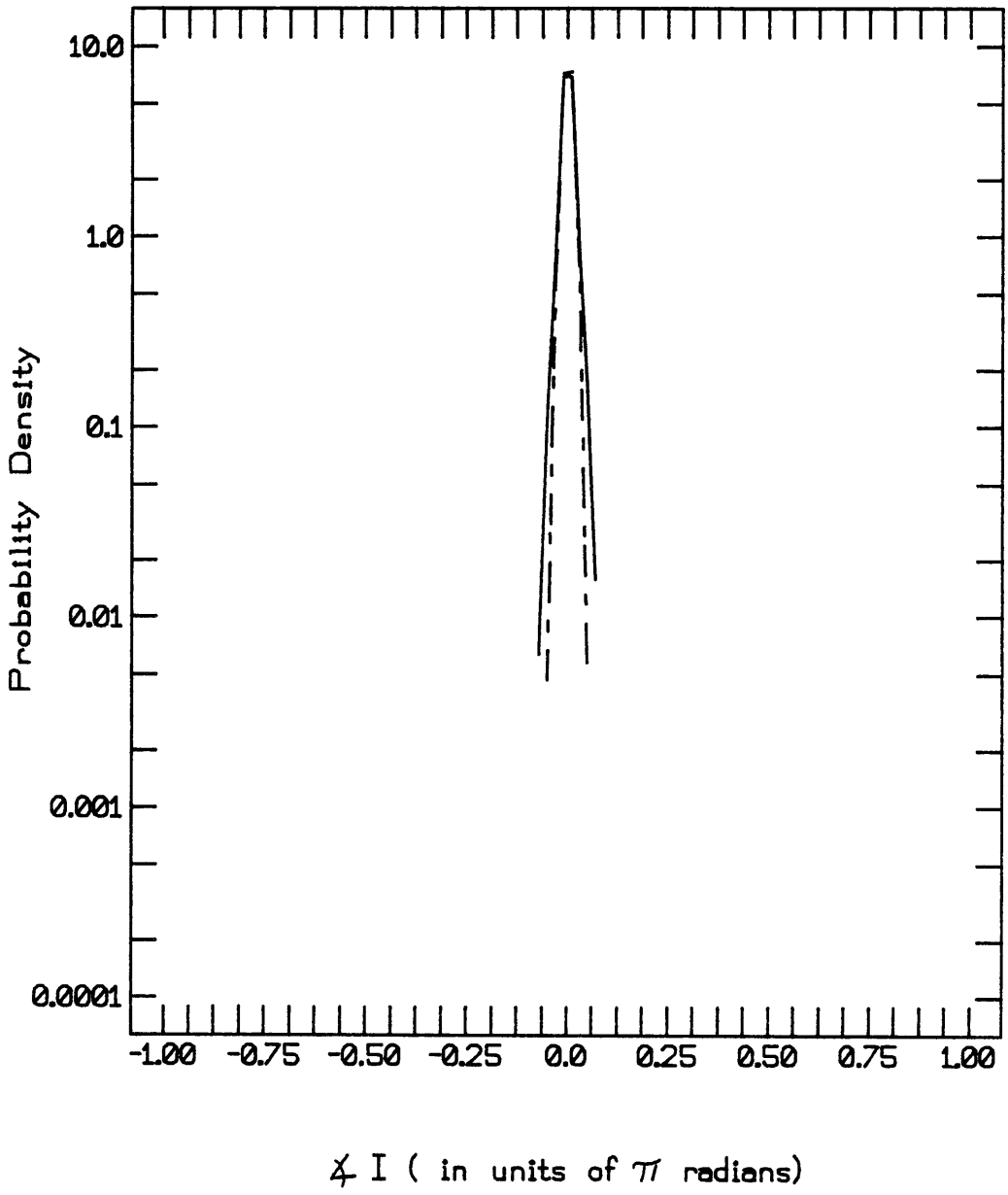
10.0
1.0
0.1
0.01
0.001
0.0001
Probability Density
-1.00
-0.75
-0.50
-0.25
0.0
0.25
0.50
0.75
1.00
∠ I (in units of π radians)

Figure 7.3

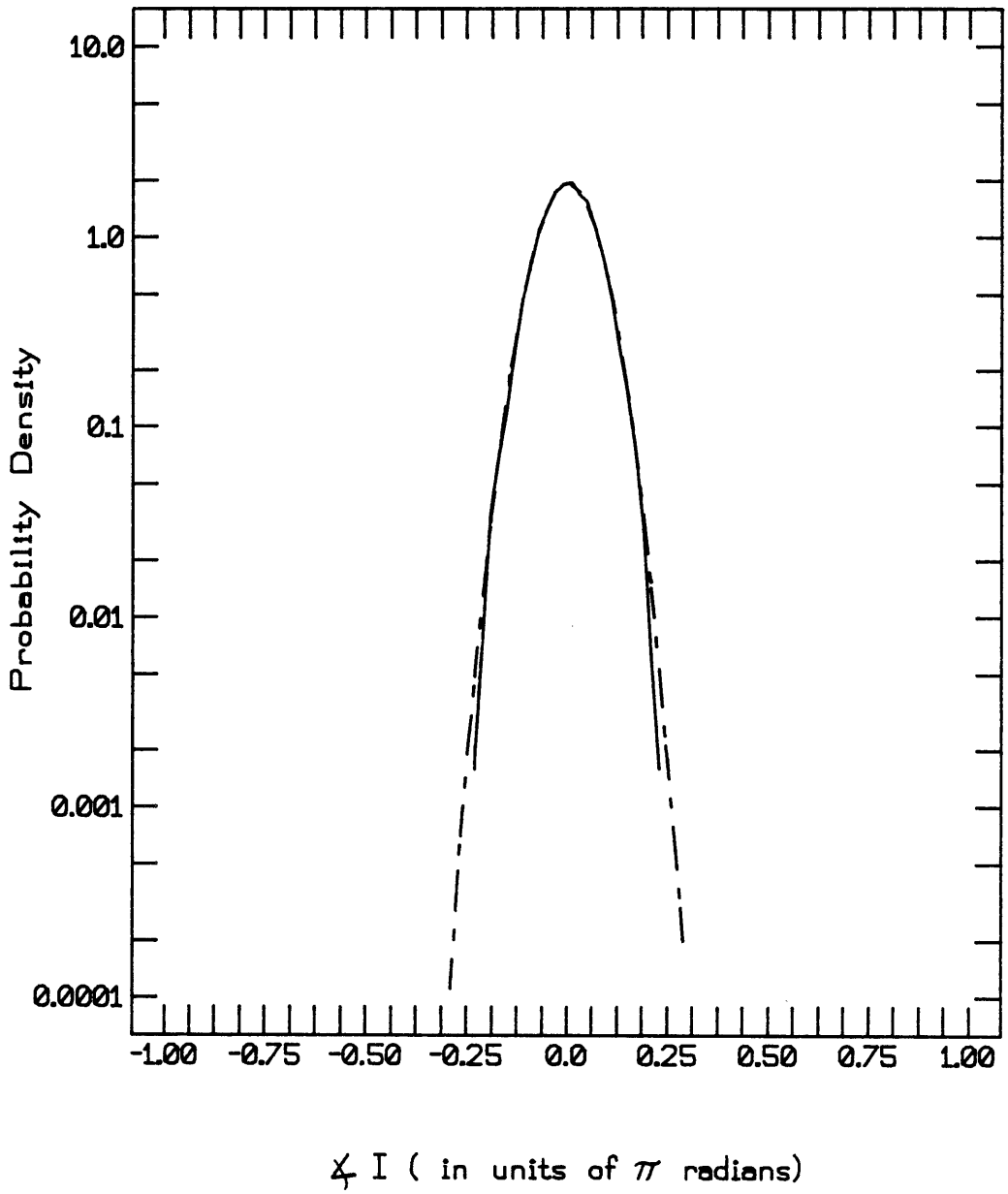
10.0
1.0
0.1
0.01
0.001
0.0001
Probability Density
-1.00
-0.75
-0.50
-0.25
0.0
0.25
0.50
0.75
1.00
∠ I (in units of π radians)

Figure 7.4

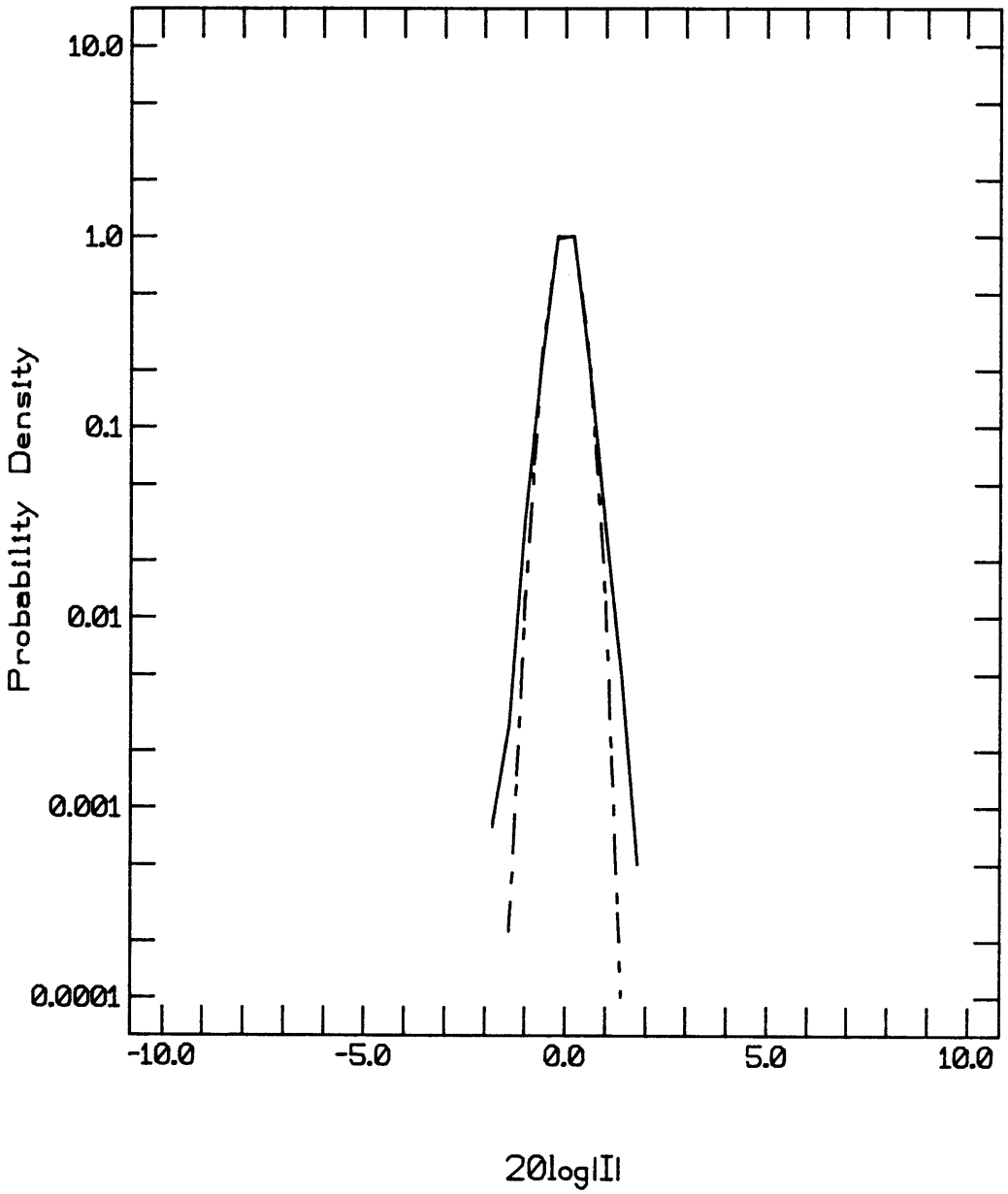
10.0
1.0
0.1
0.01
0.001
0.0001
Probability Density
-10.0
-5.0
0.0
5.0
10.0
20log|I|

Figure 7.5

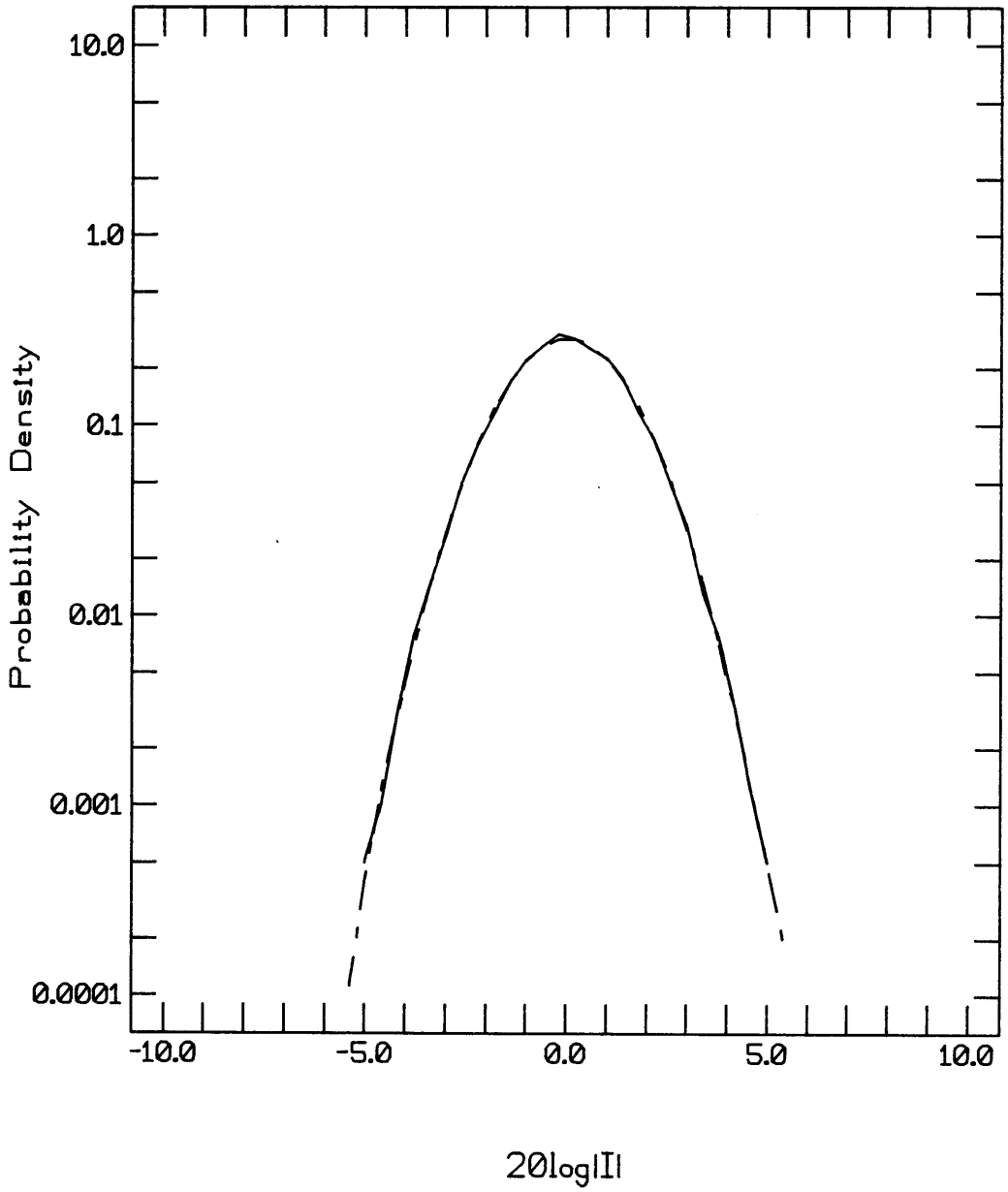
10.0
1.0
0.1
0.01
0.001
0.0001
Probability Density
-10.0
-5.0
0.0
5.0
10.0
20log|I|

Figure 7.6

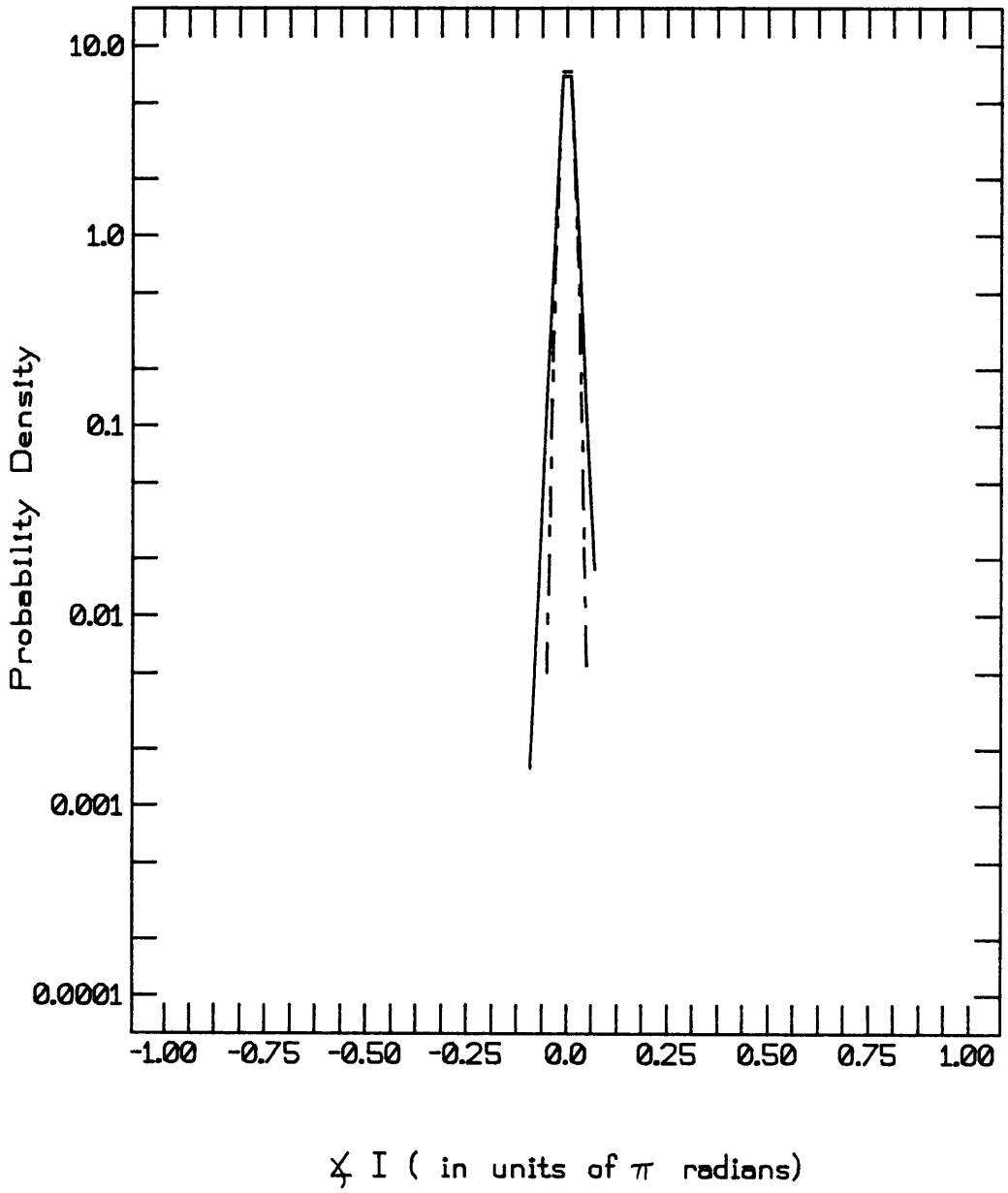
10.0
1.0
0.1
0.01
0.001
0.0001
Probability Density
-1.00
-0.75
-0.50
-0.25
0.0
0.25
0.50
0.75
1.00
∢ I (in units of π radians)

Figure 7.7

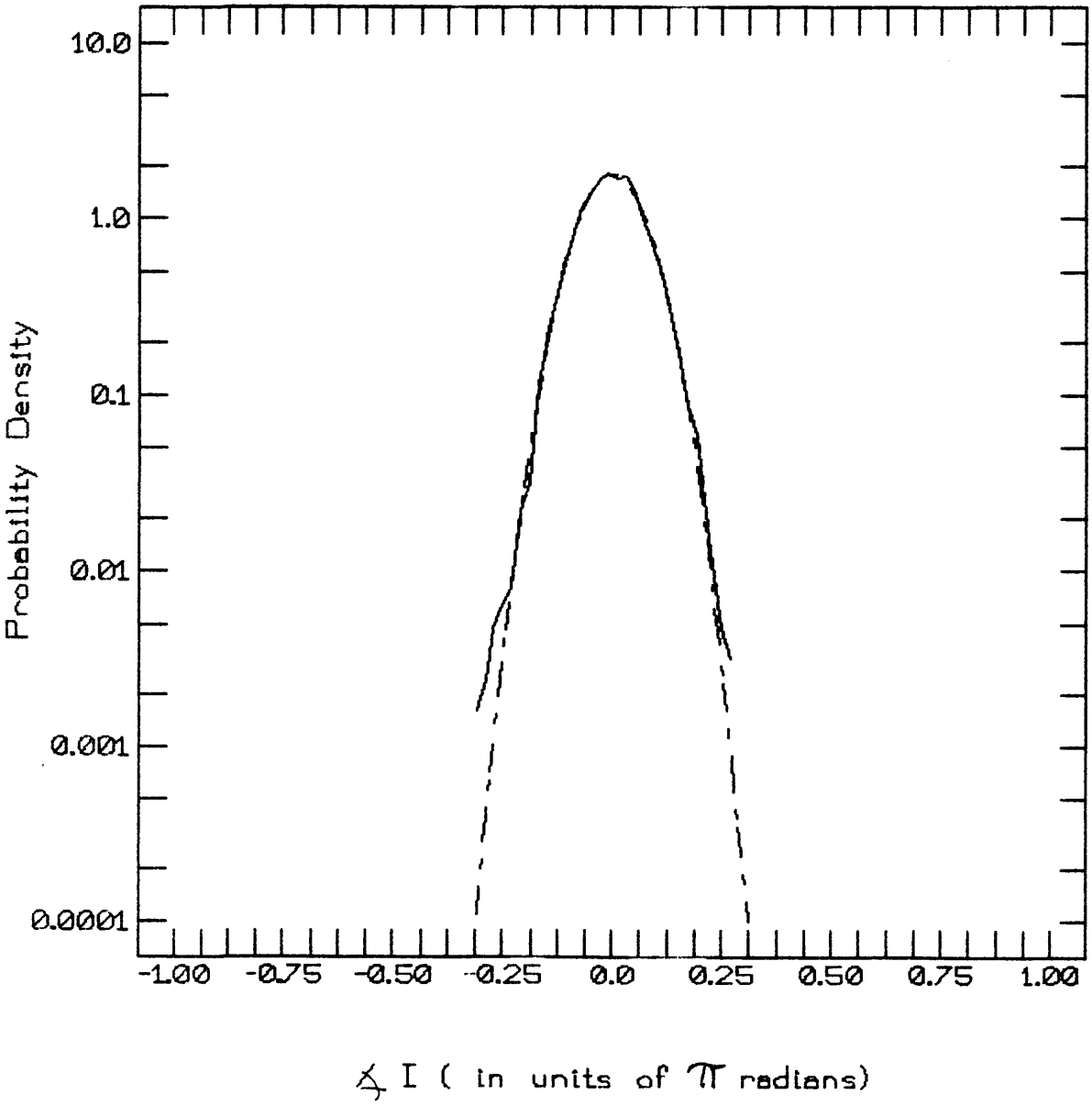
10.0
1.0
0.1
0.01
0.001
0.0001
Probability Density
-1.00
-0.75
-0.50
-0.25
0.0
0.25
0.50
0.75
1.00
∠ I (in units of π radians)

Figure 7.8

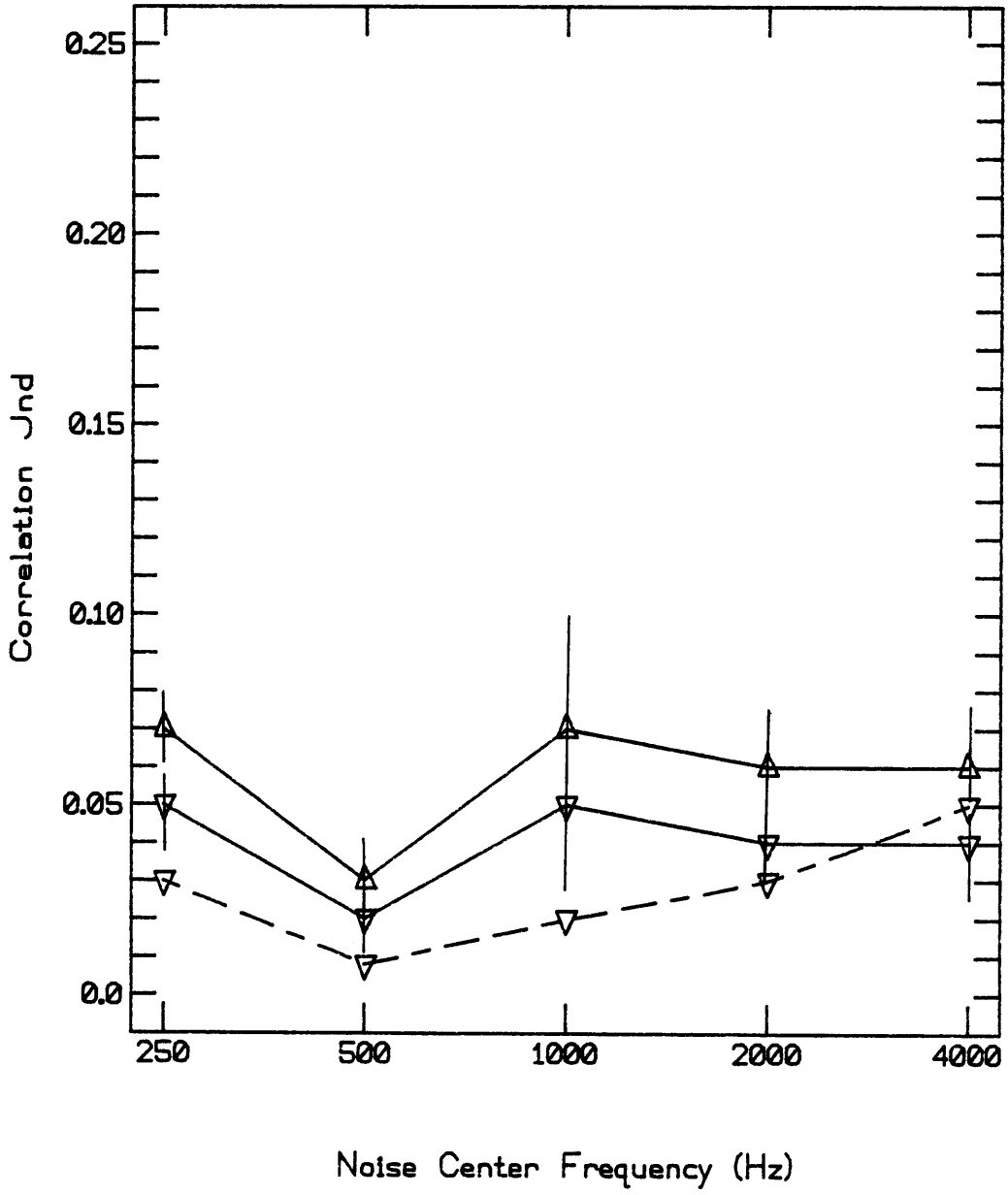
0.25
0.20
0.15
0.10
0.05
0.0
Correlation Jnd
250
500
1000
2000
4000
Noise Center Frequency (Hz)

Figure 8.1

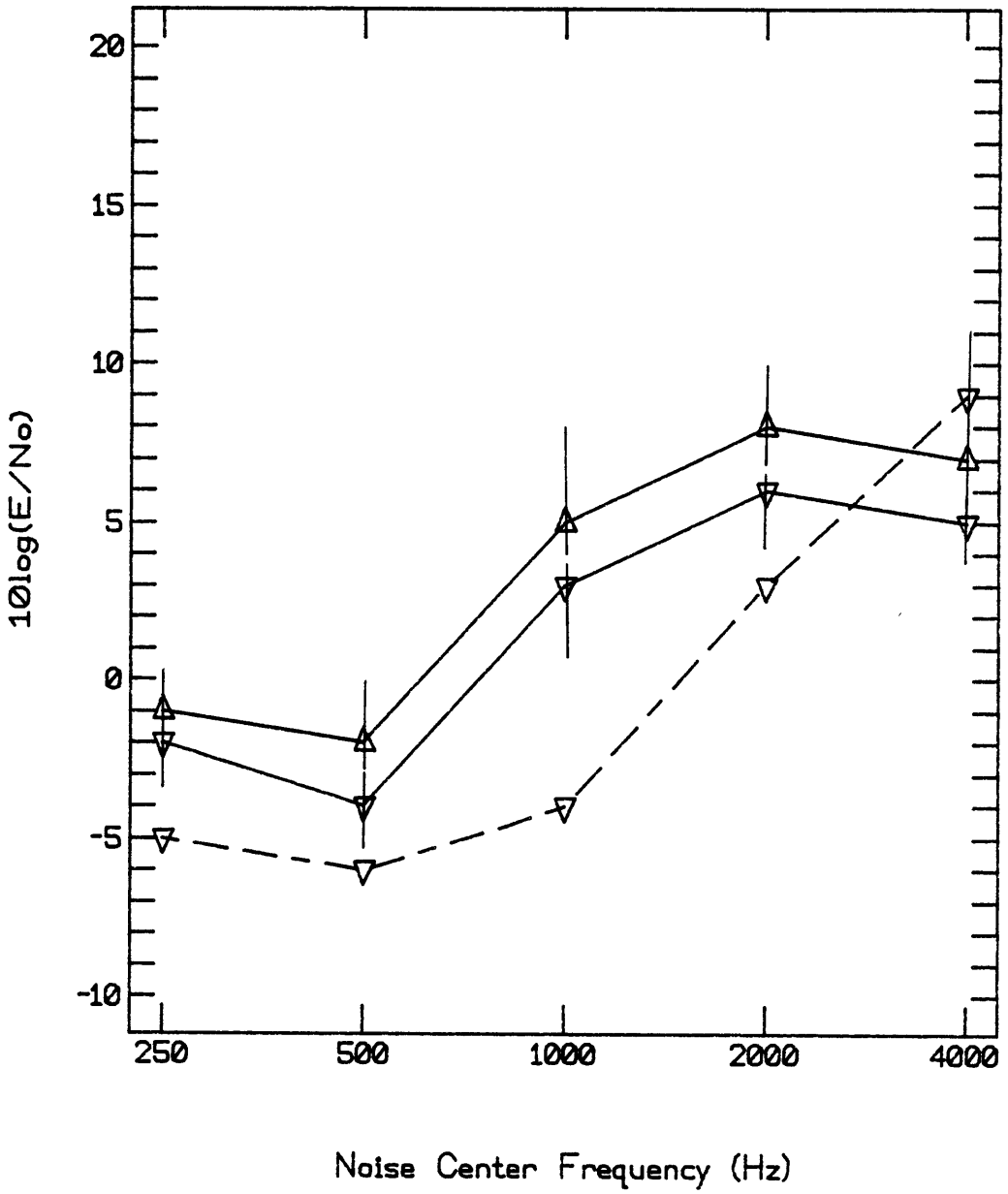
20
15
10
5
0
-5
-10
10log(E/No)
250
500
1000
2000
4000
Noise Center Frequency (Hz)

Figure 8.2

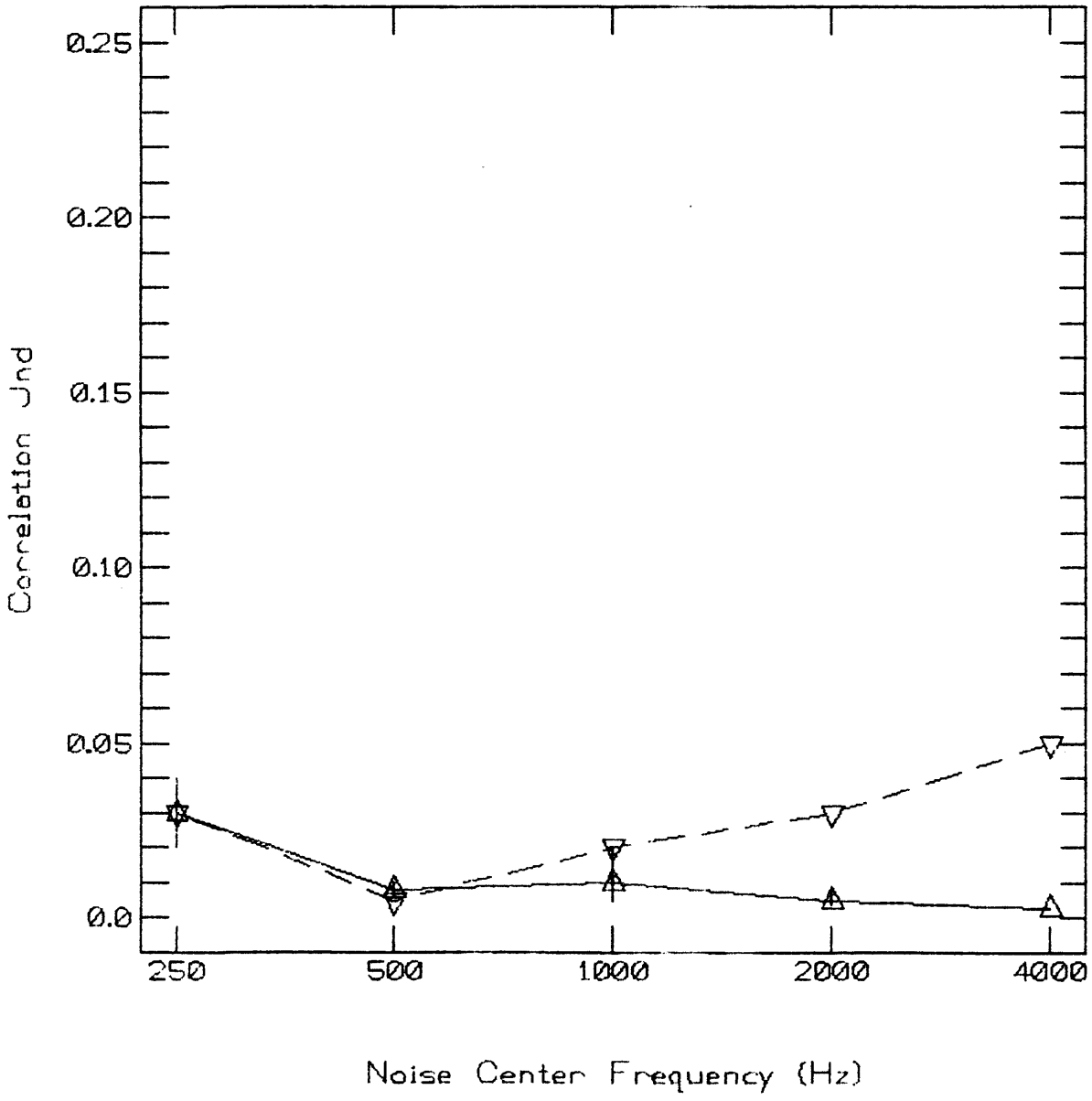
0.25
0.20
0.15
0.10
0.05
0.0
Correlation Jnd
250
500
1000
2000
4000
Noise Center Frequency (Hz)

Figure 8.3

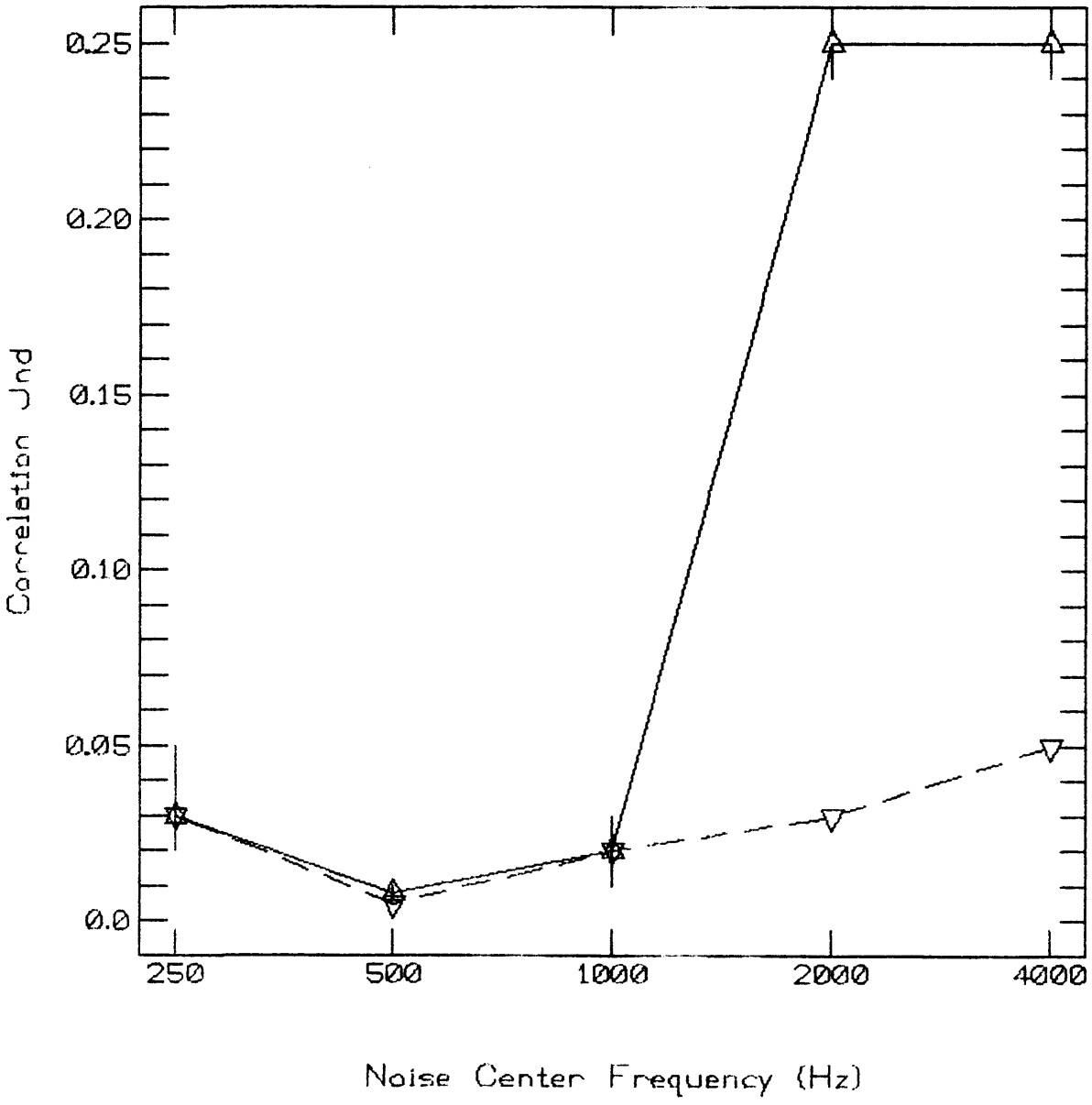
0.25
0.20
0.15
0.10
0.05
0.0
Correlation Jnd
250
500
1000
2000
4000
Noise Center Frequency (Hz)

Figure 8.4

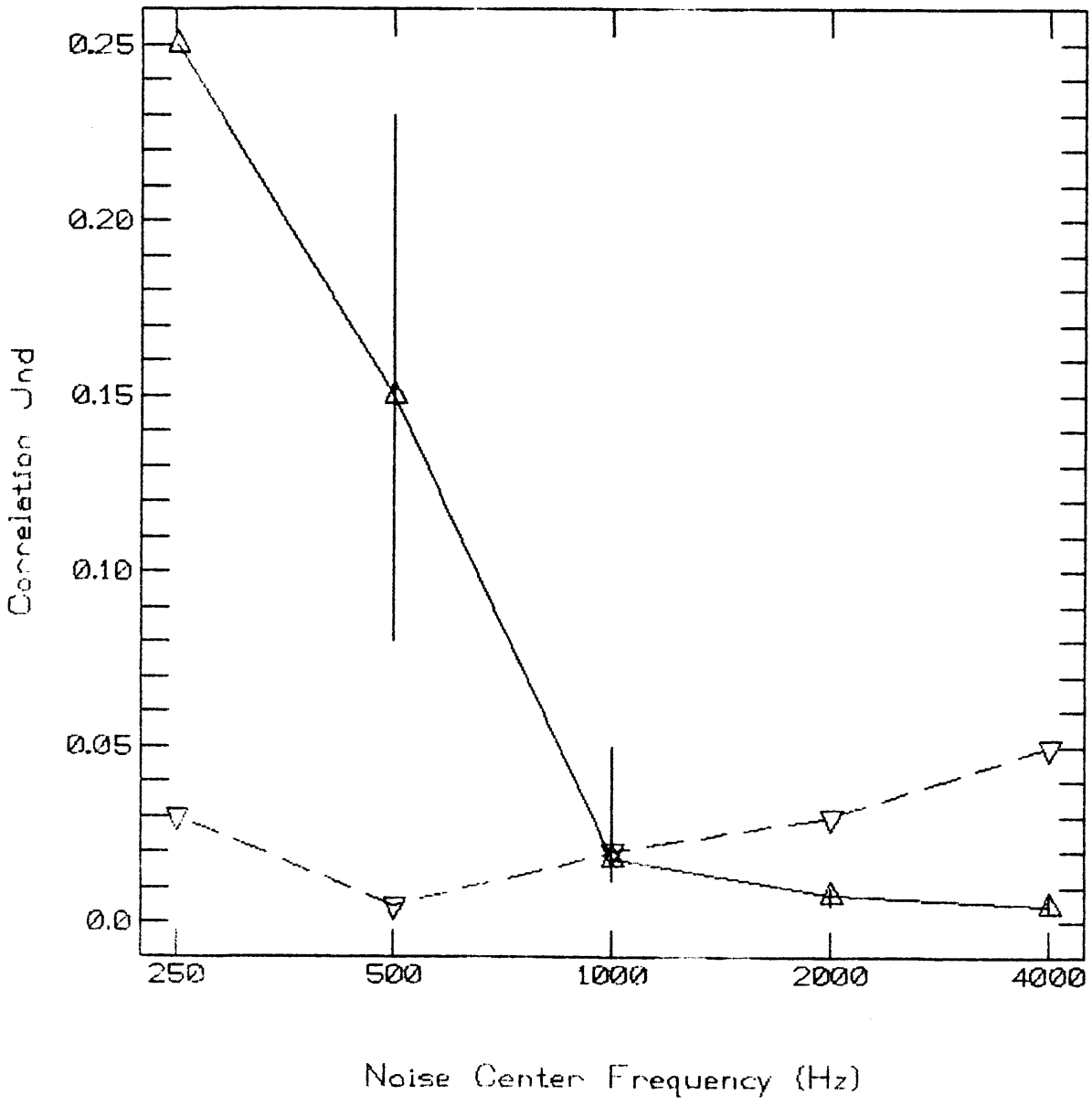
0.25
0.20
0.15
0.10
0.05
0.0
Correlation Jnd
250
500
1000
2000
4000
Noise Center Frequency (Hz)

Figure 8.5

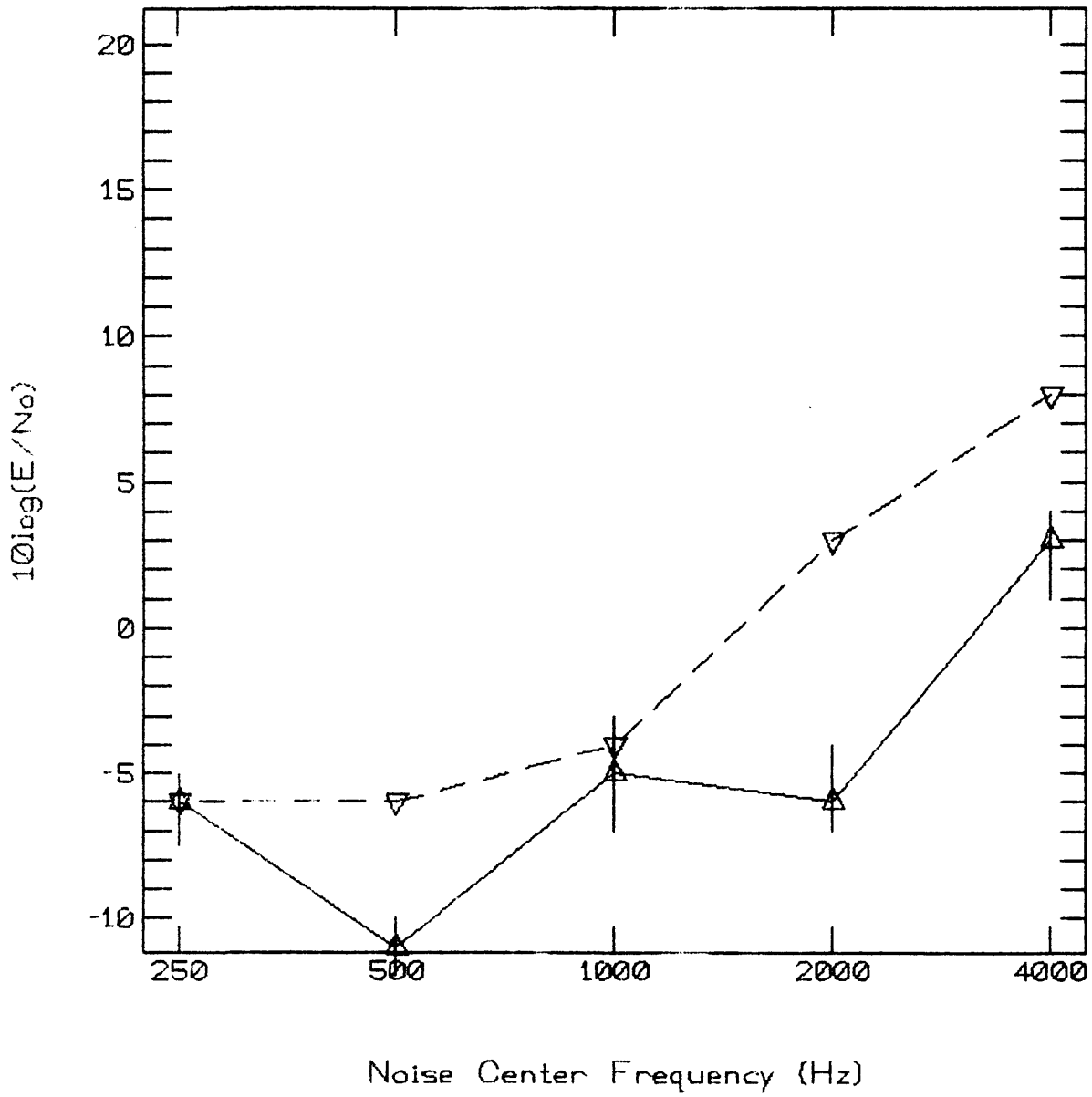
20
15
10
5
0
-5
-10
10log(E/No)
250
500
1000
2000
4000
Noise Center Frequency (Hz)

Figure8.6

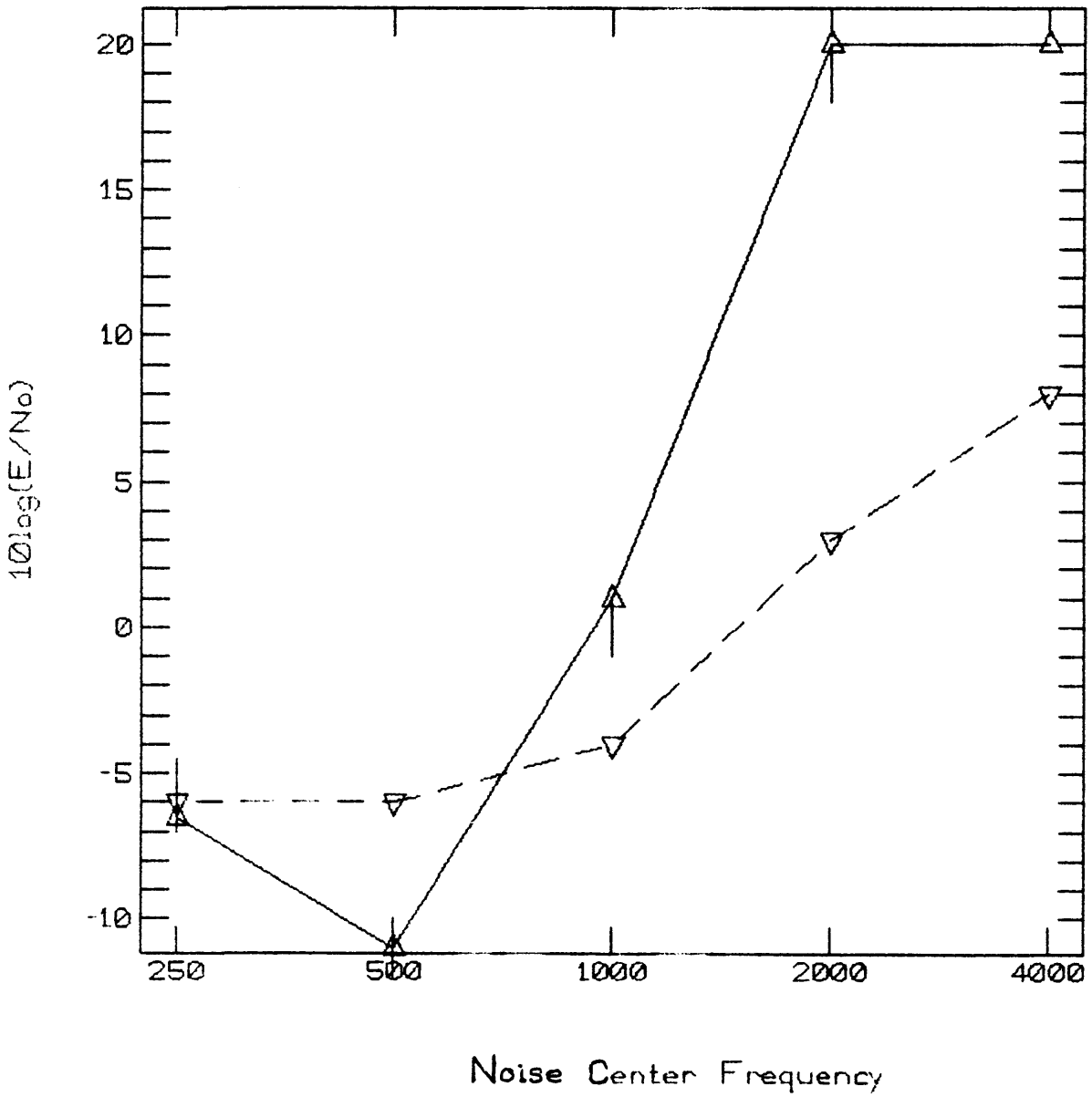
20
15
10
5
0
-5
-10
10log(E/No)
250
500
1000
2000
4000
Noise Center Frequency

Figure 8.7

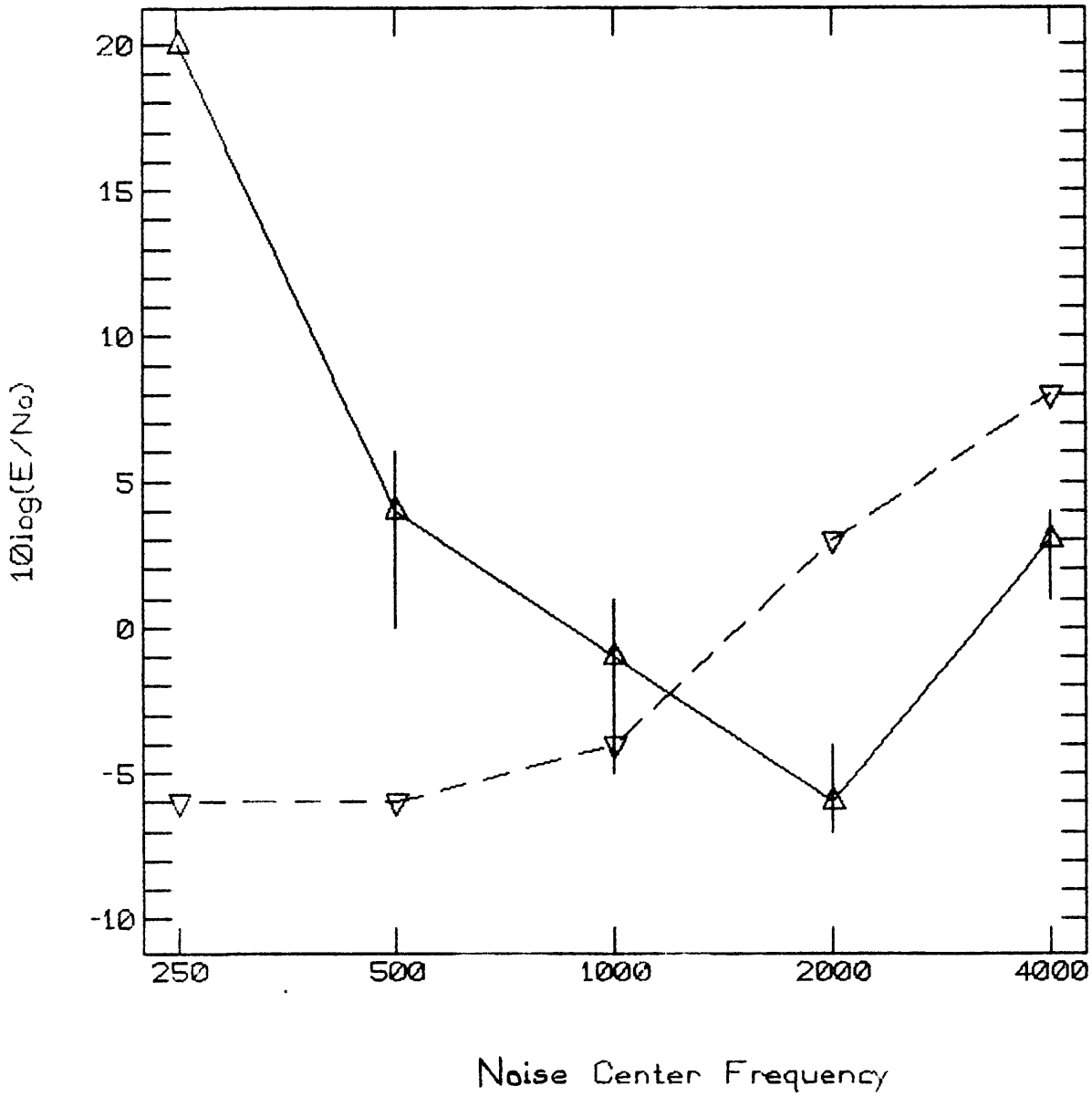
20
15
10
5
0
-5
-10
10log(E/No)
250
500
1000
2000
4000
Noise Center Frequency

Figure 8.8

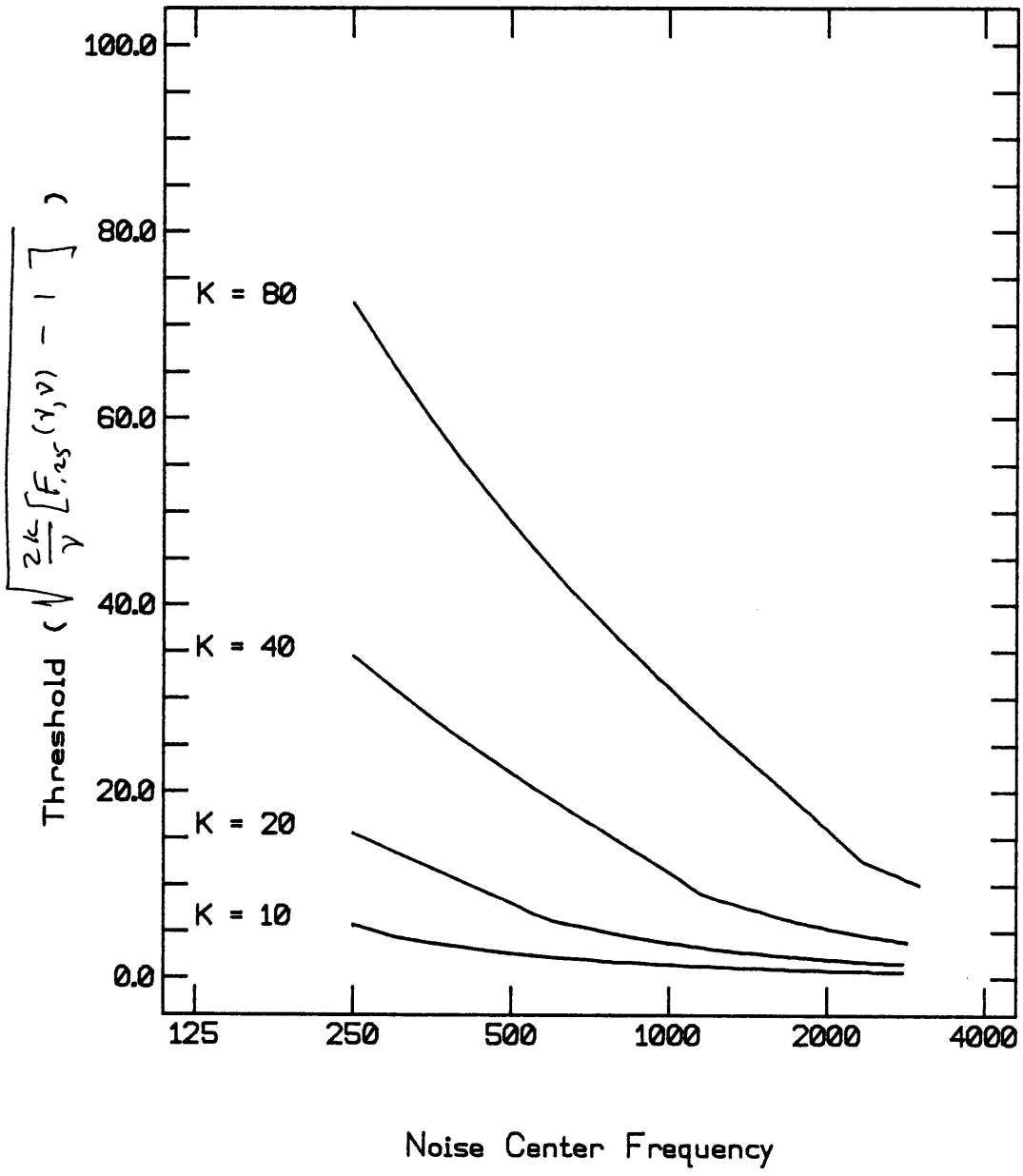
100.0
80.0
60.0
40.0
20.0
0.0
K = 80
K = 40
K = 20
K = 10
125
250
500
1000
2000
4000
Noise Center Frequency

Figure 8.9

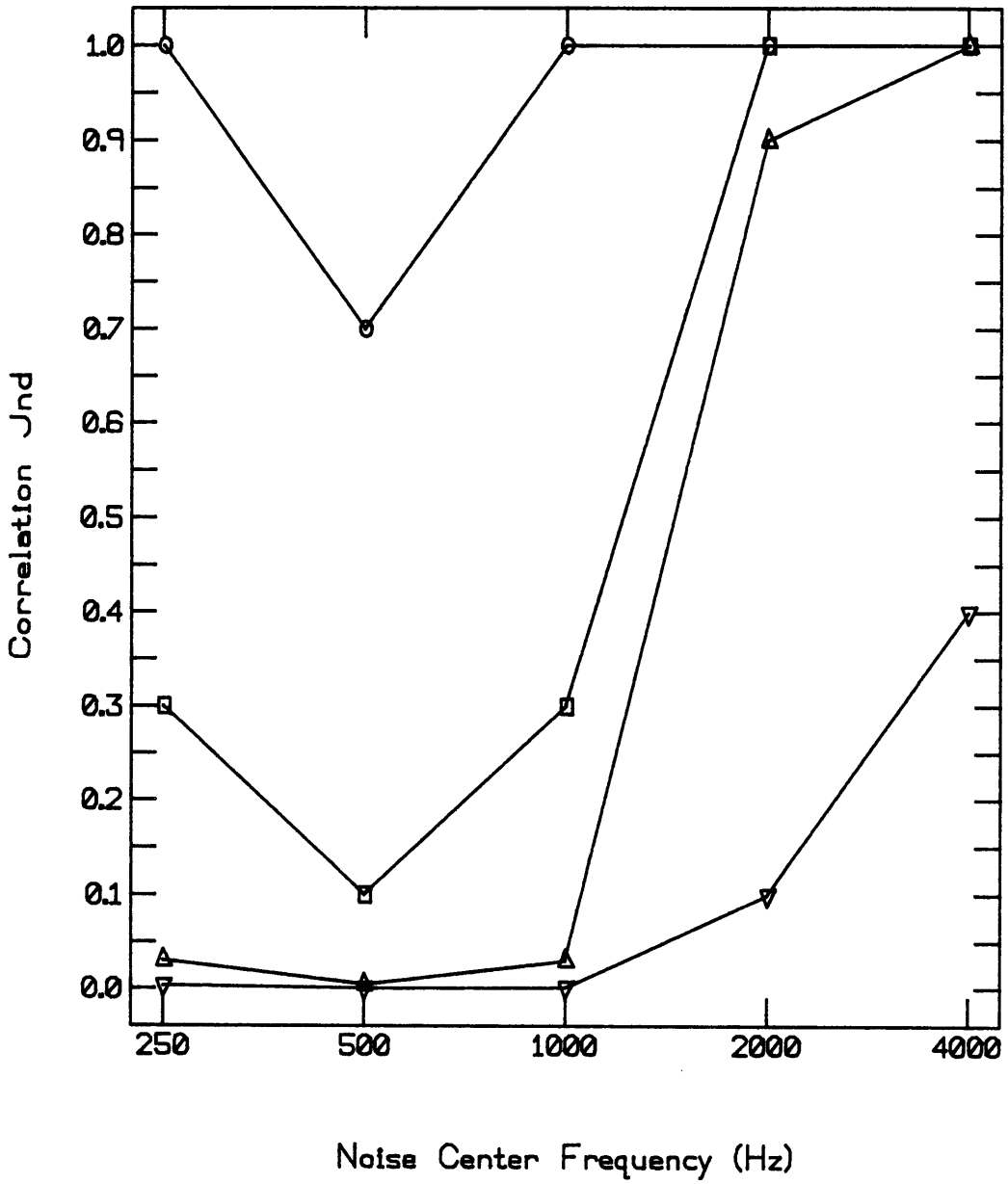
1.0
0.9
0.8
0.7
0.6
0.5
0.4
0.3
0.2
0.1
0.0
Correlation Jnd
250
500
1000
2000
4000
Noise Center Frequency (Hz)

Figure 8.10

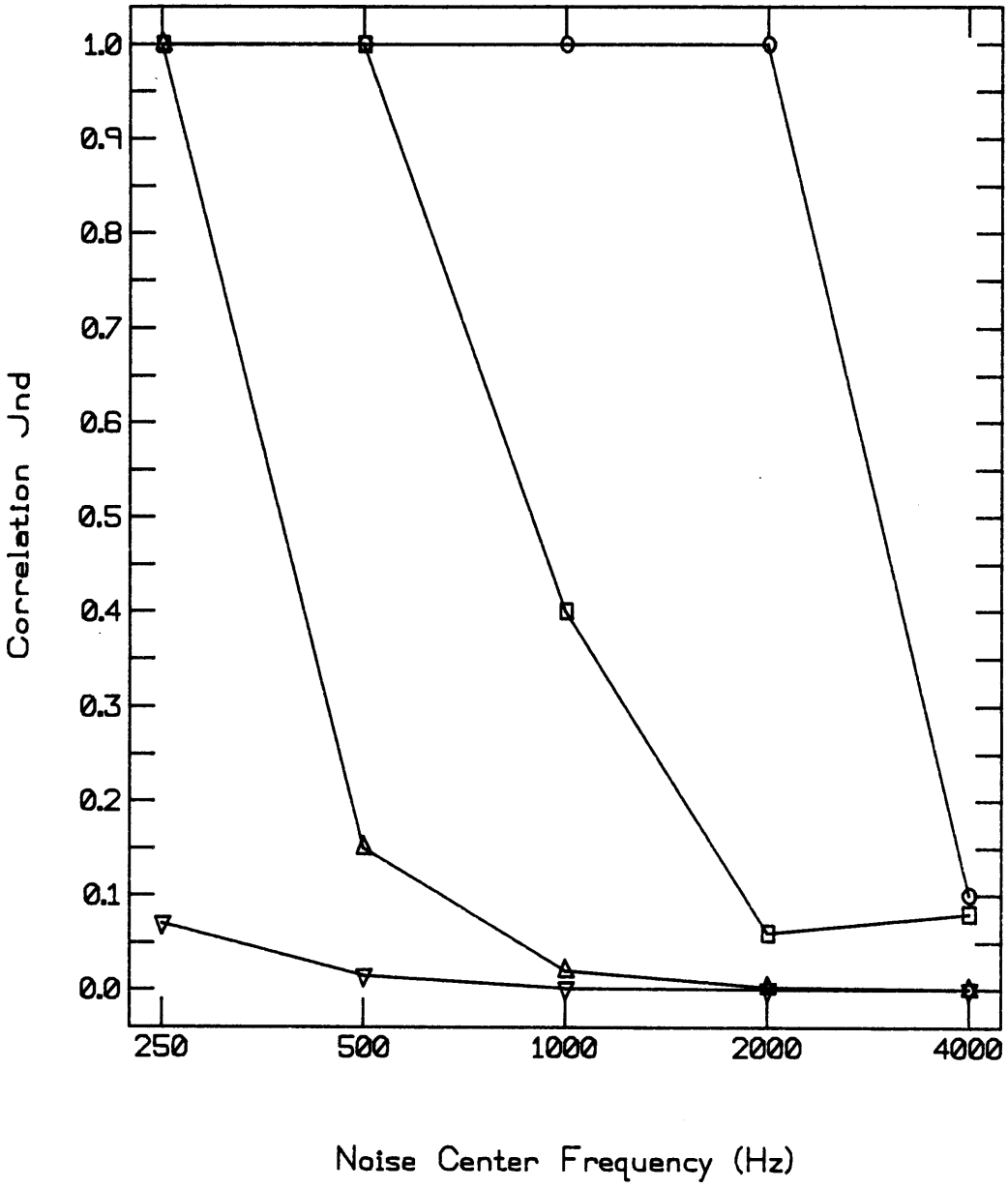
Correlation Jnd
1.0
0.9
0.8
0.7
0.6
0.5
0.4
0.3
0.2
0.1
0.0
250
500
1000
2000
4000
Noise Center Frequency (Hz)

Figure 8.11

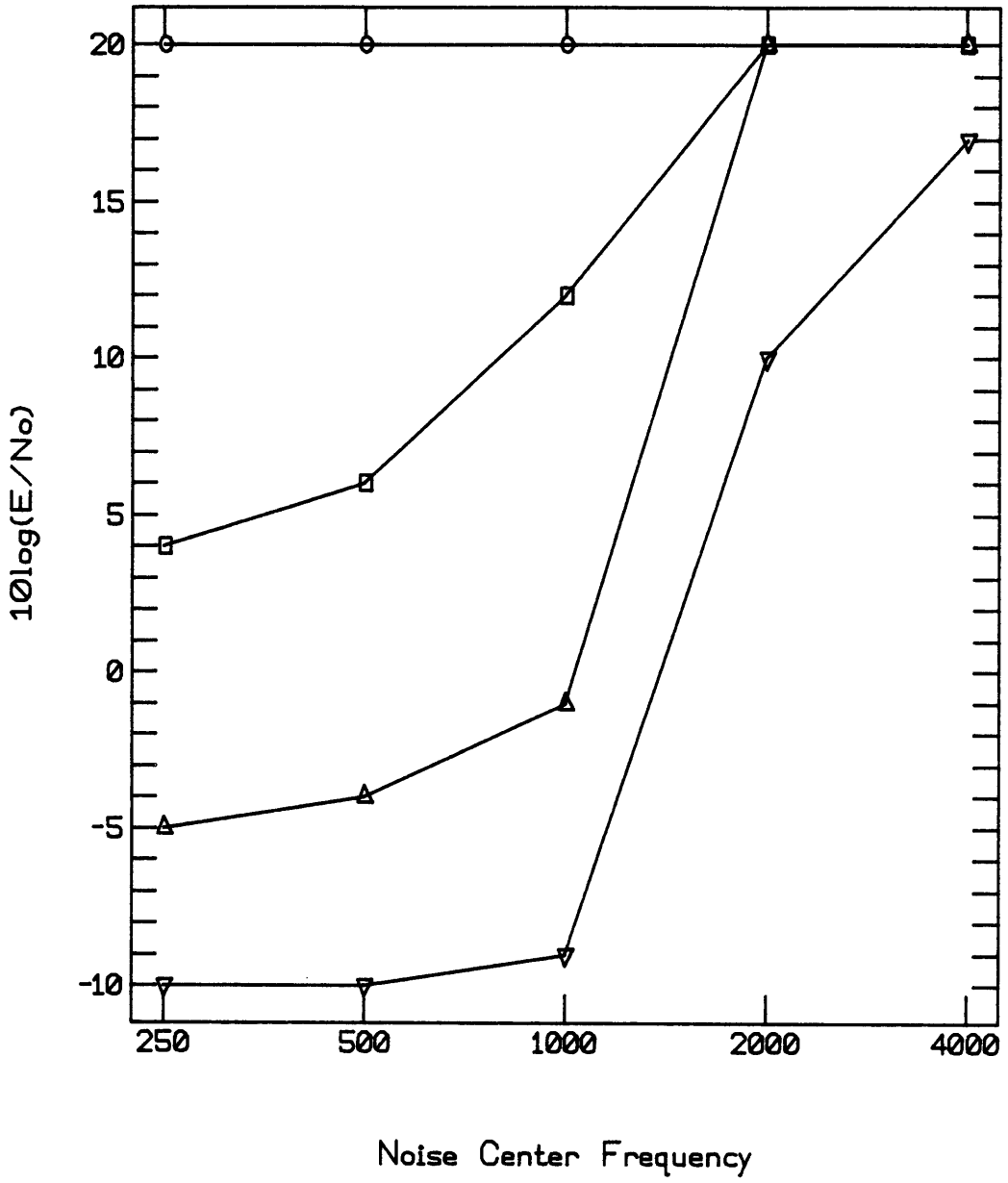
20
15
10
5
0
-5
-10
10log(E/No)
250
500
1000
2000
4000
Noise Center Frequency

Figure 8.12

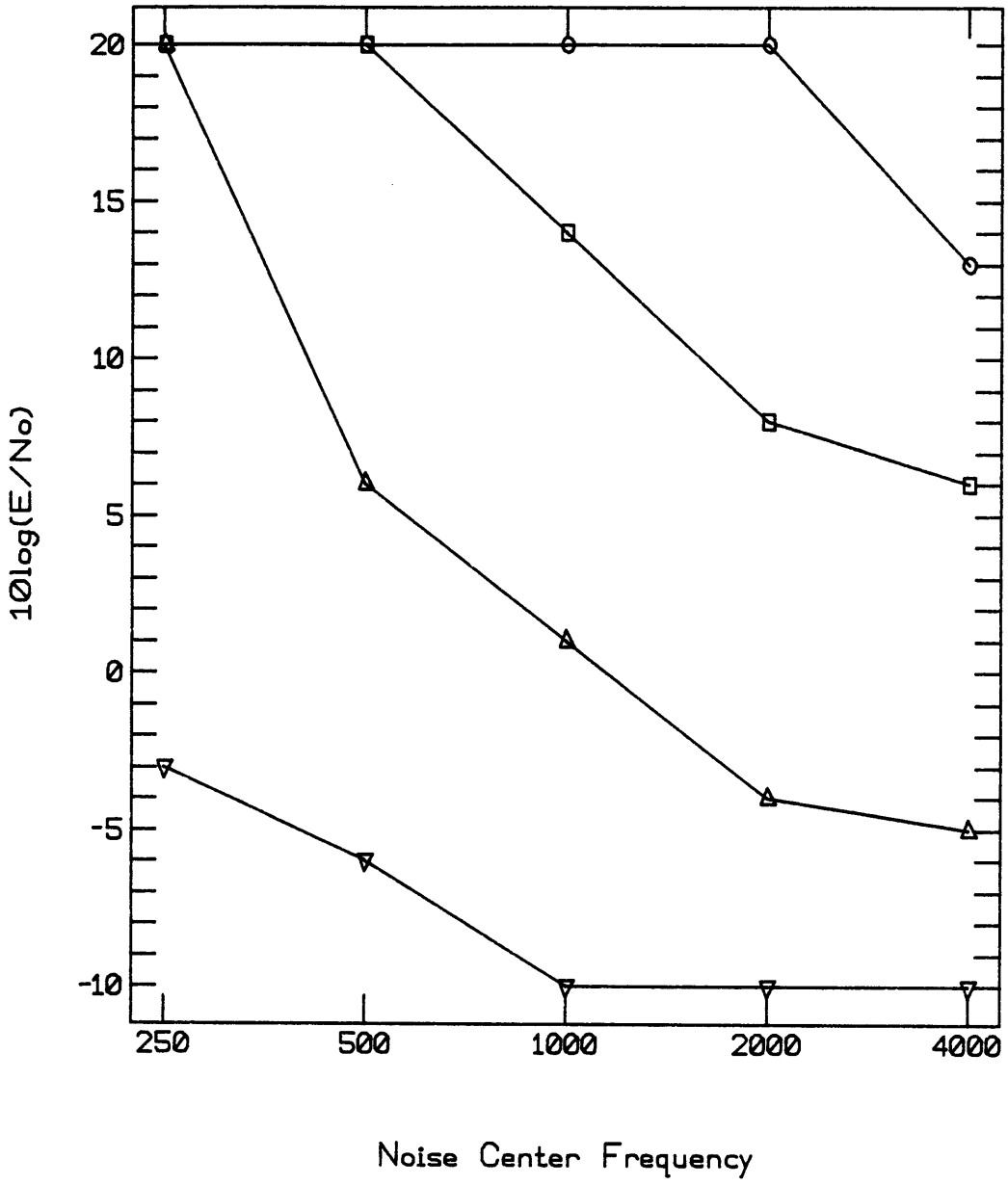
20
15
10
5
0
-5
-10
10log(E/No)
250
500
1000
2000
4000
Noise Center Frequency

Figure 8.13

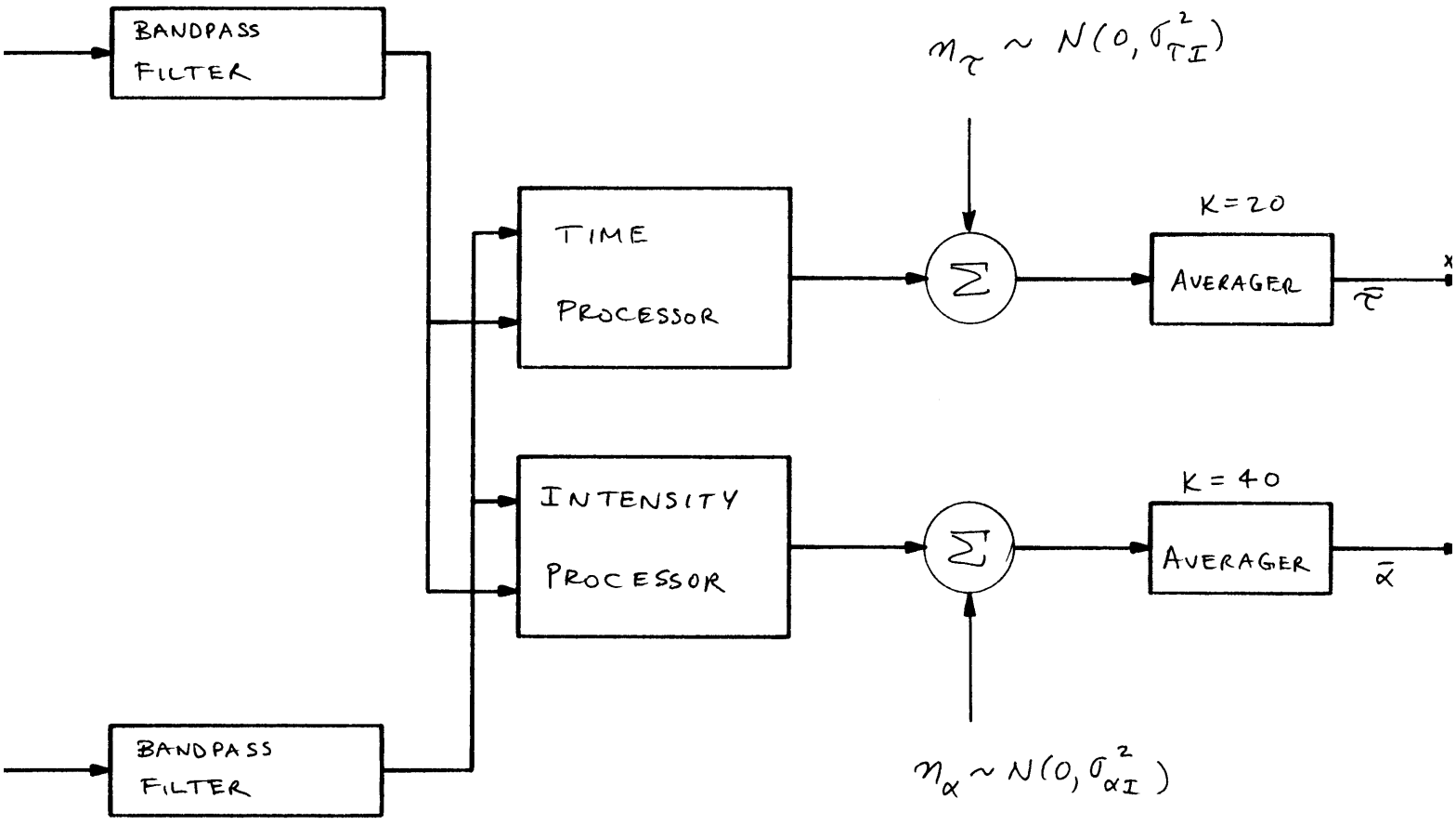
BANDPASS FILTER
BANDPASS FILTER
TIME PROCESSOR
INTENSITY PROCESSOR
$n_\tau \sim N(0, \sigma_{TI}^2)$
$n_\alpha \sim N(0, \sigma_{\alpha I}^2)$
Σ
Σ
K = 20
K = 40
AVERAGER
AVERAGER
$\bar{\tau}$
$\bar{\alpha}$

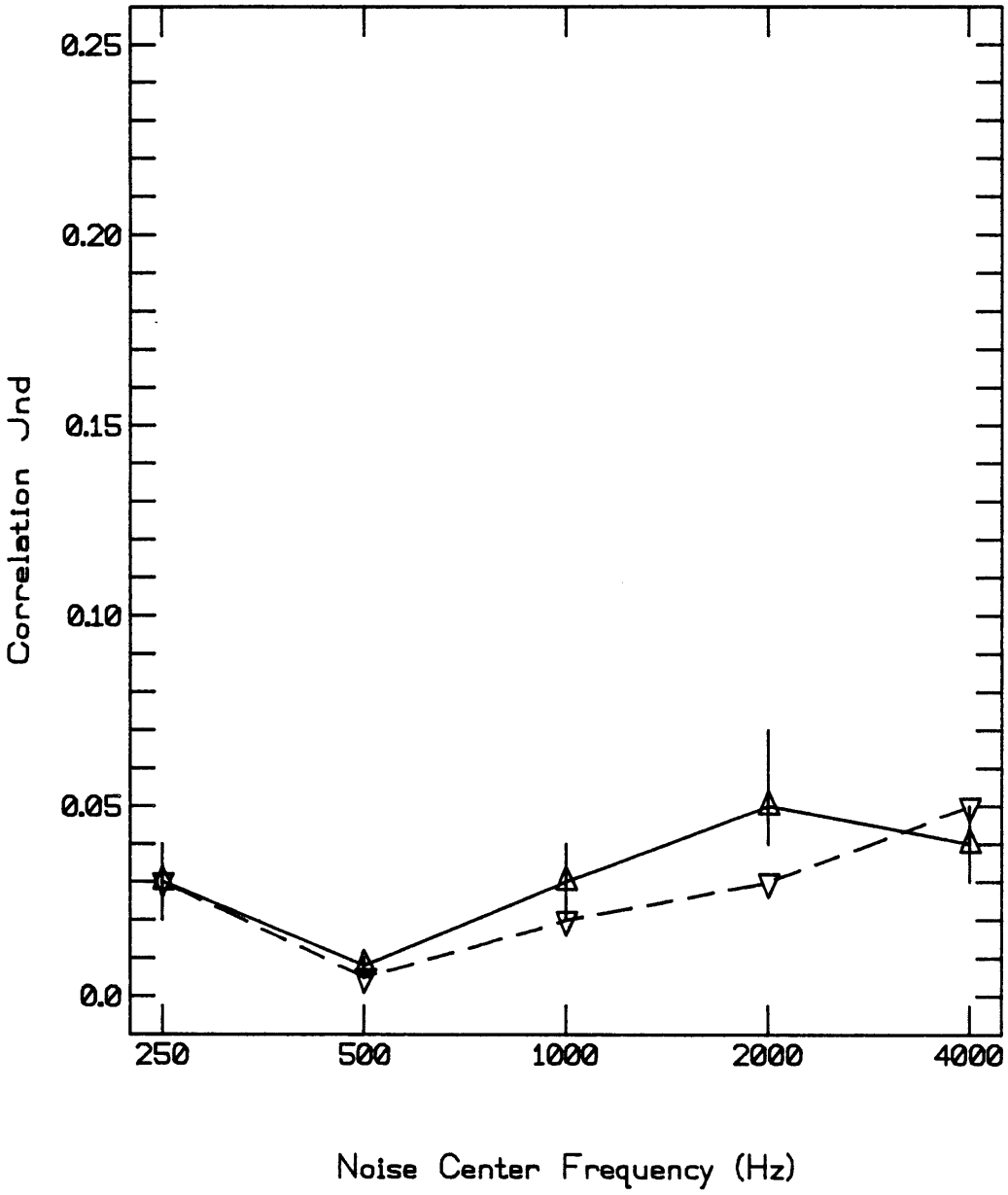
0.25
0.20
0.15
0.10
0.05
0.0
Correlation Jnd
250
500
1000
2000
4000
Noise Center Frequency (Hz)

Figure 8.15

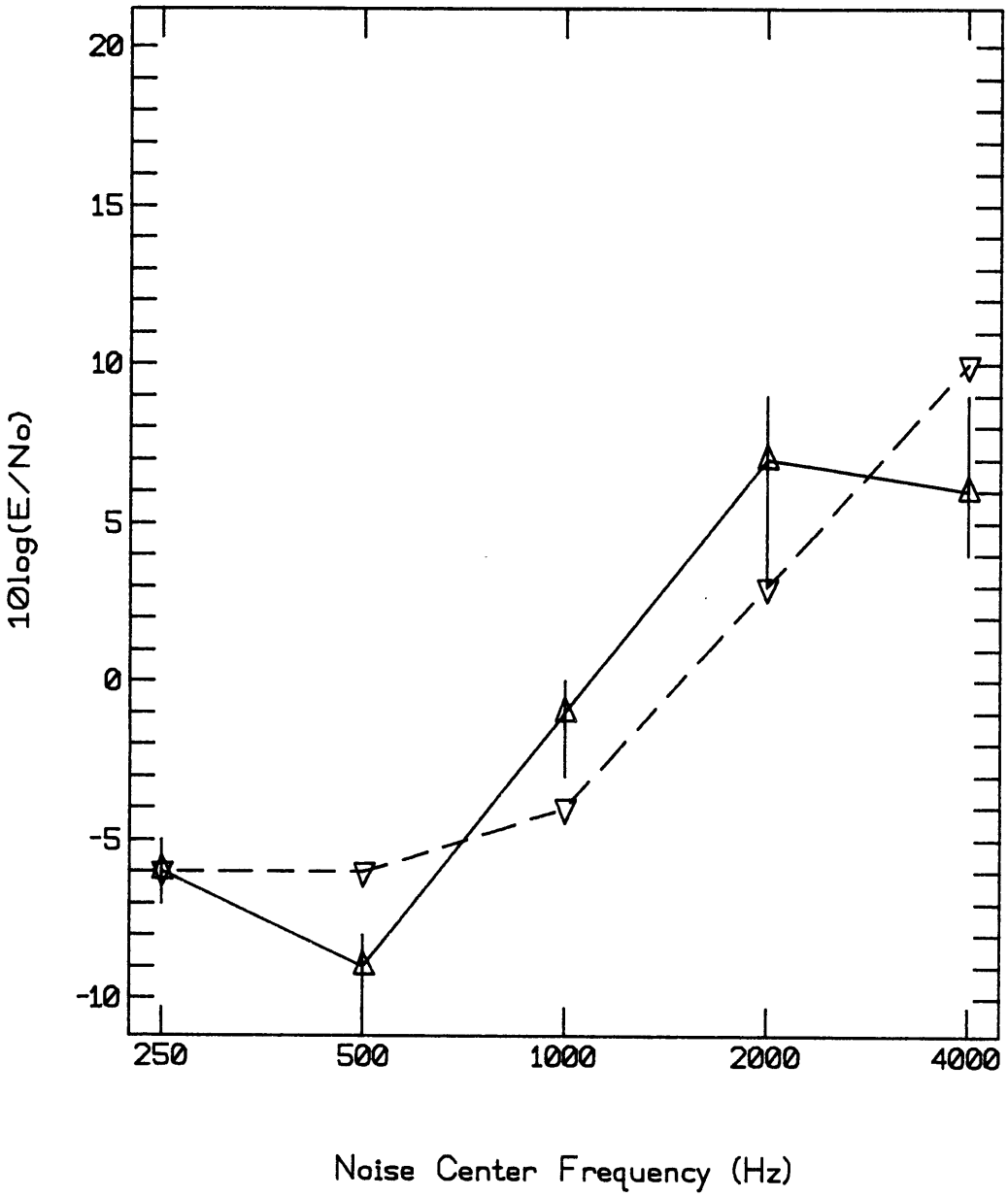
20
15
10
5
0
-5
-10
10log(E/No)
250
500
1000
2000
4000
Noise Center Frequency (Hz)

Figure 8.16

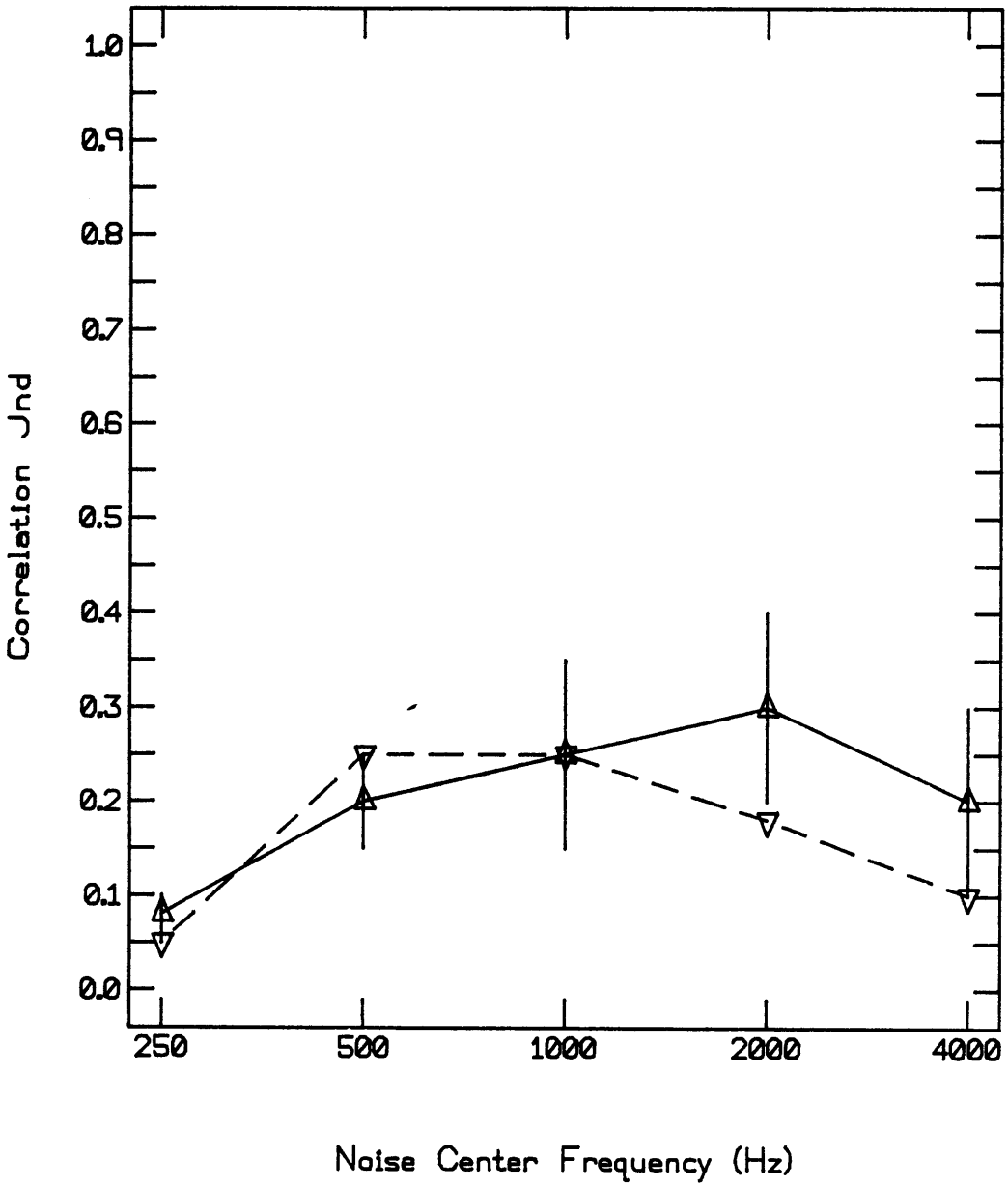
1.0
0.9
0.8
0.7
0.6
0.5
0.4
0.3
0.2
0.1
0.0
Correlation Jnd
250
500
1000
2000
4000
Noise Center Frequency (Hz)

Figure8.17

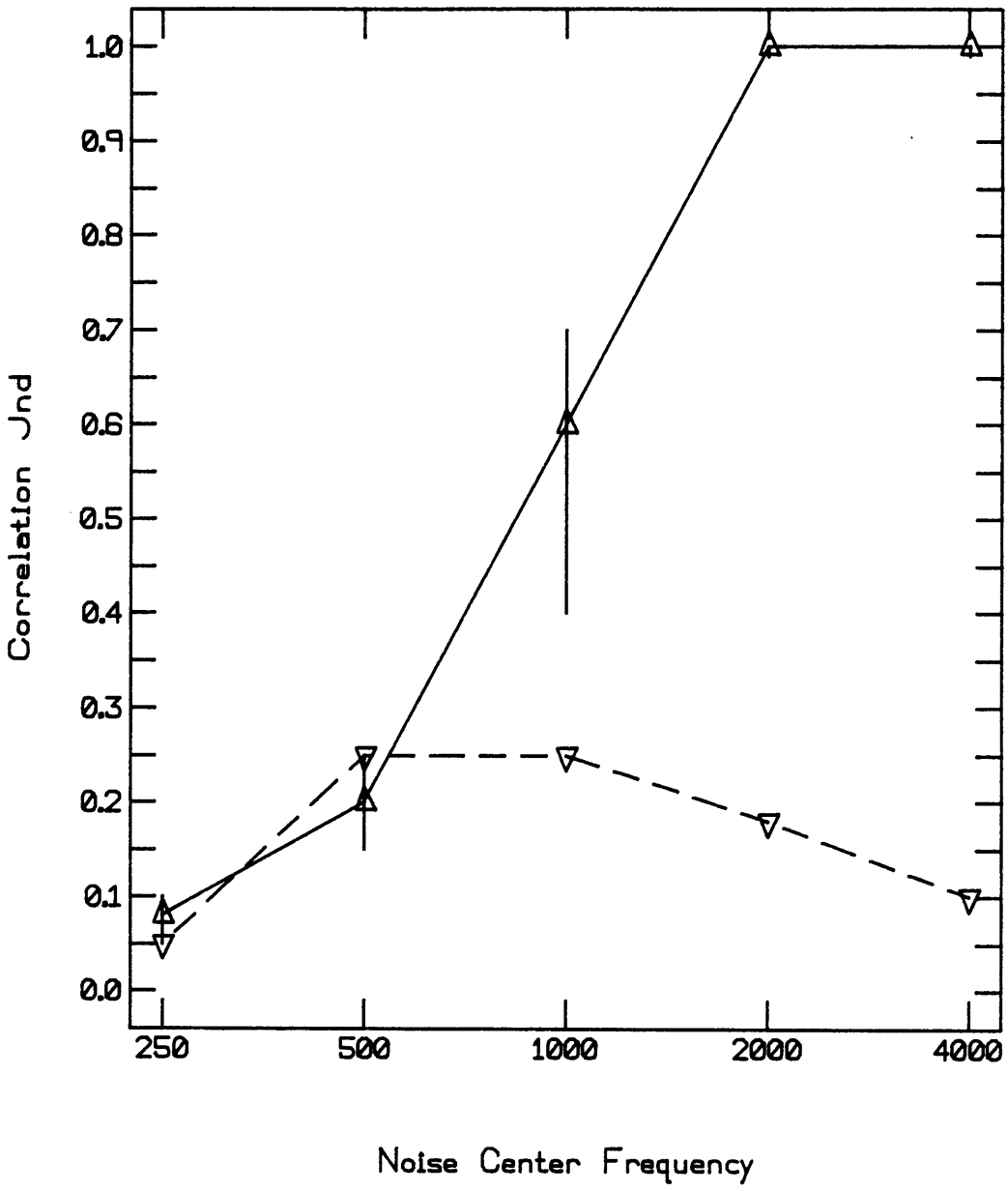
Correlation Jnd
1.0
0.9
0.8
0.7
0.6
0.5
0.4
0.3
0.2
0.1
0.0
250
500
1000
2000
4000
Noise Center Frequency

Figure 8.18

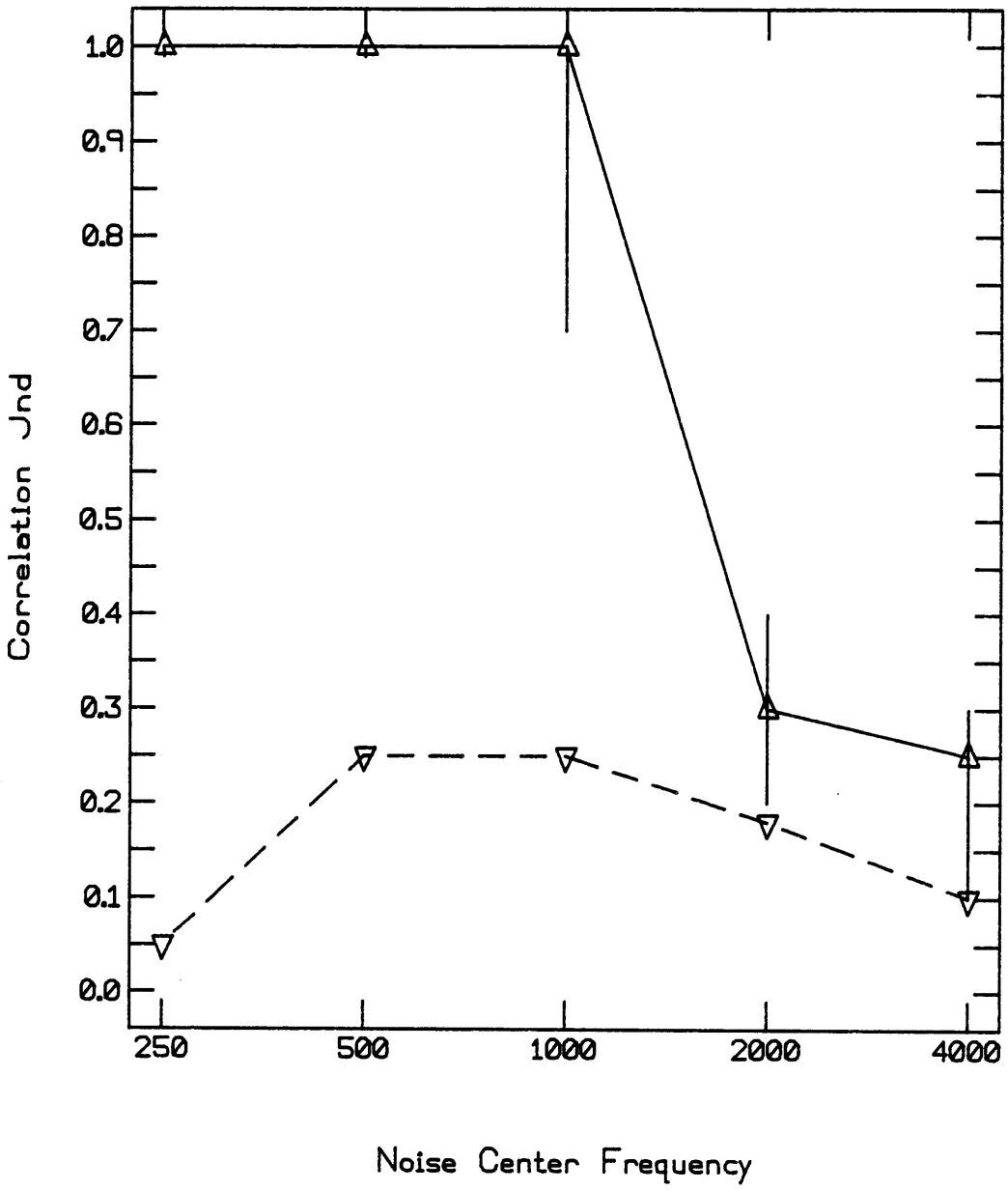
1.0
0.9
0.8
0.7
0.6
0.5
0.4
0.3
0.2
0.1
0.0
Correlation Jnd
250
500
1000
2000
4000
Noise Center Frequency

Figure 8.19

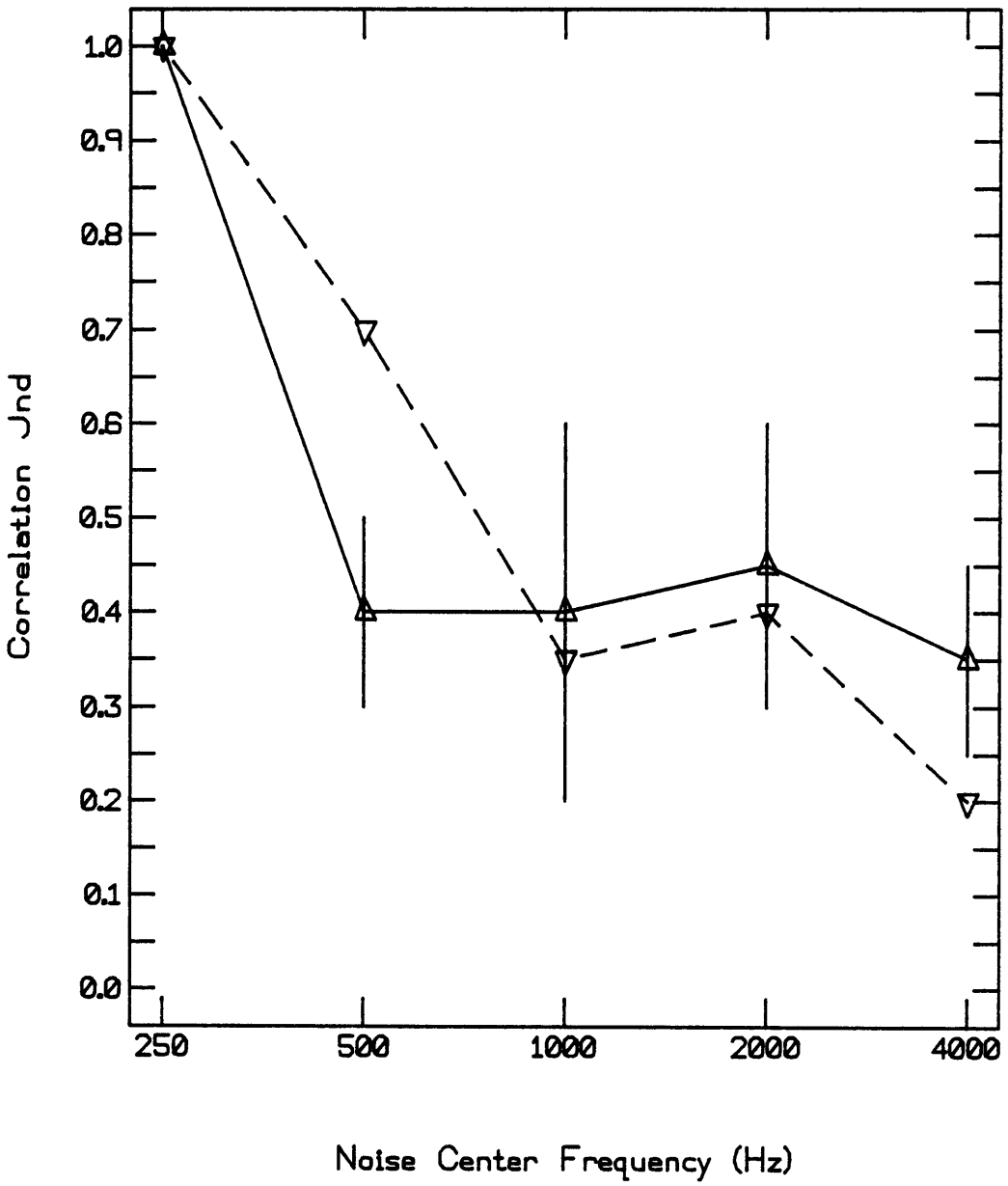
1.0
0.9
0.8
0.7
0.6
0.5
0.4
0.3
0.2
0.1
0.0
Correlation Jnd
250
500
1000
2000
4000
Noise Center Frequency (Hz)

Figure 8.20

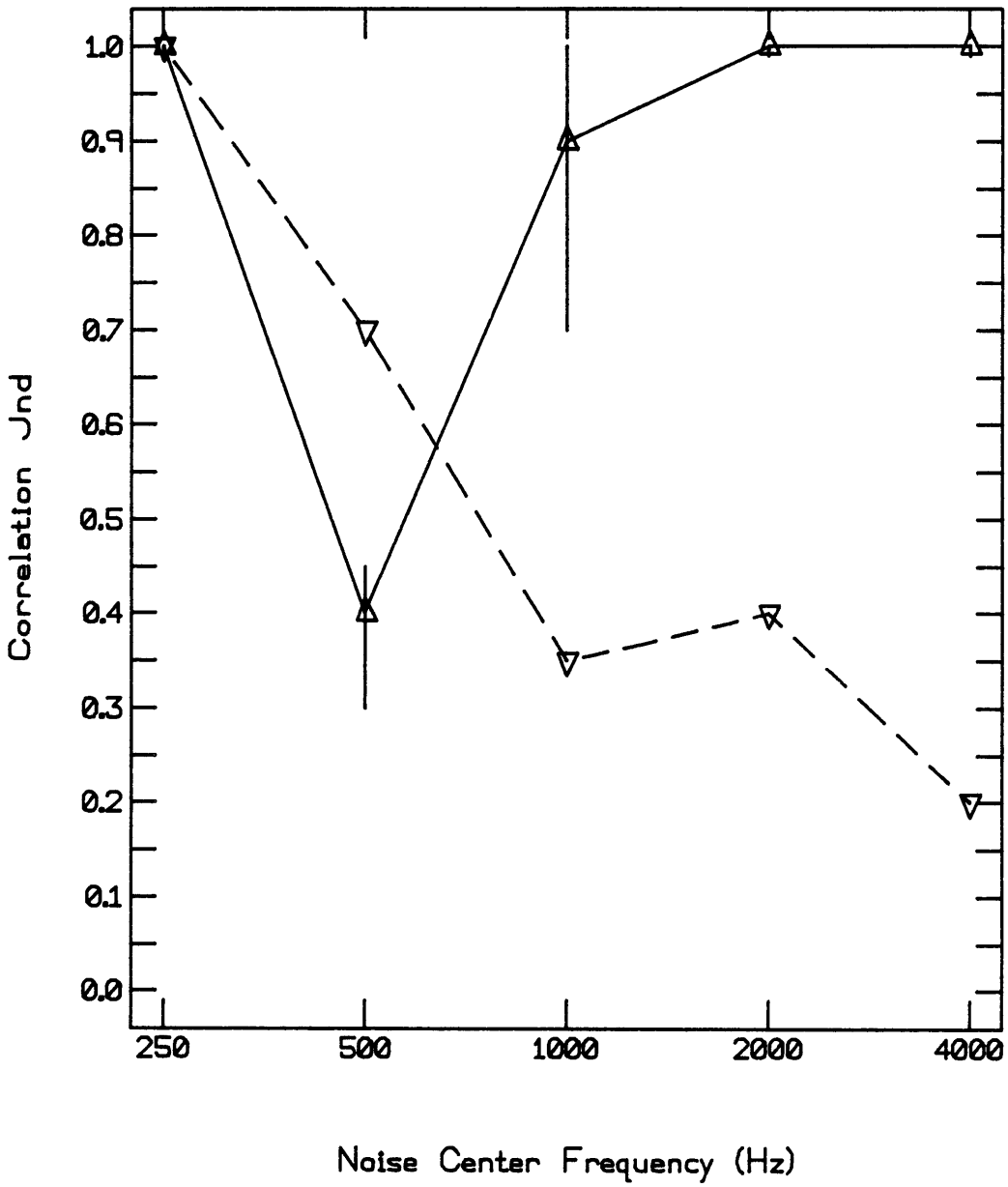
1.0
0.9
0.8
0.7
0.6
0.5
0.4
0.3
0.2
0.1
0.0
Correlation Jnd
250
500
1000
2000
4000
Noise Center Frequency (Hz)

Figure 8.21

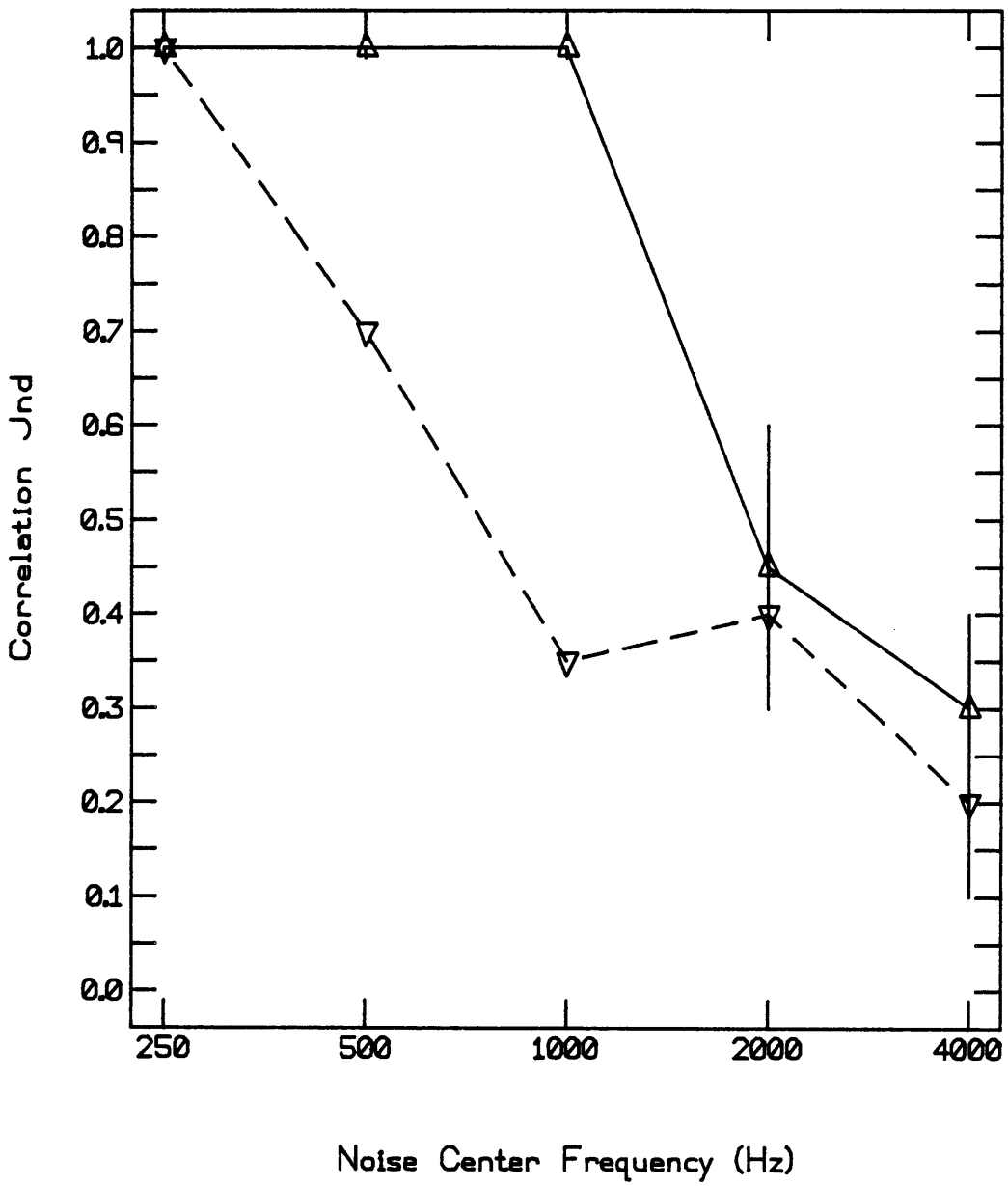
1.0
0.9
0.8
0.7
0.6
0.5
0.4
0.3
0.2
0.1
0.0
Correlation Jnd
250
500
1000
2000
4000
Noise Center Frequency (Hz)

Figure 8.22

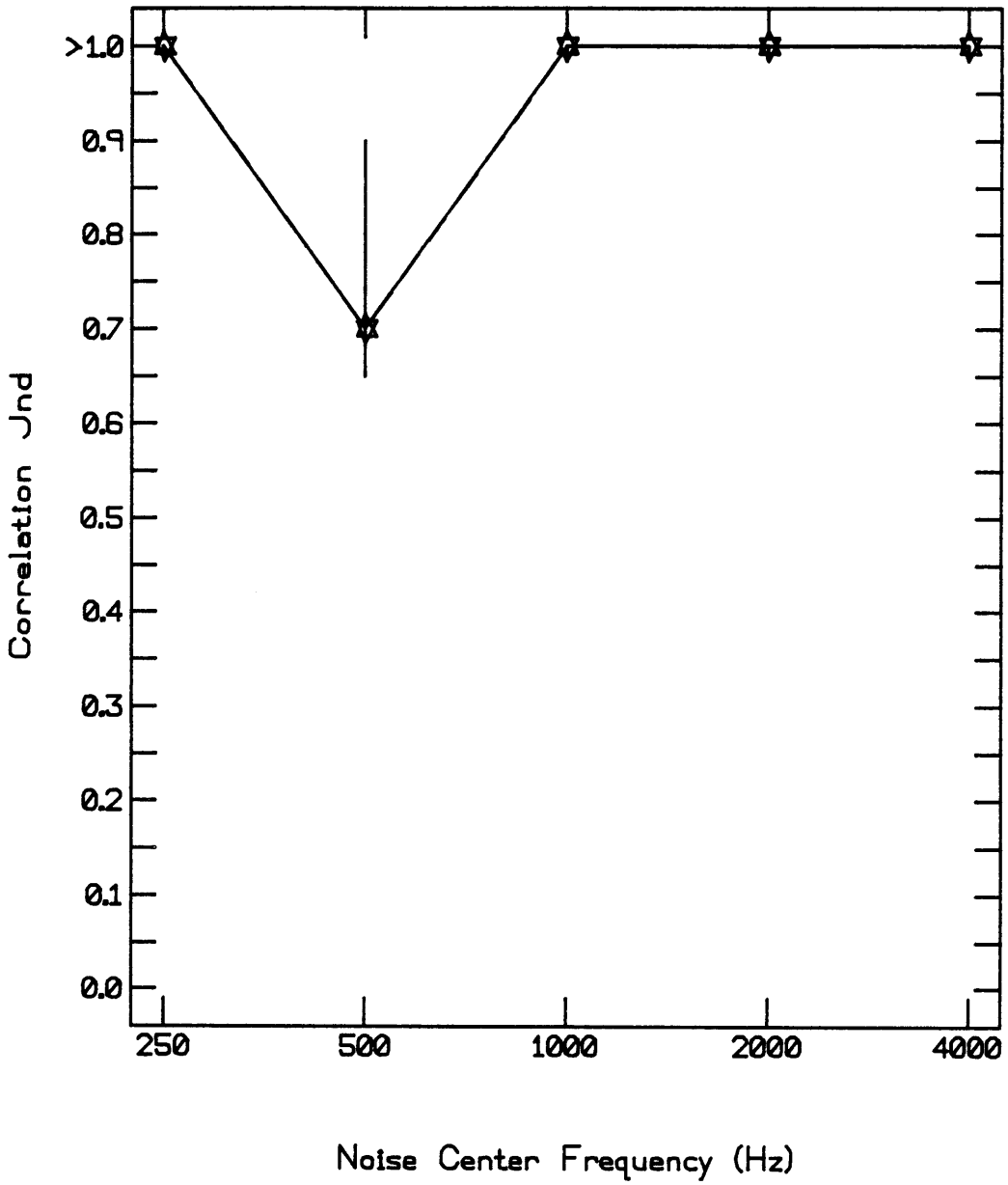
>1.0
0.9
0.8
0.7
0.6
0.5
0.4
0.3
0.2
0.1
0.0
Correlation Jnd
250
500
1000
2000
4000
Noise Center Frequency (Hz)

Figure 8.23

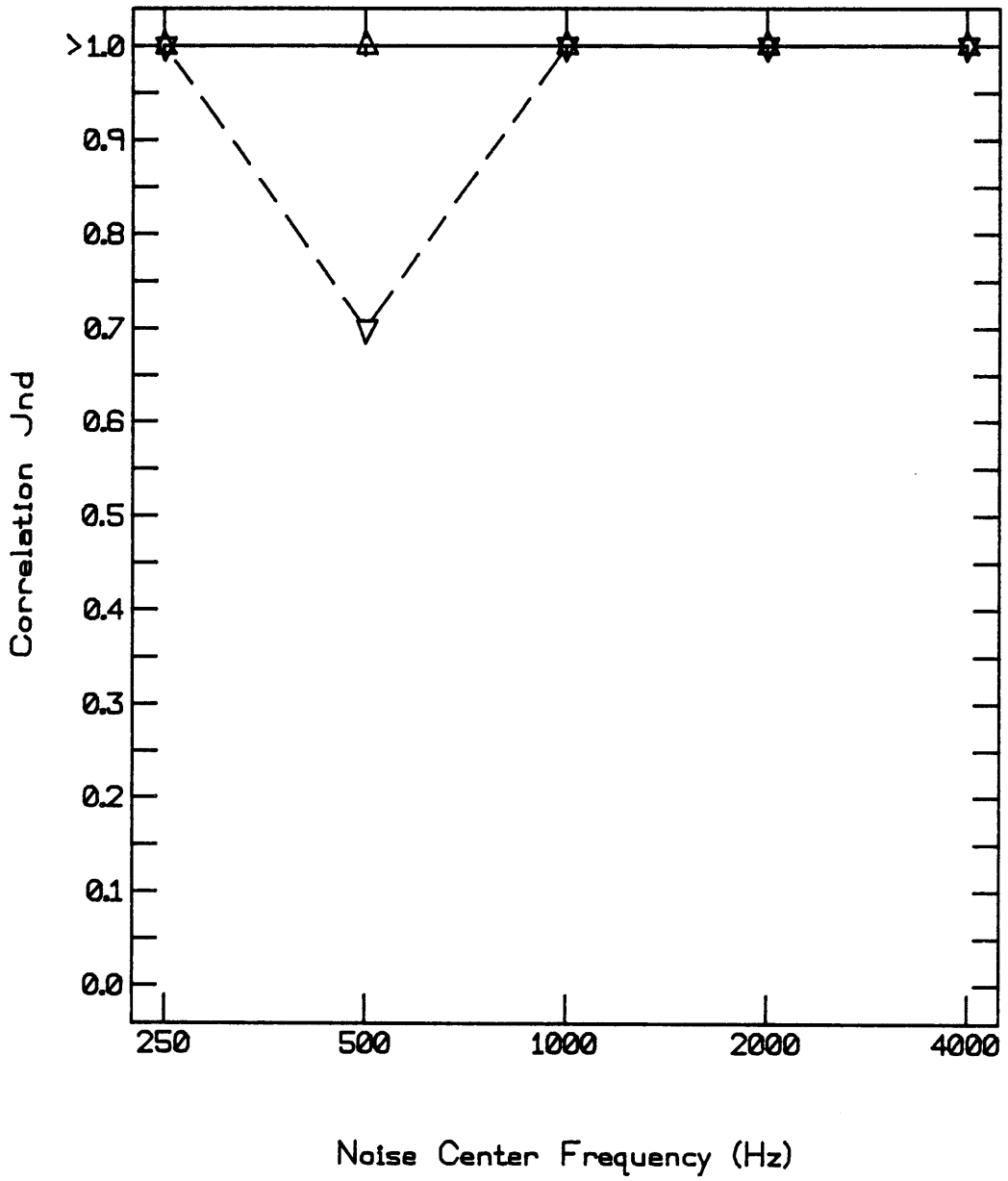
>1.0
0.9
0.8
0.7
0.6
0.5
0.4
0.3
0.2
0.1
0.0
Correlation Jnd
250
500
1000
2000
4000
Noise Center Frequency (Hz)

Figure 8.24

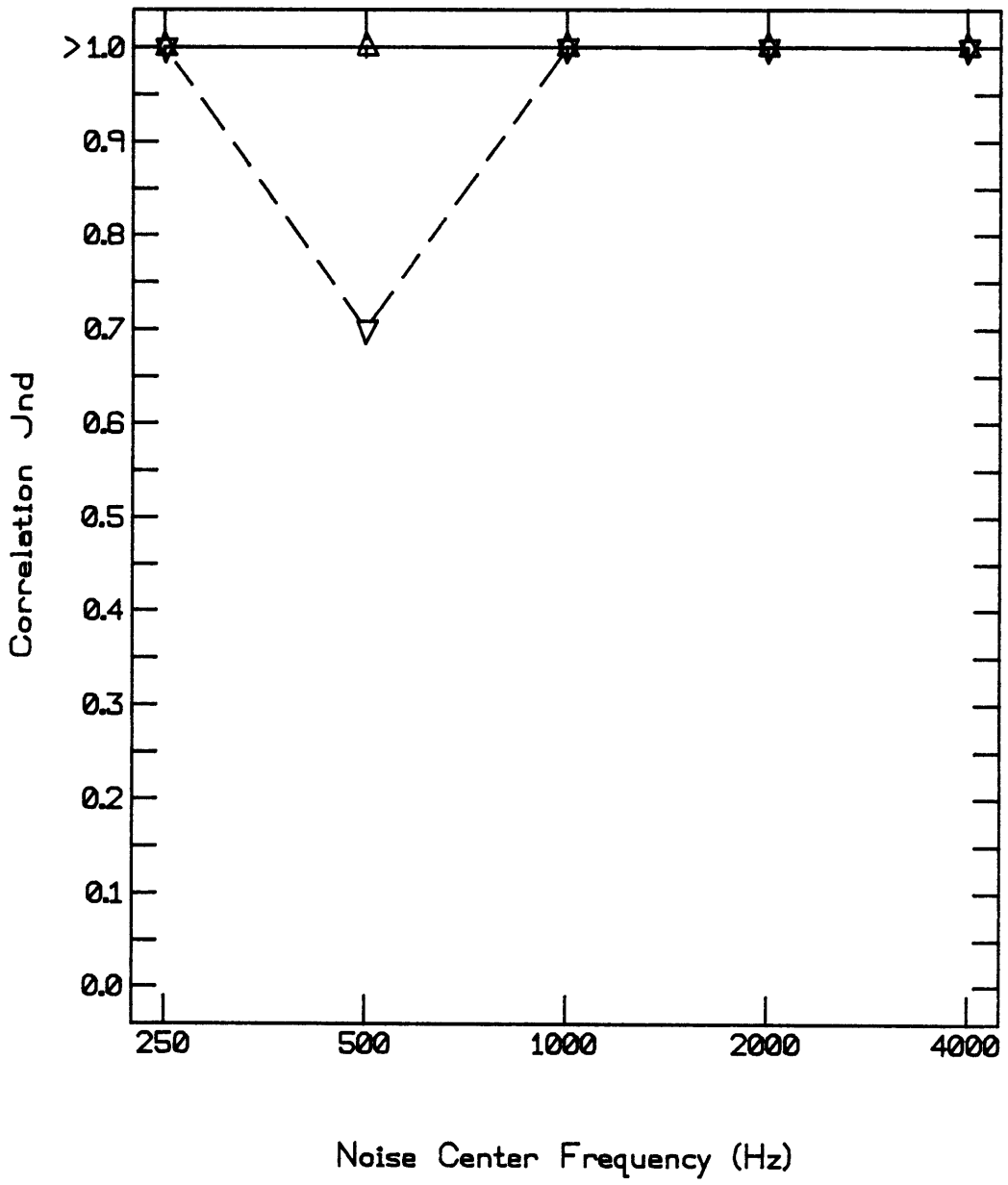
>1.0
0.9
0.8
0.7
0.6
0.5
0.4
0.3
0.2
0.1
0.0
Correlation Jnd
250
500
1000
2000
4000
Noise Center Frequency (Hz)

Figure 8.25

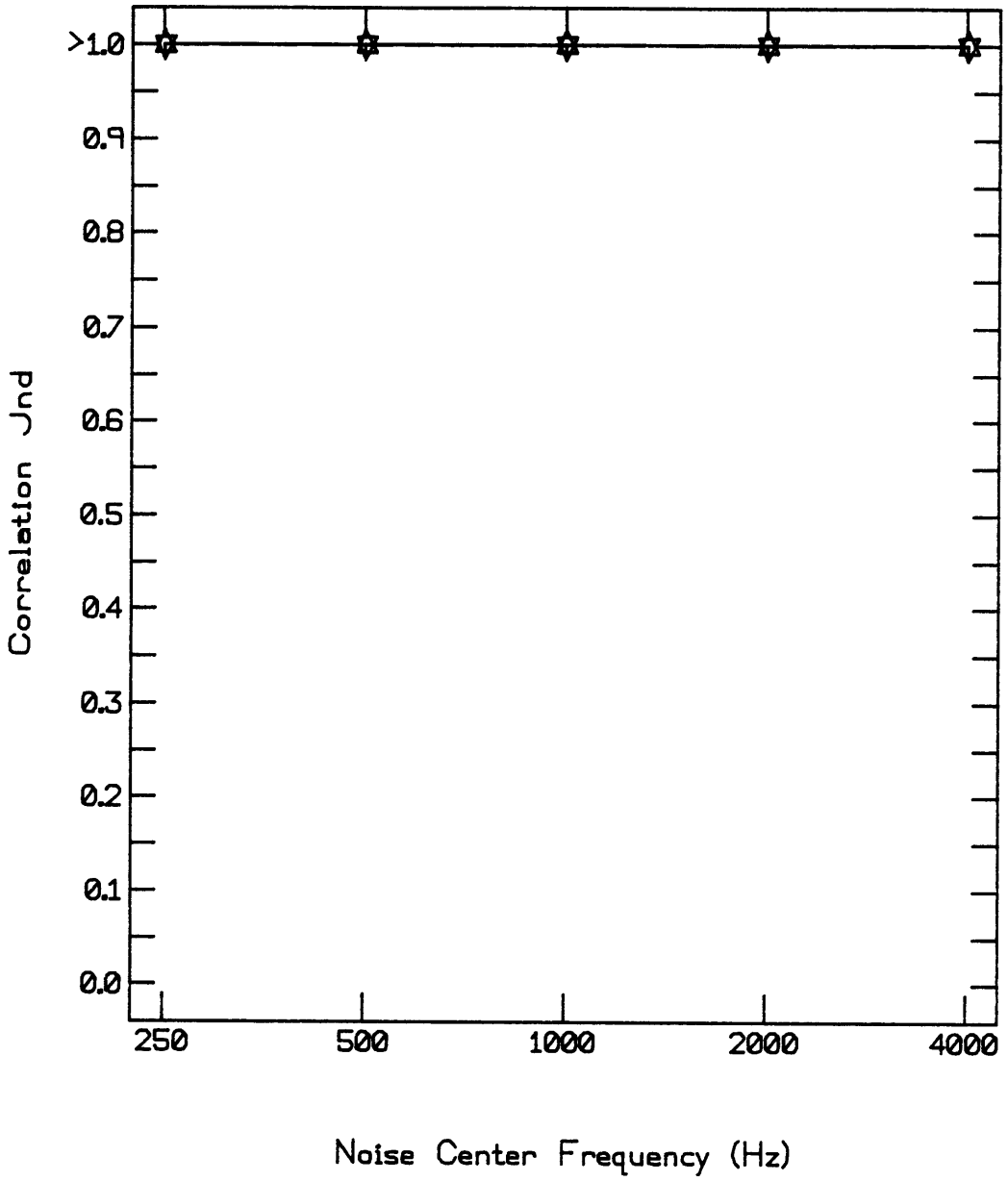
>1.0
0.9
0.8
0.7
0.6
0.5
0.4
0.3
0.2
0.1
0.0
Correlation Jnd
250
500
1000
2000
4000
Noise Center Frequency (Hz)

Figure 8.26

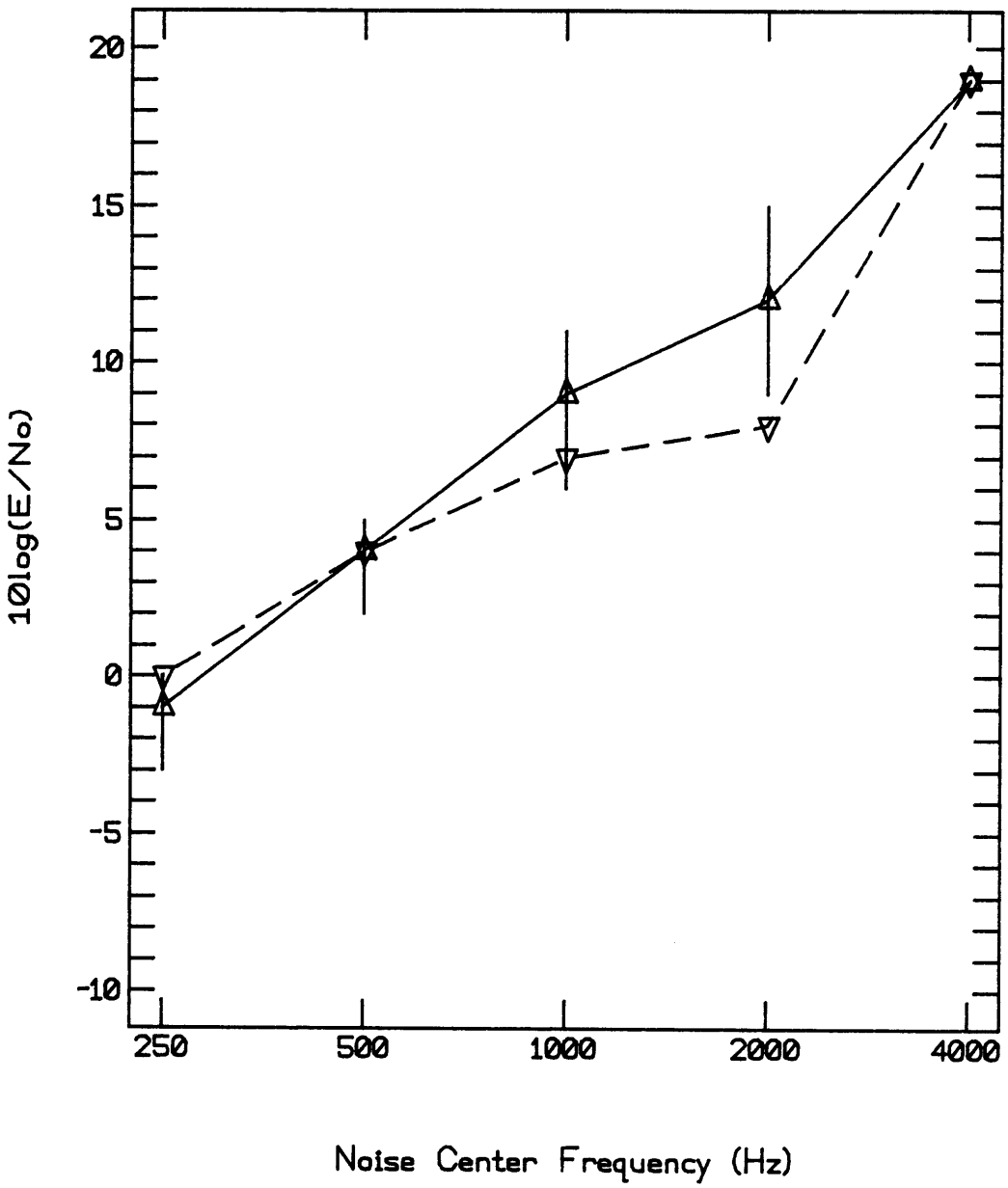
20
15
10
5
0
-5
-10
10log(E/No)
250
500
1000
2000
4000
Noise Center Frequency (Hz)

Figure8.27

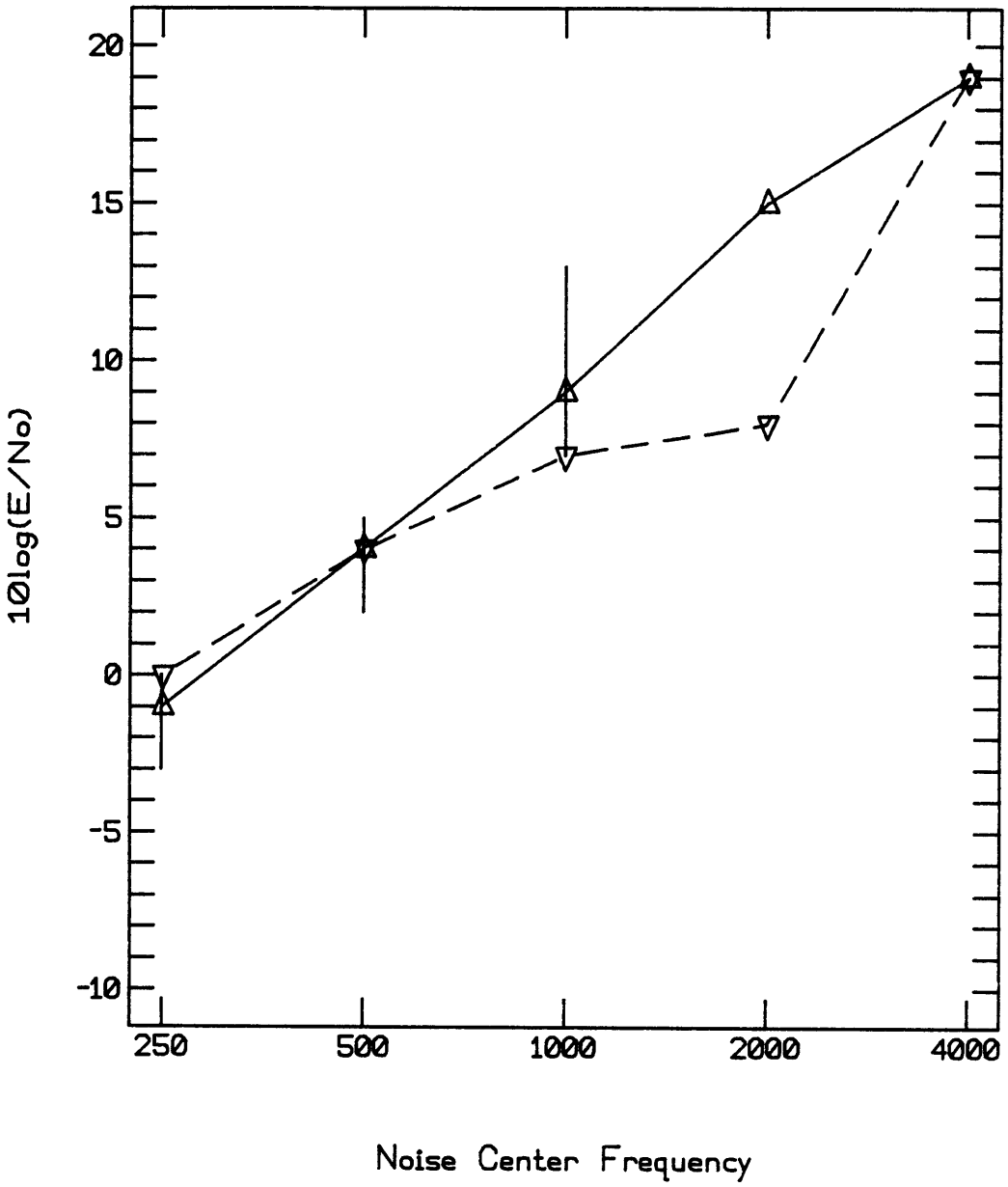
20
15
10
5
0
-5
-10
10log(E/No)
250
500
1000
2000
4000
Noise Center Frequency

Figure 8.28

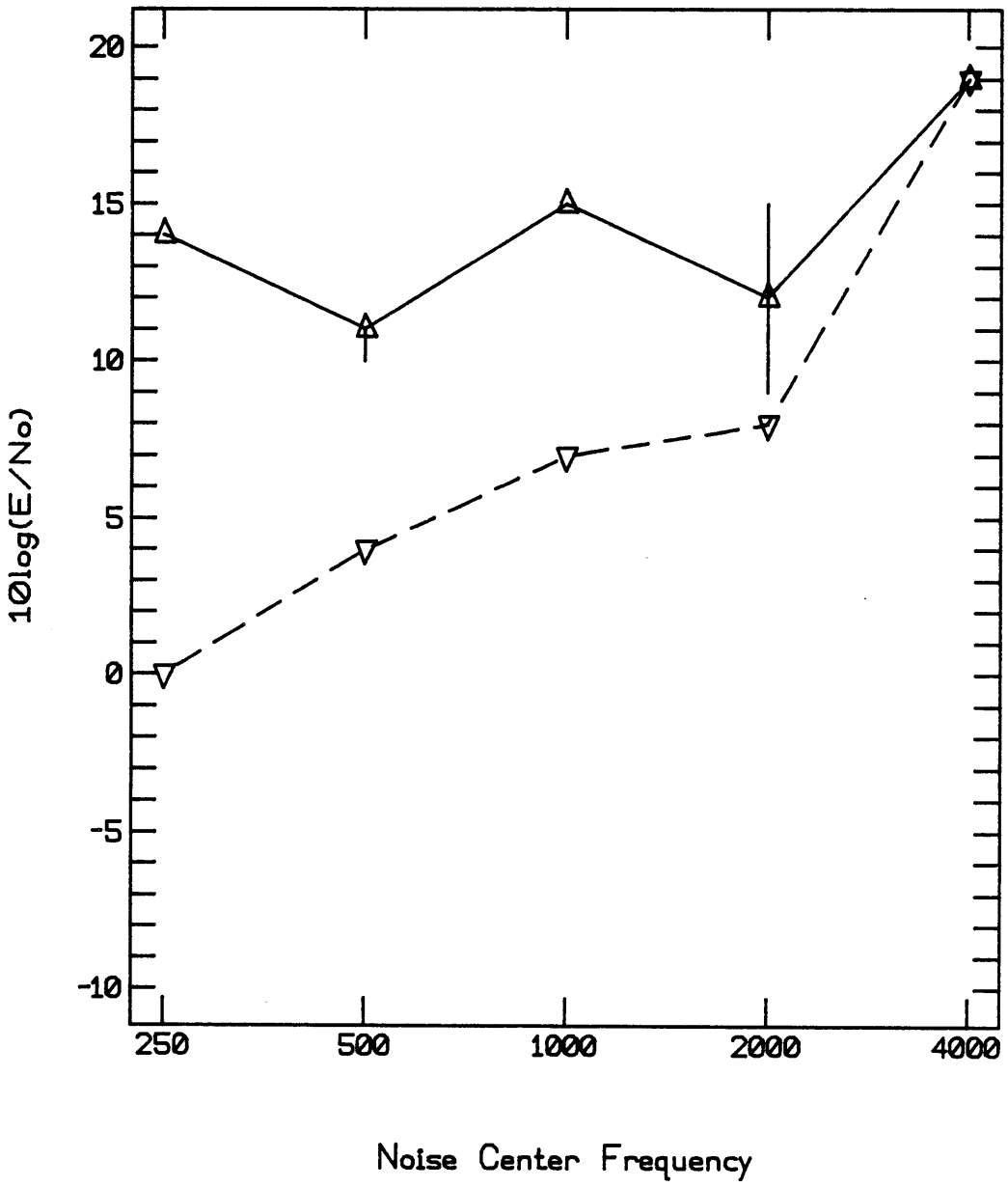
20
15
10
5
0
-5
-10
10log(E/No)
250
500
1000
2000
4000
Noise Center Frequency

Figure 8.29

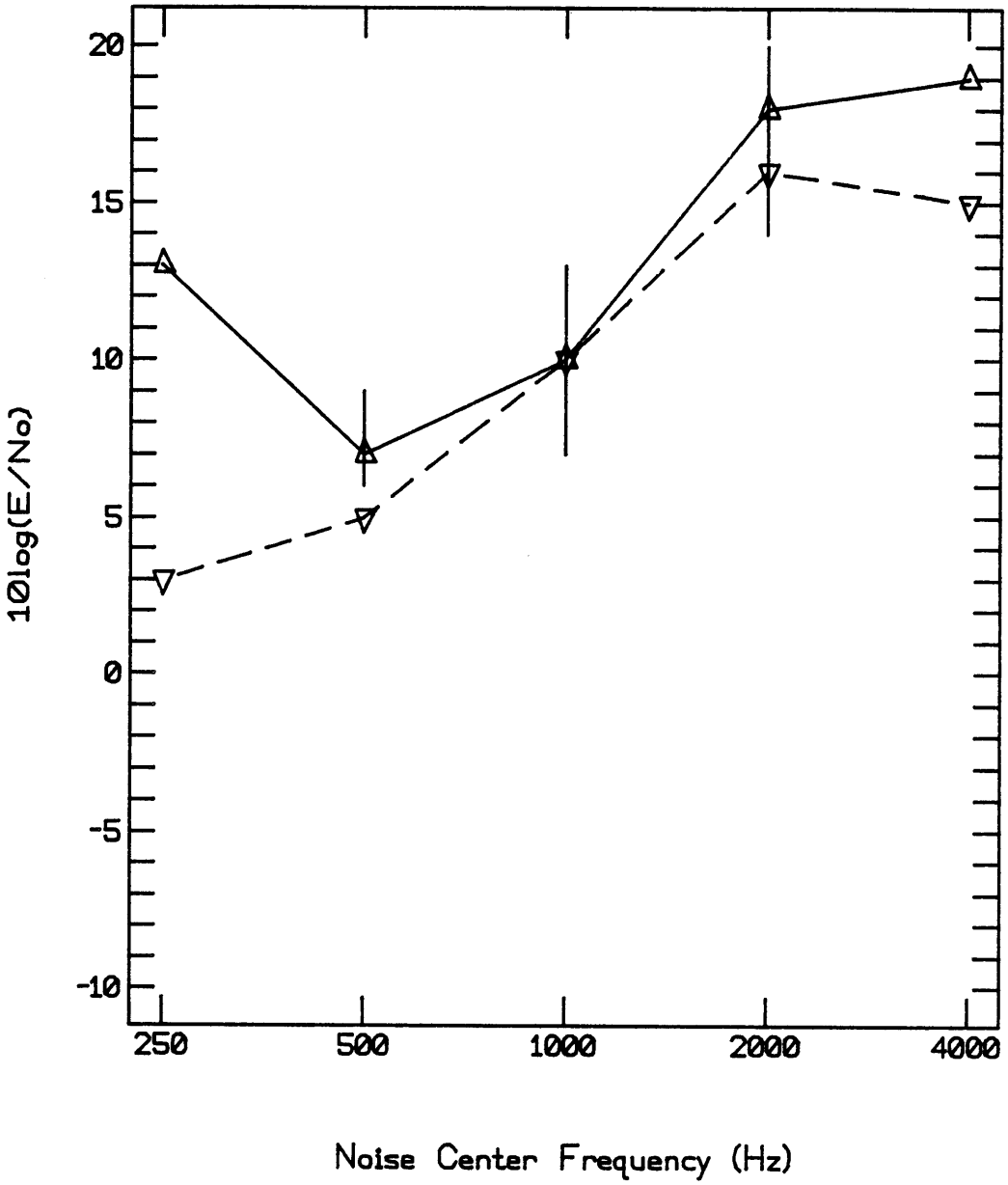
20
15
10
5
0
-5
-10
10log(E/No)
250
500
1000
2000
4000
Noise Center Frequency (Hz)

Figure 8.30

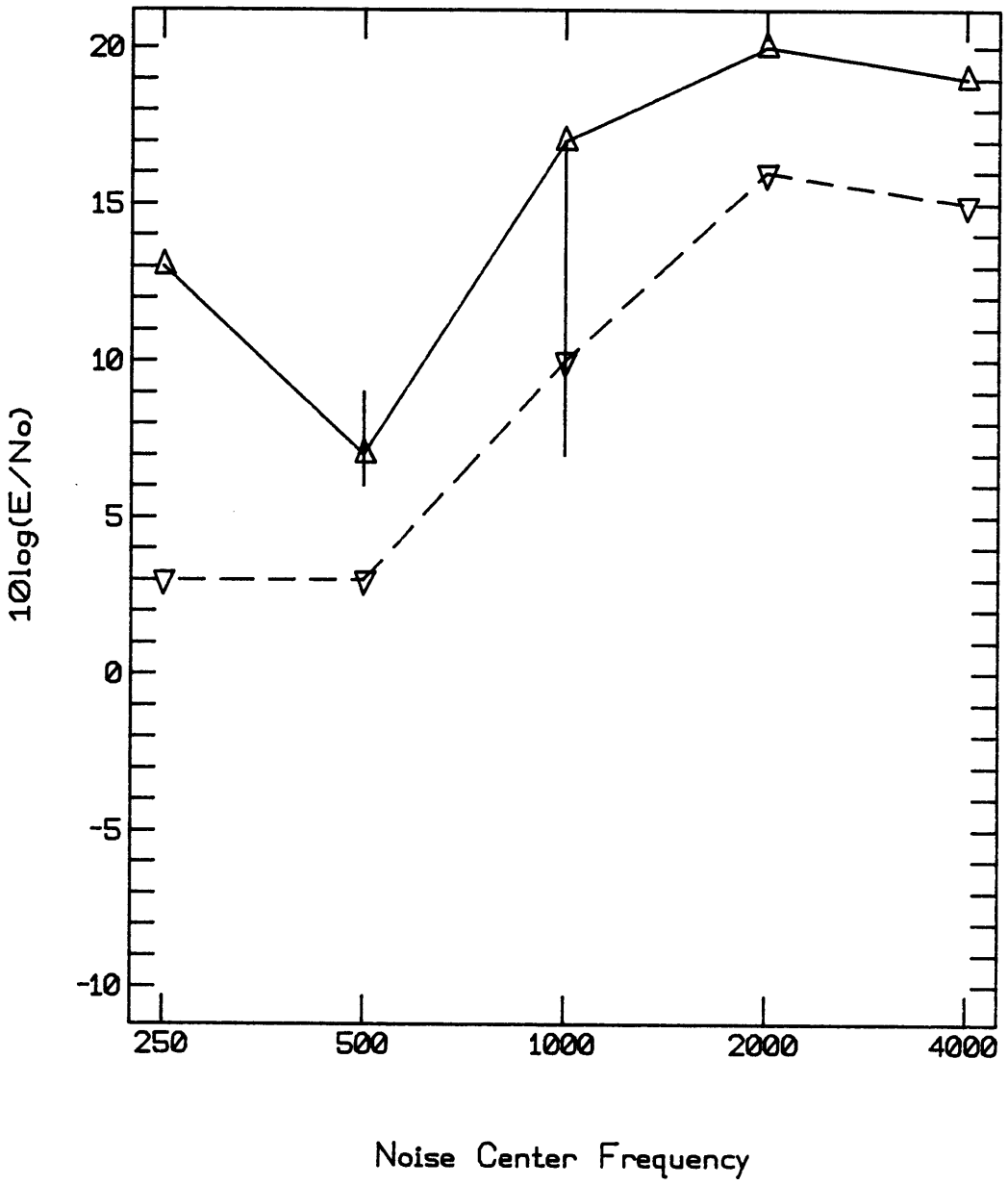
20
15
10
5
0
-5
-10
10log(E/No)
250
500
1000
2000
4000
Noise Center Frequency

Figure 8.31

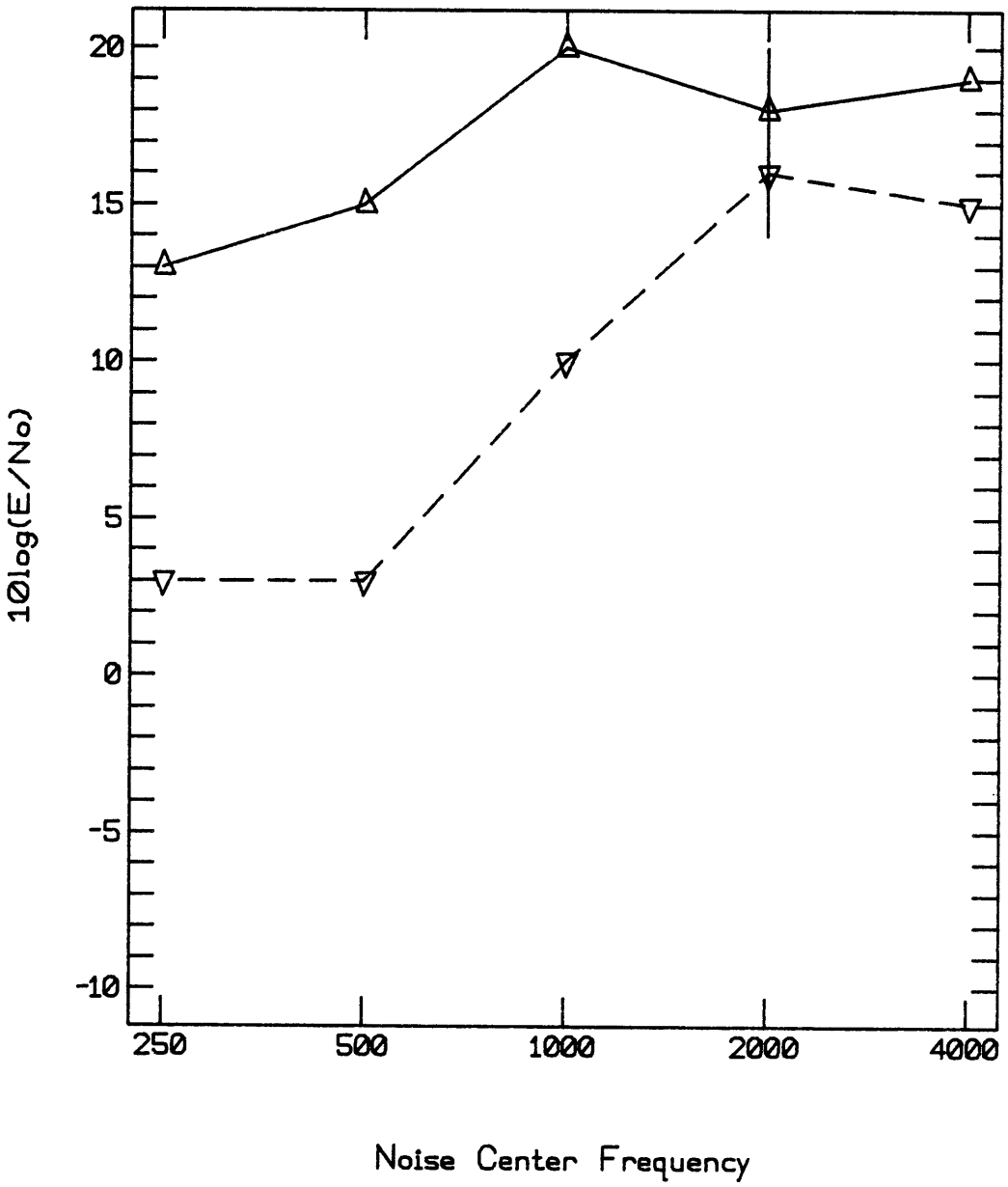
20
15
10
5
0
-5
-10
10log(E/No)
250
500
1000
2000
4000
Noise Center Frequency

Figure 8.32

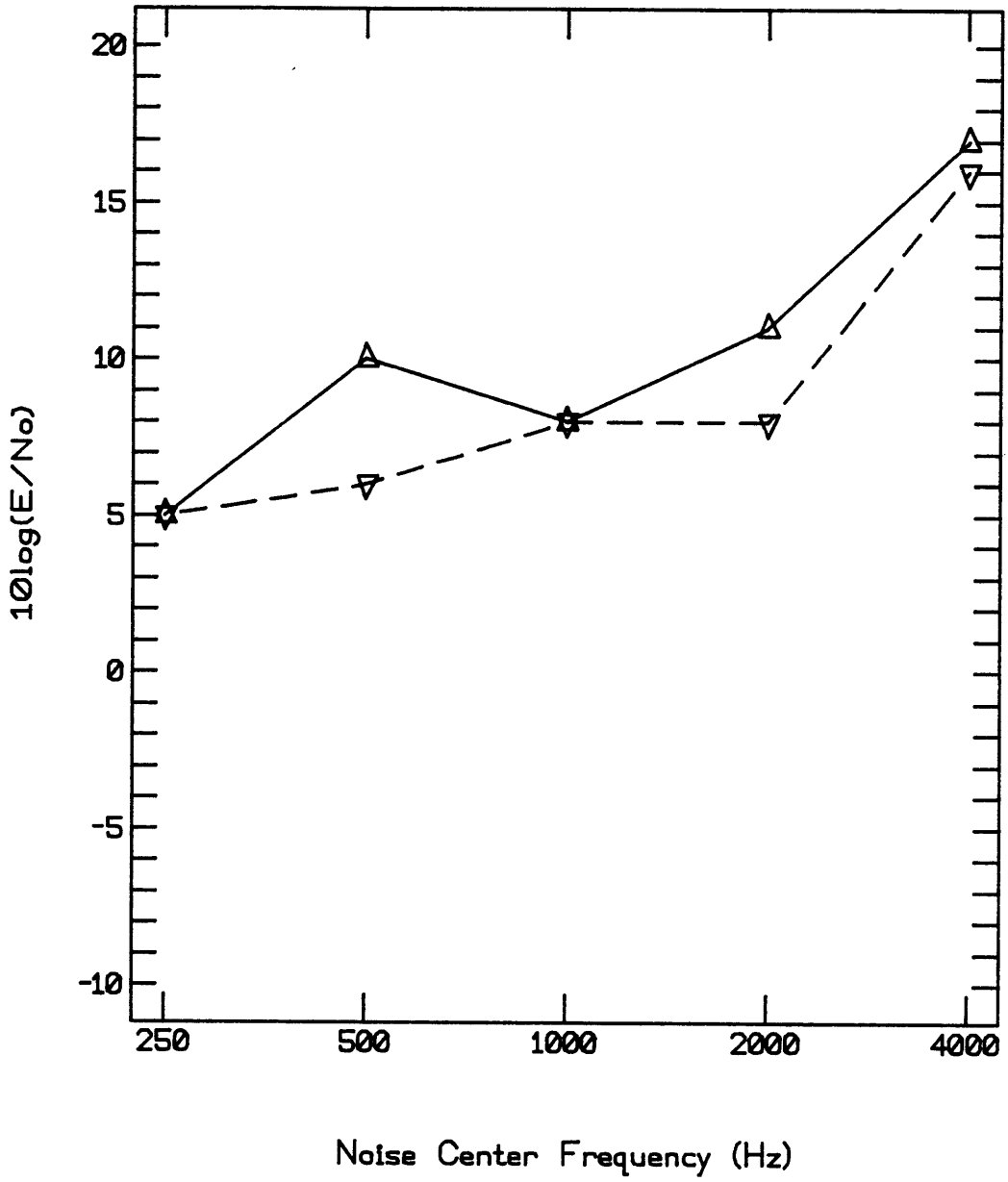
20
15
10
5
0
-5
-10
10log(E/No)
250
500
1000
2000
4000
Noise Center Frequency (Hz)

Figure 8.33

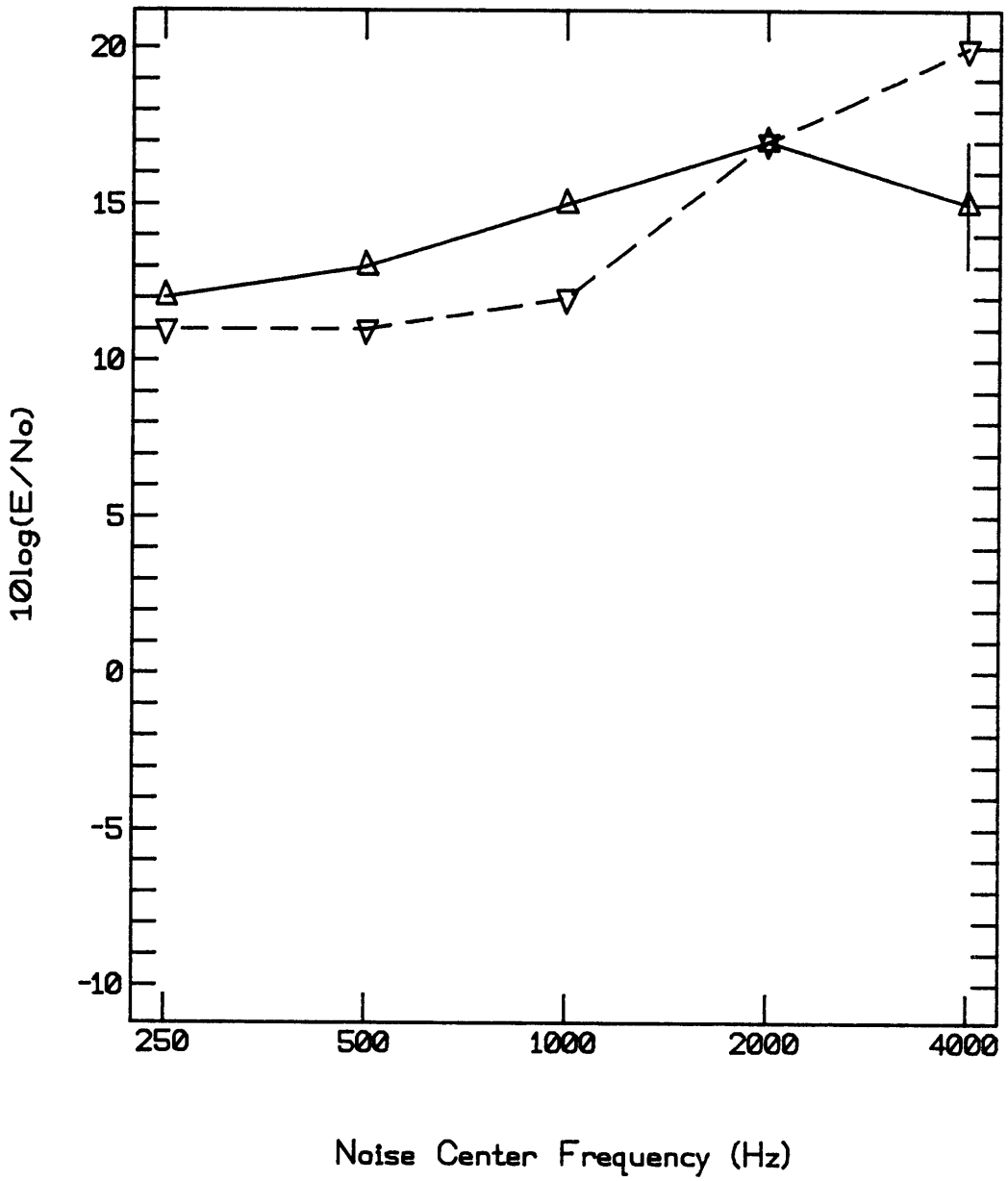
20
15
10
5
0
-5
-10
10log(E/No)
250
500
1000
2000
4000
Noise Center Frequency (Hz)

Figure 8.34

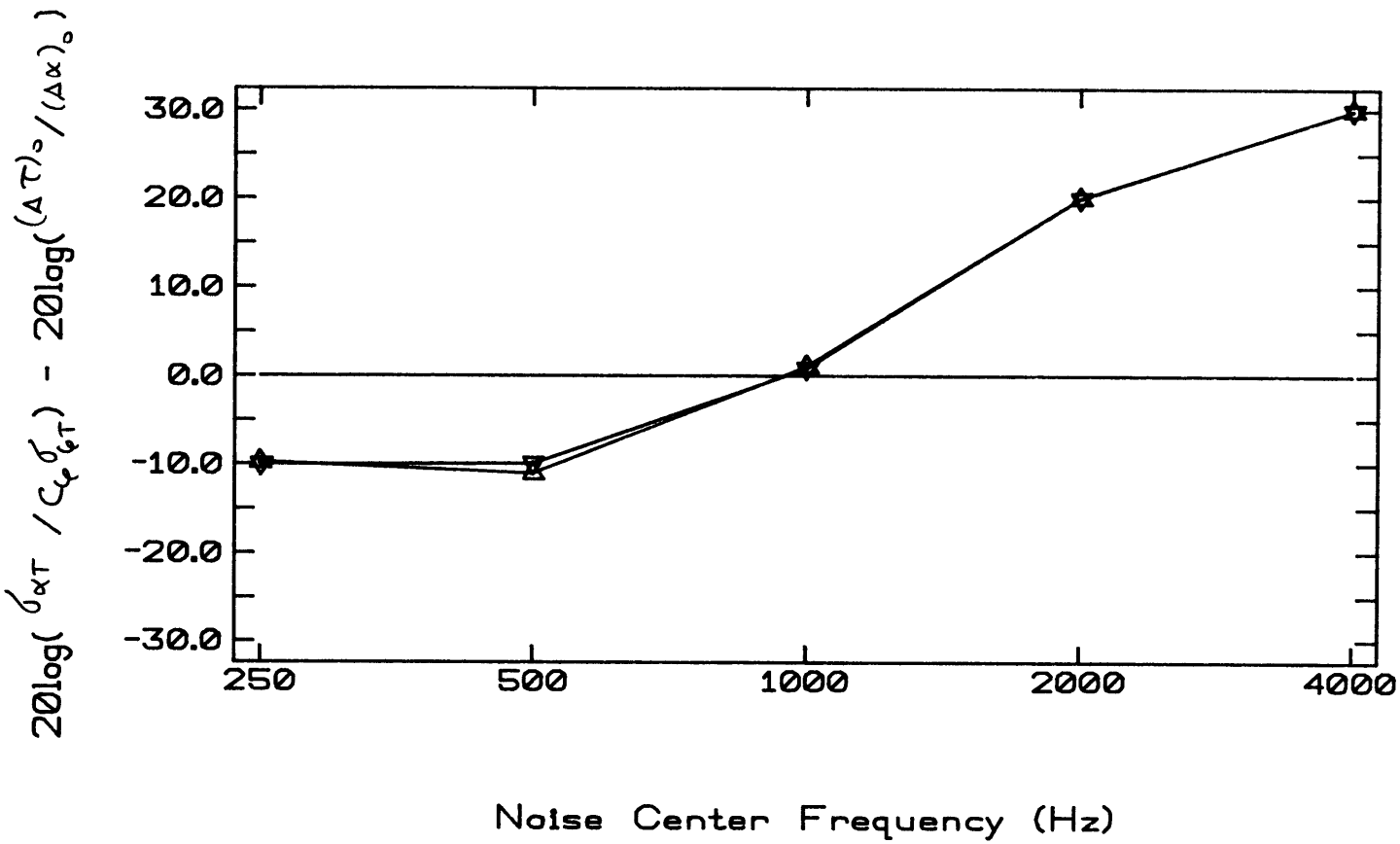
20log(σ_αT / C_φ σ_φT) - 20log((ΔT)_o / (Δα)_o)
30.0
20.0
10.0
0.0
-10.0
-20.0
-30.0
250
500
1000
2000
4000
Noise Center Frequency (Hz)

Figure 8.35

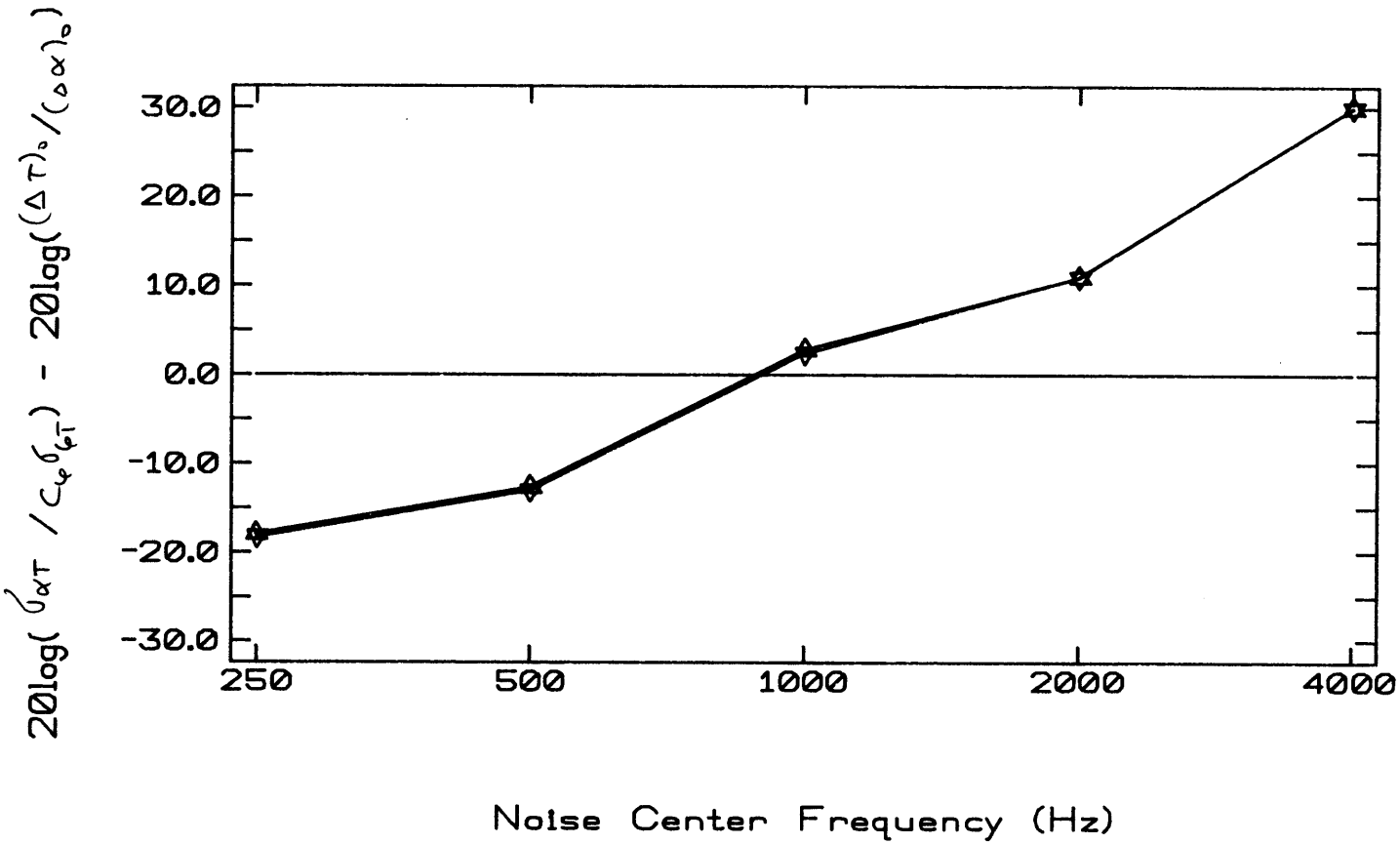
20log(σαT / Cφ σφT) - 20log((ΔT)o/(Δα)o)
30.0
20.0
10.0
0.0
-10.0
-20.0
-30.0
250
500
1000
2000
4000
Noise Center Frequency (Hz)

Figure 8.36

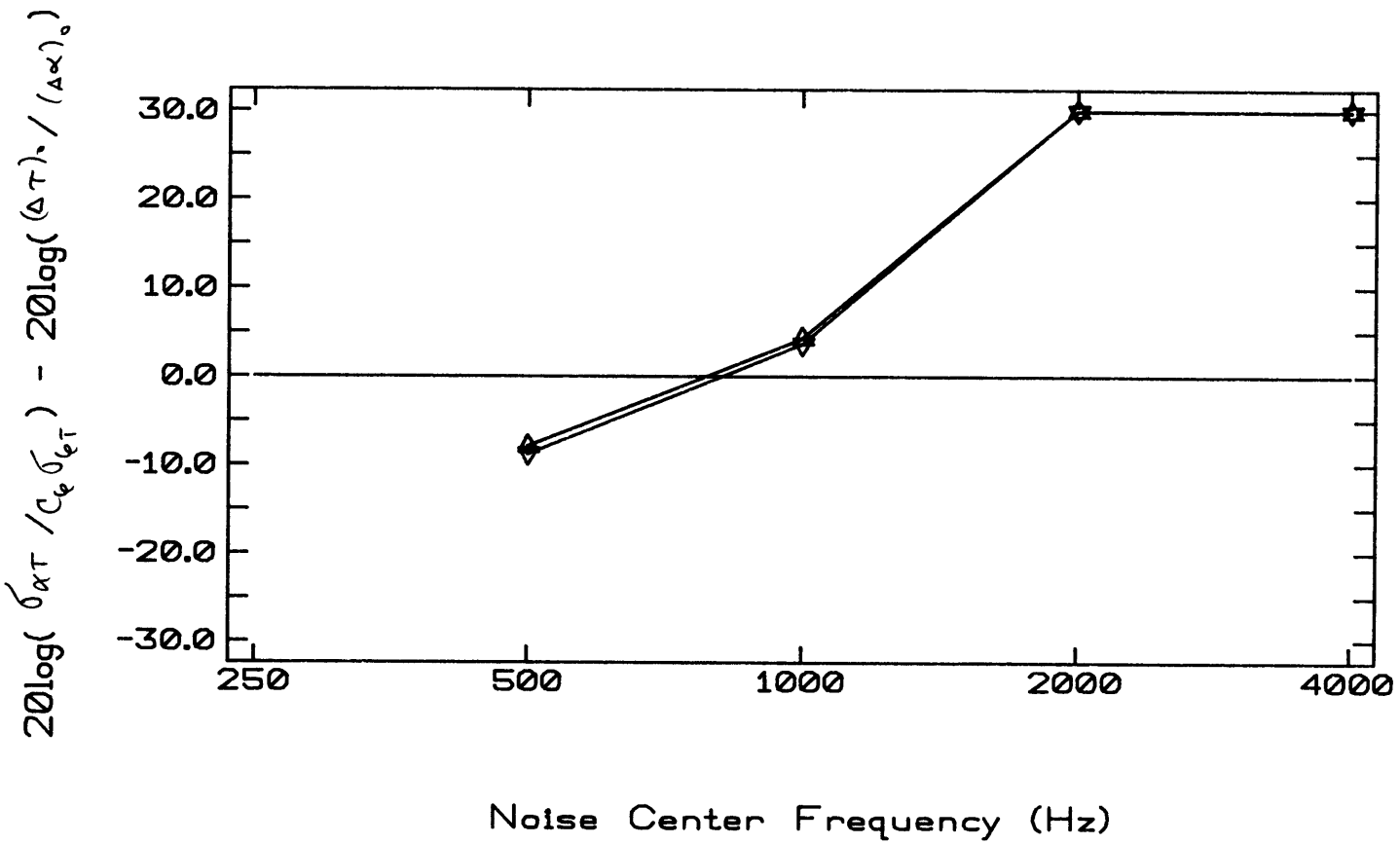
30.0
20.0
10.0
0.0
-10.0
-20.0
-30.0
250
500
1000
2000
4000
Noise Center Frequency (Hz)

Figure 8.37

Figure II.1

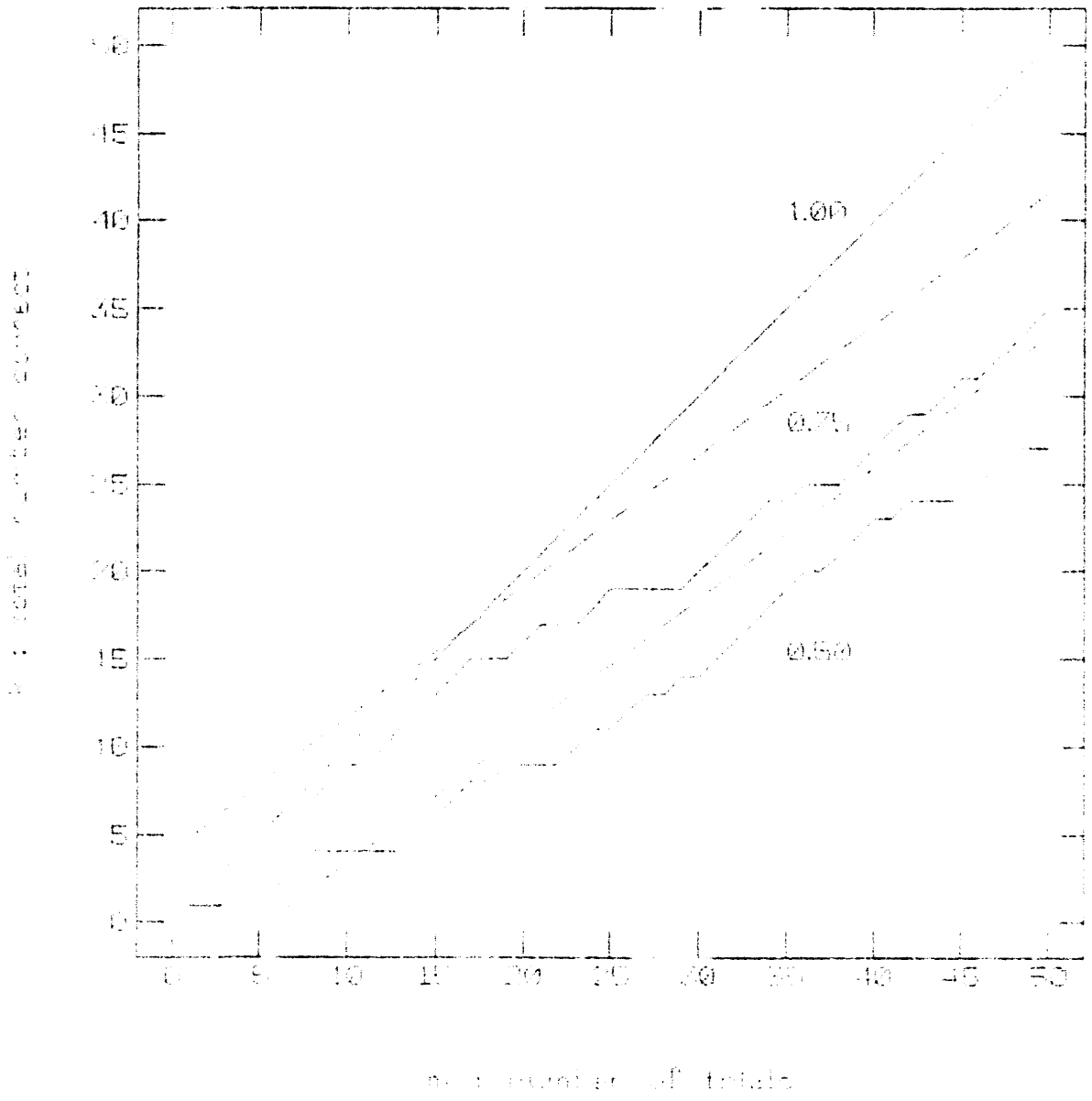

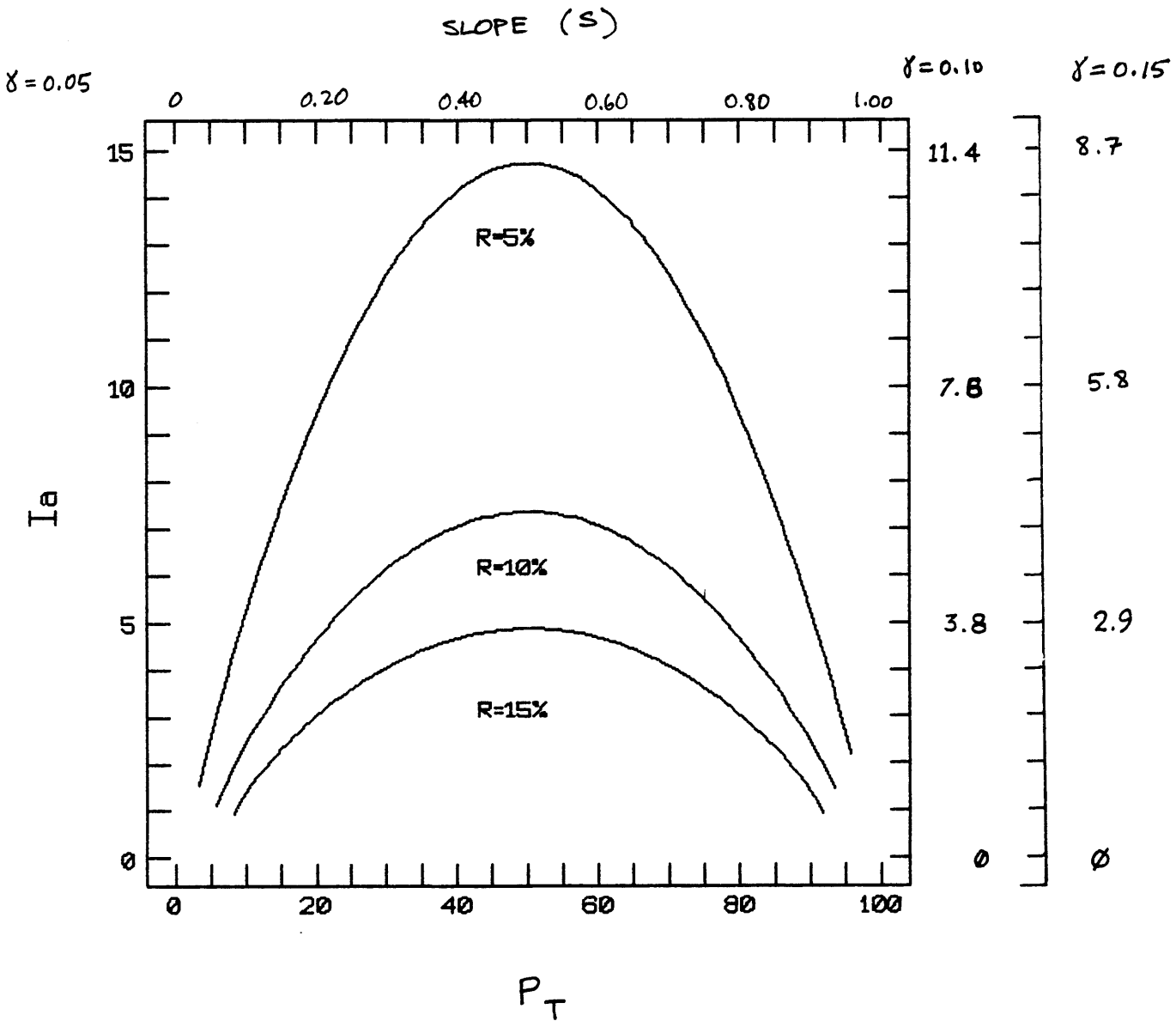
SLOPE (S)
γ = 0.05
γ = 0.10
γ = 0.15
0
0.20
0.40
0.60
0.80
1.00
15
10
5
0
11.4
7.6
3.8
0
8.7
5.8
2.9
Ø
R=5%
R=10%
R=15%
Ia
0
20
40
60
80
100
P_T

Figure II.2

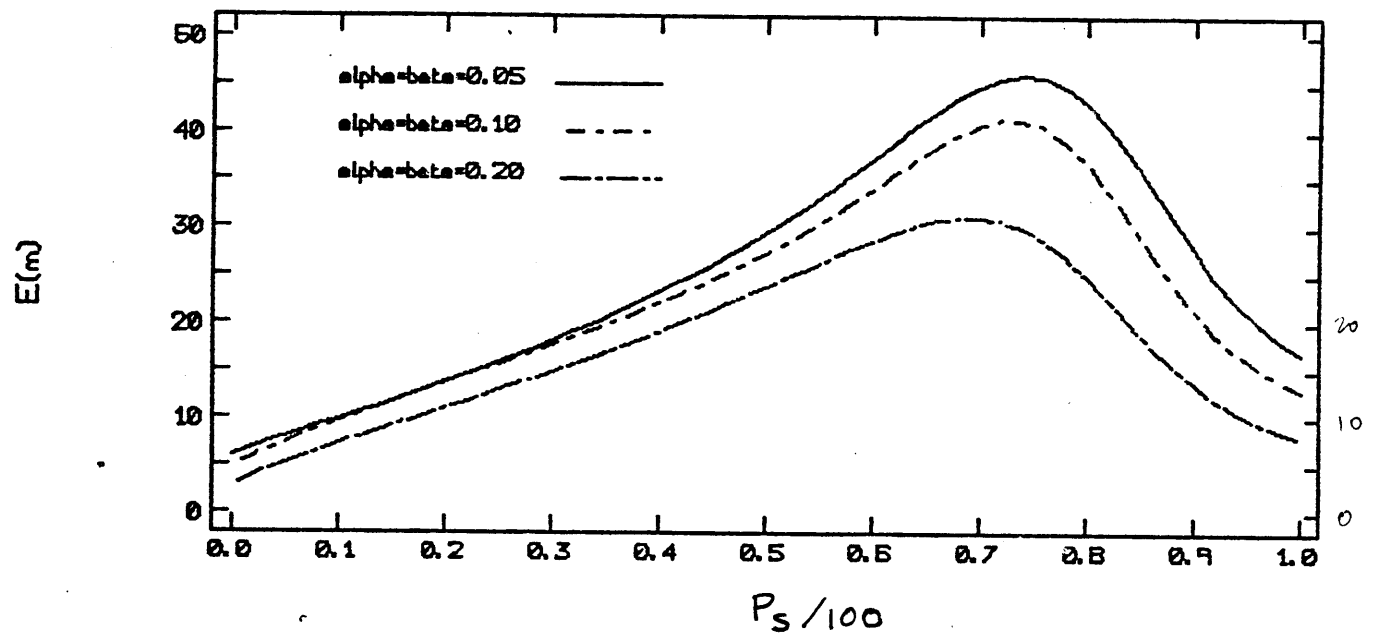
E(m)
alpha=beta=0.05
alpha=beta=0.10
alpha=beta=0.20
50
40
30
20
10
0
0.0
0.1
0.2
0.3
0.4
0.5
0.6
0.7
0.8
0.9
1.0
20
10
0
$P_S/100$

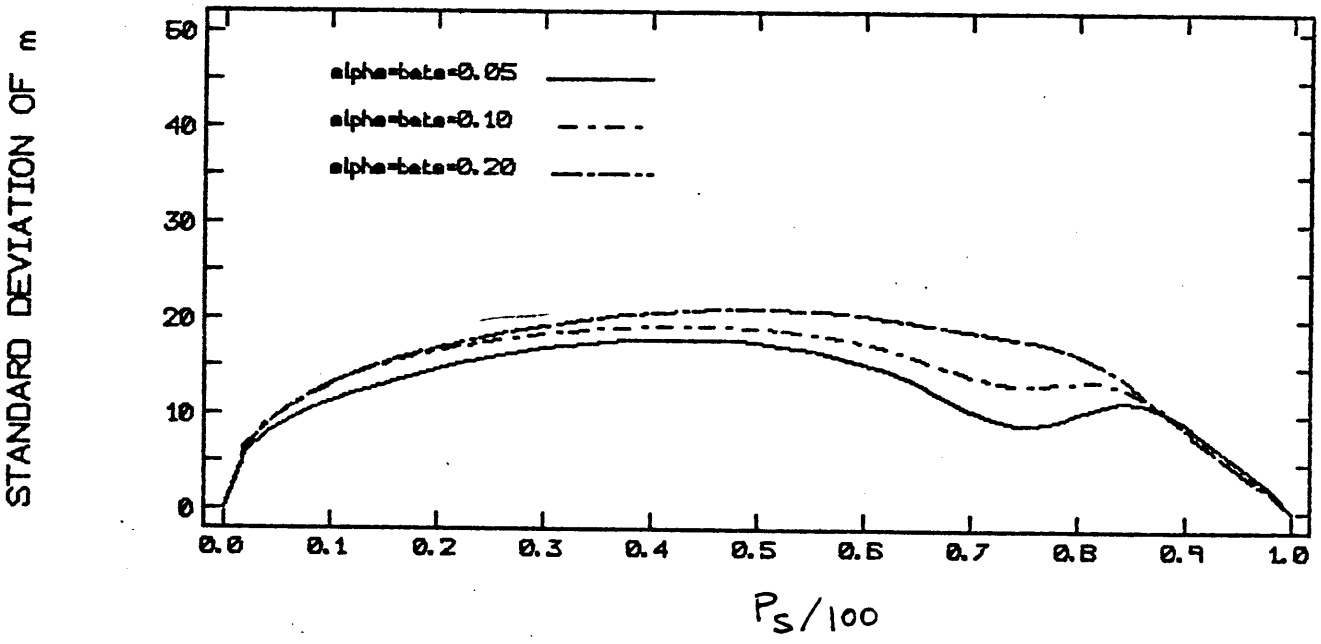
STANDARD DEVIATION OF m
alpha=beta=0.05
alpha=beta=0.10
alpha=beta=0.20
50
40
30
20
10
0
0.0
0.1
0.2
0.3
0.4
0.5
0.6
0.7
0.8
0.9
1.0
$P_S/100$

Figure II.3

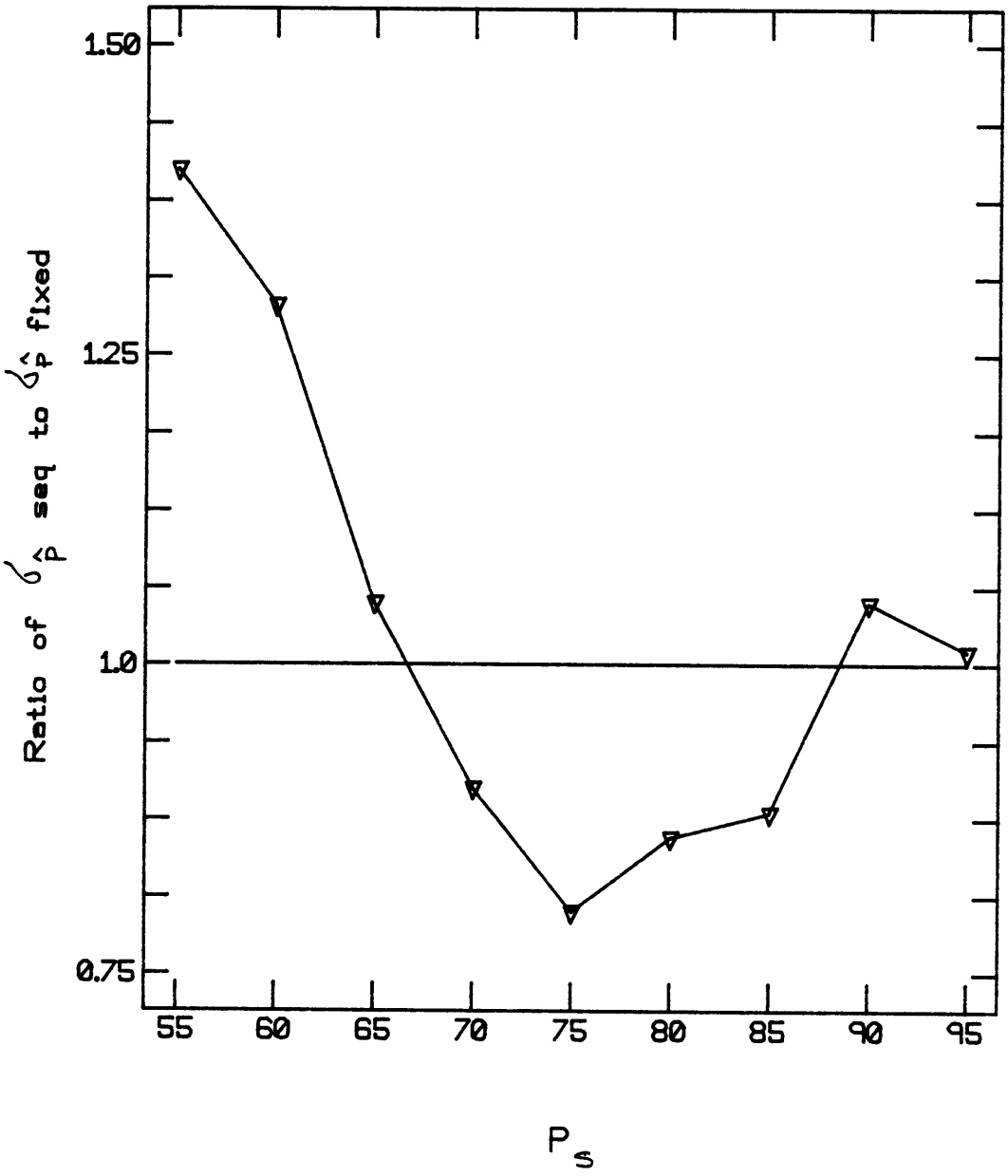
1.50
1.25
1.0
0.75
55
60
65
70
75
80
85
90
95
Ratio of $\hat{\sigma}_P$ seq to $\hat{\sigma}_P$ fixed
P_s

Figure II.4

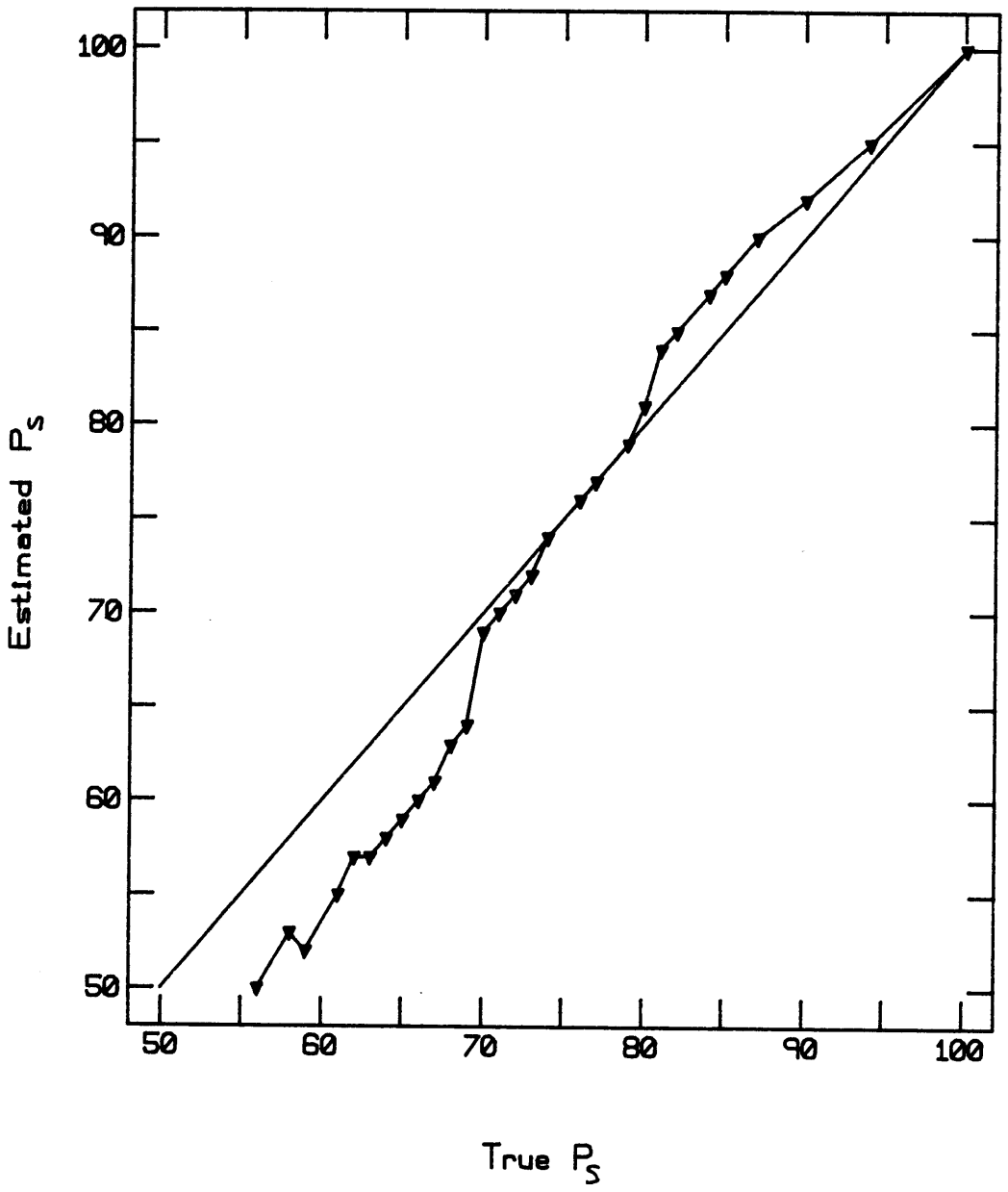

Figure II.5